MOLECULAR AND ENZYMATIC CHARACTERISATION OF MAMMALIAN PHOSPHOLIPASE C ZETA (PLCζ)

BY

MICHAIL NOMIKOS

A thesis submitted for the degree of Philosophiae Doctor

November 2005

Department of Cardiology

Wales Heart Research Institute

University of Wales College of Medicine

ProQuest LLC
789 East Eisenhower Parkway
P.O. Box 1346
Ann Arbor, MI 48106-1346

Dedicated to my Father

Acknowledgements

Firstly and foremost I would like to thank my supervisor Professor F. Anthony Lai for giving me the great opportunity to be taught and trained in his laboratory, and also for his invaluable guidance, understanding and support throughout the course of my PhD study.
I would like to express my gratitude to my second supervisor, Dr Lynda M. Blayney, for her time, patience, teaching, technical help and useful advice, which gave me the experience and courage to complete this study.
I am grateful to Dr Christopher Saunders for his excellent technical help and useful discussions all these years.
Special thanks to Professor Karl Swann for his invaluable ideas, advice and the enjoyable and productive collaboration with his group.
I would also like to thank Professor McLaughlin's group for our collaboration.
I am also grateful to Dr Spyros Zissimopoulos, Dr Christopher George and everyone else in the Wales Heart Research Institute for their help and for creating such a friendly atmosphere.
Finally I would like to express my gratitude to my family and my relatives in Greece, for their unconditional love and unending support all these years. Special thanks to my mother and my brother who deserve an award for their patience and understanding during the difficult last four years.

"Life is short, science is long, opportunity is elusive, experiment is dangerous and judgement is difficult."
Hippocrates 460-377 BC Greek physician

Papers published from this study

Nomikos, M., Blayney, L.M., Larman, M.G., Campbell, K., Rossbach, A., Saunders, C.M., Swann, K. and Lai, F.A. (2005) Role of phospholipase C-zeta domains in Ca^{2+}-dependent phosphatidylinositol 4,5-bisphosphate hydrolysis and cytoplasmic Ca^{2+} oscillations. *Journal of Biological Chemistry* **280**; 31011-31018

*Nomikos, M., *Pallavi, P., *Mulgrew-Nesbitt, A., Mihalyne, G., Zaitseva, I., Lai, F.A., Swann, K., Murray, D. and McLaughlin, S. Binding of phosphoinositide-specific phospholipase Cζ (PLCζ) to phospholipid membranes: Potential role of an unstructured cluster of basic residues. (Submitted to the *Journal of Biological Chemistry*).

* Authors contributed equally to this work.

Summary

In mammalian oocytes, the fertilising sperm evokes intracellular calcium (Ca^{2+}) oscillations that are essential for the initiation of egg activation and embryonic development. Although the exact mechanism leading to the initiation of Ca^{2+} oscillations is still unclear, accumulating evidence suggests that sperm-specific phospholipase C zeta (PLCζ), is delivered from the fertilising sperm into the ooplasm, triggering the Ca^{2+} oscillations through the inositol 1,4,5-trisphosphate ($InsP_3$) pathway. PLCζ is the smallest known mammalian PLC isoform comprising of two EF hand, a C2 and the X and Y catalytic core domains. In this study we examined the biochemical properties of recombinant bacterially expressed mouse PLCζ (mPLCζ) using the well-characterised rat PLCδ1 (rPLCδ1) as control. Using a $PtdInsP_2$ hydrolysis assay we showed that both isoforms had a similar *Km* for $PtdIns(4,5)P_2$ and that PLCζ had a much higher Ca^{2+} sensitivity, which would predict it to be active at resting Ca^{2+} concentrations in eggs. PLCζ bound with high affinity to $PtdIns(3,5)P_2$ and $PtdIns(4,5)P_2$ even though it lacks a PH domain from its sequence, which targets PLCδ1 to $PtdIns(4,5)P_2$. A series of domain deletion constructs of PLCζ were used to demonstrate the role of the EF hands on the Ca^{2+} sensitivity of PLCζ and the role of C2 domain and XY linker on its binding to $PtdInsP_2$. Luminescent PLC constructs were generated to examine their potential to elicit Ca^{2+} oscillations, quantifying their expression levels in mouse eggs. Anti-human PLCζ (hPLCζ) monoclonal antibodies were produced and their ability to block the *in vitro* hydrolysing activity of recombinant hPLCζ was tested.

Table of contents

Chapter 1

General Introduction

1.1 Calcium: A vital ionic messenger.

1.1.1 Calcium signalling- An overview.

One of the most versatile and universal signalling molecules in the human body is the calcium ion (Ca^{2+}), which serves as a dynamic messenger in regulating intracellular and extracellular events (Clapham, 1995; Berridge *et al*, 2000). The involvement of Ca^{2+} in a variety of cellular processes such as fertilisation, gene transcription, muscle contraction, cellular proliferation and cell death, shows the ability of this ion to regulate a great diversity of events (Berridge, 1993; Clapham, 1995; Berridge *et al*, 2000;). Due to these multiple roles, Ca^{2+} has to be carefully regulated within the cytoplasm. One of the controversies surrounding Ca^{2+} signals is that it can be involved in life and death. Although elevations in Ca^{2+} are necessary for it to act as a signal, subsequent increases in its levels can be fatal (Berridge, 1993). Cells avoid death either by utilising low amplitude Ca^{2+} signals or more usually by delivering the signals as transients.

In cells, Ca^{2+} signalling occurs when the Ca^{2+} concentration ($[Ca^{2+}]$) is elevated in the cytosolic compartment. The $[Ca^{2+}]$ within the cells can be controlled by a simultaneous interplay of multiple counteracting processes, which are divided into Ca^{2+} "on" and "off" mechanisms depending on whether they can increase or decrease Ca^{2+} levels (Figure 1.1), (Berridge, 1993; Petersen *et al*, 1994; Berridge *et al*, 1998; Berridge *et al*, 2000). The Ca^{2+} "on" mechanisms include channels on the plasma membrane that regulate the Ca^{2+} supply from the extracellular space, and channels on the endoplasmic reticulum or sarcoplasmic reticulum (ER and SR respectively), which act as intracellular Ca^{2+} stores (Berridge *et al*, 2000). In contrast the "off" mechanisms involve the mechanisms utilised by cells to remove internal Ca^{2+} from the cytoplasm. These events include the Ca^{2+} ATPases on the plasma membrane and ER/SR, as well as a number of exchangers that catalyse gradients of other agents providing the energy to transport Ca^{2+} out of the cells e.g. Na^{+}/ Ca^{2+} exchange (Lipp and Niggli, 1994). A vital organelle involved in the "off" mechanism events is the mitochondrion, which has a low affinity but high capacity for cytosolic Ca^{2+} and through its uniporter can

diminish cytosolic Ca^{2+} levels and minimise cellular events. Ca^{2+} can also diffuse into the nucleus (Bootman *et al*, 2001). When cells are at rest, their "on " and "off " mechanisms at equilibrium yield a cytosolic [Ca^{2+}] around 100nM. The cells become activated by subsequent raises of cytosolic Ca^{2+} levels to 1μM or more (Bootman *et al*, 2001). However prolonged elevations in Ca^{2+} levels result in irreversible damage, as described in cardiac or cerebral ischaemia (Trump and Berezesky, 1995).

Cells utilise two sources of Ca^{2+} to generate signals. Ca^{2+} can either enter from outside the cell by passing through channels spanning the plasma membrane or alternatively it can be released from internal stores through channels located in the ER or SR (Berridge, 1993; Clapham, 1995). Ca^{2+} enters via the plasma membrane through a variety of channels, such as the voltage-operated calcium channels (VOCCs), receptor-operated calcium channels (ROCCs), and store-operated calcium channels (SOCCs) (Berridge, 1997). VOCCs are employed largely by excitable cell types such as muscle and neuronal cells, where they are activated by depolarisation of the plasma membrane. ROCCs are a structurally and functionally diverse set of channels that are prevalent in secretory cells and nerve terminals. Well known ROCCs include nicotinic acetylcholine receptor and the N-methyl D aspartate receptor. These channels are activated by Ca^{2+} agonists such as ATP, serotonin, glutamate and acetylcholine, which has been found to bind to metabotropic receptors in the plasma membrane. Finally, SOCCs are thought to be activated in response to a depletion of intracellular Ca^{2+} stores elicited in response to either physiological or pharmacological agents (Bootman *et al.*, 2001).

Calcium from internal stores can be released in distinct ways. It is a highly regulatable process, mediated by the action of a variety of second messenger molecules and by the function of two types of Ca^{2+} release channels, the Inositol 1,4,5-trisphosphate Receptor ($InsP_3R$) and the Ryanodine Receptor (RyR) located in the ER (Berridge *et al*, 2000). Inositol 1,4,5-trisphosphate ($InsP_3$) is a second messenger molecule that mobilises Ca^{2+} from the ER via binding to the $InsP_3R$, which has a Ca^{2+}-dependent sensitisation to $InsP_3$. The RyR is the second major channel located in the ER. It too can be modulated

by [Ca^{2+}]. Two other compounds the nicotinic acid adenide dinucleotide phosphate (NAADP) and sphingosine 1-phosphate (S1P) have also been implicated in the Ca^{2+}-release from intracellular stores, although their receptor release channels have not been defined. All these variable mechanisms of Ca^{2+}-release from intracellular stores are discussed in detail in the following sections.

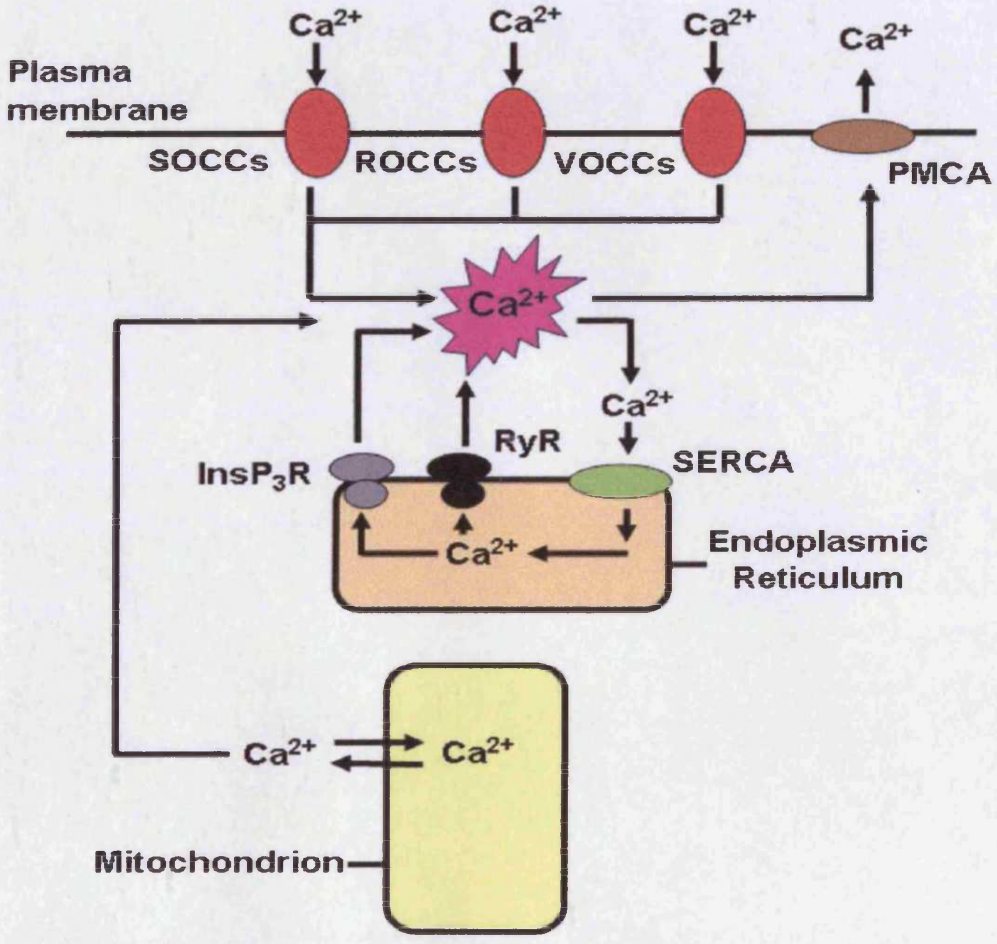

Figure 1.1 Schematic representation of Ca^{2+} "on" and "off" mechanisms employed to control Ca^{2+} concentration in the cytosolic compartment of the cells. Ca^{2+} "on" mechanisms involve SOC, ROC, VOC channels on the plasma membrane and $InsP_3R$ and RyR Ca^{2+} channels located in the endoplasmic reticulum. Ca^{2+} "off" mechanisms involve Ca^{2+}-ATPases found on the plasma membrane (PMCA) and on the endoplasmic reticulum (SERCA). In addition, mitochondrion is a vital organelle that plays an important role in Ca^{2+} homeostasis (Figure based on reports reviewed in Berridge *et al*, 1998; Berridge *et al*, 2000; Bootman *et al*, 2001).

1.1.2 Endoplasmic reticulum Ca^{2+} stores.

The endoplasmic reticulum (ER) is the primary storage organelle for Ca^{2+} in most mammalian cell types. ER is a complex system of cytoplasmic membranes arranged to form cisternae and tubules, found in all eukaryotic cells despite its high variability (Pozzan *et al*, 1994). ER consists of three separate subcompartments; the 'rough' ER, the 'smooth' ER and the nuclear envelope (NE). The 'rough' ER, which is mostly composed of cisternae and is covered with numerous ribosomes, is the major site of protein synthesis and post-translational processing in the cell. The 'smooth' ER is composed of a series of twisted ribosome-free tubules. The NE is also covered by ribosomes, but only on its cytoplasmic face. The NE surrounds the nucleus with a continuous double membrane, interrupted by highly specific structures, the nuclear pores, which act as the regulators of molecular movement into and out of the nucleus. An additional specialised form of ER is the sarcoplasmic reticulum (SR), which is only found in muscle tissue. SR consists of a series of tubules arranged around the contractile myofilaments, ensuring adequate Ca^{2+} levels for muscle contraction (Pozzan *et al*, 1994).

Measurements of free internal $[Ca^{2+}]$ in ER have been variously reported, but recent refinements in measuring techniques have enabled the free $[Ca^{2+}]$ within the ER to be estimated as at least a few hundred micromolar (μM), considerably higher than that in the cytoplasm (~100nM) (Meldolesi and Pozzan, 1998; Verkhratsky and Petersen, 1998; Meldolesi, 2001). This is in addition to Ca^{2+} ions that may be bound to the large number of Ca^{2+}-binding proteins, such as calreticulin and calcineurin found within the ER lumen (Pozzan *et al*, 1994; Meldolesi and Pozzan, 1998; Meldolesi, 2001; Sorrentino and Rizzuto, 2001). However the amount of Ca^{2+} stored in the ER is highly variable between cell types. For example the ER Ca^{2+} stores in neurons of the central nervous system are only partially full under resting conditions, and can only release small amounts of Ca^{2+} upon stimulation. The stores become responsive after conditioning depolarisation allowing Ca^{2+} influx from the extracellular medium, which is then taken up by the stores (Verkhratsky and Shmigol, 1996; Verkhratsky and Petersen, 1998).

Uptake of Ca^{2+} into the ER stores from the cytosol occurs via specialised Ca^{2+}-ATPase pumps, dubbed SERCA because they are found also in the sarcoplasmic reticulum (Pozzan *et al*, 1994; Clapham, 1995; Meldolesi, 2001; Sorrentino and Rizzuto, 2001). Three distinct SERCA genes have been identified producing proteins of approximately 110kDa, which contain ten membrane-spanning domains, a small luminal portion and a bulky cytosolic head. SERCA1 & SERCA2 undergo alternative splicing to produce two splice variants of each (SERCA1a/SERCA1b, SERCA2a/SERCA2b). The three isoforms and their splice variants are expressed differentially between most tissue types in both adults and foetal tissues, highlighting different roles for the three isoforms. In addition, an alternative Ca^{2+} pump, distinct from the SERCA pump has been recently characterised, termed the secretory pathway Ca^{2+} ATPase (Shull, 2000).

1.1.3 Mitochondria and Ca^{2+} homeostasis.

In addition to the endoplasmic reticulum other organelles, most notably the mitochondria, play important roles in many physiological processes by modulating the cytoplasmic Ca^{2+} signals (Duchen, 1999; Duchen, 2000; Hajnoczky *et al*, 2000; Rutter and Rizzuto, 2000). The uptake of Ca^{2+} into the mitochondrion does not depend on ATP hydrolysis, but on the presence of a "Ca^{2+} uniporter" located on the inner mitochondrial membrane and the driving force provided by the negative (-180mV in the matrix) membrane potential generated by the respiratory chain. Mitochondria are generally believed to act as a buffer for high levels of Ca^{2+} release from other stores (Meldolesi and Grohovaz, 2001), rather than by rapid release of Ca^{2+} from their own stores. There is evidence that Ca^{2+} uptake is mediated by a RyR channel, since ryanodine suppressed uptake into isolated heart mitochondria (Beutner *et al*, 2001).

1.1.4 $InsP_3$-mediated Ca^{2+} release.

This study is concerned with the analysis of a novel phospholipase C isoform that causes $InsP_3$-mediated Ca^{2+} release in fertilised oocytes (discussed in detail in the following sections). $InsP_3$ is generated at the plasma membrane from the hydrolysis of phosphatidyl inositol 4-5-bisphosphate [$PtdIns(4,5)P_2$] by phosphatidylinositol-specific phospholipase C enzymes (PLCs). Activation of PLCs by an intracellular signal or by a receptor results in the binding of these enzymes to $PtdIns(4,5)P_2$ substrate and cleavage of the inositol headgroup, producing freely diffusible $InsP_3$ and the membrane-bound lipid diacylglycerol (DAG). DAG can stimulate the activation of protein kinase C (PKC) and $InsP_3$ binds to $InsP_3R$ on the ER membrane, causing a conformational change and consequent opening of the $InsP_3R$ channel resulting in Ca^{2+} release from internal stores. Ca^{2+} release stops when $InsP_3$ is metabolised through the action of two enzymes, $InsP_3$-5-phosphatase or $InsP_3$-3-kinase to form the derivatives inositol 1,4-bisphosphate or Inositol 1,3,4,5-tetrakisphosphate respectively.

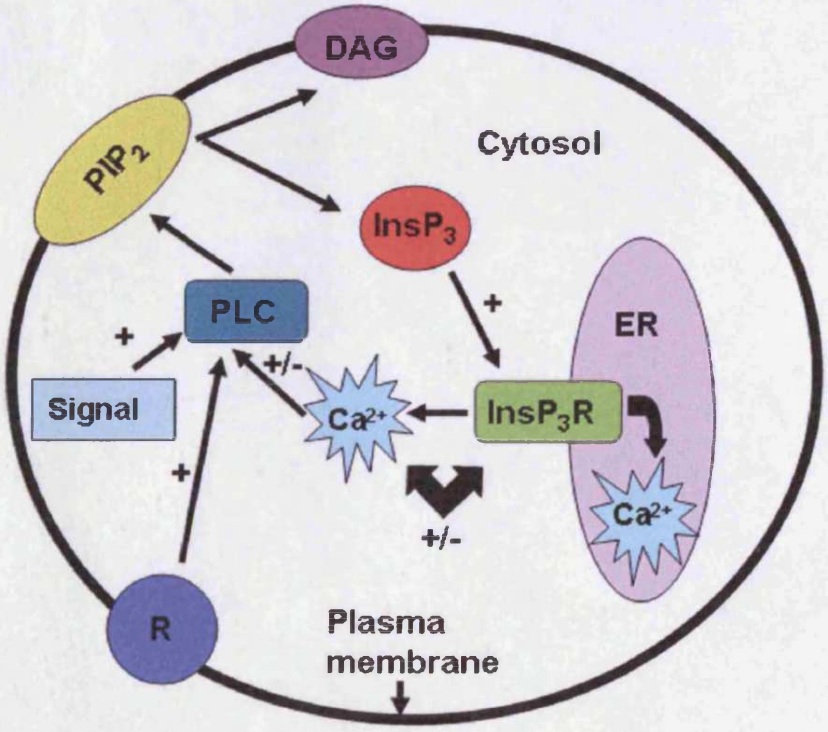

Figure 1.2 Schematic diagram of $InsP_3$-mediated Ca^{2+} release within a mammalian cell. (R is a receptor mediated event; other abbreviations are defined in the text).

1.1.5 Inositol 1,4,5-Trisphosphate Receptor.

The $InsP_3R$ is a large tetrameric channel with a total molecular mass of ~1.2 MDa and is composed of four subunits of ~2700 residues each (Patel *et al*, 1999; Taylor *et al*, 1999). Cryoelectron-microscopy studies of the native channel revealed a square-shaped particle with a side of ~12nm length (Mikoshiba, 1997). The channel pore is formed by six membrane-spanning regions, clustered at the C-terminus of the protein, contributed by the non covalent association of all four subunits (Patel *et al*, 1999; Taylor *et al*, 1999). The C-terminal membrane spanning region of $InsP_3R$ is essential for protein oligomerisation and correct targeting (Patel *et al*, 1999; Taylor *et al*, 1999). The N-terminal region possesses the $InsP_3$ binding site (Mikoshiba, 1997; Patel *et al*, 1999). The $InsP_3$ binding domain consists of a 650 amino acid sequence (Mikoshiba *et al*, 1994). The middle of the sequence is the location of phosphorylation; and in addition this region contains the binding sites for regulatory proteins. Binding of $InsP_3$ causes a conformational change in the cytoplasmic portion of this protein, resulting in the opening of the channel pore and the efflux of Ca^{2+} (Boening and Joseph, 2000). This process has been found to involve co-interaction of the N-terminal and the C-terminal cytoplasmic regions of the protein (Boening and Joseph, 2000).

Three isoforms of $InsP_3R$ have been identified; sharing 60-80% amino acid sequence identity with each other (Taylor *et al*, 1999; Thrower *et al*, 2001). In addition type 1 and 2 receptors have been described to have a number of splice variants. The $InsP_3R$ isoforms share a number of functional properties such as activation by $InsP_3$, the magnitude of the single channel current and activation by minimal Ca^{2+} concentrations of less than 250nM (Bezprozvanny *et al*, 1991; Perez *et al*, 1997; Hagorr *et al*, 1998; Ramos-Franco *et al*, 1998). The most widely studied isoform of $InsP_3R$ is the $InsP_3R1$ subtype that is highly expressed in cerebullar Purkinje cells of the central nervous system (Furuichi *et al*, 1993). The $InsP_3R1$ can be alternatively spliced at three different sites, while the $InsP_3R3$ has no splice variants. The $InsP_3R3$ is expressed in the kidney, brain, gastrointestinal epithelium, and pancreatic islets (Blondell *et al*, 1993), while $InsP_3R2$ is highly expressed in spinal cord, glial cells and cardiac myocytes. $InsP_3Rs$ are most abundantly expressed in

the ER; however their expression has been reported in the nuclear envelope, the Golgi apparatus, secretory vesicles, as well as in the plasma membrane of some cells (Taylor *et al*, 1999). At present there is no evidence linking targeting to specific membranes with isoform specificity. Even within the ER, $InsP_3R$ are differentially distributed leading to important functional consequences (Meldolesi and Pozzan, 1998).

Ca^{2+} is an important regulator of $InsP_3R$. It has a biphasic role, as in relatively low concentrations Ca^{2+} is stimulatory (μM), while at higher concentrations has been shown to be inhibitory. It is still not clear however, if Ca^{2+} acts directly by binding to the $InsP_3R$ or via other accessory proteins such as calmodulin (Taylor, 1998; Patel *et al*, 1999). Another important regulator of $InsP_3R$ is the $InsP_3$ itself since its effect appears to be more complex than simply sensitising the receptor for activation and is isoform specific (Bootman and Lipp, 1999; Taylor, 1998; Thrower *et al*, 2001). The $InsP_3R3$ is of significant importance, as it has different $InsP_3$ binding properties in comparison with the other two subtypes (O' Neil *et al*, 2002). It possesses the lowest relative affinity for $InsP_3$, and unlike the $InsP_3R1$, can be fully activated by $InsP_3$ binding even at resting cytosolic Ca^{2+} levels (O' Neil *et al*, 2002). Finally other endogenous regulators mediating $InsP_3R$ sensitisation and activation have also been reported (Patel *et al*, 1999; Thrower *et al*, 2001). These modulators include ATP, phosphorylation and accessory proteins (Patel *et al*, 1999). Micromolecular concentrations of ATP have been reported to increase channel activation, while higher concentrations have an inhibitory effect. It is believed, that ATP acts as an antagonist to $InsP_3$ ligand binding. Furthermore, the $InsP_3R$ is subject to phosphorylation by a variety of protein kinases, all of which enhance $InsP_3$-induced Ca^{2+} mobilisation irrespective of receptor subtype (Thrower *et al*, 2001). Finally, not many pharmacological regulators of $InsP_3R$ have been described. A well known inhibitor, Heparin competitively inhibits $InsP_3$ binding to its receptor (Elhrich *et al*, 1994).

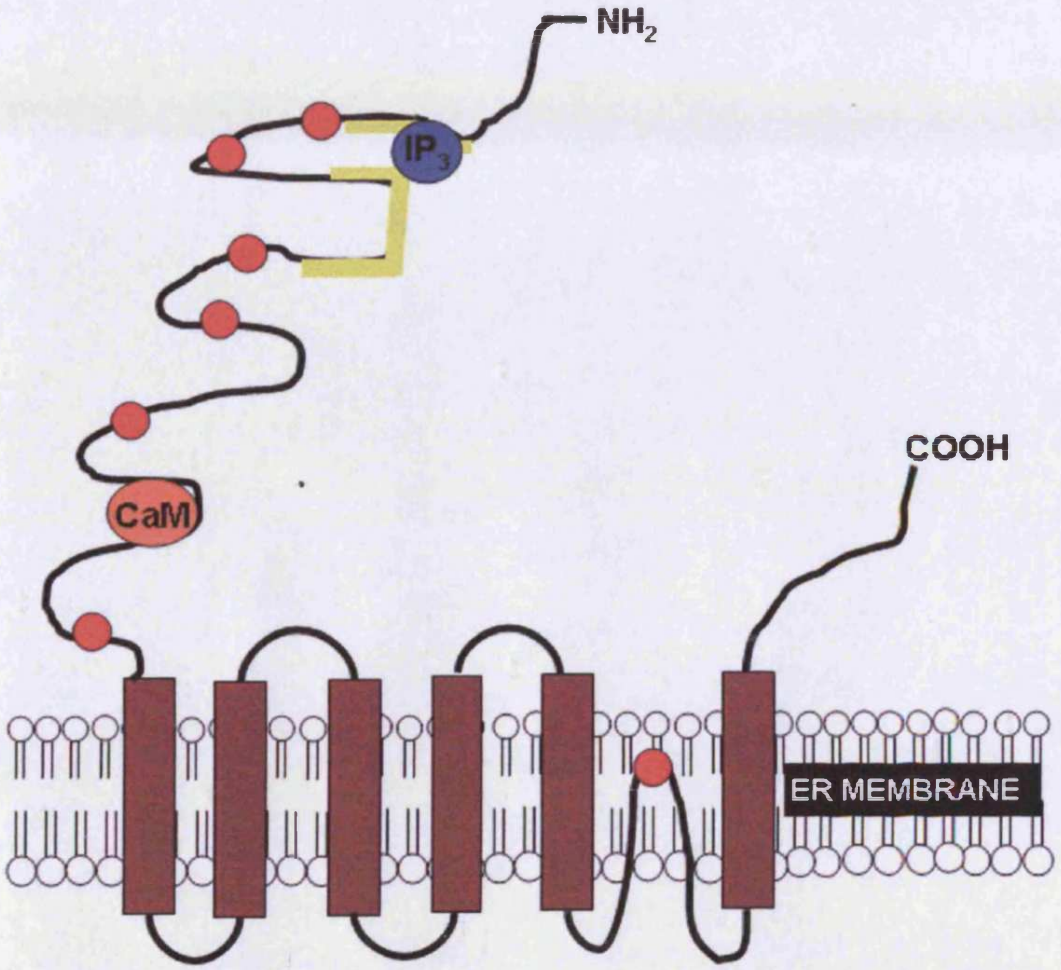

Figure 1.3 Schematic representation of the domain topology of the $InsP_3$ receptor. The six transmembrane regions at the C-terminus, several Ca^{2+} binding sites (red), a calmodulin (orange) anchoring site and the ligand binding domain (yellow) occupied by an $InsP_3$ molecule (blue) at the N-terminus.

1.1.6 Ryanodine receptor.

The Ryanodine receptor (RyR) is the second major Ca^{2+} release channel located in the ER. It is a large homotetrameric protein with a total molecular mass of ~2.2MDa composed of four subunits each containing ~5000 amino acid residues. The RyR channel was discovered by the actions of an alkaloid termed ryanodine, isolated from the stem and roots of the plant *Ryania Speciosa*. This alkaloid was capable of inducing rigid paralysis in skeletal muscles and flaccid paralysis in cardiac muscles of mammals. Ryanodine was

found to inhibit Ca^{2+} release from the SR by binding with high affinity to a protein present in the SR membrane. Incorporation of this Ryanodine binding protein complex into artificial planar lipid bilayers revealed a structure that was characteristic of an ion channel (Fill and Copello, 2002). Structural analysis of the primary amino acid sequence in the RyR showed that the transmembrane domain was clustered in the C-terminal of the RyR channel. However there is much debate with regard to how many transmembrane-spanning segments RyR contains. Estimations vary from four to ten transmembrane units (Grunwald and Meissner, 1995). The N-terminal domain of the RyR complex serves as a scaffold of proteins that modulate RyR channel function (Marx *et al*, 2000).

The RyR Ca^{2+}-release channel consists of three main isoforms named RyR1, RyR2, RyR3 that share 65% amino acid homology and each isoform possesses three major regions of diversity designated D1, D2 and D3 respectively (Sorrentino and Volpe, 1993). These regions of diversity account for the functional differences between the three RyR isoforms. The RyR1 isoform is the dominant Ca^{2+} release channel required for skeletal muscle contraction, although low levels of its expression have been identified in smooth muscle cerebellum, testis, adrenal gland and ovaries (Takeshima *et al*, 1989; Ottini *et al*, 1996). In addition RyR1 is highly expressed in Purkinje cells in the brain, while the RyR2 isoform is localised in the somata of neurons. High levels of RyR2 expression are found in heart and brain, but in lower levels RyR2 is expressed in the stomach, lung, thymus, adrenal gland and ovaries (Nakai *et al*, 1990; Giannini *et al*, 1995; Wehrens *et al*, 2005). The third isoform RyR3 is expressed in the brain, diaphragm, slow switch skeletal muscle as well as abdominal organs (Giannini *et al*, 1995; Wehrens et al, 2005). The RyR channel interacts with a large number of proteins. The first protein that was found to interact with the RyR channel in lipid bilayers was calmodulin (CaM). Cryoelectronmicroscopy studies revealed binding of CaM to the surface of RyR2 (Wehrens *et al*, 2005). The Ca^{2+}-free calmodulin has been described as an inhibitor of RyR1 function (Wehrens *et al*, 2005). Furthermore two Ca^{2+} channel –stabilising proteins calstabin1 (also known as FKBP12) and calstabin2 (alternatively known as FKBP12.6) associate with RyR1 and RyR2 respectively such that one calstabin protein is bound to each

RyR monomer (Timerman *et al*, 1993; Timerman *et al*, 1996). Calstabin1 binds with high affinity to RyR1 and RyR3 specific binding sites, while the RyR2 channel exhibits a higher affinity for calstabin2 (Timerman *et al*, 1996; Jeyakumar *et al*, 2001).

A large number of other cellular proteins including calmodulin, sorcin, calsequestrin, junctin, and triadin have been demonstrated to associate with RyR (Mackrill, 1999). This suggests that many of the physiological differences between the RyR isoforms may be due to the different protein-protein interactions. Other modulators of RyR are other cellular factors including Mg^{2+} (Coronado *et al*, 1994; Meissner, 1994), adenine nucleotides and lipid products (Meissner, 1994; Zucchi and Ronca-Testoni, 1997). A role of Ca^{2+} itself as the agonist of the channel has been suggested and this is supported by the observation that other antagonists of RyR had little or no effect in the absence of free Ca^{2+} (Coronado *et al*, 1994; Meissner, 1994; Zucchi and Ronca-Testoni, 1997).

1.1.7 cADPR-mediated Ca^{2+} release.

cADPR has been described as a mobilising messenger releasing Ca^{2+} from internal stores in a variety of cells types including plant cells, mammalian eggs, pituitary cells, pancreatic acinar and β-cells, skeletal, cardiac, and smooth muscle cells, hepatocytes and T-lymphocytes (Lee, 1997; Lee, 2001). However, the role of cADP–ribose is poorly characterised with many controversies. cADPR is a cyclic derivative of β-nicotinamide adenine dinucleotide (NAD). It is synthesised by ADP-ribosyl cyclases and metabolised by cADPR hydrolases to yield the inactive linear molecule ADPR. It has been suggested that cADPR releases Ca^{2+} through an $InsP_3$ insensitive pathway. Its activity is thought to be mediated by its interaction with RyR, which can either be direct or via other accessory proteins (Guse, 1999; Da Silva and Guse, 2000; Lee, 2001). However there are few convincing examples of a link to cellular stimulation. In addition appreciable effects of cADPR seem to exist in cells that do not express RyRs. This may indicate that

cADPR is a relatively constant endogenous regulator of Ca^{2+} or that it has cellular functions distinct from Ca^{2+} release (Bootman *et al*, 2001).

1.1.8 NAADP-mediated Ca^{2+} release.

Ca^{2+} release from internal stores by NAADP has been demonstrated in a number of different cell types from a range of eukaryotic species (Lee, 1997; Galione *et al*, 2000; Lee, 2001; Patel *et al*, 2001). NAADP is synthesised from ADP-ribosyl cyclases, by converting NADP to NAADP in a "base-exchange" reaction, substituting an amino group for a hydroxyl group. NAADP was first discovered in the sea urchin egg as a novel Ca^{2+}-mobilizing agent (Galione *et al*, 2000). The most intriguing property of NAADP (in sea urchin homogenates) is its profound self-desensitization mechanism that is unparalled by any other intracellular messenger, as sub-threshold concentrations of NAADP inactivated the NAADP-evoked Ca^{2+} release that normally shows a robust Ca^{2+} release response. However, in intact mammalian cells, only high concentrations of NAADP cause such self-desensitization (Patel *et al*, 2001). In contrast to Ca^{2+} release by $InsP_3$ or cADPR, NAADP-mediated Ca^{2+} release appears not to be modulated by divalent cations including Ca^{2+} itself (Chini and Dousa, 1995). RyRs have been proposed as target Ca^{2+} release channels for NAADP in mammalian cells. Evidence for this came from the findings that NAADP was shown activate isolated RyRs reconstituted in lipid bilayers from rabbit skeletal muscle (RyR1), (Hohenegger *et al*, 2002), and cardiac microsomes RyR2 (Mojzisova *et al*, 2001). However, RyRs are unlikely to be a target Ca^{2+} release channels for NAADP in sea urchin eggs, since depletion of ryanodine sensitive stores in egg homogenate did not significantly affect the ability of NAADP to evoke subsequent Ca^{2+} release (Galione and Ruas, 2005). Further studies are required to establish in more detail the molecular mechanisms mediating NAADP-induced Ca^{2+} release.

1.1.9 Sphingosine-1-Phosphate-mediated Ca^{2+} release.

Sphingosine-1-phosphate (S1P) is involved in the regulation of many cellular processes such as cell differentiation, mitogenesis, cell migration and apoptosis (Pyne and Pyne, 2000). S1P is formed from sphingosine through the action of sphingosine kinase in response to various extracellular stimuli (growth factors, G-protein coupled molecules, cytokines and antigens), (Pyne and Pyne, 2000). It has been demonstrated that S1P and its surrogate sphingosylphosphorylcholine induce Ca^{2+} release from internal stores of mammalian cell lines. S1P-mediated Ca^{2+} release appeared to be insensitive to certain antagonists such as heparin, nifedipine, conotoxin, Ni^{2+}, or La^{2+} suggesting that the channel responsible was distinct from the other known plasma membrane or intracellular Ca^{2+} channels (Ghosh *et al*, 1994; Kindman *et al*, 1994; Kim *et al*, 1995). A novel sphingolipid-gated Ca^{2+} release channel, named SCaMPER (for sphingolipid calcium release-mediating protein of ER), was identified with a molecular mass of 20kDa. This channel appeared to have no homology with any proteins (Mao *et al*, 1996), suggesting that S1P-mediated Ca^{2+} release mechanism maybe distinct from other intracellular release mechanisms.

1.2 Mammalian Fertilisation.

Mammalian fertilisation is the process of the union of two haploid gametes derived from the genetically distinct individuals of the same species. The gametes are morphologically distinct and are derived from germ cells contained within sexually differentiated organs within each of the parent individuals. The male gametes (spermatozoa) are produced by meiosis from germ cells (spermatogonia) within the testes and the female gametes (oocytes) are also produced by meiosis from germ cells (oogonia) located within the ovaries (Kupker *et al*, 1998).

When mammalian sperm and oocytes come into contact in the oviduct a series of steps is set in motion that can lead to oocyte activation and ultimately to the development of a diploid zygote that begins to divide by mitosis to form a mass of about 100 cells, the blastocyst. The external part will become the placenta and the internal part will become the embryo. Growth and development of the embryo into a fully-formed infant is species dependant with gestation (fertilisation to birth) lasting from ~3 weeks in the mouse to ~23 months in African elephants.

1.2.1 Oogenesis.

Oocytes are produced from the female germ cells (oogonia) within the ovary. The ovary is an endocrine organ that produces steroids to allow the development of female secondary sexual characteristics and support pregnancy. Oogonia undergo several mitotic divisions and rapid growth, and embark on a meiotic division shortly before birth (and in some cases soon after birth) of the neonate (Eppig, 1993; Tsafriri and Dekel, 1994). During meiosis of oogonia the replicated (4n) chromosomes undergo two successive reductive divisions separating a first set of chromosomes (2n) in the first polar body and a second set of replicated chromosomes after fertilisation to generate a haploid set (1n) in the egg (figure 1.4). In mammals, meiotic division proceeds as far as late prophase of the first division, before arresting under the influence of the surrounding follicular (granulosa) cells (Edwards, 1965). Maintenance of this meiotically-arrested (PI arrest) may involve hypoxanthine (produced by follicular cells), (Eppig *et al*, 1985); or high levels of cAMP, either produced locally within the oocyte, or transferred into the oocyte from granulosa cells through gap junctions (Dekel, 1988). Resumption of meiosis is accompanied by the activation of maturation promoting factor (MPF), a complex consisting of a regulatory protein cyclin B2 and a catalytic protein Cdc2 (Tsafriri and Dekel, 1994). The activity of MPF is controlled by the association of these proteins with each other. Active MPF is required for the oocyte to undergo germinal vesicle (dense nucleus of a PI arrested oocyte) breakdown (GVBD) and the formation of the 'spindle' apparatus that will segregate homologous chromosomes. Entry into a second meiotic division occurs as MPF is reactivated when newly synthesised cyclin B2 associates with Cdc2. The degradation of cyclin B2 is blocked so that eggs arrest division, before they separate their replicated chromosomes, at a stage called metaphase two (MII). This meiotic arrest is maintained by production of a cytostatic factor (CSF) produced by the surrounding follicular cells (Masui and Market, 1971). An important component of CFS is Mos protein kinase that activates the mitogen-activated protein kinase (MAPK) pathway (Sagata *et al*, 1989). Only the oocytes arrested in the MII stage can be fertilised by sperm

and remain in this meiotic arrest until intracellular signals in the oocyte following fertilisation result in resumption of division.

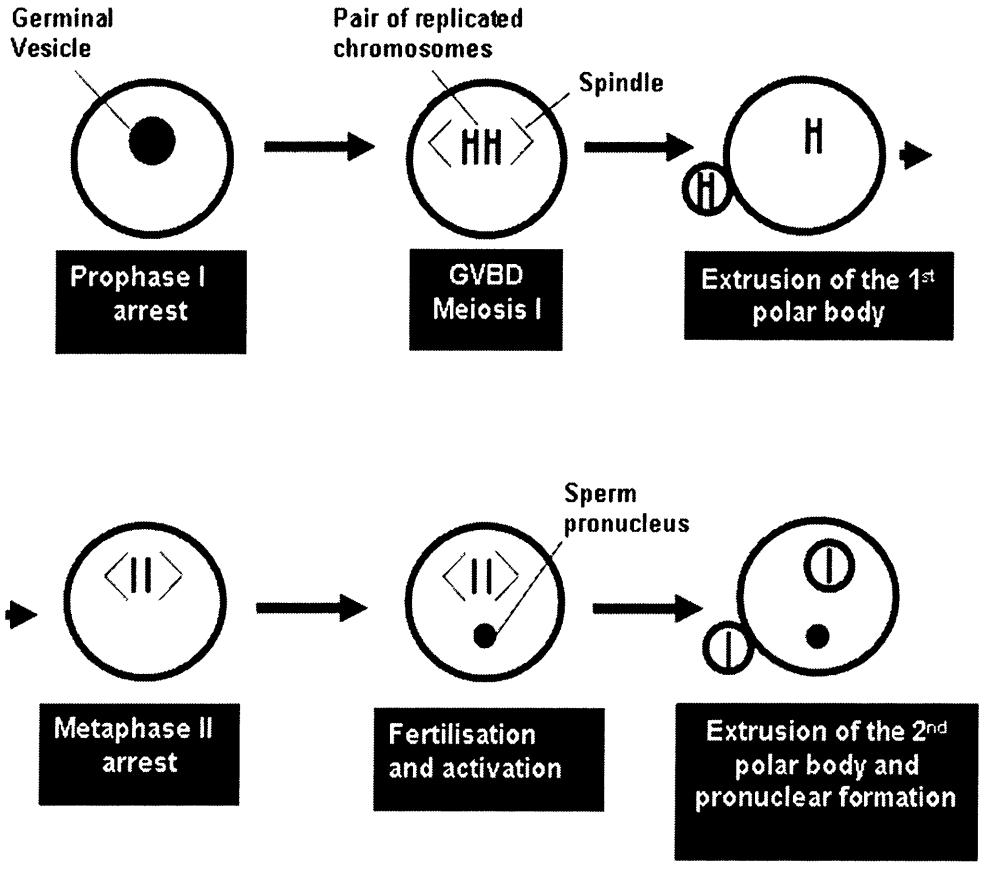

Figure 1.4 Schematic representation of the major events in oogenesis (see text for details).

1.2.2 Follicular development.

Maturation and growth of the oocyte depends on its association with the granulosa cells (follicular cells) that surround it. These granulosa somatic cells support oocyte growth and development and regulate the progression of meiosis. Likewise, oocytes promote granulosa cell proliferation, differentiation and function. Thus the communication between granulosa cells and oocytes is bidirectional and occurs throughout follicular development (Eppig, 1991)

Soon after oocytes enter meiosis the precursors to follicular somatic cells surround the oocyte in a single squamous layer to form primordial follicles. Release from meiosis I leads to proliferation of these cells, which change

shape to form several layers of cubiodal and columnar epithelium, the primary follicle. When the growing oocytes are surrounded by more than one layer of granulosa cells, the follicle is called a secondary follicle. It has been suggested that optimal development of primary and secondary follicles may require gonadotrophins (Cortvrindt *et al*, 1997). Following GBVD and release of the oocyte from PI meiotic arrest, follicular cells proliferate and a fluid-filled antrum forms within the substance of the follicular cell mass. This antrum continues to grow until the formation of a Graafian follicle. In a Graafian follicle the majority of the space within the follicle is occupied by the antrum and the oocyte is held within many granulosa cells. The formation of the follicular antrum divides the population of granulosa cells into two main groups; the cumulus cells that are associated with the oocyte and the mural granulosa cells lining the follicular wall. Although the cumulus cells loose their physical communication with the oocyte shortly before ovulation they continue to function beneficially for the oocyte by acting as a screen to remove abnormal sperm (Nottola *et al*, 1998) and by secreting hormones (such as progesterone) important for sperm capacitation and acrosome reaction (Tesarik *et al*, 1988). At ovulation, which is stimulated mainly by the follicle stimulating hormone (FSH) and oestrogen, the outer cell layers of the Graafian follicle break apart, releasing the oocyte and the follicular fluid into the uterine ducts (Rawlings *et al*, 2003).

1.2.3 Zona pellucida.

During follicular development, the oocyte also synthesises and secretes a thick oligosaccharide-based extracellular coat, the zona pellucida (ZP), which surrounds the plasma membrane of mammalian eggs. ZP is composed of three glycoproteins ZP1, ZP2 and ZP3. These proteins build a typical fibrogranular structure by noncovalent interactions presenting a complex and highly heterogenous mixture of asparagine and serine/threonine (O)-linked oligosaccharide side chains. It has been shown that the amino acid sequence of the ZP glycoproteins is highly conserved between different mammalian species. However, variable post-translational glycosylation and processing of

the polypeptide chains, as well as the variable assembling of the supra-molecular structure of the ZP matrix, lead to substantial differences of ZP structure and function between rodents (e.g. mouse) and domestic animals (e.g. pig), (Topfer-Petersen *et al*, 2000). Enzymatic removal of (O)-linked carbohydrates has been reported to abolish sperm-ZP binding. ZP3 appears to be the most important candidate to function as primary sperm receptor but also as inducer of the acrosome reaction (Flesch and Gadella, 2000). ZP has been shown to act as a block to polyspermy as the spermatozoon has to digest a path through this matrix by a combination of enzyme release and hypermotility before they can reach, bind and fuse with the plasma membrane of the oocyte. During this process the ZP also screen out biological in abnormal sperm (Morales *et al*, 1994).

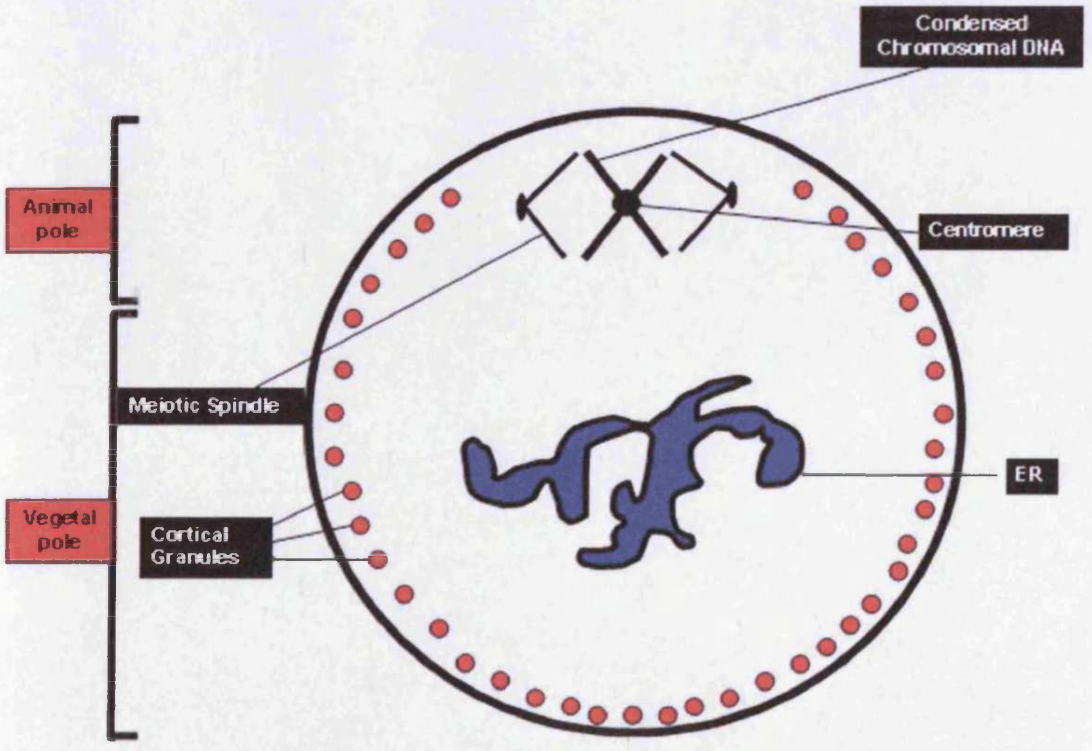

Figure 1.5 Schematic representation of a mature (MII arrested) oocyte, which contains numeral cortical granules in close proximity to the plasma membrane, ER and mitochondria and the meiotically arrested chromosomes.

1.2.4 Spermatogenesis and capacitation.

Spermatozoa are produced from male germ cells (spermatogonia) within the testis. The testes are a pair of elongated structure composed of branching seminiferous tubules embedded in stroma. There are three phases by which stem cells develop into mature spermatozoa; mitosis, meiosis and spermiogenesis (Kupker *et al*, 1998), (Figure 1.6). Stem cells (Type A spermatogonia) undergo mitosis to replace themselves and to produce cells that begin differentiation (Type B spermatogonia). In meiosis the diploid number of chromosomes present in spermatogonia is reduced to the haploid number present in mature spermatozoa. Spermatogonia have spherical or oval nuclei and rest on a basement membrane. The cells in prophase of the first meiotic division, the primary spermatocytes, go through the first meiotic division to become secondary spermatocytes. These cells quickly proceed through this stage and complete a second meiotic division. The products of the second meiotic division are called spermatids. Spermatids undergo a period of morphological development (spermiogenesis) in vesicles within overlying Sertoli cells. Sertoli cells are endocrine cells which are thought to provide structural and metabolic support to the developing sperm cells. During spermiogenesis the head (containing the nucleus and the acrosome), a midpiece (containing numerous mitochondria) and a long tail (containing a set of motile microtubules) are formed (Kupker *et al*, 1998), (Figure 1.7). Following release from the Sertoli cells the morphologically developed, but as yet non-functional spermatozoa, are transported out of the testis to an accessory storage organ, the epididymis, where they acquire their functional characteristics. Spermatozoa are then moved to the urethra, where they meet secretions (such as buffering salts, water, cholesterol, acid phosphatases and phospholipids) from various accessory glands before ejaculation to the female reproductive tract. These secretions provide essential nutrients to the ejaculated sperm.

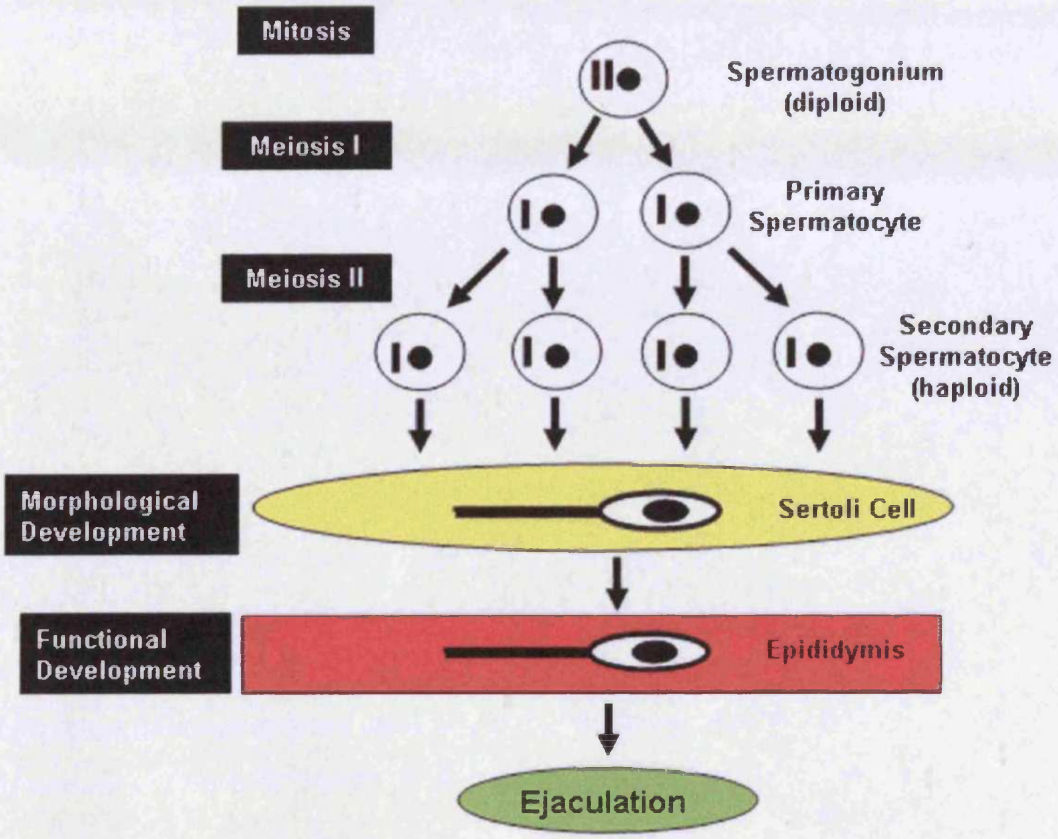

Figure 1.6 Schematic representation of genetic and morphological development of spermatozoa (see text for details).

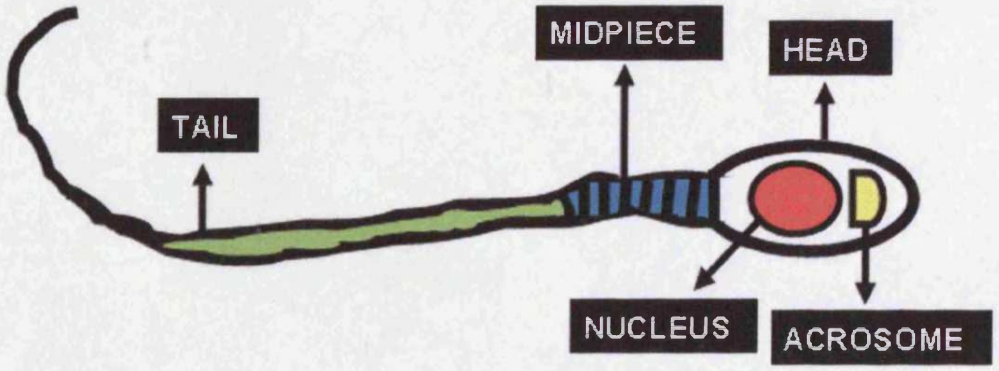

Figure 1.7 Schematic representation of a spermatozoon. The head contains a large dense nucleus (containing chromosomes) and the acrosome. The midpiece contains mitochondria which provide energy for sperm motility. The tail contains motile microtubules which are responsible for the sperm swimming movements. The tail is not shown to scale as it is ~15 times longer than the rest of the cell.

Mammalian spermatozoa are unable to fertilise the oocyte immediately after ejaculation. They require a period of incubation in the female reproductive tract where they undergo a series of biochemical modifications in order to acquire the ability to fertilise, a process defined as capacitation. During capacitation several intracellular changes occur, such as increases in intracellular Ca^{2+} and cAMP concentrations (Breitbart *et al*, 1985), cholesterol efflux, protein phosphorylation, increases in membrane fluidity and changes in swimming patterns and chemostatic motility (Breitbart, 2002). Tyrosine phosphorylation of several sperm proteins plays an important role in capacitation (Visconti and Kopf, 1998) and it has been previously demonstrated that inhibition of protein kinase A (PKA) can inhibit the capacitation of spermatozoa (Visconti *et al*, 1995). In humans reactive oxygen species (ROS) have been suggested to play an important role in capacitation-related phosphorylation of several proteins. In addition Ca^{2+} and HCO^{-3} have been suggested to play an important role in the activation of adenyl cyclase in sperm (Visconti *et al*, 1995). There is no direct evidence for a specific ligand which induces the signal transduction cascade leading to protein tyrosine phosphorylation during capacitation. However, a role for epidermal growth factor (EGF) has been suggested, as its receptor tyrosine kinase EGFR has been identified in the head of bovine sperm (Lax *et al*, 1994). Activation of EGFR leads to two essential processes for the progress of capacitation, tyrosine phosphorylation and activation of PLCγ (Spungin *et al*, 1995).

1.2.5 Attachment, acrosome reaction and membrane fusion.

Attachment of the spermatozoon to the ZP is one of the most critical steps in mammalian fertilisation. Numerous sperm proteins with high binding capacity and different zona adhesion molecules have been identified. There are also different types of ligands that are present in the sperm plasma membrane (primary sperm ligands). Several mechanisms of species-specific sperm-egg recognition have been described, such as α-1,4-galactosil transferase that binds to the oligosaccharide residues of mouse ZP3 (Miller *et al*, 1993). In rabbits, recognition is mediated by sperm autoantigens such as Sp17 found

also in human and mice testis (Richardson *et al*, 1994). In rats, the antigen 2B1 has been identified as the primary zona ligand (Jones and Jansen, 1993). In addition, a group of sperm proteins of low MW (~15kDa) termed spermadhesins has been described as zona ligands. These proteins are produced in the epididymis and in the seminal vesicles and adhere to the sperm plasma membrane during its passage to ejaculation. It has been shown that these proteins bind strongly to the ZP (Toepfer-Petersen *et al*, 1993; Dostalova *et al*, 1995). Interaction of all these molecules with the egg ZP contributes to the gamete interaction, leading to the second step of fertilisation, the induction of the acrosome reaction.

The acrosome reaction is the key event in fertilisation. It is the process which enables the sperm to penetrate the ZP. During the acrosome reaction the sperm undergoes the regulated exocytosis of its single secretory granule, the acrosome. The acrosome is a relatively large, Golgi-derived organelle and although it is surrounded by a continuous membrane, it is usually described as consisting of an 'inner' and 'outer' membrane; the former overlies the nucleus and the latter underlies the plasma membrane. The acrosome reaction involves multiple fusions between the outer acrosomal membrane and plasma membrane at the anterior region of the sperm head, extensive formation of hybrid membrane vesicles and exposure of the contents of inner acrosomal membrane. Only sperm that have completed the acrosome reaction can penetrate the ZP and fuse with the oocyte plasma membrane. A number of physiological and non-physiological inducers of the acrosome reaction have been reported including progesterone (Murase and Roldan, 1996), follicular fluid and cumulus cell secretions containing glycosaminoglycans and neoglycoproteins (Abou-Haila and Tulsiani, 2000). Progesterone mediated induction of the acrosome reaction can be blocked by tyrosine kinase inhibitors; whereas progesterone itself stimulates protein phosphorylation, suggesting that progesterone mediated signalling is transduced via protein tyrosine phosphorylation (Bonaccorsi *et al*, 1995). However, the natural agonist that induces the acrosome reaction is the ZP3. The ability of mouse ZP3 (mZP3) to induce the acrosome reaction depends upon glycan moieties as well as on the polypeptide backbone of the molecule (Abou-Haila and Tulsiani, 2000). Stimulation of ZP3 by sperm activates G

proteins of the $G\alpha_i$ family, which induce Ca^{2+} influx by stimulation of ion channels (Abou-Haila and Tulsiani, 2000). It has also been reported that activation of PLCδ4 is essential for the normal progression of acrosome reaction (Fukami *et al*, 2001). Stimulation of ZP by sperm also leads to depolarisation of sperm plasma membrane and rise in internal sperm pH that is also associated with the triggering of the acrosome reaction. Cholesterol efflux during capacitation of human spermatozoa can also cause the elevation in the internal sperm pH (Cross and Razy-Faulkner, 1997). Acrosome-reacted sperm remain bound to the ZP, apparently by binding to ZP2 (Bleil *et al*, 1988). Penetration of the ZP is achieved by a combination of sperm motility and enzymatic hydrolysis. There is evidence that an acrosomal serine protease called acrosin plays an important role in the catalysis of the latter (Yamagata *et al*, 1998).

A sperm having penetrated the ZP, reaches the perivitelline space where it will meet with the oolemma. A ZP penetrated sperm cell initially binds with the tip of its head to the oolemma. Cyritestin and fertilin-β are two candidate adhesion molecules for this binding step. Cyritestin and fertilin-β are members of the ADAM family of transmembrane proteins and have been reported to be associated with the inner acrosomal membrane of mouse sperm. Cyritestin and fertilin-β are thought to interact with an integrin on the egg plasma membrane, as sperm-oocyte fusion can be blocked by disintegrin domains from fertilin-β and cyritestin (Yuan *et al*, 1997). However, these findings are not consistent with the results of another study where cyritestin and fertilin-β knockout sperm from mice were still able to fuse at 50% of the wild type rate (Nishimura *et al*, 2001). A further member of the ADAM family, fertilin-α has been implicated in the fusion of the sperm with the oocyte plasma membrane; however its exact role remains to be elucidated (Houvila *et al*, 1996). Results of several studies indicate that CD9 in the oocyte plasma membrane has a vital function in sperm oocyte fusion in mice (Miyado *et al*, 2000). CD9 is a member of the tetraspan superfamily of integral plasma membrane proteins that associate with each other, as well as with a subset of β1 integrins (Hemler, 1998). It is believed that CD9 in the plasma membrane is associated with integrin $\alpha 6\beta 1$ to which fertilin-β binds. Thus CD9 may regulate the

interactions between integrin and fertilin that are ultimately responsible for sperm-egg fusion (Chen *et al*, 1999).

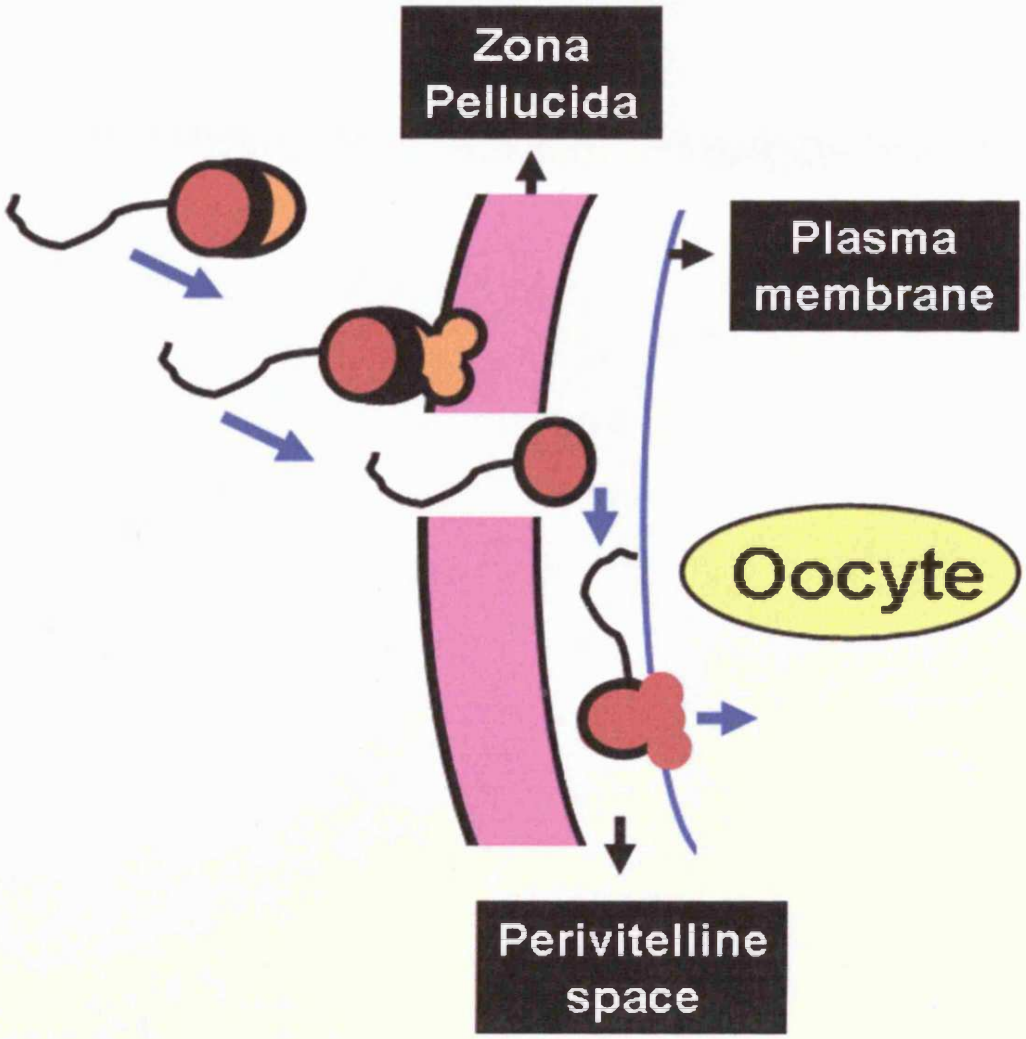

Figure 1.8 Schematic representation of sequential events during mammalian fertilization. Capacitated sperm cell binds to the egg ZP and this binding is capable of triggering the acrosome reaction. Hydrolytic enzymes secreted from the acrosome degrade the ZP and sperm cell penetrates the ZP entering the perivitelline space. After binding of the sperm cell to the oolemma, sperm cell fuses with the oocyte and is subsequently incorporated to the oocyte (Figure based on reports reviewed in Abou-Haila and Tulsiani, 2000; Flesch and Gadella, 2000).

1.2.6 Zygotic development.

To prevent polyspermy and ensure that each oocyte is fertilised by only one sperm, following sperm/oocyte fusion, a reaction between cortical granules with the oolemma occurs, in a process called cortical granule exocytosis (CGE) (Cran *et al*, 1988). The cortical granules contain enzymes that facilitate the cross-linking of oligosaccharides in the ZP, inhibiting further sperm from penetration by removing the sperm-specific binding sites that facilitate the acrosome reaction.

Following these events a series of complex biochemical reactions occur within the ooplasm leading to the activation of the oocyte and its transmutation into a developing embryo. It is widely accepted that these events are mediated by a distinct set of Ca^{2+} oscillations that occur in the oocyte following the sperm-oocyte fusion reaction (Ducibella *et al*, 2002), which last for several hours until the pronuclei is formed (Carroll, 2001). After sperm fusion, meiosis resumes from MII arrest and then follows the expulsion of one of the daughter nuclei as a second polar body, which like the first one is small, non-proliferative, and soon after degenerates. Following the polar body extrusion the remaining set of maternal chromosomes decondenses and is surrounded by a nuclear membrane, forming the pronucleus. This pronucleus moves to the middle of the cell, along with the pronucleus of the sperm head, where the chromosomes replicate and condense and the zygote undergoes the first mitotic division of development (Carroll, 2001). The zygote continues to undergo mitosis by dividing continually until a ball of 8-50 cells is developed known as morula. At this point a cavity within the cell mass transforms the embryo into a hollow sphere; the blastocyst. The blastocyst consists of an outer layer, the trophoblast, and an inner cluster of cells, that forms the foetus. The outer layer of the blastocyst develops later into the chorion, which supports the developing foetus during the prenatal stage (Lu *et al*, 2001; Piatrowska and Zerniska-Goetz, 2001). At this point the blastocyst has the same size as the original oocyte. It is still free within the female reproductive tract and hence is not accessible to nutrients. The blastocyst cavity continues to expand until it is fully formed and adheres to the uterine wall. In less than a day, the blastocyst becomes fully embedded in the vascular endometrium

continuing development and differentiation, and deriving nourishment and benefiting from waste removal via the maternal blood supply to the womb.

It is notable that the polarity of the blastocyst is related to the original sperm entry site. The distinctive Ca^{2+} oscillations in the fertilised oocyte begin at the sperm fusion site and spread rapidly throughout the cytoplasm (Degucchi *et al*, 2000). The first polar body is extruded opposite this site (Piatrowska and Zerniska-Goetz, 2001). Thus cell fate may be predetermined from the first mitosis of the fertilised zygote, dependant on the sperm-mediated fusion event in the fertilised oocyte (Lu *et al*, 2001; Piatrowska and Zerniska-Goetz, 2001).

1.2.7 Calcium oscillations during mammalian fertilisation.

As discussed above, and in all species studied, one of the earliest events of oocyte activation is an increase in the level of intracellular Ca^{2+} concentration. In most non-mammalian species such as Sea Urchin and Xenopus, the Ca^{2+} increase is a single rise but in mammals and some marine invertebrates the Ca^{2+} increase has the form of repetitive Ca^{2+} spikes (Ca^{2+} oscillations) of a constant amplitude, which continue at regular frequency for several hours after sperm-oocyte fusion (Cuthbertson and Cobbold, 1985; Swann, 1990; Miyazaki *et al*, 1993), (Figure 1.9). The frequency and duration of Ca^{2+} oscillations varies between species (Stricker, 1999). This increase in Ca^{2+} concentration is necessary and sufficient for the completion of all the events of egg activation (Schultz and Kopf, 1995) such as membrane hyperpolarisation, CGE to block polyspermy (Cran *et al*, 1988), resumption of meiosis through Ca^{2+}-dependent destruction of cyclin B (Hyslop *et al*, 2004) and pronuclear formation.

Several lines of evidence implicate the 1,4,5-trisphosphate ($InsP_3$) signaling pathway as the origin of the Ca^{2+} signals in mammalian eggs. The essential role of $InsP_3$ and the $InsP_3R$ in fertilisation has been illustrated by studies in mouse and hamster eggs, where Ca^{2+} oscillations at fertilisation can be inhibited by microinjection of antibodies that inhibit $InsP_3R$ (Miyazaki *et al*, 1992), or by downregulation of $InsP_3Rs$ (Brind *et al*, 2000; Jellerette *et al*, 2000). In addition, it has been shown that sustained injection of $InsP_3$, or repeated photorelease of caged $InsP_3$, or microinjection of the $InsP_3$ analogue adenophostin can all lead to a series of Ca^{2+} oscillations in eggs (Swann, 1994, Jones and Nixon 2000, Wu *et al*, 2001). Liberated $InsP_3$ causes Ca^{2+} release by binding to $InsP_3R$ located on the endoplasmic reticulum of eggs and oocytes (Rice *et al*, 2000, Wu *et al*, 2001). Hence, in mammalian eggs, $InsP_3$ is both necessary and sufficient to explain the Ca^{2+} oscillations observed at fertilisation. The ability of the oocyte to release Ca^{2+} is also cell-cycle dependent, displaying significant sensitivity during metaphase-II arrest the stage at which the oocyte is naturally fertilised (Marangos *et al*, 2003).

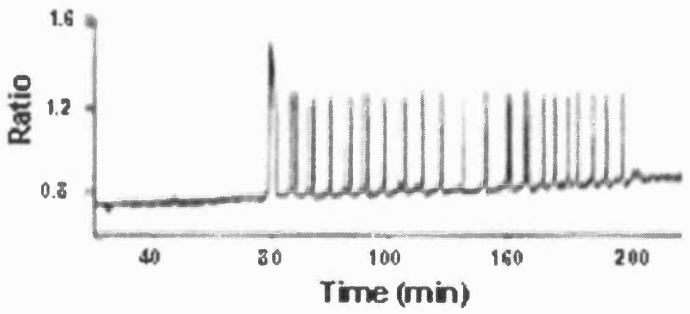

Figure 1.9 Ca^{2+}-dependant fluorescence trace showing oscillations in intracellular Ca^{2+} following *in vitro* fertilization in a mouse egg. There is a latent period between sperm-egg fusion and the beginning of Ca^{2+} oscillations (from Saunders *et al*, 2002).

1.2.8 The generation of Ca^{2+} oscillations during fertilisation.

Several hypotheses have been proposed to explain the generation of Ca^{2+} oscillations in fertilised oocytes. The earliest hypothesis known as the the 'Ca^{2+} bomb' hypothesis proposed that upon sperm-oocyte fusion, Ca^{2+} from the sperm cytosol entered the oocyte and triggered Ca^{2+}-induced Ca^{2+} release (Jaffe, 1983). However, although Ca^{2+} or its ionophore A23187 are able to induce Ca^{2+} release from intracellular stores into the oocyte (Steinhardt *et al*, 1974; Fulton and Whittingham, 1978), the [Ca^{2+}] within the sperm was not sufficient to trigger Ca^{2+} release. In particular, this hypothesis could not explain the several minutes delay between sperm-oocyte fusion and the initiation of Ca^{2+} oscillations in mammalian oocytes (Lawrence *et al*, 1997).

Similar to the 'Ca^{2+} bomb' hypothesis was the 'conduit' hypothesis, which proposed that fusion of the sperm head with the oolemma allowed Ca^{2+} influx into the oocyte, thereby overloading the Ca^{2+} stores and subsequently causing Ca^{2+} release (Jaffe, 1991). However, observations that repetitive Ca^{2+} transients during fertilisation proceeded unaltered in the absence of extracelllular Ca^{2+}, suggested that Ca^{2+} influx was not necessary to trigger Ca^{2+} oscillations during fertilisation in mammals (Swann, 1996; Jones *et al*, 1998a).

The 'Contact' hypothesis (Figure 1.10) suggested that upon sperm-oocyte membrane contact, receptor-ligand interaction on the surface of the gametes led to a series of intracellular signaling events that initiated Ca^{2+} release in the oocyte. Initially activation of PLCβ was proposed to be implicated in the initiation of Ca^{2+} release in fertilised oocytes, based on injection experiments of activators and inhibitors of α_q subunits of PLC-associated G-protein (Miyazaki, 1988; Fissore and Robl, 1994). However inhibitory antibodies to $G\alpha_q$ proteins failed to block fertilisation-induced Ca^{2+} oscillations when injected into oocytes prior to *in vitro* fertilisation (Williams *et al*, 1998), suggesting that this pathway did not contribute to the initiation of Ca^{2+} oscillations in mammalian fertilisation. A second signaling cascade proposed to be activated by the sperm-oocyte interaction was that mediated by protein tyrosine kinases (PTKs). It was thought that the Src-family of PTKs (SFKs) may activate PLCγ (Carroll *et al*, 1997; Shearer *et al*, 1999; Sato *et al*, 2000), thereby triggering

$InsP_3$-mediated Ca^{2+} release. Inhibition of PLCγ activation by overexpression of SH2 domains prevented the sperm-mediated Ca^{2+} rise in Sea Urchin eggs (Carroll *et al*, 1997). However when these experiments were performed in mammalian oocytes, overexpression of SH2 domains was incapable of inhibiting sperm-mediated Ca^{2+} release (Mehlmann *et al*, 1998; Runft *et al*, 1999). In addition, injection of recombinant PLCγ (Mehlmann *et al*, 2001) failed to show the involvement of this pathway in triggering the Ca^{2+} oscillations in mammalian oocytes.

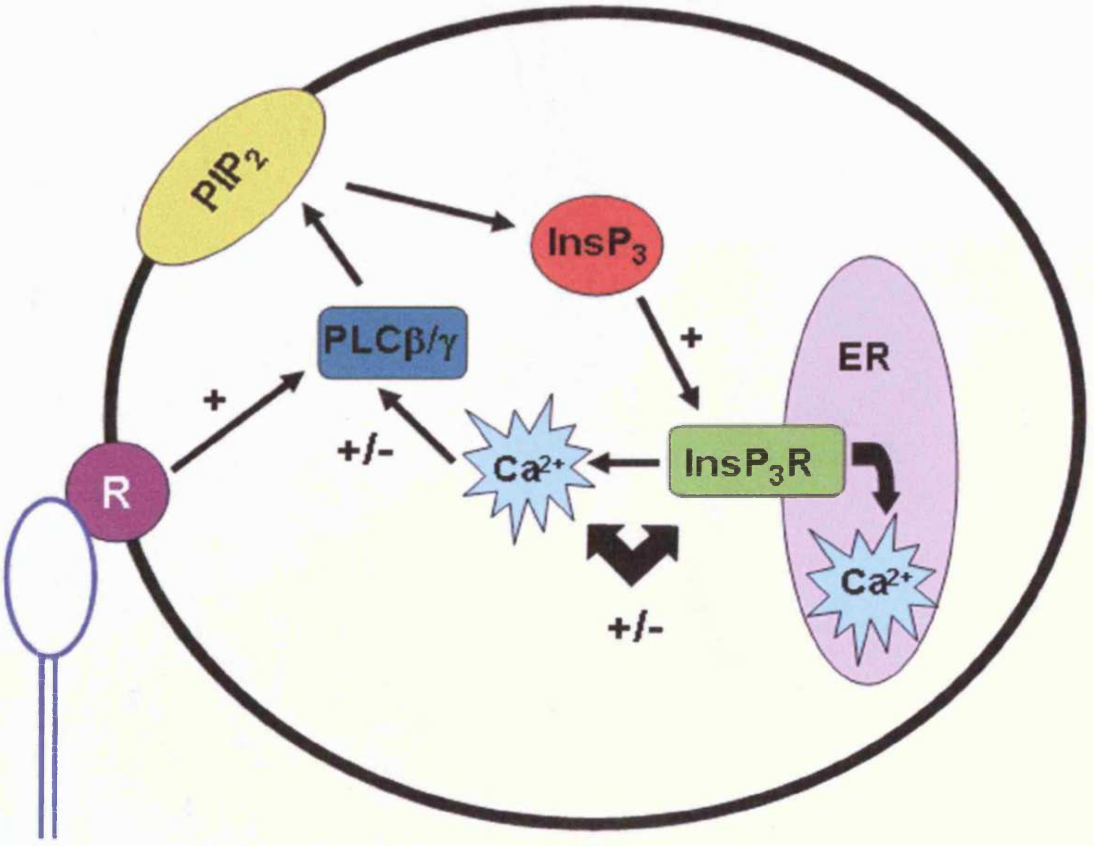

Figure 1.10 Schematic representation of the 'Contact' hypothesis. R is a receptor; other abbreviations are defined in the text.

1.2.9 The 'Sperm Factor' hypothesis.

The 'Sperm Factor' hypothesis (Figure 1.12) has recently emerged to explain the genesis of Ca^{2+} oscillations in fertilised oocytes. This hypothesis proposed that upon sperm-oocyte fusion a sperm factor (SF) was delivered into the ooplasm, capable of activating the 1,4,5-trisphosphate ($InsP_3$) signaling pathway and the subsequent Ca^{2+} oscillations in fertilised oocytes. Experimental evidence for this hypothesis came from the demonstration that injection of sperm extracts into mammalian eggs was able to trigger Ca^{2+} oscillations indistinguishable from those seen at *in vitro* fertilisation (Swann, 1990; Stricker, 1997). Additional support for this hypothesis came from the clinical technique intra-cytoplasmic sperm injection (ICSI), (Palermo *et al*, 1992), which avoids sperm-oocyte membrane contact by direct injection of intact sperm into the ooplasm. Injection of whole sperm by ICSI was able to lead to normal activation and development of the oocytes (Tesarik *et al*, 1994; Nakano *et al*, 1997). This hypothesis was also consistent with the latent period of several minutes between sperm oocyte contact and the initiation of Ca^{2+} oscillations in the oocytes (Whitaker *et al*, 1989).

1.2.10 The 'Sperm Factor' is a novel phospholipase C isoform.

Early candidates for the sperm factor were believed to be small molecules such as $InsP_3$ (Tosti *et al*, 1993), NO (Kuo *et al*, 2000) or $NAADP^+$ (Lim *et al*, 2001). Although these molecules appeared to have the ability of generating Ca^{2+} release from intracellular stores in non-mammalian species, none of these can fully mimic the response seen at *in vitro* fertilisation in mammalian oocytes (Swann, 1994), suggesting that these molecules might play an important role in the propagation of Ca^{2+} oscillations during mammalian fertilisation but none of them appears to have an oscillogenic activity itself.

More recent studies involving various fractionation techniques suggested that the sperm factor was a protein (Swann, 1996; Stricker, 1997; Wu *et al*, 1998) and is ~30-100kDa in size (Rice *et al*, 2000; Parrington *et al*, 2002). Different proteins have been hypothesised to be the sperm factor, involving a 33kDa protein termed 'oscillin' (Parrington *et al*, 1996) and a truncated form of the *kit*

receptor (Sette *et al*, 1997). However none of these proteins is capable of generating fertilisation-like Ca^{2+} responses when injected into mammalian oocytes (Wu *et al* 1998; Wolosker *et al*, 1998; Wolny *et al*, 1999).

In vitro PLC assays using sperm extracts showed that these extracts possessed a PLC activity, at least 100 times greater than that present in other tissues known to express several PLC isoforms (Rice *et al*, 2000). Uniquely the PLC activity of the sperm extracts was high even at the basal Ca^{2+} levels (~0.1μM), typical of mammalian eggs at the time of fertilisation. These observations supported the idea that the SF may be a PLC isoform itself (Figure 1.11)

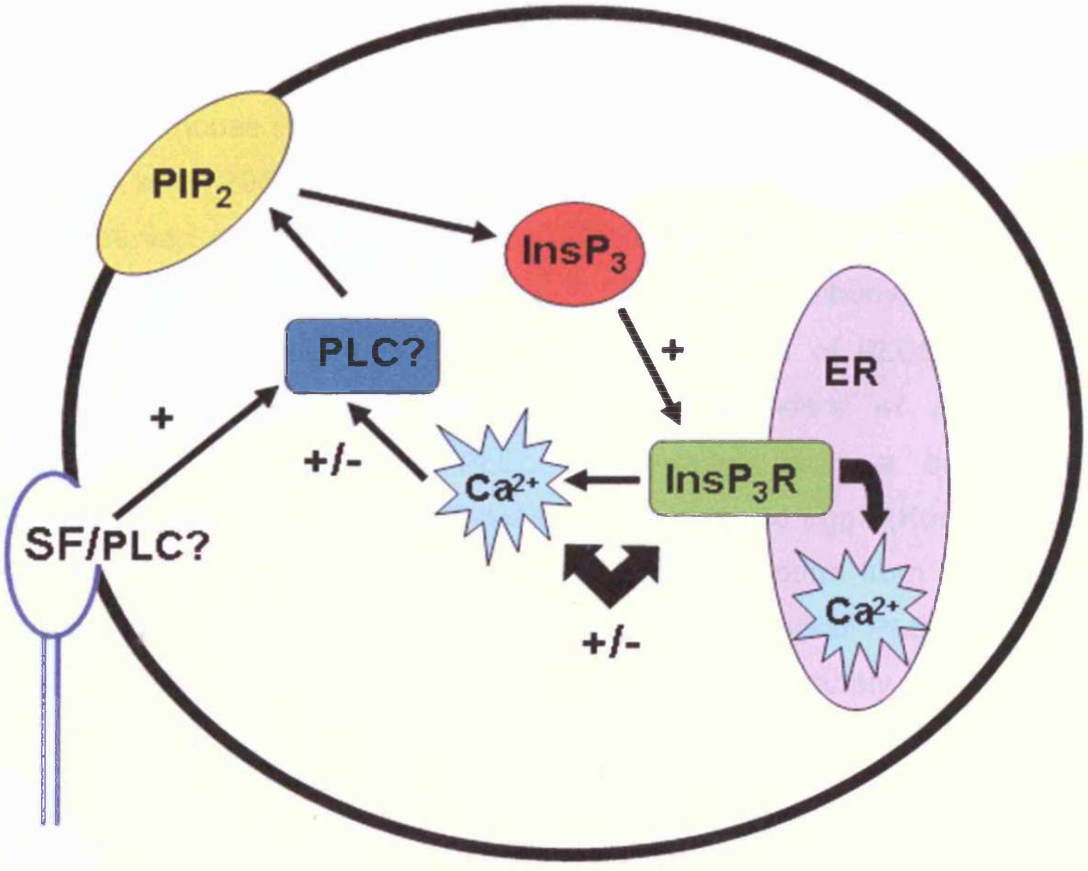

Figure 1.11 Schematic representation of the idea that the sperm factor (SF) is a PLC isoform. Following membrane fusion entry of the sperm factor, which is a PLC isoform itself, leads to hydrolysis of $PtdInsP_2$ and production of $InsP_3$ inducing Ca^{2+} release from the ER.

Several PLC isoforms have been shown to be expressed in mammalian sperm (Fukami, 2001). However microinjection of recombinant proteins corresponding to most of the known isoforms expressed in sperm failed to initiate Ca^{2+} oscillations (Jones *et al*, 2000; Parrington *et al*, 2002; Runft *et al*,

2002) or did so at non-physiological concentrations (Mehlmann *et al*, 2001). Furthermore, chromatographic fractionation of sperm extracts revealed none of the known PLC isoforms present in the fraction with the Ca^{2+} oscillogenic activity (Wu *et al*, 2001; Parrington *et al*, 2002). All these suggested that if the sperm factor was a PLC it had to be a novel isoform.

A search of a mouse expressed sequence tag (EST) database revealed potentially novel PLC sequences derived from testes. Using a mouse spermatid cDNA library and primers based on the EST sequence two-step RACE PCR amplification, produced a full length clone of a novel PLC, termed PLCζ (Saunders *et al*, 2002). PLCζ was smaller than other PLC isoforms and its expression, tested by a Northern blot screen of several tissues, showed it to be exclusive to testis. Microinjection of complementary RNA (cRNA) encoding the mouse (Saunders *et al*, 2002), human, and cynomolgus monkey PLCζ (Cox *et al*, 2002) into mouse eggs, triggered Ca^{2+} oscillations similar to those observed at fertilization. These Ca^{2+} oscillations were abolished when PLCζ was immunodepleted, by an anti-PLCζ specific antibody, from native sperm extracts (Saunders *et al*, 2002). The presence of PLCζ was also demonstrated in boar and hamster sperm (Saunders *et al*, 2002). Microinjection of recombinant PLCζ, synthesised using a baculovirus expression system triggered Ca^{2+} oscillations in mouse eggs (Kouchi *et al*, 2004). In addition another recent study reported that sperm from transgenic mice expressing short hairpin RNAs, had reduced amounts of PLCζ and Ca^{2+} oscillations following *in vitro* fertilisation terminated prematurely (Knott *et al.*, 2005). All this accumulated evidence confirmed the sperm factor to be PLCζ.

1.3 The Phosphoinositide-specific Phospholipase C family.

Mammalian phosphoinositide-specific phospholipase C (PLC) is a ubiquitous family of enzymes that play a central role in activating intracellular signal transduction pathways during early key events in the regulation of various cell functions (Katan, 1998; Rebecchi and Pentyala, 2000; Rhee, 2001). As described in section 1.1.4 these enzymes catalyse the hydrolysis of PtdIns(4,5)P_2 to generate two second messengers InsP_3 and DAG. Fourteen distinct PLC isoforms have been identified in mammals, grouped into six distinct classes, based on their domain structure and regulatory mechanisms: β (1-4), γ (1,2), δ (1-4), ε, ζ, and η (1,2) (Rhee, 2001; Saunders *et al*, 2002; Hwang *et al*, 2005; Nakahara *et al*, 2005). The existence of distinct regulatory domains in PLC isoforms renders them susceptible to different modes of activation and participation in different signalling pathways (Rhee, 2001). The domain organisation of the six types of PLC isozymes is shown in Figure 1.12.

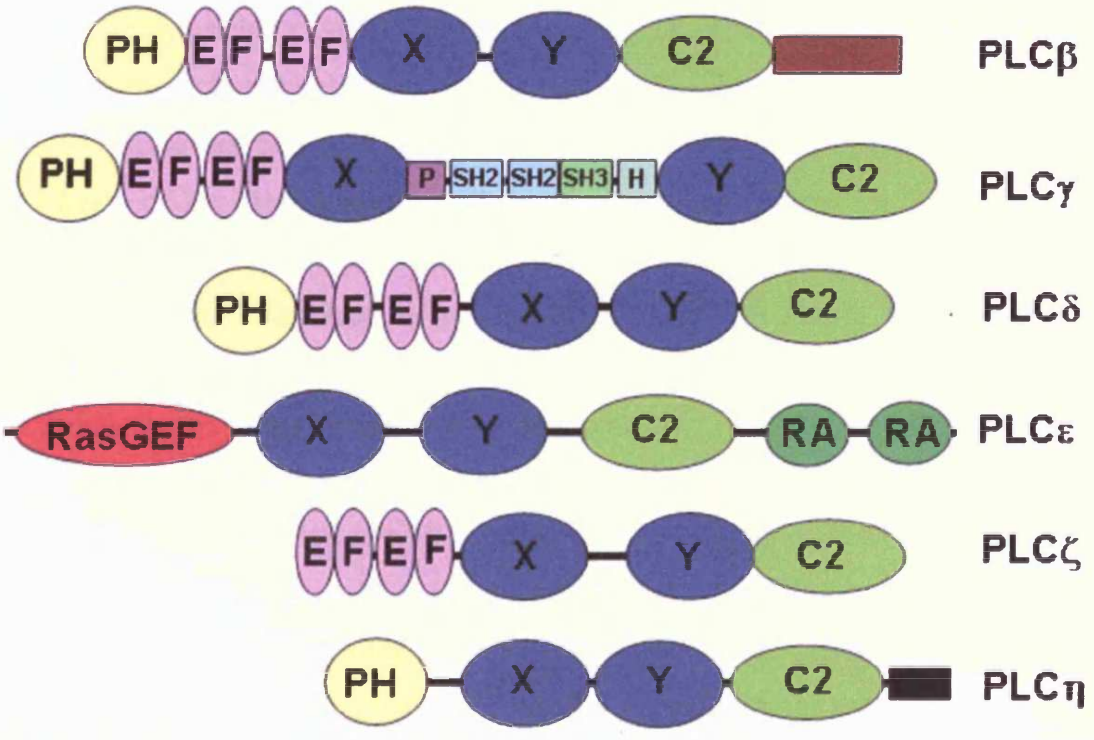

Figure 1.12 Schematic representation of domain organisation of the known PLC isoform families, illustrating the PH domain, the EF-hands, the X and Y catalytic domains, the C2 domain, the SH2 and SH3 domains, the RA domains and the RasGEF domain (illustration not to scale), (for full domain names see text).

1.3.1 Pleckstrin Homology domain.

All PLC isoforms except PLCε and PLCζ possess a Pleckstrin Homology (PH) domain. PH domains are well defined structural modules of about ~120 amino acid residues and have been identified in more than 100 different proteins. The majority of the proteins that contain PH domain require membrane association for their function. Despite the limited sequence similarity of different PH domains their three-dimensional structure is remarkably similar. The PH domain of PLCδ1 consists of seven antiparallel β strands in a barrel-like structure with one half of the barrel consisting of a three stranded sheet, another of a four stranded sheet and a bottom formed by C-terminal alpha helix (Figure 1.13), (Williams, 1999). Structural analysis of the PH domain of PLCδ1 has revealed specific $InsP_3$/PtdIns(4,5)P_2 binding residues within the protein structure (Ferguson *et al*, 1995; Essen *et al*, 1996). This is supported from other studies that demonstrated that the PH domain of PLCδ1 binds PtdIns(4,5)P_2 and $InsP_3$ with high affinity and this binding is directly related to enzyme activity (Lomasney *et al*, 1996; Yagisawa *et al*, 1998). Nevertheless the basic amino acids (Lys30, Lys32, Arg40 and Lys57) located in the inositol phosphate binding pocket of the PH domain of PLCδ1 are not well conserved in the PH domains of PLCβ and PLCγ (Rhee, 2001). This could explain the high affinity of the PH domain of PLCγ isozymes for PtdIns(3,4,5)P_3 and not for PtdIns(4,5)P_2. PH domains of PLCβ isozymes bind strongly to membranes regardless of the presence of phosphoinositides (Rebecchi and Pentyala 2000). The PH domain of PLCβ1 has recently been shown to specifically bind to PtdIns(3)P and this interaction appears to be responsible for the membrane recruitment of this enzyme in cells in which PtdIns 3-kinase is activated (Rhee, 2001). In addition the PH domains of PLCβ2 and PLCβ3 have been shown to bind the G-protein subunit Gβγ (Wang *et al*, 2000), whereas $G\alpha_q$ binds the PH domains of PLCβ1 and PLCβ2 (Wang *et al*, 1999), highlighting a role for the PH domain of some PLCs in determining the specificity of interaction with activated G-protein subunits. The most recently identified PLC isoform, PLCη (Hwang *et al*, 2005) also possesses a PH domain, but little is known about its structural and functional characteristics.

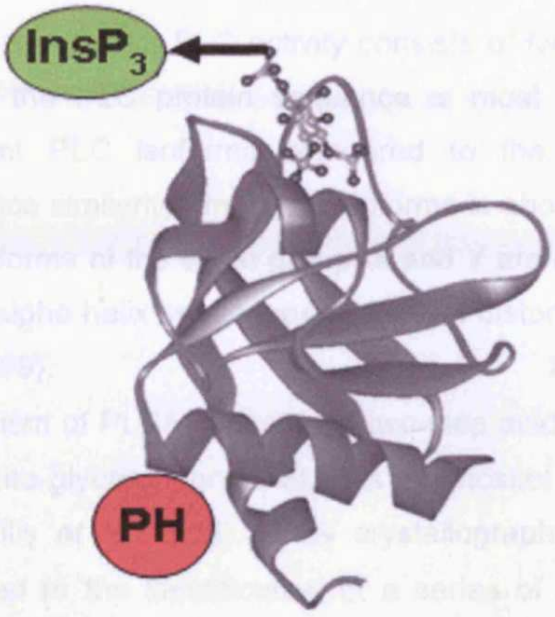

Figure 1.13 A schematic representation of the PLCδ1 PH domain showing the $InsP_3$ binding pocket (adapted from Rebecchi and Pentyala, 2000).

1.3.2 Elongation Factor hand domains.

The Elongation Factor (EF) hand domains, consisting of four helix-loop-helix motifs are divided in two pairwise lobes. EF hands occur in pairs because one loop stabilises the other (Williams, 1999). These domains form a flexible link between the X/Y catalytic domain and the PH domain. In PLCδ1, EF hands possess Ca^{2+} binding residues (Essen *et al*, 1996), which have also been identified in various other calcium binding proteins such as calmodulin. In PLCδ1, the first pair of EF hands has been shown to be essential for an efficient interaction of the PH domain with $PtdIns(4,5)P_2$ in the plasma membrane (Yamamoto *et al*, 1999). The second pair of EF hands interacts with the C2 domain probably stabilising enzyme folding, since truncations of the second EF hand in PLCγ and PLCδ1 rendered the enzymes inactive (Emori *et al*, 1989; Nakashima *et al*, 1995). In PLCδ1, point mutations of amino acid residues Asp-153, Asp-157 and Glu-164, within the EF hand domains, appeared to be very sensitive to the activity of the enzyme, affecting its core structure (Nakashima *et al*, 1995).

1.3.3 XY catalytic domain.

The catalytic core necessary for PLC activity consists of two domains, the X and Y. This part of the PLC protein sequence is most highly conserved between the different PLC isoforms compared to the other regulatory domains. The sequence similarity among all isoforms is about 60%, but much higher among the isoforms of the same group. X and Y are organised in eight repetitive beta sheet/alpha helix sequences, forming a distorted barrel (Ellis *et al*, 1998; Williams, 1999).

The catalytic mechanism of PLCδ1 employs a two-step acid/base catalysis of the inositol 1-phosphate-glycerol bond that links the inositol headgroup to the DAG lipid anchor (Ellis *et al*, 1998). X-ray crystallography of recombinant PLCδ1 protein has led to the identification of a series of residues that are essential for catalysis, and are highly conserved between PLC isozymes. These residues include His-311, His-356, Glu-341, Asp-343, and Glu-390 (Essen *et al*, 1997). This suggests that all PLC isozymes employ a similar mechanism of $PtdInsP_2$ catalysis, and the differences in enzyme kinetics are likely to be due to the influence of other regulatory domains on the X/Y barrel. Other critical residues in the active site for enzyme function are those involved in the binding of the Ca^{2+} ion. In PLCδ1, Ca^{2+} binding is co-ordinated by the side chains of Asn-312, Glu-341, Asp-343 and Glu-390 (Rebecchi and Pentyala, 2000). Although other domains in PLC have the potential to bind Ca^{2+}, the single catalytic Ca^{2+} ion seems to be most critical for the enzyme function. This is supported by studies of a PLC-δ1 mutant missing other calcium binding sites located in the C2 domain and it had the same activation constant (K_{act}) for Ca^{2+} (~1.4 μM) as the wild-type PLC (Grobler and Hurley, 1998). Surrounding the active site is a ridge of hydrophobic residues, Leu-320, Tyr-358, Phe-360, Leu-529, and Trp-555 (Essen *et al*, 1996). It has been proposed that this ridge serves to promote the insertion of the X/Y barrel into the membrane surface, a process required for full enzymatic activity. This is supported by studies of PLC-β1 -β2, -γ1, and -δ1 in which raising the surface pressure of phospholipid monolayers to levels equivalent to, or slightly beyond, the packing densities found in membrane bilayers, profoundly inhibited the catalytic activity (Boguslavsky *et al*, 1994; James *et al*, 1997).

A network of hydrogen bonds and salt-bridges orientates the PtdIns(4,5)P_2 within the active site by its phosphate ring substituents at inositol positions 4 and 5, while hydrolysis takes place at position 1. Lys-438 and Lys-440, interact with the phosphomonoester at position 4 of the inositol-(4,5)-diphosphate ring and Ser-522 and Arg-549 interact with the phosphomonoester at position 5. These residues are highly conserved between the PLCβ, -γ and -δ isozymes (Rebecchi and Pentyala, 2000). Arg-549 not only orients the PtdIns(4,5)P_2 in place but also acts as a substrate determiner. Amino acid substitutions of this positively charged amino acid to progressively non-polar amino acids changed the substrate preference from to PtdIns(4,5)P_2 to PtdIns (Wang *et al*, 1996).

There is an interruption between strands four and five of the catalytic domain, which gives rise to a large loop, the XY linker sequence, which differs considerably between PLC isozymes. In the PLCδ group, the XY linker is relatively short (46 amino acids). Proteolysis of this highly negatively charged region leads to activation of the enzyme (Williams, 1999; Rebecchi and Pentyala, 2000). Interactions of different cellular factors with this sequence have not been elucidated and there are possibilities of regulation that have not been explored. The XY linker sequence of PLCβ and PLCε is about 110 and 190 residues long respectively. PLC γ possesses additional developed regulatory domains between X and Y domains (Figure 1.12), and their functions are discussed in section 1.3.6.

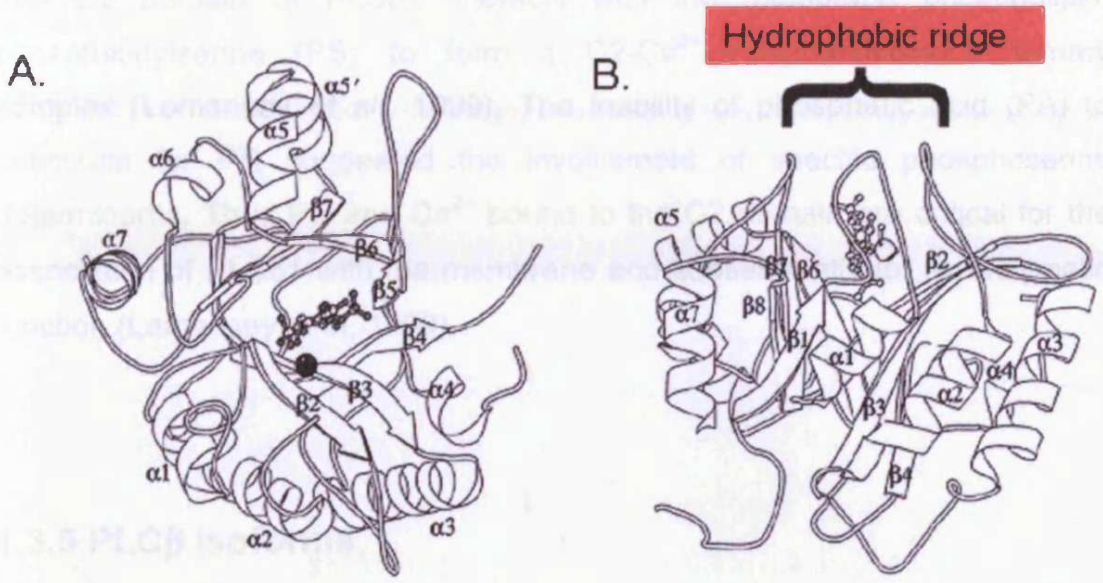

Figure 1.14 A. Ribbon representation of the PLCδ1 catalytic domain/$InsP_3$ complex. $InsP_3$ is shown as a ball and stick model. A bound Ca^{2+} ion is shown as a black sphere. **B.** View of the active site rotated by approximately 90°. The position of the hydrophobic ridge, which penetrates the membrane, is seen more clearly with this orientation (adapted from Ellis *et al*, 1998).

1.3.4 PKC-homology type II domain.

The PKC-homology type II (C2) domain comprises ~120 amino acid residues and has been identified in numerous proteins, including all isoforms of protein kinase C, phospholipase A, synaptotagmin and PLC. The C2 domain was first identified in protein kinase C and its function was implicated in Ca^{2+}-dependent phospholipid interactions (Nalefski and Falke, 1996). The C2 domain of PLCδ1 consists of an antiparallel β-sandwich, composed of eight well-conserved β-sheets, linked by variable peptide loops (Williams, 1999). It has been well documented that most C2 domains bind Ca^{2+}, a critical determinant for the activity of their enzymes (Zheng *et al*, 2000). However, there are domains that do not bind Ca^{2+} ions, such as the C2 domains of the ApIII PKC and P13K-C2β. These domains bind phospholipids with low affinity and little specificity (Hurley and Misra, 2000). Ca^{2+}-affinities are dependent on the presence of phospholipids or other ligands. The C2 domain of $cPLCA_2$ binds two Ca^{2+} ions in the absence or presence of membrane phospholipids, while the C2 domain of PLCδ1 binds three Ca^{2+} ions (Hurley and Misra, 2000).

The C2 domain of PLCδ1 interacts with the membrane phospholipid, phosphatidylserine (PS) to form a C2-Ca^{2+}-phosphatidylserine ternary complex (Lomansey *et al.*, 1999). The inability of phosphatic acid (PA) to substitute for PS suggested the involvement of specific phosphoserine determinants. Thus PS and Ca^{2+} bound to the C2 domain are critical for the association of PLCδ1 with the membrane and subsequently for its enzymatic function (Lomansey *et al*, 1999).

1.3.5 PLCβ isoforms.

PLCβ (1-4) isoforms differ in their tissue distribution and in their modes of activation by G-proteins. PLCβ1 is the most widely expressed isoform, with the highest concentrations found in specific regions of the brain. Expression of PLCβ2 is greatest in hemopoietic cells. PLCβ3 is widely expressed, with the highest concentrations found in brain, liver, and parotid gland, while expression of PLCβ4 is highly expressed in the retina and certain neuronal cells (Rebecchi and Pentyala, 2000; Rhee, 2001).

The catalytic activities of PLCβ isoforms are mediated by α- and βγ subunits of heterotrimeric G-proteins (Figure 1.15). G-proteins consist of α, β and γ subunits that are stably associated in an inactive GDP bound state. Interaction between a G-protein and a seven membrane spanning G-protein coupled receptor stimulated by an agonist, such as bradykinin, bombesin, angiotensin, histamine, vasopressin, acetylcholine or α1 adrenergic receptor. The ligand binding event promotes the exchange of GDP for GTP on the Gα subunit leading to the dissociation of this subunit from the stable Gβγ dimer. This triggers G-protein-mediated signalling, which in turn activates PLCβ isoforms. Hydrolysis of the GTP bound to the Gα subunit by its intrinsic GTPase activity, results in the turn off of this G-protein-mediated signalling. This process can be regulated by a family of proteins termed RGS (regulators of G protein signalling), leading to the reassociation of the GDP-bound α subunit with the βγ dimmer (Rhee, 2001).

G-protein α subunits are divided into four subfamilies $G_s\alpha$, $G_i\alpha$, $G_q\alpha$ and $G_{12}\alpha$. All four members of the $G\alpha_q$ subfamily (α_q, α_{11}, α_{14}, and α_{16}) have been described to activate PLCβ isoforms to a different extend, but fail to activate PLCγ, PLCδ and PLCε (Taylor *et al*, 1991; Smrcka *et al*, 1993; Lopez *et al*, 2001). The PLCβ isoforms possess an additional, unique 400 amino acid carboxyl terminal tail attached to the C2 domain (Figure 1.12). It has been demonstrated that a set of basic residues, which cluster in regions within this C-terminal tail, are responsible for the binding of PLCβ to the activated $G\alpha_q$ subunits (Park *et al*, 1993; Wu *et al*, 1993).

The Gβγ dimer activates the mammalian PLCβ isoforms, with the exception of PLCβ4. These Gβγ subunits may originate from stimulation of pathways linked to $G_i\alpha$. However, the α subunits of the $G_i\alpha$ family do not themselves interact directly with PLCβ isoforms. PLCβ1 is the least sensitive to Gβγ, in contrast with PLCβ2 and PLCβ3 which are strongly activated by these subunits (Smrcka and Sternweis, 1993; Lee *et al*, 1994). The region responsible for the interaction of PLCβ with Gβγ is the PH domain. This is supported by a study where a chimeric PLCδ1 molecule in which the PH domain was replaced with that of PLCβ2, showed the same degree of activation by Gβγ as the intact PLCβ2 (Wang *et al*, 2000). In addition truncation of the COOH-terminal extension of PLCβ2, generated enzymes that were not activated by $G\alpha_q$ but were sensitive to Gβγ activation (Lee *et al*, 1993).

It has also been proposed that the PLCβ isozymes might be targeted to the membrane environment through their interaction with adapter proteins known as Na^+/K^+ exchanger regulatory factors (NHERFs). Interaction is achieved through a C-terminal sequence (Ser/Thr)-X-(Val/Leu)-COOH of PZD binding motifs, which is found in all PLCβ isozymes (Hwang *et al*, 2000).

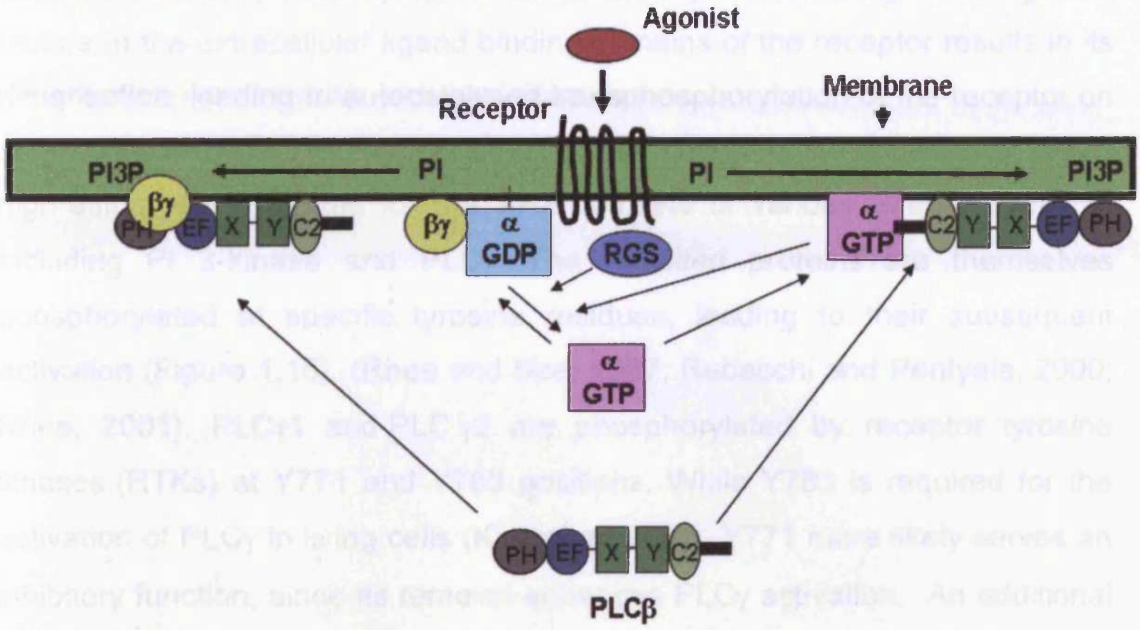

Figure 1.15 Schematic representation of the G-protein coupled receptor-mediated activation of PLCβ isoforms. Both the α_q subunit of G_q and βγ subunits activate PLCβ. Membrane localisation of the enzyme might be promoted by an interaction of the PH domain with the PI3P. RGS proteins act as receptor-specific down-regulators of the Gα subunits (Figure based on review reported by Rhee, 2001).

1.3.6 PLCγ isoforms.

Two mammalian PLCγ isoforms have been identified. PLCγ1, which is ubiquitously expressed; and PLCγ2, which although it is expressed widely, is characterised by a high level of expression in cells of hematopoeitic origin. Activation of PLCγ isoforms mobilises internal calcium stores and triggers multiple protein kinase pathways that control or modulate important cellular processes such as cell division, transformation, differentiation, shape, motility, and apoptosis (Rebecchi and Pentyala, 2000).

PLCγ is distinguished from the other PLCs by the possession of three Src homology domains (two SH2 domains followed by a SH3 domain) inserted in the XY linker region (Figure 1.12). SH2 domains play an important role in the activation of PLCγ by targeting the enzyme to the tyrosine-autophosphorylated receptors (Rhee and Bae, 1997; Rebecchi and Pentyala, 2000).

Some growth factor receptors such as platelet-derived growth factor (PDGF), epidermal growth factor (EPG) and nerve growth factor (NFG) receptors

possess intrinsic protein tyrosine kinase activity. The binding of the growth factors to the extracellular ligand binding domains of the receptor results in its dimerisation, leading to autocatalysed transphosphorylation of the receptor on specific intracellular tyrosine residues. These phosphorylated residues act as high-affinity binding sites for the SH2 domains of various effector proteins, including PI 3-kinase and PLCγ. The recruited proteins are themselves phosphorylated at specific tyrosine residues, leading to their subsequent activation (Figure 1.16), (Rhee and Bae, 1997; Rebecchi and Pentyala, 2000; Rhee, 2001). PLCγ1 and PLC γ2 are phosphorylated by receptor tyrosine kinases (RTKs) at Y771 and Y783 positions. While Y783 is required for the activation of PLCγ in living cells (Kim *et al*, 1991), Y771 more likely serves an inhibitory function, since its removal enhances PLCγ activation. An additional site, Y1254, is located at the C-terminus of PLCγ1, but its role has not been elucidated and it is absent from PLCγ2 (Rebecchi and Pentyala, 2000).

Different receptor tyrosine kinases (RTKs) possess different numbers of autophosphorylation sites. RTKs for NGF and PDGF possess a single autophosphorylation site that binds to the SH2 domains of PLCγ1, while the EGF receptor contains multiple potential binding sites with different affinities for PLC (Soler *et al*, 1994). Deletion of these PLC recognition sites blocks RTK-catalysed tyrosine phosphorylation of PLCγ1 and its activation (Rebecchi and Pentyala, 2000).

Protein tyrosine phosphatases (PTPases) play an important role in tyrosine protein kinase pathways, and thereby in PLCγ activation. It is thought that some PTPases are recruited to activated receptor complexes, where they dephosphorylate effector molecules, such as PLCγ. Inhibition of PTPases is necessary to increase the steady-state level of protein tyrosine phosphorylation, and is regulated by reactive oxygen species (ROS), (Rebecchi and Pentyala, 2000; Rhee, 2001).

In addition to its tyrosine residues, PLCγ can also be phosphorylated on selected serine and threonine sites, in response to growth stimulants (Wahl *et al*, 1989). The major site appears to be the S1248 and it can be phosphorylated by either PKA or PKC. However, Serine/Threonine phosphorylation of PLCγ is thought not to be sufficient for PLCγ activation,

and it is more likely that Serine/Threonine phosphorylation of the receptor and associated proteins represents the critical step in desensitising various effector pathways, including PLCγ activation (Rebecchi and Pentyala, 2000).

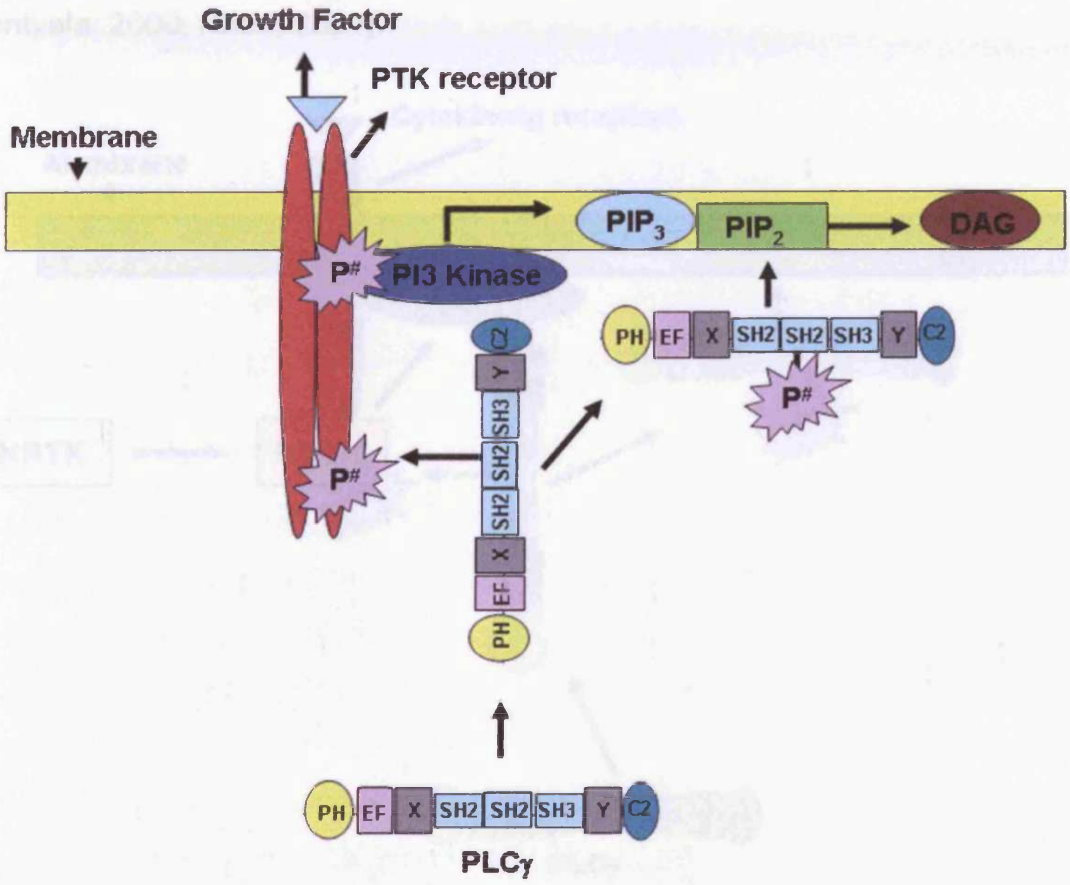

Figure 1.16 Schematic representation of growth factor-mediated activation of PLCγ. Growth factor stimulation triggers autophosphorylation of protein tyrosine kinase receptor, on tyrosine residues which function as docking sites for PLCγ and PI3-kinases. The PI3-kinases product, PIP_3, serves to anchor PLCγ to the membrane after its dissociation from the protein tyrosine kinase (Figure based on reviews reported by Rebecchi and Pentyala, 2000; Rhee, 2001).

Components of the immune system express a variety of receptors (including B- and T-cell receptor complexes, receptors for the Fc regions IgE, IgG, IgA, and IgM, and for cytokines such as interleukin IL1, IL4, IL5, and IL7) that regulate cell proliferation, differentiation, and apoptosis. These receptors comprise multiple polypeptide chains that do not possess intrinsic tyrosine kinase activity but oligomerise, forming a functional receptor unit. These receptor sites recruit nonreceptor tyrosine kinases (NRTKs), including Src, Syc, and Tec families. Similar to RTKs, the recruited NRTKs are themselves phosphorylated, recruiting other effector proteins that contain SH2 domains,

including PLCγ1 and PLCγ2 isoforms, which are tyrosine phosphorylated at similar sites targeted by RTKs (Figure 1.17). The ligand binding site of these receptors is composed of variable chains, which are noncovalently associated with invariants subunits and confer binding specificity (Rebecchi and Pentyala, 2000; Rhee, 2001).

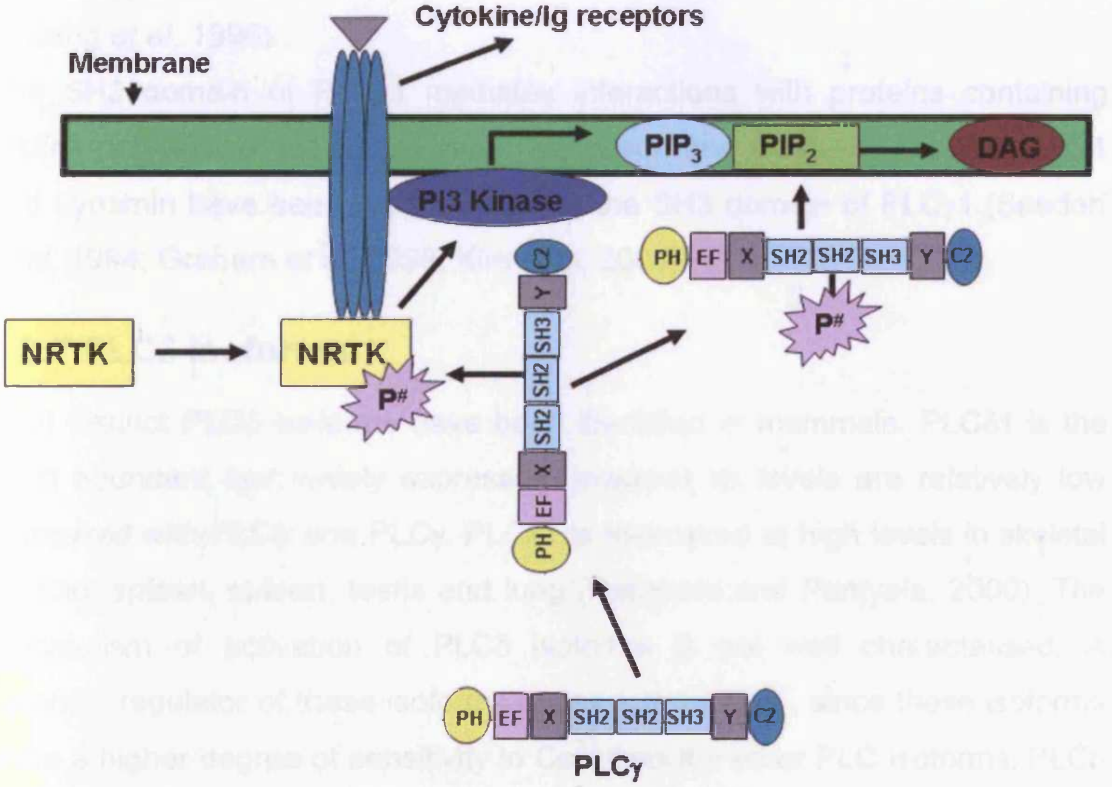

Figure 1.17 Schematic representation of antigen-receptor-mediated activation of PLCγ. Stimulation of a cytokine or Ig receptor causes oligomerisation of the receptor and recruitment of nonreceptor tyrosine kinases (NRTKs). NRTKs are autophosphorylated recruiting PLCγ and PI3-kinases, which are phosphorylated at similar sites targeted by RTKs, leading to their activation. (Figure based on reviews reported by Rebecchi and Pentyala, 2000; Rhee, 2001).

PLCγ isoforms are also under the control of G protein-coupled receptors (GPCRs), which lack an intrinsic PTK activity. These receptors trigger similar pathways stimulated by growth factors, antigens, and cytokines, including the ras/MAPK/ERK pathways. Activation of GPCRs indirectly (and the intermediary proteins remain to be clearly identified) induce tyrosine phosphorylation of activated RTKs. These then function as if bound with growth factor, recruiting the usual set of signalling molecules, including PLCγ (Rebecchi and Pentyala, 2000; Rhee, 2001).

Other mechanisms of PLCγ activation have been proposed. Phosphatic acid (PA) has been described as an activator of both tyrosine phosphorylated and unphosphorylated forms of PLCγ1, increasing their affinity for substrate vesicles (Jones and Carpenter, 1993; Zhou *et al*, 1999). Arachidonic acid also has been shown to stimulate the activity of PLCγ independently of tyrosine phosphorylation in the presence of the microtubule associated protein tau (Hwang *et al*, 1996).

The SH3 domain of PLCγ1 mediates interactions with proteins containing proline-rich sequences (PXXP motif), (Pawson and Nash, 2000). Cbl, SOS1 and dynamin have been reported to bind the SH3 domain of PLCγ1 (Seedorf *et al*, 1994; Graham *et al*, 1998; Kim *et al*, 2000).

1.3.7 PLCδ isoforms.

Four distinct PLCδ isoforms have been identified in mammals. PLCδ1 is the most abundant and widely expressed, however its levels are relatively low compared with PLCβ and PLCγ. PLCδ1 is expressed at high levels in skeletal muscle, spleen, spleen, testis and lung (Rebecchi and Pentyala, 2000). The mechanism of activation of PLCδ isoforms is not well characterised. A potential regulator of these isoforms appears to be Ca^{2+}, since these isoforms show a higher degree of sensitivity to Ca^{2+} than the other PLC isoforms. PLCδ isoforms are activated by $[Ca^{2+}]$ in the range of 10^{-7} to 10^{-5} M. Ca^{2+} binding is necessary for the enzymatic function of PLCδ1. The binding of Ca^{2+} to the EF hands is essential for an efficient interaction of the PH domain with $PtdInsP_2$ (Yamamoto *et al*, 1999). Ca^{2+} binding to the catalytic domain is critical for the activity (Essen *et* al, 1996; Grobler and Hurley, 1998), and its binding to the C2 domain leads to the formation of a C2-Ca^{2+}-phosphatidylserine ternary complex, essential for the association of PLCδ1 with the membrane (Lomansey *et al*, 1999). All these roles for Ca^{2+} suggest that an increase in $[Ca^{2+}]$ might be sufficient to trigger activation of PLCδ1.

Another potential regulator of PLCδ isoforms has been proposed to be a GTP-binding protein termed high-molecular-weight G-protein (G_h). This protein has a molecular weight of ~80kDa, possesses transglutaminase activity (TGII) and has been suggested that it binds and activates PLCδ1 (Feng *et al*, 1996).

PLCδ1 has been described to be an effector of oxytocin receptor signaling via the activation of G_h. This interaction has been shown to stimulate PLCδ1 (Park *et al*, 1998). Conversely a more recent study showed that α1-AR couples to PLCδ1 via an interaction with G_h protein (Nakaoka *et al*, 1994), resulting in a significant inhibition of PLCδ1 activity (Murthy *et al*, 1999).

PLCδ1 is also regulated by phospholipids. Of all phospholipids tested, sphingomyelin has been described as the most effective inhibitor. Inhibition of PLCδ1 activity by sphingomyelin is promoted by spermine and Ca^{2+}, and is suppressed by sphingosine (Matecki and Pawelczyk, 1997; Pawelczyk and Lowenstein, 1997). The regulation of PLCδ1 activity and targeting to membranes and $PtdInsP_2$ is further discussed in section 7.6 (including a schematic diagram), with respect to the role of its individual functional domains and a comparison with the biochemical properties of PLCζ is made.

PLCδ-related proteins have also been described in higher plants, such as *Arabidopsis thaliana*, *Glycine max*, *Solanum tuberosum* and *Pisum sativum*. These proteins similarly to PLCζ, lack an N-terminal PH domain, as well as the first pair of EF hands. Despite the lack of these domains plant PLCs retain the overall PLC enzymatic properties. These enzymes exhibit catalytic activity on $PtdIns(4,5)P_2$ responding to Ca^{2+} in the range of 0.1-10μM (Rebecchi and Pentyala, 2002).

1.3.8 PLCε isoform.

Two human PLCε splice variants of 1994 and 2303 residues, which differ only in their N-termini and a rat isoform of 2281 residues have been reported. These enzymes are expressed in a variety of tissues, most abundantly in the heart (Rhee, 2001). PLCε lacks a PH domain and EF hands from its sequence. In these PLC isoforms a Ras-GEF-like domain is present towards the N-terminus and two Ras binding domains (RA1 and RA2) at the C-terminus (Figure 1.12), (Kelley *et al*, 2001; Rhee, 2001). The presence of the RasGEF and RA domains suggested a bifunctional regulatory potential of PLCε acting both as an effector of Ras and an activator of downstream Ras-GTPase signalling pathways.

RA domains are conserved in a variety of proteins and interact directly with the Ras-family GTPases. These are small monomeric proteins, which play an important role in many cellular processes including cell growth, differentiation and oncogenesis (Ponting and Benjamin, 1996; Rhee, 2001). It has been described that the RA2 domains of rat PLCε binds H-Ras in a GTP-dependant manner and a single amino acid substitution (e.g. K2150E) in the RA2 domain is able to disrupt this interaction. In contrast, RA1 binds H-Ras with a low affinity and in a GTP-independent manner (Kelley *et al*, 2001; Song *et al*, 2001). PLCε is most closely related to PLCβ isoforms and can therefore be expected to share some functional characteristics. Like PLCβ isoforms, PLCε can be stimulated by a range of Gα subunits, most potently by $G\alpha_{12}$ (Lopez *et al*, 2001). Gβγ subunits have also been shown to stimulate PLCε activity (Wing *et al*, 2001).

1.3.9 PLCη isoforms.

PLCη1 and PLCη2 are the most recently identified PLC isoforms (Hwang *et al*, 2005; Nakahara *et al*, 2005). PLCη1 is an 115kDa protein and of the PLC families is most closely related to PLCδ1. PLCη gene is transcribed to several splice variants. The transcript encoding the 115kDa protein is restricted to the brain and lung. *In situ* hybridisation analysis with brain revealed that PLCη1 is expressed abundantly only in nerve tissues such as cerebral cortex, hippocampus, zona incerta and cerebellar Purkinje cell layer. Recombinant PLCη1 exhibited Ca^{2+}-dependent catalytic activity on PtdIns(4,5)P_2 with maximal activity at 10μM of [Ca^{2+}] (Hwang *et al*, 2005).

PLCη2 was identified in mouse brain. It is composed of 1164 amino acids with a molecular mass of 125kDa. PLCη2 has high homology with PLCη1 but contains an additional 290 amino acids at the C-terminus. PLCη2 exhibited high Ca^{2+}-sensitivity. This enzyme is activated at [Ca^{2+}] as low as 10nM. *In situ* hybridisation with brain showed that PLCη2 is particularly abundant in pyramidal cells of the hippocampus, cerebral cortex and olfactory bulb. These organs have been described to contribute to memory formation suggesting that PLCη2 may be involved in this function (Nakahara *et al*, 2005).

1.4 Aims of this study.

PLCζ protein is approximately 70 kDa and is most closely related to PLCδ1, with the exception that it lacks a PH domain from its sequence (Saunders *et al.*, 2002). In mouse PLCζ, a tandem pair of EF hands (residues 20-150) at the N-terminus is followed by the catalytic XY domain and a C2 domain (residues 521-625). The linker sequence between the X (residues 168 to 307) and Y (residues 386-502) domains is slightly longer in PLCζ (308-385) than in PLCδ1 (residues 441-491). Figure 1.18 represents the crystal structure of PLCδ1 lacking the PH domain. As PLCζ and PLCδ1 are closely related, it is possible that these proteins share a similar 3D-structure.

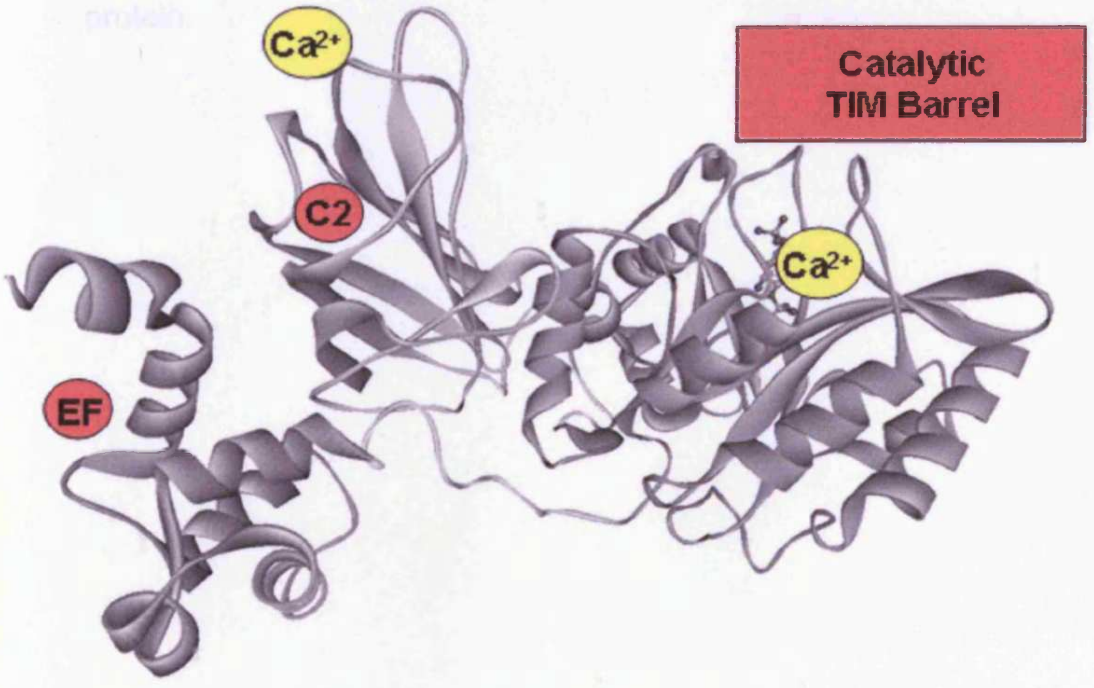

Figure 1.18 Representation of crystal structure of PLCδ1 lacking the PH domain (Essen *et al*, 1996). Three Ca^{2+} ions bind to the C2 domain and one the X/Y barrel of PLCδ1 (Figure adapted from Rebecchi and Pentyala, 2000).

PLCζ is effective at causing Ca^{2+} oscillations in eggs at very low concentrations (e.g. 10fg/egg) (Saunders *et al*, 2002, Kouchi *et al*, 2004, Fujimoto *et al*, 2004). In contrast, other studies have shown that PLC isoforms of the β, γ or δ class are either ineffective (Jones *et al*, 2000), or at least much less effective than PLCζ at causing Ca^{2+} release when microinjected in eggs

(Runft *et al*, 2002, Kouchi *et al*, 2004). The specific reason(s) for this are currently unexplained.

The aims of this thesis are:

- to characterise the enzymatic properties of recombinant mouse PLCζ (mPLCζ) *in vitro*, with respect to $PtdInsP_2$ hydrolysis and Ca^{2+} sensitivity.
- to study the importance of each mPLCζ domain on the *in vitro* enzymatic activity, targeting mechanisms and the *in vivo* oscillogenic activity of this protein.
- to produce a mouse anti-PLCζ monoclonal antibody, with the aim of blocking the hydrolytic and consequently the oscillogenic activity of this protein.

Chapter 2

Materials and Methods

2.1 Materials.

2.1.1 General Laboratory Reagents and Chemicals.

All reagents and chemicals were of analytical grade and were obtained from Sigma or Calbiochem unless otherwise stated. All reagents and equipment for protein and DNA gel electrophoresis were obtained from BioRad unless otherwise stated.

2.1.2 General Biological Reagents.

- $CaCl_2$, 1M stock: a 1M solution was filter sterilised and stored at 4°C.
- CH_3COONa, 3M: a 3M solution was adjusted to pH 5.3 using glacial CH_3COOH. Filter sterilised.
- Chloroform:Methanol:Conc.HCl (100:100:0.6): Mixed in the fume hood and stored in a sealed glass container at 4°C.
- Chloroform:Phenol:Isoamyl alcohol (25:24:1): Mixed in fume hood and stored in sealed glass container at 4°C.
- DEPC-H_2O: 1ml/L DEPC was added to deionised H_2O, mixed well, solution incubated overnight at room temperature and autoclaved.
- DNA loading buffer, 5X stock: 50% v/v glycerol, 0.25% w/v orange G, 5x TAE.
- EGTA 0.5M stock: Dissolved in H_2O at pH 8.0, adjusted using NaOH. Filter sterilised and stored at 4°C.
- Ethanol, 80% stock: an 80% v/v solution was filter sterilised.
- IPTG, 0.1M stock was filter sterilised and stored at -20 °C.
- Isopropanol, an 80% v/v solution was filter sterilised.
- L-Arabinose, 20 % w/v stock was filter sterilised and stored at -20 °C
- Molecular weight DNA markers: obtained from Gibco.
- NaCl, 5M stock was filter sterilised and stored at 4°C.
- PBS: 137mM NaCl, 2.7mM KCl, 4.3mM Na_2HPO_4, 1.4mM KH_2PO_4, adjusted to pH 7.4 using HCl, autoclaved and stored at 4°C.

- Phosphate Buffer: 500mM NaCl, 20mM Na_2HPO_4, adjusted to pH 7.4 and filter sterilised.
- PtdInsP$_2$ calcium buffer: 0.8ml 0.5M EGTA (pH 8.0), 0.2ml 1M $CaCl_2$, 9ml H_2O. Filter sterilised and stored at 4°C.
- PtdInsP$_2$ hydrolysis buffer: 2ml 0.2M Tris-HCl pH 6.8, 800µl 10mg/ml BSA, 7µl β-Mercaptoethanol, 5.2ml H_2O. Filter sterilised and stored at 4°C for no more than 2 weeks.
- Sodium Cholate, 20% stock was filter sterilised and stored at 4°C.
- TAE, 50X stock: 2M Tris, 2M acetic acid, 50mM EDTA

2.1.3 Protein Biochemistry Reagents.

- Ammonium persulphate: 10% w/v: always made fresh.
- Carbonate coating buffer 1X: 0.15M Na_2CO_3, 0.35M $NaHCO_3$ adjusted to pH 7.4 using HCl. Filter sterilised.
- Molecular weight protein markers: pre-stained 'Kaleidoscope Broad Range' markers (BioRad).
- Protease inhibitor cocktail, 25X (Roche).
- Protein loading buffer, 5X stock: 0.3M Tris, 10% w/v SDS, 50% v/v glycerol, 0.025mM EDTA, 0.25% w/v bromophenol blue, adjusted to pH 6.8 using HCl.
- Running buffer, 5X stock: 15g/L Tris, 72g/L glycine, 5g/L SDS.
- Semi-dry transfer buffer: 48mM Tris, 39mM glycine, 0.0375% w/v SDS, 20% v/v methanol.
- TBS, 10X Stock: 0.2M Tris, 1.37M NaCl, adjusted to pH 7.5 using HCl.
- TBS-T buffer: 1X TBS, 0.1% v/v Tween-20.
- Tris, 0.5M: a 0.5M solution was adjusted to pH 6.8 using HCl.
- Tris, 1.5M: a 1.5M solution was adjusted to pH 8.8 using HCl.

2.1.4 Bacterial Cell Culture Reagents.

All growth media were obtained from Sigma and sterile plastic glassware from Fisher. All glassware was washed in detergent-free water and autoclaved (135°C, 90 min) before use. Growth media were autoclaved under the same conditions prior to the addition of antibiotics. All procedures were carried out in a sterile fume hood, where all the surfaces were cleaned with 70% v/v ethanol before and after use.

- LB broth: 10g/L tryptone, 5g/L yeast extract, 5g/L NaCl. Autoclaved. Medium cooled to <50°C before antibiotic addition. Stored at 4°C.
- LB-agar medium: LB broth, 15g/L agar. Autoclaved. Medium cooled to <50°c before antibiotic addition. Stored at 4°C once poured.
- Ampicillin, 1000X stock: 100mg/ml, dissolved in deionised H_2O, filter sterilised, stored at -20°C.
- Chloramphenicol, 1000X stock: 100mg/ml, dissolved in deionised H_2O, filter sterilised, stored at -20°C.

2.1.5 Monoclonal Antibody Production and Cell Culture Reagents.

All media were obtained from Sigma. All procedures were carried out in a sterile fume hood, where all the surfaces were cleaned with 70% v/v ethanol before and after use. All media stored at 4°C.

- For 500ml of F10 medium: 435ml RPMI 1640, 50ml FCS, 5ml Penicillin/Streptomycin (5000 IU/ml), 5ml glutamine (200mM), 5ml Sodium Pyruvate (100mM) and 0.5 Fungizone (250μg/ml).
- F15 medium: F10 medium plus further 5% (v/v) FCS.
- F15+ HAT medium: 392ml F15 medium plus 4ml Aminopterin (0.1mM) and 4ml Hypoxanthine (25mM)/Thymidine (4mM).
- F10 medium + HT: 396ml F10 medium plus 4ml Hypoxanthine (25mM)/Thymidine (4mM).
- Polyethylene Glycol 1500.

2.1.6 Monoclonal Antibody Purification Reagents.

All Buffers were made in our Laboratory and stored at 4°C.

- Binding Buffer A: 1.5M Glycine/NaOH, 3M NaCl, pH 9.0.
- Elution Buffer B: 0.2M Glycine/HCl, pH 2.5.
- Neutralisation Buffer C: 1M Tris/HCl, pH 9.0.

2.1.7 Radiolabelled Phosphatidylinositol-4,5-biphosphate.

0.01 mCi/ml (0.37 MBq/ml) of [^{3}H]PtdInsP$_2$ in a methylene chloride: ethanol: water (20:10:1) solution, in a sealed ampoule was obtained from NEN. The ampoule was opened carefully under fume hood, [^{3}H]PtdInsP$_2$ was dried under N_2 gas and diluted with 450μl of 10mM Tris-HCl pH 7.5.

2.1.8 Oligonucleotides.

Custom oligonucleotide primers were ordered from Sigma-Genosys and were obtained as lyophilised pellets. Pellets were resuspended in an appropriate volume of sterile deionised H_2O to give stock solutions of 100μM, according to manufacturer's instructions. Working aliquots of 20μM or 3.2μM, as appropriate, were prepared by dilution with H_2O and all primers stored at -20°C. A list of all primers used in this study is given in Appendix III.

2.1.9 Plasmid Vectors.

2.1.9.1 pGEX-5X-2.

Vector pGEX-5X-2 was obtained from Amersham. pGEX-5X-2 contains the coding sequence for glutathione-S-transferase (GST), with the vector multiple cloning site at the 3' end of GST. Expression of the fused protein is induced in *E. Coli* bacteria by addition of optimal IPTG to the bacterial media. The vector carries the ampicillin resistance gene for selection in *E. Coli*.

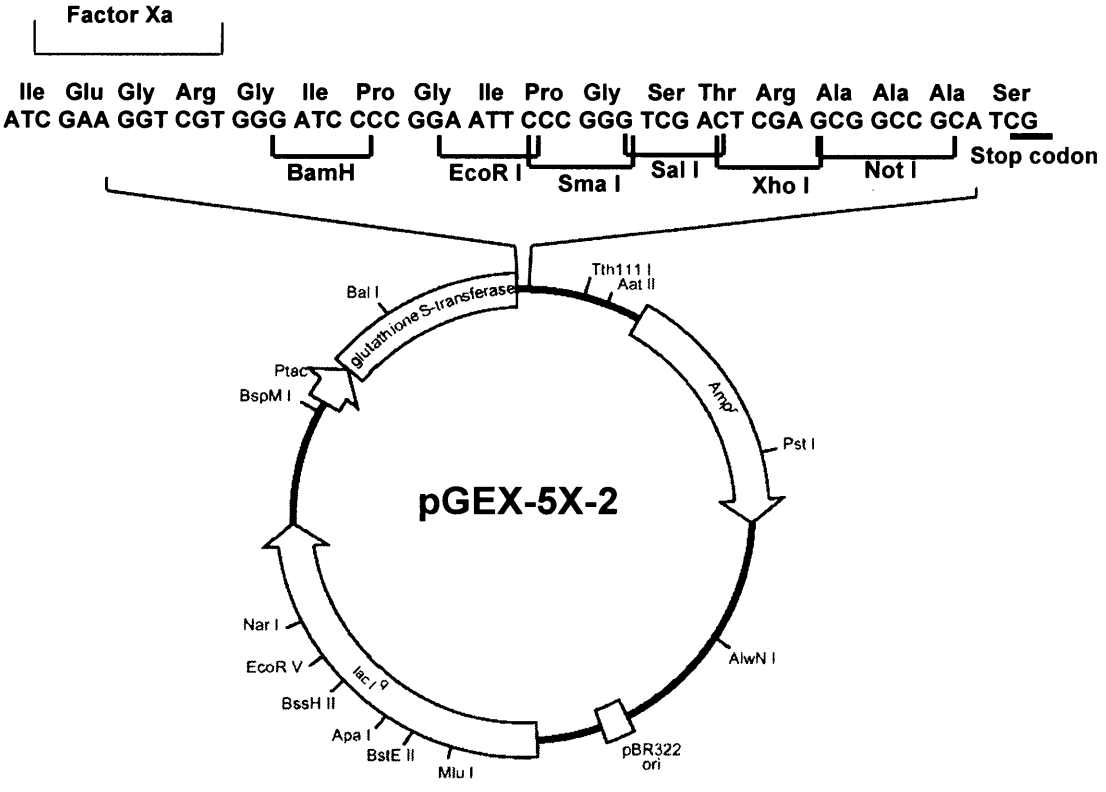

Figure 2.1 Vector map of pGEX-5X-2 (courtesy of Amersham).

2.1.9.2 pCR™ 3.

Vector pCR™ 3 was obtained from Invitrogen. This vector contains a T7 promoter upstream of the MCS, for *in vitro expression* of recombinant proteins in the TNT T7 Quick coupled transcription and translation system, and for cRNA synthesis. The vector carries the ampicillin resistance gene for selection in *E. Coli.*

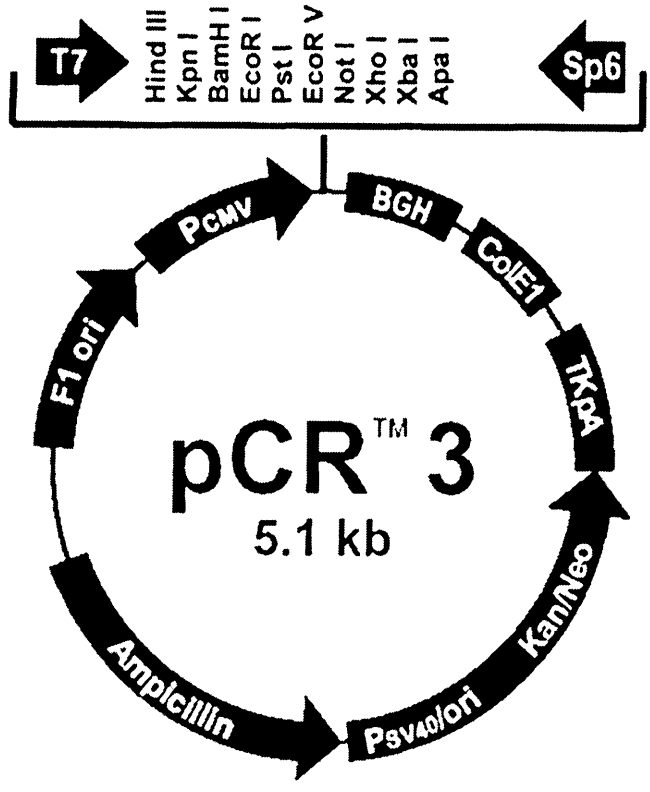

Figure 2.2 Vector map of pCR™ 3 (courtesy of Invitrogen).

2.1.9.3 pTarget.

pTarget was obtained from Promega. Like the pCR™ 3, this vector contains a T7 promoter upstream of the MCS, for *in vitro expression* of recombinant proteins in the TNT T7 Quick coupled transcription and translation system, and for cRNA synthesis. The vector carries the ampicillin resistance gene for selection in *E. Coli*.

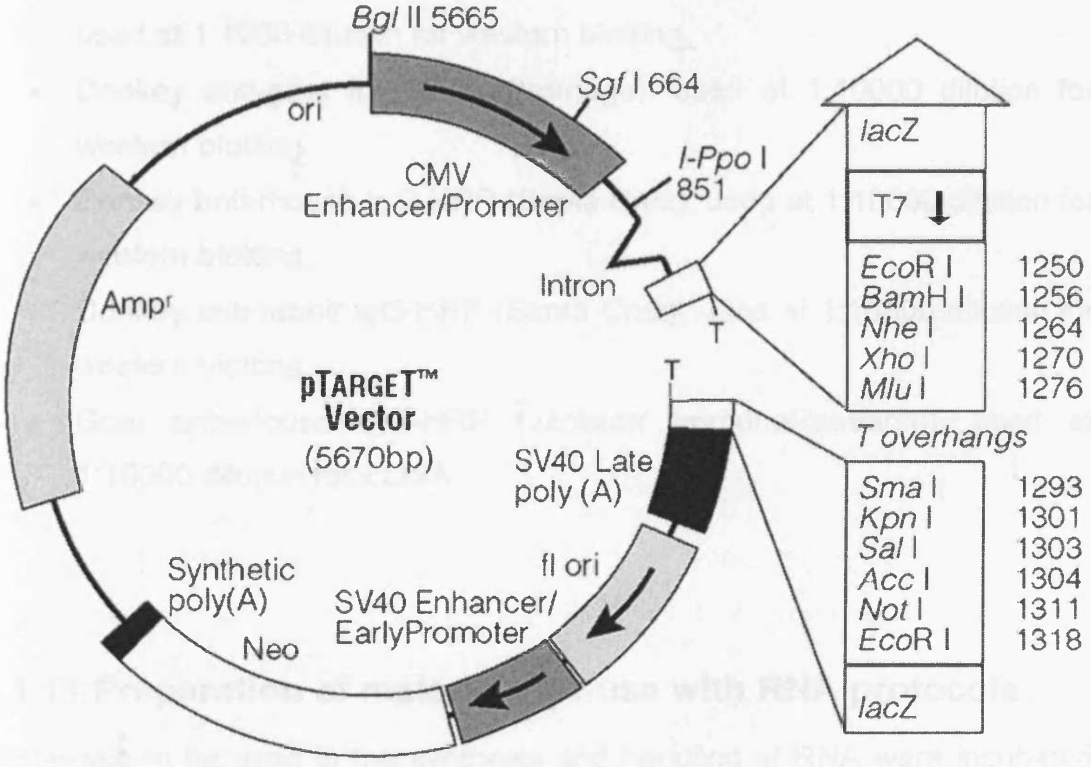

Figure 2.3 Vector map of pTarget (courtesy of Promega).

2.1.10 Antibodies.

The following antibodies were used in this study:

- Ab-T103, rabbit polyclonal, raised against glutathione-S-transferase. Used at 1:5000 dilution for western blotting.
- Ab-cMyc, mouse monoclonal, raised against the cMyc epitope (9E10, Santa Cruz), used at 1:1000 dilution for western blotting.
- Ab-Anti-Luciferase goat polyclonal, raised against recombinant luciferase from North American firefly *Photinus Pyralis* (Promega), used at 1:1000 dilution for western blotting.
- Donkey anti-goat IgG-HRP (Promega), used at 1:10000 dilution for western blotting.
- Donkey anti-mouse IgG-HRP (Santa Cruz), used at 1:10000 dilution for western blotting.
- Donkey anti-rabbit IgG-HRP (Santa Cruz), used at 1:10000 dilution for western blotting.
- Goat anti-mouse IgG-HRP (Jackson ImmunoResearch), used at 1:10000 dilution for ELISA.

2.1.11 Preparation of materials for use with RNA protocols.

All vessels to be used in the synthesis and handling of RNA were incubated overnight in diethylpyrocarbonate (DEPC), (0.1% v/v) and then autoclaved. RNA protocols were performed in an isolated part of the laboratory, and all bench tops were treated with RNaseZAP (SIGMA) RNase inhibitor before work began.

2.1.12 Computer Software and Data Analysis.

Numerical data were stored in spreadsheets and plotted in graphical form using Excel (Microsoft) and Prism unless specifically stated otherwise in methods. Data were expressed as mean ± standard error. Standard curves for protein concentration analysis were generated by the least squares fit method.

Stained protein gels and western blots were scanned at 300dpi using a densitometer (GS-700, BioRad) and image processing performed using Photoshop 4.0 (Adobe).

DNA and protein sequence analysis were performed using software available at the ExPASy (http://www.expasy.ch/tools/dna.html), European Bioinformatics Institute (http://www.ebi.ac.uk/services) and NCBI (http://www.ncbi.nlm.nih.gov) websites.

2.1.13 Health and Safety / Legal procedures.

All reagents were handled and stored as recommended by manufacturer's safety sheets. All experiments were carried out in accordance with COSHH regulations and local college regulations.

Animal immunisation and sacrifice was carried out by Biomedical Services, UWCM, in accordance with HM Home Office schedule one procedures and licence.

2.2 Methods.

Standard molecular and biochemical techniques were performed according to procedures described in *Molecular Cloning: A Laboratory Manual* (CSH) or *Short Protocols in Molecular Biology* (Wiley).

2.2.1 Molecular Biology Techniques.

2.2.1.1 PCR amplification of DNA.

PCR reactions were carried out according to reagent manufacturer's instructions, using a Progene (Techne) PCR machine. Phusion (Finnzymes) and *Pfu* (Promega) DNA polymerases were used for the generation of high fidelity PCR products, while *Taq* (Promega) was used for diagnostic reactions only. A typical example for the reaction mixture and cycling conditions is given in Tables 2.1 and 2.2. Following analysis of PCR products by agarose gel electrophoresis, PCR products were purified using the QIAquick PCR purification kit (Qiagen), which employs a DNA-binding column, according to the manufacturer's instructions.

Table 2.1 Typical PCR Reaction Mix

Reagent	Final Concentration	Typical Volume
PCR buffer	1X	5µl of 10X stock (or 10µl of 5X stock for phusion)
*$MgCl_2$	2.5mM	2.5µl of 50mM stock
dNTP mix	0.2mM	0.5µl of 20mM stock
Forward primer	0.4µM	1µl of 20µM stock
Reverse primer	0.4µM	1µl of 20µM stock
DNA template	10-500ng total	0.5µl of 200ng/µl
DNA polymerase	1u total (or 0.4u Phusion)	0.5 µl of 2u/µl stock
Nuclease-free H_2O	Up to 50µl	39µl (or 36.8µl for phusion)
*$MgCl_2$ is already included in the Phusion and *Pfu* reaction buffers		

Table 2.2 Thermal Cycling Conditions

Step	Temperature	Time	Total number of cycles
Initial Denaturation	94°C	2 min	1
Denaturation Annealing Extension	94°C 50-65°C* 72°C	1 min 1 min 45 sec - 3 min**	32
Final Extension	72°C	10 min	1

* Annealing temperature typically 2-5°C below calculated melting temperature of primers

** Extension time dependant on size of PCR product. Typically for *Taq* polymerase time=1min/kb, for *Pfu* polymerase, time=1.25min/kb and for Phusion time=0.25min/kb

For Phusion polymerase temperature and time of each step was slightly different.

2.2.1.2 Agarose gel electrophoresis.

DNA fragments were analysed by agarose gel electrophoresis and compared against DNA molecular weight markers. Depending on the percentage of agarose gel required (table 2.3), the appropriate concentration of ultra-pure agarose (Eurogentec) was added to TAE buffer (1X) and heated in a microwave oven until the agarose completely dissolved resulting in a clear solution. The solution was allowed to cool to <50°C and ethidium bromide was added to a final concentration of 0.2μg/ml. The solution was poured into a gel tray, assembled according to manufacturer's instructions (BioRad), and a comb inserted to mould the wells. Once gel was set, DNA samples in DNA-loading buffer (1X) were loaded, along with standard DNA molecular weight markers (invitrogen). Electrophoresis was then carried out in a gel tank containing fresh TAE (1X) at a constant voltage (typically 80V). Electrophoresis was stopped when the dye front had migrated approximately three quarters through the gel. The gel was then visualised on a UV transluminator and the image acquired using documentation system (BioRad) and Quantity One software (BioRad).

Table 2.3. DNA separation by Agarose Gel Electrophoresis.	
Agarose % (w/v)	**Effective range of resolution of linear DNA (kb)**
0.5	30 to 1
0.7	12 to 0.8
1.0*	10 to 0.5
1.2	7 to 0.4
1.7	3 to 0.2
2.0*	2 to 0.1
*Typically, 1% was used for products >1kb and 2% was used for products <1kb.	
Table reproduced from Short Protocols in Molecular Biology (Wiley).	

2.2.1.3 Cloning of DNA fragments.

Plasmid DNA was digested with the appropriate endonuclease enzymes, typically 1μg of DNA in a 20μl reaction for 2hr at 37°C, in the appropriate buffers according to the manufacturer's instructions. For double digests using restriction enzymes with incompatible buffers, the two digests were performed sequentially in their own buffers. Following the digestion of DNA with the first restriction enzyme the single DNA digest was purified using the QIAquick PCR purification kit (Qiagen) and then the appropriate enzyme for the second digest was added in its own buffer.

DNA fragments to be subcloned were separated by gel electrophoresis, extracted from the agarose gels and purified using the QIAEX II gel extraction kit (Qiagen). The extracted agarose gel slices were dissolved in a high salt buffer (QuiexI), containing DNA-binding beads (QuiexII) at 50°C for 10mins. The beads were sedimented by centrifugation at 15,000g for 1 min (Microfuge R, Beckman). The beads were washed once with high salt buffer and twice with a 70% ethanol buffer. DNA was eluted from the beads with the appropriate volume of dH_2O.

Ligations were carried out using a molar ratio of 3:1 of insert to vector (typically 300ng: 100ng). The ligation was performed using 2U T4 DNA ligase (NEB) in supplied 1X buffer and incubated at room temperature overnight. The ligation mixture was subsequently used for transformation into chemically competent *E. Coli* bacteria.

2.2.1.4 Bacterial cell culture.

Three different strains of *E. Coli* were used for molecular biology techniques in this study; DH5α (Promega), TOP10F (Invitrogen) and BL21-derivative *Rosetta*(DE3)pLysS (Novagen). Bacteria were cultured at 37°C under aseptic conditions in LB medium, either in suspension with rotation at 225 rpm (Innova 4300 shaker incubator, New Brunswick) or on solid support medium LB-agar plates (plate incubator, Heraeus). For bacteria transformed with plasmid DNA, the growth medium was supplemented with the appropriate antibiotic (typically ampicillin at 100μg/ml and/or chloramphenicol at 40μg/ml). For long term storage of positive clones, frozen glycerol stocks of the host bacteria were prepared. 0.5ml of a saturated overnight culture were pelleted by centrifugation at 10,000g for 5 min (Avanti J-25, Beckman), resuspended in 1ml of sterile LB:glycerol 1:1 v/v, (containing the appropriate antibiotic) and stored at -80°C. Bacteria were revived from stock by streaking a sample of the frozen stock on an LB-agar plate (containing the appropriate antibiotic) to produce individual colonies.

The cell density of growing cultures, where required, was determined by measuring the absorbance at 600nm (A_{600}) of an appropriately diluted cell suspension. Cell density was calculated using the formula: 1unit $A_{600} \cong 1x10^9$ cells/ml.

2.2.1.5 Preparation of competent bacteria.

Chemically competent DH5a, TOP10F and *Rosetta* (DE3)pLysS cells were prepared in our laboratory using the $CaCl_2$ method. One colony of competent cells was grown in 10ml of LB medium (with the appropriate antibiotic) overnight at 37°C in a shaker incubator. The next morning 3ml of the overnight culture was added in 300 ml LB (with the appropriate antibiotic) and grown at 37°C with shaking (225rpm). The growth was stopped when the A_{600} had reached 0.5. The culture was then transferred to a Beckman centrifuge tube and incubated on ice for 1 h. The cells were then centrifuged at 6,000g for 10min at 4°C. The supernatant was discarded and the pellet was resuspended gently in 0.5 volume of chilled 50mM $CaCl_2$ and incubated for 30

min on ice. The cells were then centrifuged again under the same conditions and the pellet resuspended in 0.1 volume of cell storage solution (50mM $CaCl_2$, 20% glycerol (w/v). After a gently mix the cells were aliquoted 100 μl into small eppendorfs and immediately snap frozen on dry ice for 30 min before transfer to the -80°C freezer. The cells could be successfully used for efficient transformation for up to 6 months.

2.2.1.6 Transformation of competent bacteria.

Frozen aliquots (100μl) of chemically competent *E. Coli* were thawed on ice. Up to 5μl (5-10ng DNA) of the ligation reaction was added directly to the cells and mixed gently. Bacteria were incubated on ice for 30mins and then heat shocked at 42°C water bath for 45sec and put back on ice for further 5mins. 900μl LB broth medium was added to the cell suspension and incubated at 37°C for one hour with shaking at 225rpm. Two unequal volumes of the cell culture [typically 100μl and 900μl (concentrated to100μl by centrifugation)] were plated on LB-agar plate containing the appropriate antibiotic. Culture plates were incubated inverted at 37°C overnight.

2.2.1.7 Analysis of recombinant plasmids.

A number of colonies were screened for the presence of the recombinant plasmid as follows: a colony was picked from the plate with a sterile pipette tip and transferred to a PCR reaction containing primers specific to the subcloned insert. Following cycling, the PCR reactions were analysed by agarose electrophoresis as above. Any colonies that appeared positive for the correct insert were analysed by restriction digest following plasmid DNA purification. Plasmid DNA purification was performed following the protocol supplied with the Wizard® Plus SV Minipreps purification system (Promega): 5ml of LB medium containing the appropriate antibiotic were inoculated with the colony and grown overnight at 37°C with shaking at 225rpm. The next day cells were pelleted by centrifugation at 6000g for 10min (Allegra 6R, Beckman) and resuspended in 250μl Resuspension buffer. Bacteria were

lysed by addition of 250μl Lysis buffer for 5mins at room temperature. 10μl alkaline phosphatase was then added and the mixture incubated at room temperature for 5 additional minutes. In this step bacterial endonucleases and other enzymes that could influence the results of the preparation in a negative way were cleaved and denatured. 350μl Neutralisation buffer was then added to stop the lysis reaction and precipitate acid-insoluble cell contents. Lysate was centrifuged at 21,000g for 10mins (Microfuge R, Beckman), and the supernatant added to a spin column containing an immobilised DNA-binding membrane. The spin column was centrifuged at 21,000g for 1min to draw the lysate through the membrane. The membrane was washed twice with an 80% ethanol buffer, and DNA eluted with 50μl dH_2O.

Purified recombinant plasmids were screened for the presence of the correct insert and correct orientation by restriction mapping. Typically, double digests were performed with one enzyme cutting once in the insert sequence and the other cutting the vector sequence once. Additional digests were performed to confirm the result of any positive clones. Verified positive cloned were grown to stationary phase in 200ml LB (with appropriate antibiotic) overnight at 37°C with shaking at 225rpm. Plasmid DNA was prepared using the Wizard® PureFection system (Promega), which employs paramagnetic DNA-binding beads, and stored at -20°C. Plasmid DNA was again verified by restriction mapping and direct DNA sequencing using the BigDye terminator sequencing kit (Perkin-Elmer) in a GeneAmp 2400 PCR system (Perkin-Elmer) and ABI Prism 377 sequencer (Perkin-Elmer) according to the manufacturer's instructions.

2.2.1.8 Quantification of DNA.

DNA concentration was determined by spectrophotometric quantification of a 1:100 dilution sample (in duplicate) by measuring the absorbance at 260nm (A_{260}) in a quartz cuvette using a Perkin-Elmer MBA2000 spectrophotometer. The concentration was automatically calculated using the equation: 1unit A_{260} = 50μg/ml of double stranded DNA.

2.2.1.9 *In Vitro* transcription/translation.

In vitro expression of protein was performed using the TNT T7 Quick System obtained from Promega, according to manufacturer's instructions. The system is based on a rabbit reticulocyte lysate supplemented with T7 RNA polymerase for expression of recombinant proteins cloned downstream of a T7 promoter. 1μg of plasmid DNA was added to the reticulocyte lysate (containing T7 RNA polymerase, nucleotides, amino acids (except methionine), salts and ribonuclease inhibitor) and 1μl of 1mM non-radioactive methionine. The reaction mix was incubated for 90 min at 30°C and analysed by western blotting, as detailed in section 2.2.2.3.

2.2.1.10 Synthesis of cRNA.

10μg of recombinant plasmid was linearised by restriction digestion (NdeI) overnight, in order to produce run-off transcripts of equal length, downstream of the 3' end of the insert. The linearised plasmid was then purified by phenol:chloroform:isoamyl alcohol extraction: the reaction was mixed with 1 volume of phenol:chloroform:isoamyl alcohol (25:24:1, pH 8.2) and vortexed for 1min. The mixture was centrifuged at 14,000g for 2min at 4°c (Microfuge R, Beckman) and the upper, nucleic acid-containing aqueous phase transferred to a new tube. This step was repeated and the final nucleic acid solution was mixed with 1 volume isopropanol and 0.1 volumes 3M sodium acetate (pH 5.2), vortexed briefly, and incubated at -80°C for 45 min. The solution was then centrifuged at 15,000g for 30min at 4°C and the DNA pellet was air-dried, resuspended with 5μl DEPC-H_2O and 1μl anti-RNAase, mixed carefully by pippeting up and down and transferred to a DEPC-treated eppendorf tube. cRNA was then synthesised using the mMESSAGE mMACHINE® RNA transcription system (Ambion) according to manufacturer's instructions: In the 6μl of the linearised and purified plasmid, 10μl of 2XNTP/CAP, 2μl of 10X Reaction Buffer and 2μl of T7 enzyme mix to a final volume of 20μl. The tube containing the mixture was flicked gently and incubated at 37°C for 1 hr. 1μl (2U/μl) of DNAase was then added to the

mixture to disrupt the DNA template, and the mixture was incubated at 37°C for 15min. The RNA transcripts generated were then poly-Adenylated using the Poly(A) Tailing Kit (Ambion) according to manufacturer's instructions as summarised in table 2.4:

Table 2.4 cRNA Polyadenylation

Amount	Component
20μl	mMessage mMachine reaction
36μl	Nuclease-free Water
20μl	5X E-PAP Buffer
10μl	25mM $MnCl_2$
10μl	10mM ATP
4μl	E-PAP Enzyme

The 100μl reaction mixture was incubated at 37°C for 2 hr. The recovery of cRNA was achieved by Lithium chloride (LiCl) precipitation by addition of 1.5 volumes of LiCl and the reaction mixture was incubated at -80°C overnight, to allow RNA precipitation. The RNA was pelleted by centrifugation at 21,000g for 30 min at 4°C. The pellet was washed with 1ml of 70% ethanol and recentrifuged to maximise the removal of unincorporated nucleotides. The RNA pellet was air-dried and resuspended in 1μl anti-RNAase and 9μl DEPC-H_2O. Yield was quantified by spectrophotometry of a known dilution at 280nm, where 1 unit $A_{280} \equiv 50\mu g/ml$ of single stranded RNA. The cRNA solution was diluted to 2μg/μl with DEPC-H_2O, and stored at -80°C in 2μl aliquots.

2.2.2 Protein Biochemistry Techniques.

2.2.2.1 SDS-polyacrylamide gel electrophoresis.

Proteins were analysed by SDS-polyacrylamide gel electrophoresis (SDS-PAGE) and compared against protein molecular weight (MW) markers (Rainbow MW markers, BioRad) as follows: depending on the size of the proteins to be analysed, a separating gel of the appropriate concentration was prepared according to table 2.5. The polymerisation mixture was poured into a gel casting system according to manufacturer's instructions (BioRad) and overlaid with a layer of water. Once the gel had set, the water was poured off and the remainder blotted carefully with filter paper. The stacking gel mixture was poured on top of the separating gel and a comb was inserted to form the wells. The stacking gel was always 4% and was prepared as separating gel with the only difference of using a 0.5M Tris pH 6.8 buffer. Once the stacking gel was set, the plates were clamped into an electrode assembly which was transferred to a tank and submerged in running buffer. The comb was then removed. Protein samples, which had been heated to 95°C for 5min in 3X loading buffer containing 10% w/v DTT, were loaded (20μl per well) alongside standard MW markers. Electrophoresis was carried out at constant voltage (typically 140 V) until the dye front reached the bottom of the separating gel.

Table 2.5 Separating Gel Formulation.

Gel %	**8%**	**10%**	**12%**	**15%**
Protein sizes	**>70kDa**	**30–100kDa**	**15-50kDa**	**<30kDa**
Acrylamide/Bis (37.5:1), 40%	2ml	2.5ml	3ml	3.75ml
H_2O	5.345ml	4.845ml	4.345ml	3.595ml
Tris, 1.5M, pH8.8	2.5ml	2.5ml	2.5ml	2.5ml
SDS, 10%	100μl	100μl	100μl	100μl
Ammonium persulphate, 10%	50μl	50μl	50μl	50μl
TEMED	5μl	5μl	5μl	5μl

2.2.2.2 Transfer of proteins to membranes.

Proteins from SDS-PAGE gels were transferred to a polyvinylidene difluoride (PVDF), (Immobilon-P, Millipore) membrane using a semi-dry transfer apparatus (BioRad). The SDS-PAGE gel and membrane were pre-equilibrated in semi-dry transfer buffer for 30min at room temperature (PVDF membranes were pre-soaked in methanol for 1min). The transfer apparatus was assembled according to the manufacturer's instructions, with the membrane between the gel and the anode. The proteins were transferred by electrophoresis at a constant current (20V) for 1hr at 4°C.

2.2.2.3 Western blot analysis.

After protein transfer, the membrane was incubated in TBS-T buffer containing 5% (w/v) non-fat milk protein (Marvel), (TBS-T/Marvel) for 4hr at room temperature. Primary antibodies were added in the appropriate dilution (see 2.1.9) in TBS-T/Marvel overnight at 4°C. The membrane was then washed three times (10 min each wash) with TBS-T/Marvel, the secondary antibody was added in an appropriate dilution in TBS-T/Marvel and incubated at room temperature for 1hr. The membrane was then washed three times (10 min each wash) with TBS-T. Immunoreactive bands were detected using Super Signal West Dura (Pierce) and a BioRad ChemiDoc gel documentation system for image capture.

2.2.2.4 Determination of protein concentration.

Protein concentration was determined using the BCA assay kit (Pierce) according to manufacturer's instructions. The method is based on the colour change produced by the reduction of Cu^{2+} to Cu^{+} by protein (in alkaline medium) and subsequent chelation of the Cu^{+} ion by bicinchoninic acid (BCA). The assay was performed in a 96-well plate and the absorbance read at 560nm in a Multiscan EX (Labsystems) plate reader using the Genesis (Labsystems) software program. Sample measurements were taken in triplicate for three appropriate dilutions. These were then compared to a

standard curve produced by measurement of various known concentrations of BSA (62.5μg/ml – 2mg/ml) using the same method.

2.2.2.5 Enzyme-Linked Immunosorbent Assay (ELISA).

Mice tail bleeds prior to fusion, supernatant secreted from hybridoma clones and finally purified monoclonal antibodies were all screened for antibody titres by ELISA. The well of a falcon Pro-bind ELISA plate were coated with 100μl (0.5μg) of peptide diluted in carbonate coating buffer. The plate was covered with a plastic film and incubated at 4°C overnight. Next morning the wells were washed 3 times with PBS/Tween 20 (0.05%), blocked by addition of 100μl 3% BSA/PBS per well and the plate incubated for 1 hr at room temperature wrapped in plastic film. The wells were washed again 3 times with PBS/Tween 20. 100μl of the desired antibody diluted in PBS or 200μl of undiluted supernatant from hybridoma clones added to each well and the plate incubated for 1 hr at room temperature. The wells were washed 3 times with PBS/Tween 20 and 100μl of diluted Peroxidase-conjugated secondary antibody added to each well following 1 hr incubation of the plate at room temperature. The wells were then washed for last time 3 times with PBS/Tween 20. 100μl of diluted OPD substrate (4 tablets, 12ml H_2O, 5μl 30% H_2O_2), (DAKO), was added to each well and the plate incubated for 10 min at room temperature. The reaction was stopped by addition of 100μl H_2SO_4 (0.5M) and the absorbance was then measured at 490nm.

2.2.2.6 Expression and purification of GST-tagged fusion proteins.

E. Coli Rosetta(DE3)pLysS bacteria were transformed with the appropriate pGEX construct recombinant GST-fusion vectors as described above. A 10ml culture of LB containing Ampicillin (100μg/ml) was inoculated with one colony of transformed bacteria and grown at 37°C overnight in a shaking incubator. A larger culture of LB/Amp (typically 1L) was inoculated with 5ml of the overnight culture and grown at 37°C in a shaking incubator until the optical

density, measured by absorbance at 600nm, as above, reached 0.5. Then protein expression was induced by addition of 500μg/ml (final concentration) IPTG, and the culture medium incubated at 25°C for 4hrs with shaking at 225rpm. The cells were harvested by centrifugation at 6,000g (Avanti J-25, Beckman) for 10min at 4°C. The pellet was resuspended in 30ml/L (relative to original culture vol.) PBS containing 1X total protease inhibitor cocktail (Roche). The cell suspension was then sonicated 3 times for 20sec at 4°C, to lyse the bacteria and then centrifuged at 15,000g (Allegra 6R, Beckman) for 15min to remove cell debris. 1ml of washed GSH-sepharose beads (Glutathione-Sepharose 4B, Amersham) were added to the lysate and the suspension mixed at 4°C for 2hrs. The suspension was centrifuged at 500g for 15min (Allegra 6R, Beckman) and the supernatant (flow through for column only) removed. The beads were then washed three times with 10ml PBS per 1ml of beads. Elution of GST-fusion proteins was achieved with 2 washes of 3ml elution buffer per ml of beads. The combined elutes were dialysed overnight (Snakeskin dialysis tubing 10kDa MWCO, Pierce) in PBS buffer at 4°C. The dialysed protein was then concentrated with centrifugal concentrators (Millipore) and assayed for concentration by BCA protein assay (Pierce). Finally the proteins were stored at -80°C in PBS buffer containing 40% glycerol, 2mM DTT and protease inhibitors.

2.2.2.7 Expression and purification of 6his-tagged fusion proteins.

Expression of 6his-tagged proteins was achieved as described above for expression of GST-tagged fusion proteins, but protein expression was induced by addition of L-arabinose (0.1% final concentration) and the culture medium incubated at 25°C for 3hrs with shaking at 225rpm. The cells were harvested by centrifugation at 6,000g (Avanti J-25, Beckman) for 10min at 4°C to and the pellet was resuspended in 20ml/L (relative to original culture vol.) phosphate buffer (pH 7.4) containing the appropriate protease inhibitors (as above). The cell suspension was sonicated 3 times for 20sec at 4°C, and then centrifuged at 15,000g (Allegra 6R, Beckman) for 15min. 6his-tagged

fusion protein was then purified from the soluble lysate using Probond Metal-Binding resin (Invitrogen). 2ml of resin was used per 1 L of starting culture. Resin was washed 3X10ml of phosphate buffer, then added to the lysate and placed on a roller for 1 hr at room temperature. The mixture was then passed through a 10ml gravity flow chromatography column with unbound proteins removed from the packed resin by washing with 10ml of phosphate buffer. The column was further washed 3 times with 3 different washing buffers (500mM NaCl and 20mM phosphate) with different pH (7.4, 6.3, 5.5) until the final elution of protein with 5ml of phosphate buffer (pH 4.0). The eluted protein was dialysed, concentrated and stored at -80°C in PBS containing 40% glycerol, 2mM DTT and protease inhibitors as previously described for GST-tagged fusion proteins.

2.2.2.8 PtdInsP$_2$ hydrolysis assay.

PtdInsP$_2$ hydrolysing activity of recombinant PLC constructs was assayed as described previously (Katan and Parker, 1987), with some modifications. The final volume of the assay mixture was 50 μl containing 100 mM NaCl, 0.4% sodium cholate (w/v), 2 mM $CaCl_2$, 4 mM EGTA, 20 μg bovine serum albumin, 5 mM 2-mercaptoethanol and 20mM Tris-HCl buffer, pH 6.8. The final concentration of PtdInsP$_2$ in the reaction mixture was 220 μM, containing 0.05 μCi [^{3}H]PtdInsP$_2$. The assay conditions were optimised for linearity with 10 min incubation of 20 pmol PLC protein sample at 25°C being chosen. Reactions were stopped by addition of 0.25 ml chloroform/methanol/concentrated HCl (100:100:0.6 v/v) followed by 0.075 ml of concentrated HCl. The mixture was vortexed and centrifuged at 2000 x *g* for 2 min, then 0.2 ml of the upper, aqueous phase was removed and added to 10 ml Optiphase 'Hisafe' 3 Scintillation cocktail (Wallac) and the radioactivity determined by liquid scintillation spectrofluorimetry (Packard Tri-Carb 2100TR). In assays to determine dependence on PtdInsP$_2$ concentration, 0.05 μCi [^{3}H]PtdInsP$_2$ was mixed with cold PtdInsP$_2$ to give the appropriate final concentration. In assays examining the Ca^{2+} sensitivity, Ca^{2+}

buffers were prepared by EGTA/$CaCl_2$ admixture, as described previously (Fabiato, 1981). In the assays to monitor pH dependence of the PLCs, Tris-HCl buffers were prepared over the range of pH 5.2 to 8.6.

2.2.2.9 Binding of recombinant proteins to lipids on PIP strip membranes.

PIP strips (Molecular Probes) were pre-blocked for 2 hours with binding buffer [TBS-T containing 3% BSA (lipid free)]. 100pmol of recombinant GST-fusion protein was incubated in 5 ml of TBS-T for 4 hours at room temperature. After washing 3 times with binding buffer, protein binding was visualised using the anti-GST (T103) polyclonal antibody. PIP strips were incubated with 5 ml of binding buffer containing the anti-GST antibody overnight at 4°C, followed by three 15-minute washes to remove unbound protein. PIP strips were subsequently incubated for 1 h at room temperature with an (HRP)-coupled secondary antibody diluted in the same binding buffer followed by three 15-minute washes with TBS-T. Detection of HRP-coupled antibodies was achieved using Super Signal West Dura (PIERCE) and a BioRad ChemiDoc gel documentation system for image capture.

2.2.2.10 Centrifugation/activity assay for measuring the binding of recombinant PLC proteins to phospholipid vesicles (performed in USA by Pallavi P.).

The centrifugation technique described in detail by Buser and McLaughlin, 1998 and Arbuzova *et al*, 2001 was used to measure the binding of recombinant mPLCζ to sucrose loaded PC/PS/PIP_2 Large Unilamellar Vesicles (LUVs). We mixed ~ 5nM GST-mPLCζ with sucrose-loaded LUVs in a Ca^{2+}-free solution. The mixture was centrifuged at 100,000 × g for 1 hr and the supernatant, which contained the unbound enzyme, was collected. A $PtdInsP_2$ hydrolysis assay was used to determine the concentration of mPLCζ in the supernatant (unbound enzyme). Aliquots of the supernatant were added to micelles formed from 33:33:33:1 PC/PS/PE/PIP_2 containing a trace amount

of [^{3}H]-PtdInsP$_2$, then hydrolysis was initiated by adding $CaCl_2$. 75 µl samples were removed at different times and the reaction was terminated by adding 375 µl ice-cold 10% trichloroacetic acid and 50 µl 10% (v/v) Triton X-100. The samples were incubated on ice until a white precipitate formed. Following centrifugation at 14,000 × g for 5 min, the supernatant was removed and mixed with 1ml of 2:1 chloroform/methanol. The upper phase of this mixture was transferred to a scintillation vial to determine the concentration of methanol-soluble [^{3}H]InsP$_3$ products.

The molar partition coefficient K, given by the equation:

$$\frac{[P_m]}{[P_{total}]} = \frac{K[L]}{(1+K[L])} \qquad \text{(Equation 1)}$$

where [P_m] is the concentration of enzyme partitioned onto the membrane; [P_{total}] is the total concentration of enzyme in solution and [L] is the accessible lipid concentration. We applied Equation 1 to the experimental data and obtained a value for K that was the reciprocal of the lipid concentration required to bind 50% of the peptide.

2.2.3 Cell Biology Techniques.

2.2.3.1 Preparation and handling of gametes.

Female MF1 mice were superovulated by injection of Human Chorionic Gonadotrophin (hCG) (Intervet). Eggs were collected 13.5-14.5hrs later as described by Lawrence *et al*, 1998, and maintained in 100μl droplets of H-KSOM under mineral oil at 37°C. Microinjection of the eggs was carried out 14.5-15.5hrs after hCG injection.

2.2.3.2 Microinjection and measurement of intracellular Ca^{2+} and luciferase expression.

Mouse eggs were washed in H-KSOM and microinjected as described previously (Saunders *et al*, 2002) with cRNA diluted in injection buffer (120mM KCl, 20 mM Hepes, pH 7.4). The volume injected was estimated from the diameter of cytoplasmic displacement caused by the bolus injection. All injections were 3-5% of the egg volume. In experiments with untagged PLCζ, Ca^{2+} changes were monitored with a CCD-based imaging system using a Zeiss Axiovert 100, with illumination from a monochromator (Photonics) controlled by MetaFluor v4.0 (Universal Imaging Corp.). Eggs were loaded for 10 min with 4μM Fura red-AM (Molecular Probes), dissolved in DMSO + 5% (w/v) pluronic acid, and the loading medium was supplemented with sulfinpyrazone, which helps prevent compartmentalization and extrusion of the dye (Lawrence *et al* 1998).

For experiments with luciferase-tagged PLCζ, eggs were microinjected with the appropriate cRNA mixed with an equal volume of 1mM Oregon Green BAPTA dextran (Molecular Probes) in KCl Hepes buffer. Eggs were then maintained in H-KSOM with 100μM luciferin and imaged on a Nikon TE2000, or Zeiss Axiovert 100 microscope equipped with a cooled intensified CCD camera (Photek Ltd, UK). Ca^{2+} was monitored in these eggs for 4 hours after injection by measuring the Oregon Green BAPTA dextran fluorescence with low-level excitation light from a halogen lamp. At the end of Ca^{2+} measurements, the same set of eggs were then monitored for luminescence by integrating light emission (in the absence of fluorescence excitation) for 20

minutes using the same cooled CCD camera. The fluorescence signals were typically 10-100 times greater than the luminescence signals. Ca^{2+} measurements for an egg were considered valid only if the same egg was also luminescent. Groups of eggs verified as being luminous, were then collected and placed in a test tube containing PBS with 1mM Mg.ATP + 100μM luciferin that was held in a custom-made luminometer equipped with a cooled S20 photomultiplier tube (Electron Tubes Ltd, UK). The eggs were then lysed with 0.5% Triton X-100 and the steady state light was compared to that emitted from calibrated amounts of recombinant firefly luciferase (Sigma). The amount of luciferase activity measured for each group of eggs was then divided by the number of luminous eggs to obtain the mean value for protein expression of each type of PLCζ-LUC. These experiments were performed by Karen Campbell (collaboration with Professor Karl Swann's group).

2.2.4 Monoclonal Antibody Production Techniques.

2.2.4.1. Mice immunisation.

8 Balb/c mice were immunised. 100μl of antigen (100μg) was mixed with 100μl complete Freunds adjuvant and emulsified until the mixture was thick and creamy. Mice were immunised using a 20 gauge needle. 3-4 weeks later mice were immunised as above but emulsion was made with incomplete Freunds adjuvant. 14 days later tail bleeds were taken and serum antibody titres were tested by ELISA. The mouse that gave the highest response to the antigen was marked and boosted with 100μl (100μg) antigen in PBS only. 3 days later the fusion was carried out.

2.2.4.2 Preparation of myeloma cells.

2 weeks before fusion, Sp2 mouse myeloma cells were thawed and grown in F10 medium keeping the density at $5x10^5$ to10^6 cells/ml. For the fusion $5x10^7$ cells are required.

2.2.4.3 Preparation of peritoneal macrophages.

Peritoneal macrophages were added during the fusion and cloning procedures because of their ability to produce factors stimulating cell growth and to phagocytose dead cells and debris. A Balb/c mouse was sacrificed and saturated in 70% ethanol. The skin was opened carefully and 10ml of ice-cold RPMI was injected through an 18 gauge needle into the peritoneal cavity avoiding piercing the gut. Without removing the needle the abdomen of the mouse was massaged gently and the medium was withdrawn slowly. The cells were then placed into a 50 ml falcon tube centrifuged at 1200 rpm for 10 min and resuspended in required volume of the appropriate medium.

2.2.4.4 Fusion.

The mouse with the highest immune response to the antigen was sacrificed by a staff member of the animal house unit, saturated in 70% ethanol and transferred to Class II laboratory. The spleen was removed aseptically and any excess of fatty acid tissue trimmed away. The spleen was then resuspended in 20ml of cold RPMI and homogenised gently in a sterilised round glass homogeniser until a cell suspension was formed. The spleen cells were transferred into a falcon tube. Spleen cells and harvested myeloma cells (in a separate falcon) were then washed three times in RPMI at 4°C by centrifugation (Allegra) at 1200 rpm for 5 min. Both cell populations were counted (a mouse spleen typically yields to approximately 10^8 spleen lymphocytes) and mixed together in a 2 spleen cells: 1 myeloma cell ratio in a 50ml falcon tube. The mixed cells were washed once with warm RPMI (37°C), the supernatant was discarded and the tube was inverted for a few minutes to leave the pellet as dry as possible. 1.5 ml of prewarmed (at 37°C) 50% PEG 1500 solution was added to the pellet dropwise for 60 seconds with continual gentle agitation. The mixture was then diluted to 20ml by dropwise addition of prewarmed (at 37°C) RPMI maintaining a gentle agitation. The tube was then filled to 50 ml with the same medium and cells were centrifuged at 1200 rpm for 10 min at room temperature. The supernatant was discarded, the pellet of fused cells resuspended in F15+HAT (prewarmed at 37°C) at a density of 10^6 spleen cells per ml and the cell suspension was plated out into 6 sterile 24-well-plates (0.5ml per well) containing an equal volume (0.5ml per well) of F15+HAT with the appropriate peritoneal macrophages.

2.2.4.5 Post-fusion, feeding and screening.

The wells were observed every few days to check for any contamination, myeloma cell death and subsequent hybridoma growth. One week after the fusion, 0.5 ml of medium was removed from each well and replaced with 0.5 ml of fresh F10+HAT medium. The cells were fed in this manner as required. When the hybridoma clones had grown (few mm in diameter) usually two weeks after the fusion, 200μl of supernatant from each well was collected and

screened by ELISA for clones producing the desired antibody. The contents of the wells appeared to be positive by ELISA were cloned as soon as possible to ensure that the non-producing clones did not overgrow the clone of interest.

2.2.4.6 Cloning by limiting dilution.

Peritoneal macrophages were prepared, resuspended in F10+HAT medium and 100 μl were plated out per well into 3X 96 well plates per original well that was cloned. The hybridoma cells from the original well were harvested, counted and diluted in F10+HAT medium to 100 viable cells per 50μl. Subsequently they were diluted by 3 fold dilutions to give 30, 10, 3, 1, 0.3 and 0.1 cells per 50μl. 50μl of each dilution was equally distributed to the 3X 96 well plates containing the macrophages. After 8-14 days clones appeared in some wells. The wells containing a single clone were marked and the supernatant screened by ELISA for antibody production. The positive wells were selected and expanded to 24-well-plates. Positive wells were recloned 3 times to ensure monoclonality and then expanded into flasks for large scale antibody production.

2.2.4.7 Monoclonal antibody isotyping.

Isotyping of monoclonal antibodies was achieved using Isostrip, a mouse monoclonal antibody isotyping Kit (Roche) according to manufacturer's instructions: Culture supernatant was diluted with PBS (1:10). A development tube was opened and 150 μl of diluted supernatant was added, mixed and incubated at room temperature for 30 seconds until all the latex beads had dissolved. An Isostrip was added to the solution and left for 5 minute until the positive bands were developed and the end of the strip was cut off. The isotype was determined by the position of the bands appeared on the IsoStrip.

2.2.4.8 Freezing cells.

The cell population was centrifuged at 1200 rpm for 5 min at room temperature. The supernatant was removed and the dry pellet was resuspended with 0.5 ml RPMI medium. 0.5 ml of freezing medium (FCS:20% DMSO, 1:4) was added and immediately transferred to a freezing ampoule. Freezing ampoules were placed upright in a freezing box containing isopropyl alcohol (IPA), which ensures a cooling rate of 1C/min that required for optimum cel viability, and transferred for storage into a -80 freezer. After a few days, ampoules were transferred to liquid nitrogen for long term storage.

2.2.4.9 Monoclonal antibody purification.

Monoclonal antibody was purified from crude supernatant using the Montage® Antibody Purification kit (MILLIPORE) according to manufacturer's instructions. The kits include Montage Spin Columns pre-packed with PROSEP-G media plugs for antibody purification by centrifugation. PROSEP-G media was equilibrated with 10ml Binding Buffer A by centrifuging the spin column at 500g for 5 min. Crude supernatant was pipetted into the column and the spin column was centrifuged at 100g for 20 min. The spin column was then washed with 20ml of Binding Buffer A by centrifugation at 500g for 5 min to remove any unbound contaminants. The bound IgG antibody was eluted with 10ml Elution Buffer B by centrifugation at 500g for 5 min in a new centrifuge tube, containing Neutralisation Buffer C to bring the sample to neutral pH. The eluted antibody was concentrated in the Amicon Ultra-15 centrifugal filter device with 30 NMWL.

Chapter 3

Expression and enzymatic characterisation of recombinant mouse Phospholipase C zeta (mPLCζ).

3.1 Introduction.

As described in Chapter 1, sperm-specific PLCζ elicits fertilisation like Ca^{2+} oscillations and subsequent early embryonic development when microinjected into mammalian eggs (Saunders *et al*, 2002; Cox *et al*, 2002). One unusual feature of PLCζ is that is effective at causing Ca^{2+} oscillations in eggs at very low concentrations (e.g. 10 fg/egg), (Saunders *et al*, 2002; Fujimoto *et al*, 2004; Kouchi *et al*, 2004). In contrast, other studies have shown that PLC isoforms of the β, γ or δ class are either ineffective (Jones *et al*, 2000), or much less effective than PLCζ at causing Ca^{2+} release, when microinjected in eggs (Mehlmann *et al*, 2001; Runft *et al*, 2002; Kouchi *et al*, 2004). The specific reason(s) for this are unclear particularly as little is known about the biochemical characteristics of PLCζ.

Our initial goal was to determine the enzymatic properties and characteristics of mouse mPLCζ *in vitro*. Since PLCζ expression is exclusive to sperm, *in vitro* studies of its activity necessitated the production of recombinant protein. We used a bacterial system to express recombinant mPLCζ, as this system allowed large quantities of protein to be expressed and purified quickly and at low cost.

As a control against which the biochemical properties of mPLCζ could be compared, we chose recombinant rat PLCδ1 (rPLCδ1) that could be expressed and purified using the same bacterial system. PLCζ is similar to PLCδ1 with the only apparent distinction that it lacks the PH domain (Figure 1.13). The structure of PLCδ1 molecule, including all the critical residues for the $PtdInsP_2$ binding and hydrolysis has been determined by X-ray crystallography (Essen *et al*, 1996; Essen *et al*, 1997). In addition, PLCδ1 is the best biochemically characterised isoform of PLC families (Katan and Williams, 1997; Katan, 1998; Williams, 1999).

After successful expression and purification of recombinant mPLCζ and rPLCδ1, an *in vitro* [^{3}H]$PtdInsP_2$ hydrolysis assay was used to explore their enzymatic properties and characteristics. To assess the affinity of these recombinant proteins for different phosphinositides an overlay assay was used. In addition to this approach; and in collaboration with Professor

McLaughlin's group (Department of Physiology and Biophysics, Stony Brook University), we used a centrifugation/activity assay to measure the binding of the recombinant proteins to phospholipids vesicles.

3.2 Results.

3.2.1 Cloning of mPLCζ into pGEX-5X-2 vector.

mPLCζ was amplified by PCR from the original cDNA clone using the appropriate primers to incorporate a 5'-EcoRI site and a 3'-SalI site for cloning into pGEX-5X-2 expression vector (Figure 3.1).

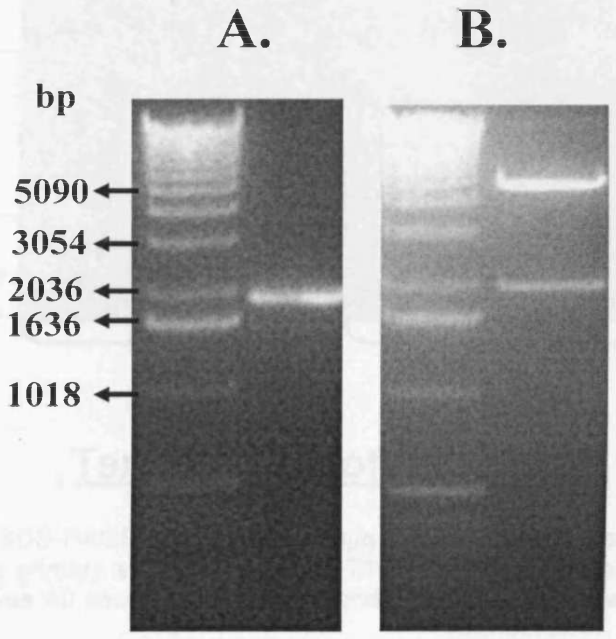

Figure 3.1 A. 1% agarose gel showing the product of PCR screen of a positive clone from transformation of pGEX-5X-2-mPLCζ ligation mixture into *E. coli* TOP10 cells. Colony DNA was screened using the same oligonucleotide primers used in amplification of mPLCζ. The band between 1.9 and 2.0kb represents the mPLCζ insert. **B.** 1% agarose gel showing the products of enzymatic digestion of DNA mini-prep corresponding to the same positive clone, using EcoRI and SalI restriction enzymes. The 4.9kb band represents the pGEX-5X-2 vector and the band between 1.9 and 2.0kb represents the mPLCζ insert.

3.2.2 Optimisation of expression of recombinant GST-mPLCζ.

3.2.2.1 Optimisation of temperature and time of induction.

The optimal temperature for the expression of GST-mPLCζ protein was determined by growing the cultures at 25 and 30°C. The cultures were induced with 0.1mM of IPTG for 1, 4 and 6 hours. Soluble fractions of the protein were produced as described in section 2.2.2.6, and it can be shown

from Figure 3.2 that the conditions for maximum protein production were 25°C for 4 hours of induction.

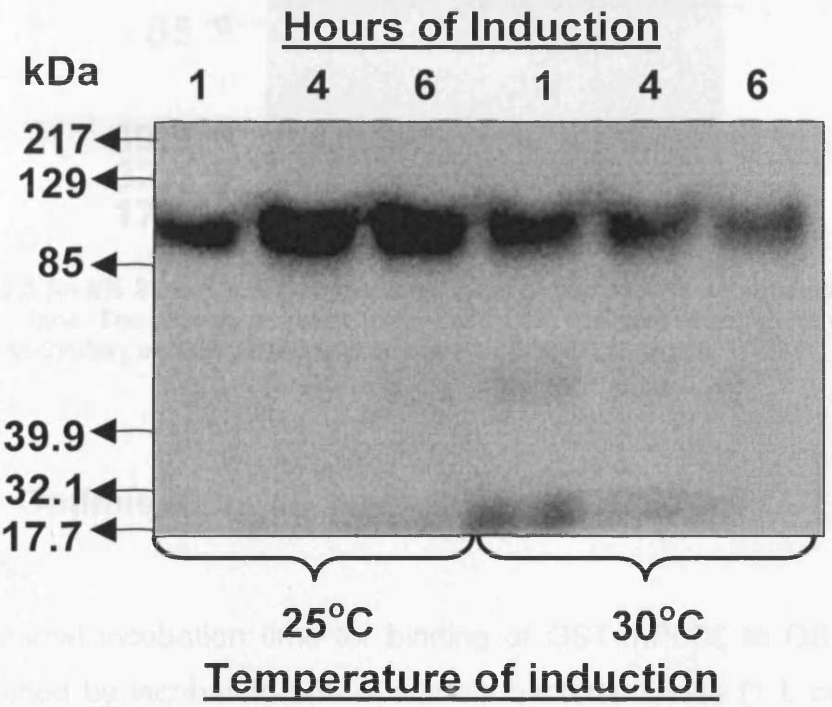

Figure 3.2 An 8% SDS-PAGE gel was used. 30μg of bacterial lysate supernatant was loaded into each lane. The primary antibody used was T103, which recognises the GST moiety. The time of exposure was 40 seconds and the secondary antibody used was an anti-rabbit HRP conjugate.

3.2.2.2 Optimisation of inducing agent (IPTG).

Four different IPTG concentrations (0.05, 0.1, 0.5 and 1mM) were used to induce the cultures for 4 hours at 25°C. The soluble fractions after bacterial breakage analysed by western blot (Figure 2.3) and the results suggested that 0.5mM of IPTG was sufficient for maximum protein production.

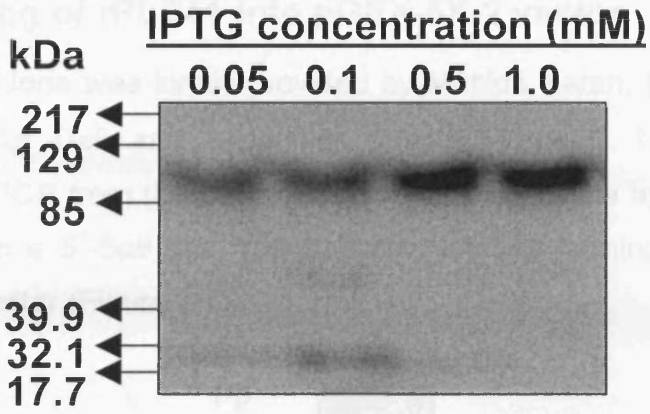

Figure 3.3 An 8% SDS-PAGE gel was used. 30μg of bacterial lysate supernatant was loaded into each lane. The primary antibody used was T103. The time of exposure was 45 seconds and the secondary antibody used was an anti-rabbit HRP conjugate.

3.2.3 Optimisation of purification of GST-mPLCζ with GST beads.

The optimal incubation time for binding of GST-mPLCζ to GST beads was determined by incubating 5ml of soluble bacterial lysate (1 L original culture was used in this experiment resulting in 20ml of soluble bacterial lysate of 13mg/ml concentration) with 0.25ml of GST-beads for 10, 30, 60 and 120 minutes at 4°C (to avoid protein degradation). GST-mPLCζ was eluted with 3 ml of 10mM glutathione and elutes were analysed by western blot (Figure 3.4). Results suggested that 120 minutes incubation was sufficient for maximum protein binding to the beads.

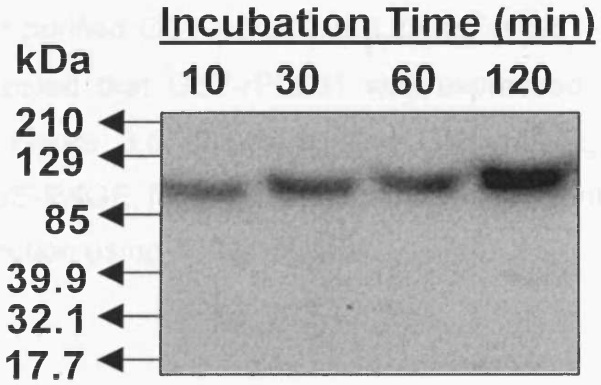

Figure 3.4 An 8% SDS-PAGE gel was used. 15μl of elutes were loaded into each lane. The primary antibody used was T103. The time of exposure was 10 seconds and the secondary antibody used was an anti-rabbit HRP conjugate.

3.2.4 Cloning of rPLCδ1 into pGEX-5X-2 vector.

The rPLCδ1 clone was kindly provided by Matilda Katan, (Cancer Research UK Centre for Cell and Molecular Biology, London, UK). rPLCδ1 was amplified by PCR from the original cDNA clone using the appropriate primers to incorporate a 5'-SalI site and a 3'-NotI site for cloning into pGEX-5X-2 expression vector (Figure 3.5).

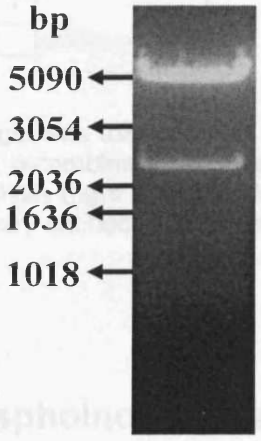

Figure 3.5 1% agarose gel showing the products of enzymatic digestion of DNA mini-prep corresponding to a positive clone of pGEX-5X-2-rPLCδ1, using SalI and NotI restriction enzymes. The 4.9kb band represents the pGEX-5X-2 vector and the band at approximately 2.4 kb represents the rPLCδ1 insert.

3.2.5 Large-scale production of recombinant GST-mPLCζ and GST-rPLCδ1.

We used all the optimised parameters to express and purify large quantities of GST-mPLCζ and GST- rPLCδ1. 1 L of starting culture typically resulted in a yield of 0.3mg of purified GST-mPLCζ and 2.4mg of GST-rPLCδ1. This 8 fold difference suggested that GST-rPLCδ1 was expressed at higher levels in bacterial cells. Figure 3.6 shows purified GST-mPLCζ and GST-rPLCδ1 analysed by SDS-PAGE followed by Coomassie Brilliant-Blue staining and immunoblot detection using T103 antibody.

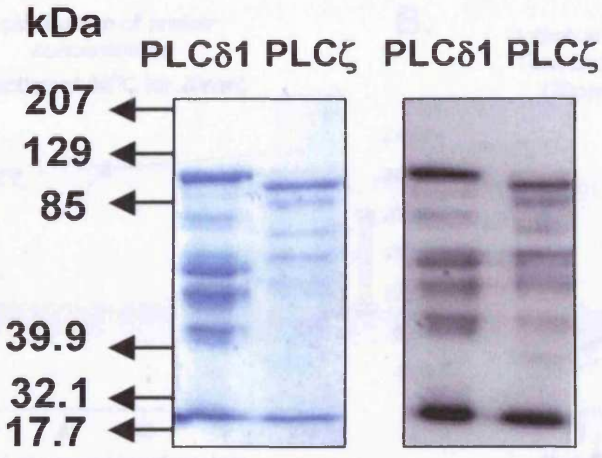

Figure 3.6 An 8% SDS-PAGE gel was used. 1μg of purified GST-mPLCζ and GST-rPLCδ1 was loaded into each lane and recombinant proteins analysed by Coomassie Brilliant-Blue (left panel) and immunoblot analysis (right panel) using T103 antibody. The time of exposure was 30 seconds and the secondary antibody used was an anti-rabbit HRP conjugate.

3.2.6 Assay of phosphoinositide-specific phospholipase C activity.

The $PtdInsP_2$ hydrolysis activity of recombinant PLC proteins was assessed by hydrolysis of $[^3H]PtdInsP_2$ (see 2.2.2.8). Hydrolysis of $[^3H]PtdInsP_2$ to $[^3H]InsP_3$ was optimised for PLC activity by varying a series of parameters including reaction time, reaction temperature and protein concentration. Linearity of $[^3H]PtdInsP_2$ cleavage was obtained by 20pmol of recombinant protein incubated with 220μM $[^3H]PtdInsP_2$ for 10 minutes at 25°C (Figure 3.7).

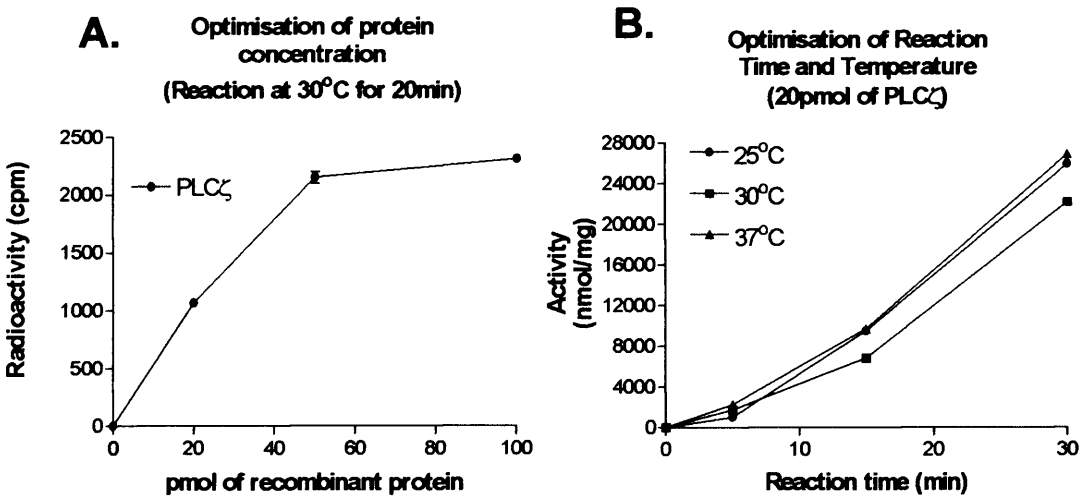

Figure 3.7 Optimisation of [^{3}H]PtdInsP$_2$ hydrolysis assay. A. Optimisation of protein concentration. Enzyme assays were performed using different concentrations of recombinant GST-mPLCζ ranging from 20 to 100pmol, at 30°C for 20 min. B. Optimisation of time and temperature of reaction. Enzyme assays were performed using 20pmol of recombinant GST-mPLCζ at variable temperatures (ranging from 25°C to 37°C) and times of reaction (ranging from 5 to 30 min), n=2 ± s.e.m, using 2 different batches of recombinant protein. Each experiment was performed in duplicate.

3.2.7 Comparison of hydrolysing activity of recombinant GST-mPLCζ and GST-rPLCδ1 .

Following optimisation of the PtdInsP$_2$ hydrolysis assay, hydrolysing activities of GST-mPLCζ and GST-rPLCδ1 were estimated at ambient Ca^{2+} (no addition of EGTA). For negative control we used purified GST. GST-mPLCζ and GST-rPLCδ1 showed an activity of 410±30nmol/min/mg and 1319±28nmol/min/mg respectively (Figure 3.8).

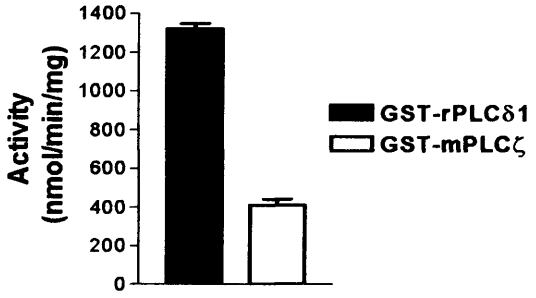

Figure 3.8 PtdInsP$_2$ hydrolysis activity of GST-mPLCζ and GST-rPLCδ1 (20 pmol) using the standard [^{3}H]PtdInsP$_2$ cleavage assay , n=2 ± s.e.m, using 2 different batches of recombinant protein. Each experiment was performed in duplicate.

3.2.8 Production of recombinant, bacterially expressed mPLCζ-6his protein.

GST is a very efficient tag to purify fusion proteins but is a relatively large tag (26KDa). In order to test whether GST tag had any effect on the conformation of GST-mPLCζ and thus on its hydrolytic activity, it was necessary to compare the hydrolytic activity of GST-mPLCζ with the activity of another recombinant bacterially expressed mPLCζ with a smaller tag. For this reason we expressed and purified (see 2.2.2.7) recombinant mPLCζ-6his (a pBad-mPLCζ construct kindly provided by Dr Chris Saunders). Figure 3.9 shows a Coomassie and a western blot of purified mPLCζ-6his protein.

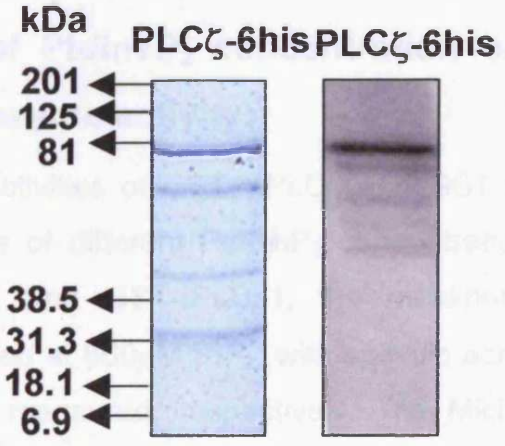

Figure 3.9 A 10% SDS-PAGE gel was used. 1μg of purified mPLCζ-6his was loaded into each lane and recombinant protein analysed by Coomassie Brilliant-Blue (left panel) and immunoblot analysis (right panel) using an anti-c-myc antibody. The time of exposure was 60 seconds and the secondary antibody used was an anti-mouse HRP conjugate.

3.2.9 Comparison of hydrolysing activity of GST-mPLCζ and mPLCζ-6his.

Hydrolysing activity of mPLCζ-6his was estimated using the standard [^{3}H]PtdInsP$_2$ hydrolysis assay and compared to that of GST-mPLCζ (Figure 3.10). Activities appeared to be very similar since GST-mPLCζ showed an activity of 400±26nmol/min/mg and mPLCζ-6his an activity of 370±38nmol/min/mg.

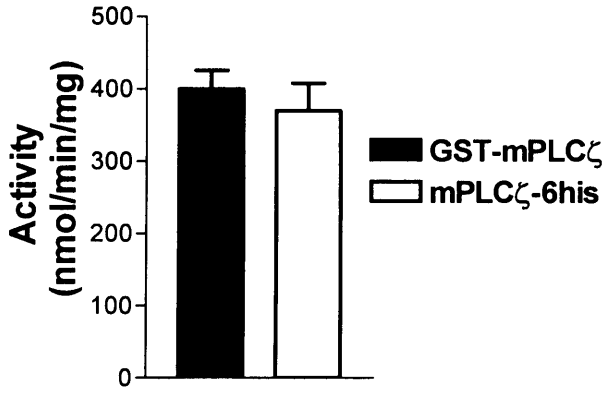

Figure 3.10 $PtdInsP_2$ hydrolysis activity of GST-mPLCζ and mPLCζ-6his (20 pmol) using the standard [^{3}H]$PtdInsP_2$ cleavage assay , n=2 ± s.e.m, using 2 different batches of recombinant protein. Each experiment was performed in duplicate.

3.2.10 Effect of $PtdInsP_2$ concentration on GST-mPLCζ and GST-rPLCδ1 enzyme activity.

The hydrolysing activities of GST-mPLCζ and GST-rPLCδ1 were estimated over a wide range of different $PtdInsP_2$ concentrations (Figure 3.11A). For both GST-mPLCζ and GST-rPLCδ1, the maximum hydrolysing enzyme activity was obtained at 660μM PIP_2, with specific activity values of 1884 and 770 nmol/min/mg measured, respectively. The Michaelis-Menten constant, *Km*, was calculated by a Lineweaver-Burk reciprocal plot for both recombinant proteins and was very similar, with PLCζ having a *Km* value of 87μM in comparison to 75μM for rPLCδ1 (Figure 3.11B).

A.

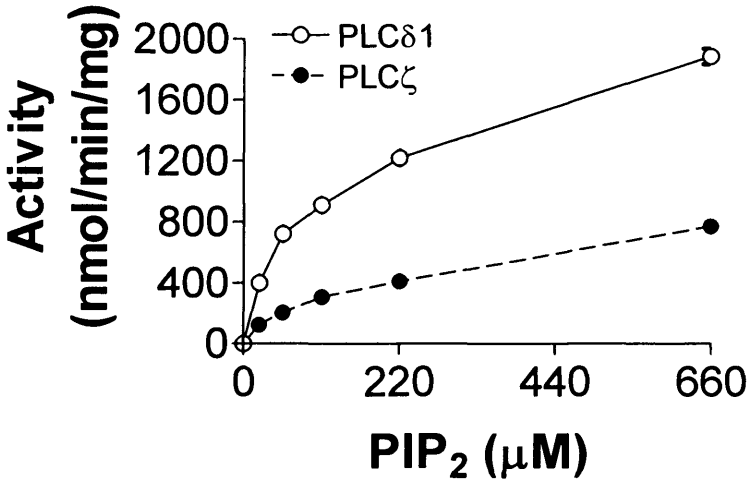

B.

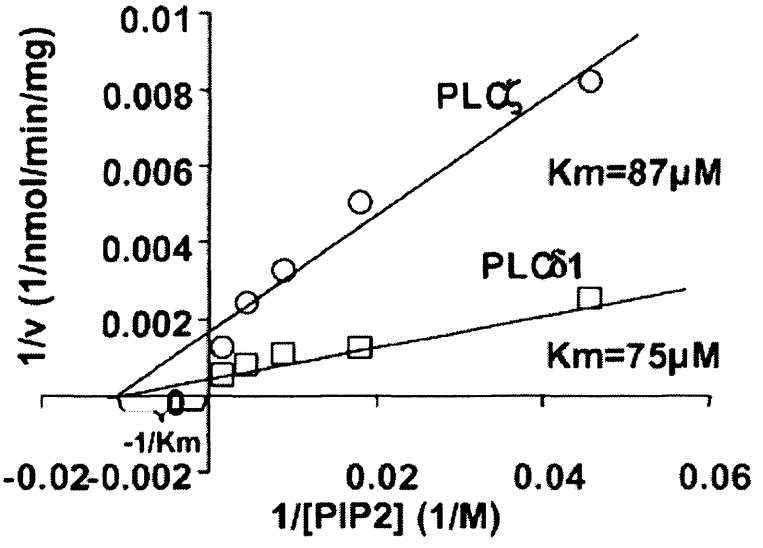

Figure 3.11 A, [^{3}H]PIP_2 hydrolysis assay of PLCδ1 and PLCζ activities as a function of PIP_2 concentration. **B**, Lineweaver-Burk reciprocal plots for determination of the *Km* for PIP_2, yielding values of 75μM and 87μM for PLCδ1 and PLCζ respectively. For A, n=2 ± s.e.m, using 2 different batches of recombinant proteins and each experiment was performed in duplicate.

3.2.11 Calcium and pH dependence of recombinant GST-mPLCζ and GST-rPLCδ1.

We tested the ability of GST-mPLCζ and GST-rPLCδ1 to hydrolyse [^{3}H]PtdInsP$_2$ at different Ca^{2+} concentrations ranging from 0.1mM to 0.1nM (Fig. 11A), and at different pH values ranging from 5.2 to 8.6 (Figure 11B). Although GST-rPLCδ1 and GST-mPLCζ had common enzymatic properties with regards to PtdInsP$_2$, the Ca^{2+} dependence of their activities were markedly different (Figure 3.12A). GST-mPLCζ was activated between 0.01 and 0.1μM Ca^{2+}, whereas the threshold for GST-rPLCδ1 was 0.1μM, with maximum activity at about 100μM. The EC_{50} was 82nM (Hill constant, 4.3) for GST-mPLCζ and 6.0μM (Hill constant, 1.5) for GST-rPLCδ1 (calculated from Figure 11A). GST-mPLCζ showed maximal activity over a broad pH range, varying between 5.2 and 6.0, in contrast with GST-rPLCδ1, which displayed an optimum pH at 6.0 (Figure 3.12B).

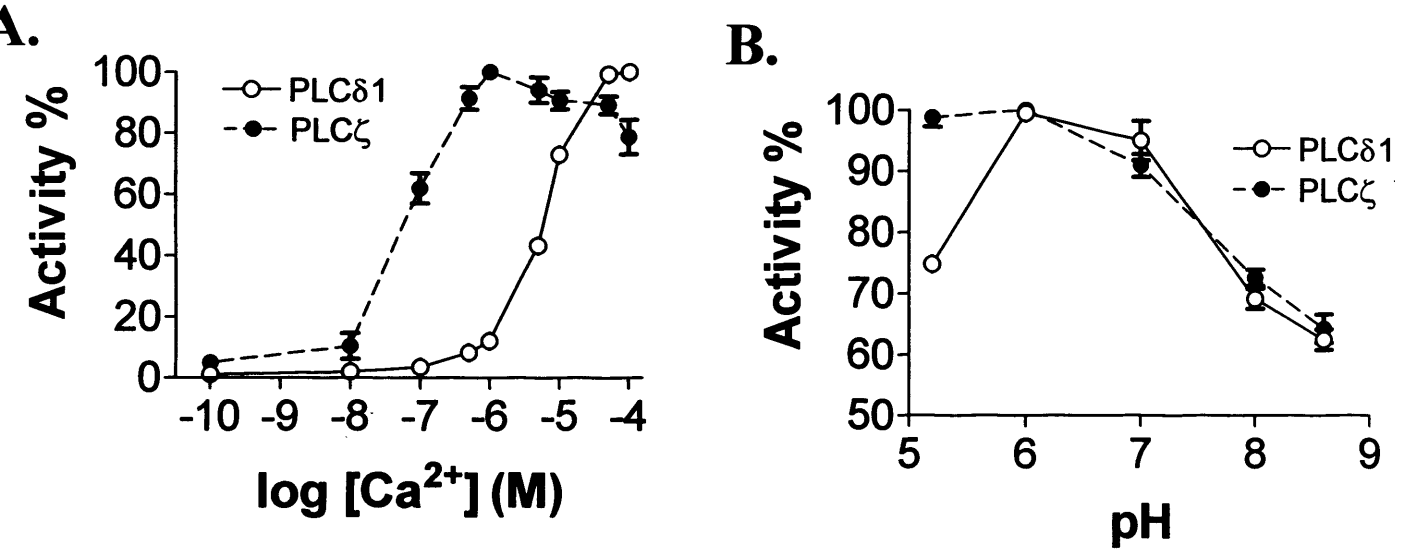

Figure 3.12 A, Effect of [Ca^{2+}] on the PtdInsP$_2$ hydrolysis activity of rPLCδ1 and mPLCζ. Enzyme assays were performed in different free [Ca^{2+}] ranging from 0.1mM to 0.1nM, as outlined in Experimental Procedures. **B**, Effect of pH on enzyme activity of rPLCδ1 and mPLCζ. The pH of the reaction was varied between pH 5.2 and pH 8.6, as outlined in Materials and Methods. For all assays, n=2 ± s.e.m, using 2 different batches of recombinant proteins and each experiment was performed in duplicate.

3.2.12 Binding of GST-mPLCζ to phosphoinositides on 'PIP' strips.

PLCδ1 targets membrane using its PH domain, which is lacking from the full-length PLCζ sequence. To determine the ability of GST-mPLCζ to specifically bind to inositol phosphoinositides, we used an overlay assay to test the binding of recombinant protein to phosphoinositides and lipids that were spotted onto nitrocellulose membrane (PIP strips) as described previously (Varnai *et al*, 2002). For comparison and in addition to rPLCδ1, we used a number of negative and positive controls. These include a truncated construct of rPLCδ1 (ΔPHδ1) in which the N-terminal PH domain was deleted; the PH domain of rPLCδ1 (δ1PH) and the GST moiety, all produced as recombinant GST proteins.

3.2.12.1 Cloning of ΔPHδ1 and δ1PH into pGEX-5X-2 vector.

ΔPHδ1 was amplified by PCR from the original rPLCδ1 clone using the appropriate primers to incorporate a 5'-SalI site and a 3'-NotI site. δ1PH was amplified by PCR from the original rPLCδ1 clone using the appropriate primers to incorporate a 5'-EcoRI site and a 3'-SalI site for cloning into the pGEX-5X-2 expression vector (Figure 3.13).

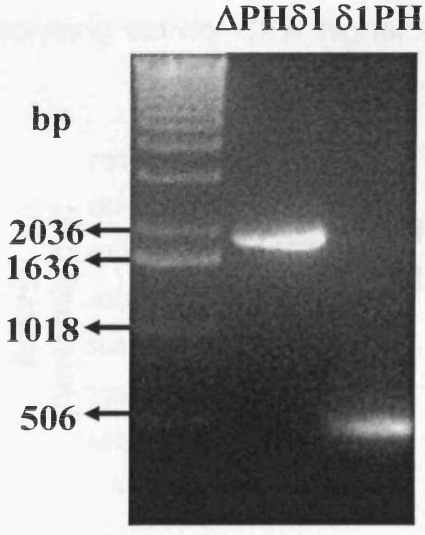

Figure 3.13 1% agarose gel showing the products of PCR screen of positive clones from transformation of pGEX-5X-2-ΔPHδ1 and pGEX-5X-2-δ1PH ligation mixtures into *E. coli* TOP10 cells. Colony DNA was screened using the same oligonucleotide primers used in amplification of these constructs.

3.2.12.2 Expression and purification of ΔPHδ1 and δ1PH as GST-tagged fusion proteins.

We expressed and purified recombinant GST-tagged ΔPHδ1 and δ1PH. Figure 3.14 shows a Coomassie and a western blot of purified recombinant proteins.

Figure 3.14 An 8% SDS-PAGE gel was used. 1μg of purified GST-ΔPHδ1 and GST-δ1PH was loaded into each lane and recombinant proteins analysed by Coomassie Brilliant-Blue (left panel) and immunoblot analysis (right panel) using T103 antibody. The time of exposure was 20 seconds and the secondary antibody used was an anti-rabbit HRP conjugate.

3.2.12.3 Comparison of hydrolysing activity of GST-ΔPHδ1 and GST-mPLCζ.

Hydrolysing activity of GST-ΔPHδ1 was estimated using the standard [^{3}H]PtdInsP$_2$ hydrolysis assay and compared to that of GST-mPLCζ. GST-ΔPHδ1 showed a hydrolysing activity 67% higher than that of GST-mPLCζ (Figure 3.15).

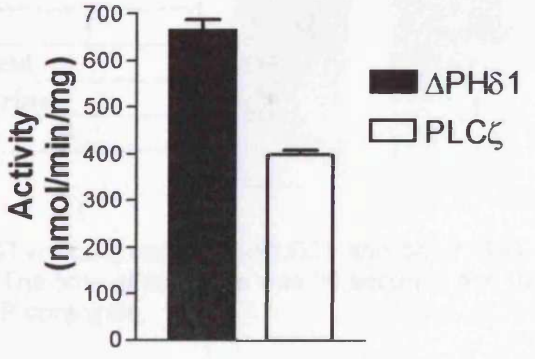

Figure 3.15 PtdInsP$_2$ hydrolysis activity of GST-mPLCζ and GST-ΔPHδ1 (20 pmol) using the standard [^{3}H]PtdInsP$_2$ cleavage assay , n=2 ± s.e.m, using 2 different batches of recombinant protein. Each experiment was performed in duplicate.

3.2.12.4 Binding of GST-mPLCζ to phosphoinositides.

PIP strips were incubated with 100pmol of each recombinant protein overnight at 4°C and bound GST-recombinant protein was detected after washing, using a western bloting with the polyclonal antibody T103. As shown in Figure 3.16, GST-rPLCδ1 and GST-mPLCζ showed similar inositol binding profiles for PtdIns(4)P, PtdIns(5)P PtdIns(3,5)P_2 and PtdIns(4,5)P_2. GST-δ1PH showed high affinity for these phosphoinositides but GST-ΔPHδ1 showed greatly diminished binding compared to both full length GST-rPLCδ1 and GST-mPLCζ. GST itself showed no binding under the same conditions. This result was a first indication that GST-mPLCζ could target PtdIns(4,5)P_2 without a PH domain, suggesting that other domains in its sequence might be involved in targeting to phosphoinositides.

Spot #	PIP Strips
1	Lysophosphatic acid
2	Lysophosphatidylcholine
3	Phosphatidylinositol (PI)
4	PI(3)P
5	PI(4)P
6	PI(5)P
7	Phosphatidylethanolamine
8	Phosphatidylcholine
9	Sphigosine 1phosphate
10	PI(3,4)P2
11	PI(3,5)P2
12	PI(4,5)P2
13	PI(3,4,5)P3
14	Phosphatidic acid
15	Phosphatidylserine
16	Blank

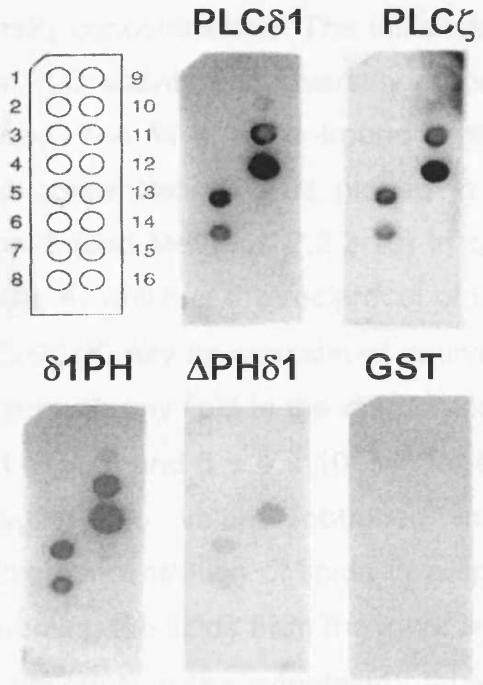

Figure 3.16 Binding of GST-mPLCζ and GST-rPLCδ1 and other GST control constructs to various phosphoinositides. The time of exposure was 60 seconds and the secondary antibody used was an anti-rabbit HRP conjugate.

3.2.13 Inclusion of $PtdInsP_2$ in the membrane significantly enhances the binding of GST-mPLCζ to phospholipid vesicles.

Recombinant GST-rPLCδ1 and GST-mPLCζ proteins were expressed and purified in our laboratory and sent to USA (Department of Physiology and Biophysics, Stony Brook University), where Payal Pallavi measured the binding of these catalytically competent proteins to phospholipids vesicles, using a centrifugation/activity assay (See section 2.2.2.10). In the experiments performed, the binding of the active enzyme to vesicles was monitored. Enzyme was mixed with sucrose-loaded phospholipid vesicles. Centrifugation was used to remove the vesicles and the bound enzyme. The concentration of active GST-mPLCζ remaining in the supernatant was determined by using it to hydrolyse radioactive [^{3}H]$PtdInsP_2$ in micelles. Figure 3.17A illustrates the rate of [^{3}H]$PtdInsP_2$ hydrolysis of the unbound enzyme remaining after binding to vesicles of 3 different PC/PS/$PtdInsP_2$ concentrations. The initial slopes of these curves were proportional to the PLC activity and inversely proportional to the lipid vesicle concentration added. The % enzyme bound to the lipid vesicles as a function of these lipid concentrations was plotted in Figure 3.17B, which show the fit of Equation 1 (see Methods 2.2.2.10) in order to determine the molar partition coefficient, K, which is the reciprocal of the lipid concentration that binds 50% of the PLCζ (K may be considered equivalent to the 1:1 association constant of a protein with any lipid in the membrane). We deduced $K = 4 \pm 0.5 \times 10^2\ M^{-1}$ for 2:1 PC/PS and $6 \pm 4 \times 10^3\ M^{-1}$ for 66:33:1 PC/PS/$PtdInsP_2$ vesicles by averaging the values obtained in three independent experiments. The effective concentration of lipids in a spherical cell of diameter 10 μm is ~10^{-3} M (assuming the lipids from the inner leaflet of the plasma membrane are dissolved uniformly in the cytoplasm); thus, PLCζ must have a molar partition coefficient of $K \geq 10^3\ M^{-1}$ to anchor a significant fraction of the enzyme to the plasma (and/or internal) membranes of a human egg. The results in Figure 3.17 suggest that mPLCζ can bind significantly to inner leaflet of a plasma membrane that contains a typical physiological mole fraction (1%) of $PtdInsP_2$. Curiously, the binding affinity of GST-mPLCζ for

PC/PS/PtdInsP$_2$ vesicles is only slightly lower than that of GST-rPLCδ1, even though the former lacks a PtdInsP$_2$-targeting PH domain. Specifically, if we assume that mPLCζ forms a 1:1 complex with PtdInsP$_2$, as does the PH domain of rPLCδ1, then K = $6x10^3$ M^{-1} corresponds to an 1:1 association constant of $6x10^5$ (K_d ~2 uM), which is only ~2-fold less than the binding constant for the PH domain for PtdInsP$_2$ in a PC/PS/PtdInsP$_2$ membrane (Rebecchi and Pentyala, 2000). GST-PLCζ bound equally well to PC/PS/PtdInsP$_2$ vesicles when we substituted PtdIns(3,5)P$_2$ for PtdIns(4,5)P$_2$ (data not shown); in contrast, GST-rPLCδ1 did not bind significantly to PC/PS/PtdIns(3,5)P$_2$ vesicles (data not shown). GST-rPLCδ1, did not bind significantly to PC/PS/PtdIns(3,5)P$_2$ vesicles (not shown). This result was expected from previous work that demonstrates the PH domain of rPLCδ1 binds with high specificity to PtdIns(4,5)P$_2$ (Lemmon and Ferguson, 2000; Lemmon, 2003). Thus mPLCζ lacks the specificity of rPLCδ1 for the 4,5 versus 3,5 phosphoinositide head group, but it is clear that strongly selects polyvalent phosphoinositides.

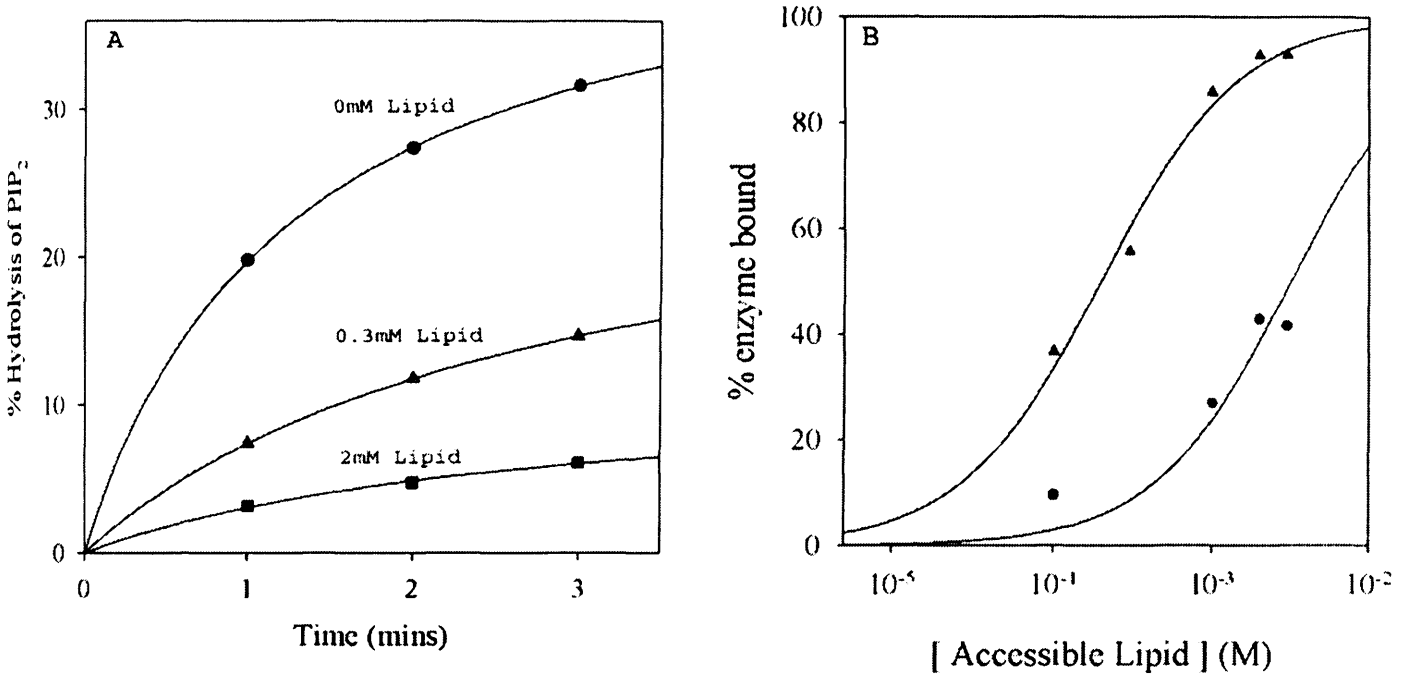

Figure 3.17 A Plot of the % radioactive $PtdInsP_2$ hydrolysed in micelles versus time after addition of supernatant containing PLCζ from an ultracentrifugation experiment. In the centrifugation experiment, ~5 nM of GST-mPLCζ was mixed with 66:33:1 PC/PS/$PtdInsP_2$ LUVs present at an accessible lipid concentration of 0mM [•], 0.3 mM [▲] and 2 mM [■]. The initial slopes are proportional to the GST-mPLCζ concentration. **B** Plot of % GST-PLCζ bound to 2:1 PC/PS [•] and to 66:33:1 PC/PS/$PtdInsP_2$ [▲] vesicles vs. accessible lipid concentration. The curves show the best fits of Equation 1 to the data. The molar partition coefficients (K) for binding of the enzyme to 2:1 PC/PS and 66:33:1 PC/PS/$PtdInsP_2$ vesicles are 3.5×10^2 M^{-1} and 5×10^3 M^{-1} respectively. The average and SD for three similar experiments are: $(4 \pm 0.5) \times 10^2$ M^{-1} (n=3) for 2:1 PC/PS and $(6\pm4)\times10^3$ M^{-1} (n=3) for 66:33:1 PC/PS/$PtdInsP_2$ vesicles.

3.1 Discussion.

We have examined the enzymatic properties of recombinant mPLCζ and its binding characteristics to $PtdInsP_2$, in comparison to rPLCδ1. Full-length mPLCζ and rPLCδ1 were produced as GST-tagged fusion proteins in a bacterial expression system. Coomassie and western blot analysis showed each to be expressed with minimal degradation products (Figure 3.6). To test whether GST moiety had any effect on the conformation of mPLCζ and thus its enzymatic activity, recombinant bacterially expressed mPLCζ-6his tagged protein was produced (Figure 3.9). Activities of both GST-mPLCζ and mPLCζ-6his appeared to be very similar (Figure 3.10), suggesting that the GST had no effect on the activity of GST-mPLCζ.

A previous study by others (Kouchi *et al*, 2004), expressed his-tagged recombinant mPLCζ using the Baculovirus/Sf9-cell expression system. In comparison, the specific activity of our GST-mPLCζ was 2 fold lower. This variance possibly resulted from the different expression and purification systems. However there was a striking similarity in the Ca^{2+} sensitivity in both studies, each of which compared the activity of recombinant mPLCζ to that of rPLCδ1. Our assays of GST-rPLCδ1 were consistent with this earlier work as we found the EC_{50} for Ca^{2+}-dependance of GST-rPLCδ1 to be 6μM. In contrast GST-mPLCζ appeared to be 100 times more sensitive with an EC_{50} of 82nM, which is within the range of reported resting Ca^{2+} concentrations in eggs. GST-mPLCζ was maximally active at 1μM Ca^{2+} but GST-rPLCδ1 was not fully activated until 30μM. We found that the dependency of GST-mPLCζ activity on Ca^{2+} had a Hill coefficient of 4.3 suggesting the binding of 4 Ca^{2+} molecules/protein. This is greater than the report of 0.9 by Kouchi *et al.* The reason for this difference is unclear. It is unlikely to be a systematic difference in the assay since the calculated EC_{50} and Hill coefficients for the Ca^{2+}-dependence of rPLCδ1 were very similar between the two studies (1.5 and 1.7 respectively), (Kouchi *et al.* 2004). The different Ca^{2+} sensitivity and Hill coefficient between mPLCζ and rPLCδ1 could explain why PLCζ is so effective at causing Ca^{2+} oscillations in mouse eggs while PLCδ1 has been reported to be much less effective (Kouchi *et al*, 2004).

The dependence of GST-mPLCζ and GST-rPLCδ1 activity on the PtdIns(4,5)P_2 concentration was determined (Figure 3.11A). Lineweaver-Burk reciprocal plot were used to calculate the Michaelis constant *Km* for these recombinant proteins (Figure 3.11B). The *Km* values were very similar, 87μM for GST-mPLCζ and 75μM for GST-rPLCδ1, denoting that the enzymes have similar affinity for their substrate PtdIns(4,5)P_2. This result is consistent with the X and Y active site domains being highly conserved throughout the PI-PLC family and is in reasonable agreement with the value for his-tagged PLCδ3 (142μM) in another study (Pawelczyc and Matecki, 1997a).

The activities of GST-mPLCζ and GST-rPLCδ1 were compared over a broad range of pH (Figure 3.12B). The optimum range was 5.2 to 6.0 for GST-mPLCζ and 6.0 for GST-rPLCδ1.

The PH domain is well characterised with regard to targeting of PLC enzymes to a PtdIns(4,5)P_2 source (Lemmon *et al*, 1995; Varnai *et al*, 2002). It has been shown that high affinity binding of PtdIns(4,5)P_2 to the PH domain of PLCδ1 leads to an enhanced enzyme activity (Lomansey *et al*, 1996). Since PLCζ lacks a PH domain, its ability to bind to phosphoinositides and especially PtdIns(4,5)P_2, was tested using a 'PIP' strip overlay assay. For comparison, constructs of rPLCδ1 lacking the PH domain (GST-rΔPHδ1) and the rPLCδ1 PH domain alone (GST-rδ1PH) were made. GST alone was used as negative control. Full-length GST-rPLCδ1 and GST-mPLCζ showed a very similar profile of binding specificity and magnitude of binding for PtdIns(4)P, PtdIns(5)P, PtdIns(3,5)P_2 and PtdIns(4,5)P_2 (Figure 3.16). The GST-rδ1PH domain construct showed high affinity for these phosphoinositides as demonstrated by others (Varnai *et al*, 2002), and the GST moiety alone showed no binding under the same conditions. In contrast, the binding of GST-rΔPHδ1 was greatly diminished, even though in the *in vitro* hydrolysis assay showed a 67% higher activity than that of GST-mPLCζ (Figure 3.15). The loss of the PH domain from rPLCδ1 resulted in loss of phosphoinositide binding suggesting that this was the primary domain to target rPLCδ1 to PtdInsP_2. However mPLCζ must target PtdIns(4,5)P_2 through other domains in its sequence.

For further confirmation of this result, another set of experiments was performed in collaboration with Professor McLaughlin's group (Department of Physiology and Biophysics, Stony Brook University). Recombinant GST-rPLCδ1 and GST-mPLCζ proteins were prepared (in our laboratory) and sent to USA, where Payal Pallavi measured the binding of these catalytically competent proteins to phospholipids vesicles, using a centrifugation/activity assay. GST-mPLCζ bound to a 2:1 PC/PS membrane with too low affinity ($K \sim 10^2\ M^{-1}$) to anchor a significant fraction of the enzyme to the PC/PS component of a biological membrane (Fig 3.17). Interestingly incorporating a physiological (1%) mole fraction of $PtdInsP_2$ into 2:1 PC/PS vesicles significantly (~15 fold) enhanced binding of the enzyme (Figure 3.17). This suggested that the affinity of mPLCζ for PC/PS/$PtdInsP_2$ membranes is strong enough to be biologically significant. This enhancement in GST-mPLCζ binding with the incorporation of $PtdInsP_2$ was reminiscent of GST-rPLCδ1, which has a PH domain that binds with high affinity to $PtdIns(4,5)P_2$ to form a stoichiometric 1:1 complex of known structure (K_d = 2μM for PC/$PtdIns(4,5)P_2$ membrane). However GST-mPLCζ, lacking a PH domain, did not distinguish between $PtdIns(3,5)P_2$ and $PtdIns(4,5)P_2$ isoforms. This data confirmed the 'PIP' strip data showing that mPLCζ has a high binding affinity for $PtdInsP_2$ and further investigation of which PLCζ domains may contribute to that binding is required.

Chapter 4

Role of EF hand, XY catalytic and C2 domains on the enzymatic activity and targeting of mPLCζ.

4.1 Introduction.

In chapter 3 we investigated the enzymatic properties of PLCζ using recombinant bacterially expressed mPLCζ protein. We demonstrated two critical properties of mPLCζ. Using a $PtdInsP_2$ hydrolysis assay we showed a high Ca^{2+} sensitivity for mPLCζ compared with rPLCδ1, which was likely to enable PLCζ to trigger Ca^{2+} release in cells at the resting Ca^{2+} state. We also showed high binding affinity of mPLCζ for $PtdInsP_2$, although this protein lacked the PH domain from its sequence, which is responsible for rPLCδ1 binding to $PtdIns(4,5)P_2$. mPLCζ showed high affinity for $PtdIns(3,5)P_2$ and $PtdIns(4,5)P_2$ in both overlay and centrifugation/activity assays.

The aim of this chapter was to investigate the role of EF hands, XY catalytic and C2 domains on the hydrolysing activity and Ca^{2+} sensitivity of PLCζ, and its ability to bind $PtdInsP_2$. A series of domain deletion constructs of mPLCζ were expressed in the same bacterial system used previously and purified as GST-tagged fusion proteins. These deletion constructs were used to study the importance of each mPLCζ domain on the hydrolysing activity and Ca^{2+} sensitivity of this protein. The C2 domains and XY linkers of mPLCζ and rPLCδ1 were expressed and purified as GST–tagged fusion proteins. We used a 'PIP' strip overlay assay to assess their binding affinity for polyvalent and monovalent phosphoinositides. Finally deletion constructs, together with a PLCζ mutant of the XY linker region, were used to investigate the contribution of each domain on the binding affinity of mPLCζ for $PtdInsP_2$ by calculating the *Km* value for each construct.

4.2 Results.

4.2.1 Cloning of mPLCζ domain-deletion constructs into pGEX-5X-2 vector.

In order to examine the role of distinct structural domains on the enzymatic activity of mPLCζ, four domain-deletion constructs of mPLCζ were made. Figure 4.1A schematically illustrates the full-length mPLCζ and the various domain-truncated mPLCζ versions, which have one or both EF hands removed (ζΔEF1 and ζΔEF1,2 respectively), the C2 domain deleted (ζΔC2) or all the above domains absent (ζXY), and their sequence coordinates. mPLCζ domain-deletion constructs were amplified by PCR from the original cDNA clone using the appropriate primers to incorporate a 5'-EcoRI site and a 3'-SalI site for cloning into pGEX-5X-2 expression vector (Figure 4.1B).

A.

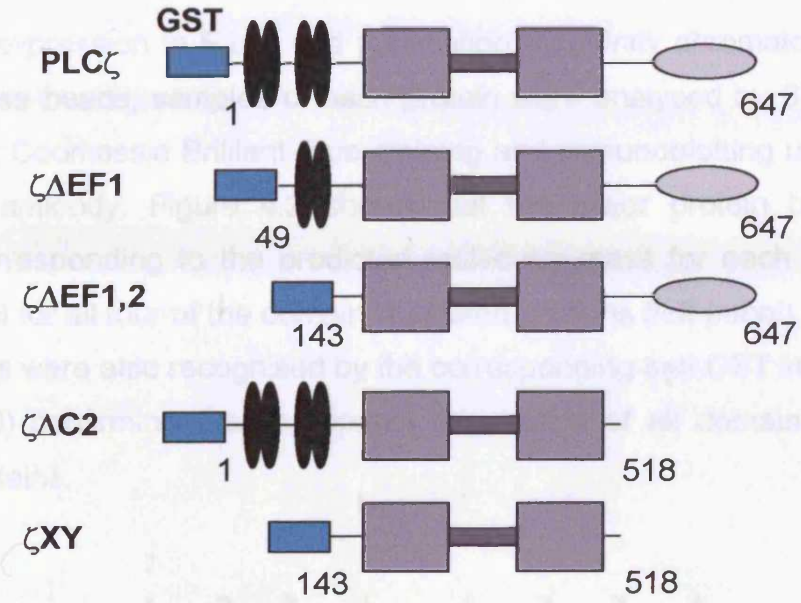

B.

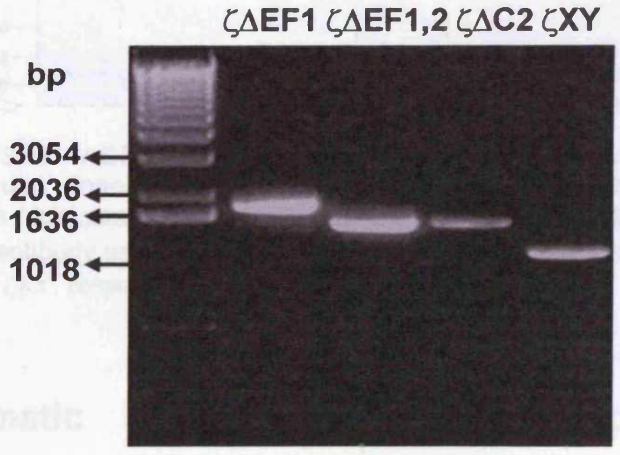

Figure 4.1 A. Schematic representation of domain-deletion constructs of mPLCζ. **B.** 1% agarose gel showing the products of PCR screen of a positive clone from each deletion construct. DNA from each colony was screened using the same oligonucleotide primers used in amplification of each deletion construct.

4.2.2 Expression and purification of mPLCζ domain-deletion constructs.

Following expression in *E.coli* and purification by affinity chromatography to GST agarose beads, samples of each protein were analysed by SDS-PAGE followed by Coomassie Brilliant-Blue staining and immunoblotting using T103 polyclonal antibody. Figure 4.2 shows that the major protein band, with mobility corresponding to the predicted molecular mass for each construct, was present for all four of the domain-truncated proteins (left panel) and these major bands were also recognised by the corresponding anti-GST immunoblot (right panel) confirming the appropriate expression of all domain-truncated mPLCζ proteins.

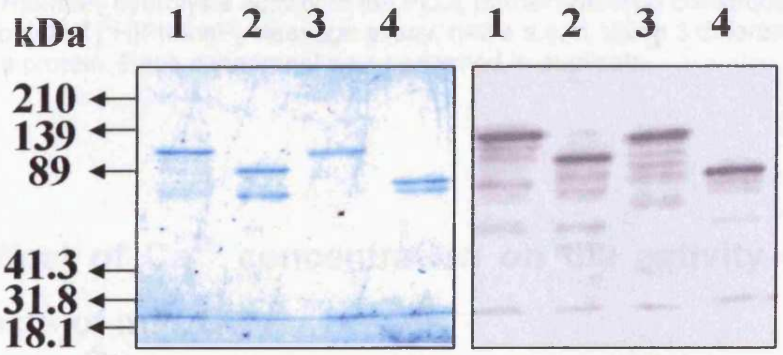

Figure 4.2 An 8% SDS-PAGE gel was used. 1μg of purified protein was loaded into each lane and recombinant proteins analysed by Coomassie Brilliant-Blue (left panel) and immunoblot analysis (right panel) using T103 antibody. The time of exposure was 30 seconds and the secondary antibody used was an anti-rabbit HRP conjugate. Lanes 1-4 show ζΔEF1, ζΔEF1,2, ζΔC2 and ζXY, respectively.

4.2.3 Enzymatic activity of mPLCζ domain-deletion constructs.

Enzymatic activity for each of the recombinant proteins, determined using the standard [^{3}H]PtdInsP$_2$ hydrolysis assay showed that every domain-deletion construct retained some of the enzymatic activity exhibited by the full length PLCζ. The histogram of Figure 4.3 plots the specific enzymatic activity values obtained for each protein, and reveals that the PLCζ proteins lacking either one or both EF hand domain, or the C2 domain retained about 70% of the

activity of the full-length PLCζ protein. Even the XY catalytic domain alone exhibited well over half of the activity of the full-length PLCζ. These data suggest that the mPLCζ catalytic site alone, comprising the X and Y domains, is capable of binding and hydrolysing $PtdInsP_2$ containing micelles and that the C2 and EF hand domains are not essential for enzymatic activity *in vitro*.

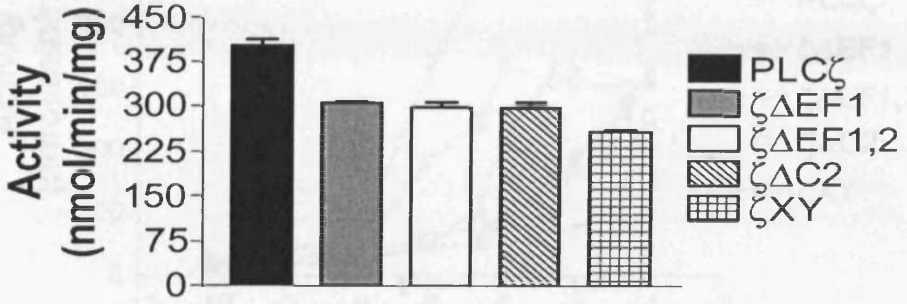

Figure 4.3 $PtdInsP_2$ hydrolysis activity of the PLCζ domain-deletion constructs (20 pmol) using the standard [^{3}H]$PtdInsP_2$ cleavage assay, n=3 ± s.e.m, using 3 different batches of recombinant protein. Each experiment was performed in duplicate.

4.2.4 Effect of Ca^{2+} concentration on the activity of deletion constructs of mPLCζ.

To examine the role of selected domains on the Ca^{2+} sensitivity of PLCζ activity, we tested the ability of the domain-deletion constructs of PLCζ to hydrolyse [^{3}H]$PtdInsP_2$ at different Ca^{2+} concentrations ranging from 0.1mM to 0.1nM (Figure 4.4). Figure 4.4A illustrates the Ca^{2+}-dependence of specific $PtdInsP_2$ hydrolytic activity for the full-length PLCζ and each of the truncated proteins, and these are also shown normalised to the maximum specific activity in Figure 4.4B. Table 4.1 summarises the EC_{50} and Hill coefficients of PLCζ and deletion constructs. Deletion of EF1 increased 10 fold the EC_{50} and reduced the Hill coefficient from 4.3 to 2.2. Deletion of both EF hands led to a dramatic increase of the EC_{50} of PLCζ (from 82 nM to 30 μM) and a decrease of the Hill coefficient from 4.3 to 0.6. Deletion of the C2 domain did not change the EC_{50} of PLCζ but reduced the Hill coefficient from 4.3 to 1.1.

Finally, deletion of both EF hands and C2 domain (PLCζ-XY) dramatically changed the EC_{50} and Hill coefficient (62μM and 0.3 respectively).

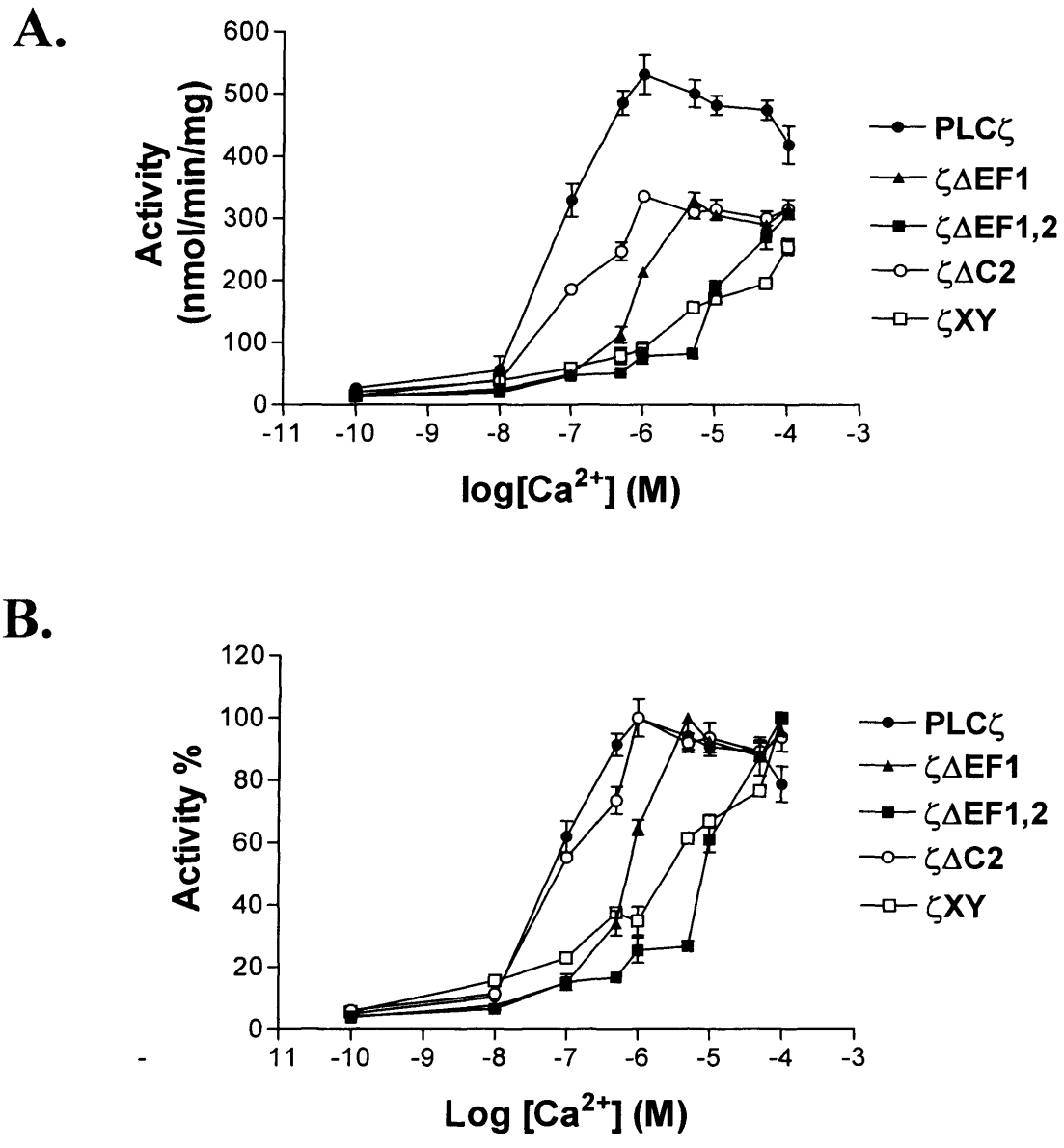

Figure 4.4 A, Effect of varying $[Ca^{2+}]$ from 0.1mM to 0.1nM on the specific $[^3H]PtdInsP_2$ hydrolysis activity of domain-deletion constructs of PLCζ. **B**, Effect of $[Ca^{2+}]$ on the normalised % activity of deletion constructs. For these assays n=2 ± s.e.m, using 2 different batches of recombinant proteins. Each experiment was performed in duplicate.

PLC protein	Ca^{2+} dependence EC_{50} (nM)	Hill cofficient
PLCζ	82	4.3
ζΔEF1	734	2.2
ζΔEF1,2	30,000	0.6
ζΔC2	85	1.1
ζXY	62,000	0.3

Table 4.1 Summary of the EC_{50} and Hill coefficients of Ca^{2+}-dependent enzyme activity determined for the full-length mPLCζ and its domain-deletion GST-tagged fusion proteins.

4.2.5 Binding of C2 domain and XY linker of mPLCζ to phosphoinositides on 'PIP' strips.

Since C2 domain of mPLCζ appeared not to be critical for its hydrolysing activity and Ca^{2+} sensitivity, we assumed that this domain might play another role in mPLCζ function, such as binding to phosphoinositides. Additionally, in mPLCζ, the sequence between the conserved X and Y catalytic domains (XY linker) is both longer and contains a cluster of basic residues not found in the unstructured homologous region of rPLCδ1 (Figure 4.5). We hypothesised that this basic cluster in PLCζ could interact with acidic lipids, and that this may facilitate of anchoring the enzyme to biological membranes. To test the binding of C2 domains and XY linkers to phosphoinositides and lipids on 'PIP' strips, as described previously with full-length recombinant proteins, we expressed and purified the GST-tagged C2 domain and XY linker of mPLCζ and rPLCδ1 (Figure 4.6).

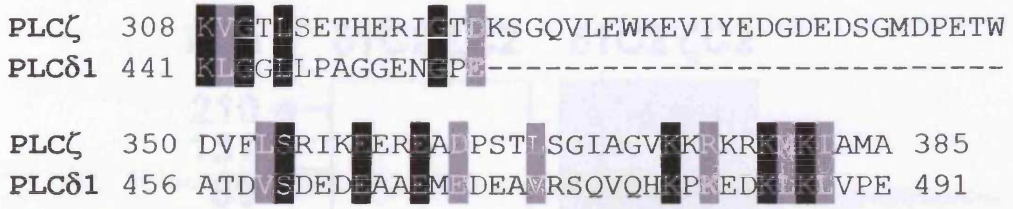

Figure 4.5 ClustalW alignment of mPLCζ and rPLCδ1 XY linkers. Identical amino acids are shown in shaded black boxes; conservative substitutions are boxed in grey.

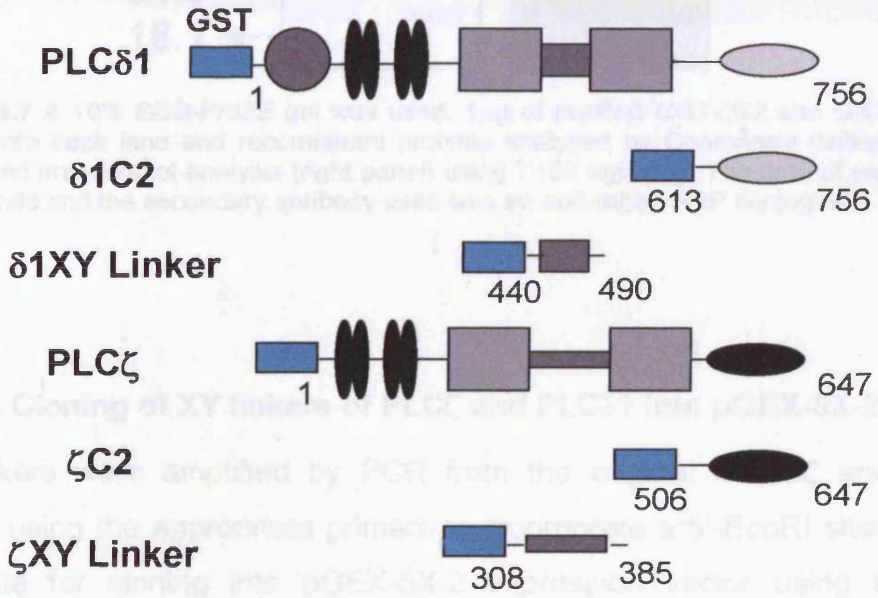

Figure 4.6 Schematic representation of C2 domain and XY linker of mPLCζ and PLCδ1 and their sequence coordinates.

4.2.5.1 Expression and purification of C2 domains of mPLCζ and rPLCδ1 as GST-tagged fusion proteins.

The C2 domain of mPLCζ had been previously cloned by Dr Chris Saunders into pGEX-1λt vector. Also, the C2 domain of rPLCδ1 had been cloned by Dr Llewellyn Cox into pGEX-4T-3 expreesion vector. Both constructs were kindly provided and recombinant GST-tagged C2 domains were expressed and purified. Purified proteins were analysed by SDS-PAGE followed by Coomassie Brilliant-Blue staining and immunoblot analysis (Figure 4.7).

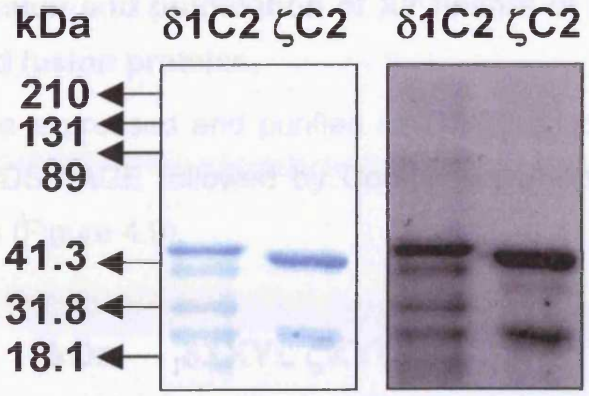

Figure 4.7 A 10% SDS-PAGE gel was used. 1μg of purified GST-ζC2 and GST-δ1C2 was loaded into each lane and recombinant proteins analysed by Coomassie Brilliant-Blue (left panel) and immunoblot analysis (right panel) using T103 antibody. The time of exposure was 15 seconds and the secondary antibody used was an anti-rabbit HRP conjugate.

4.2.5.2 Cloning of XY linkers of PLCζ and PLCδ1 into pGEX-5X-2 vector.

XY linkers were amplified by PCR from the original mPLCζ and rPLCδ1 clones using the appropriate primers to incorporate a 5'-EcoRI site and a 3'-SalI site for cloning into pGEX-5X-2 expression vector using the same restriction sites (Figure 4.8).

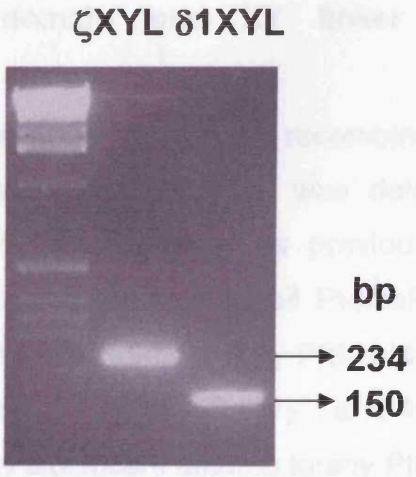

Figure 4.8 2% agarose gel showing the products of PCR screen of a positive clone from each construct. DNA from each colony was screened using the same oligonucleotide primers used in amplification of each construct.

4.2.5.3 Expression and purification of XY linkers of mPLCζ and rPLCδ1 as GST-tagged fusion proteins.

XY linkers were expressed and purified as GST-tagged fusion proteins and analysed by SDS-PAGE followed by Coomassie Brilliant-Blue staining and immunoblotting (Figure 4.9).

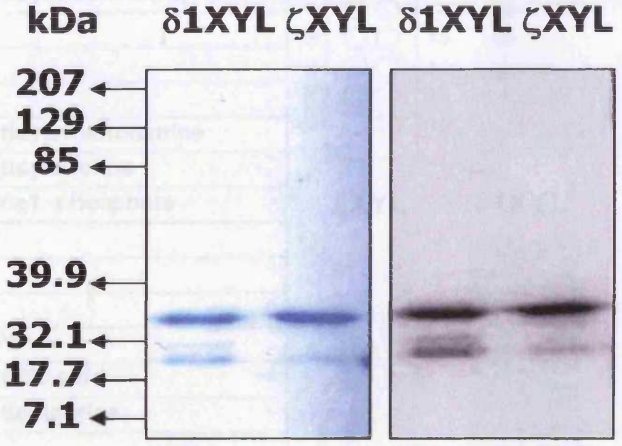

Figure 4.9 A 10% SDS-PAGE gel was used. 1μg of purified GST-ζXY linker and GST-δ1XY linker was loaded into each lane and recombinant proteins analysed by Coomassie Brilliant-Blue (left panel) and immunoblot analysis (right panel) using T103 antibody. The time of exposure was 10 seconds and the secondary antibody used was an anti-rabbit HRP conjugate.

4.2.5.4 Binding of C2 domain and XY linker of mPLCζ to phosphoinositides.

PIP strips were incubated with 100pmol of each recombinant protein at 4°C overnight and bound GST-recombinant protein was detected by western blotting using the T103 polyclonal antibody, as previously described. As shown in Figure 4.10, ζC2 bound strongly to all PtdInsPs and showed a reduced but remarkable affinity for PtdIns(3,5)P_2, PtdIns(4,5)P_2. The protein also showed a reduced affinity for PtdIns(3,4)P_2 and PtdIns(3,4,5)P_3. In contrast δ1C2 did not show any significant binding to any PtdInsP or PtdInsP_2, except some low affinity binding to PtdIns(5)P and PtdIns(4)P. The XY linker of PLCζ bound strongly not only to all PtdInsPs but to PtdIns(3,5)P_2 as well. The protein also showed some reduced affinity binding to PtdIns(3,4)P_2 and PtdIns(4,5)P_2, as well as to PtdIns(3,4,5)P_3 and phosphatic acid. The XY

linker of PLCδ1 and the negative control GST showed no binding to any phosphoinositides under the same conditions.

Spot #	PIP Strips
1	Lysophosphatic acid
2	Lysophosphatidylcholine
3	Phosphatidylinositol (PI)
4	PI(3)P
5	PI(4)P
6	PI(5)P
7	Phosphatidylethanolamine
8	Phosphatidylcholine
9	Sphigosine1 -phosphate
10	PI(3,4)P2
11	PI(3,5)P2
12	PI(4,5)P2
13	PI(3,4,5)P3
14	Phosphatidic acid
15	Phosphatidylserine
16	Blank

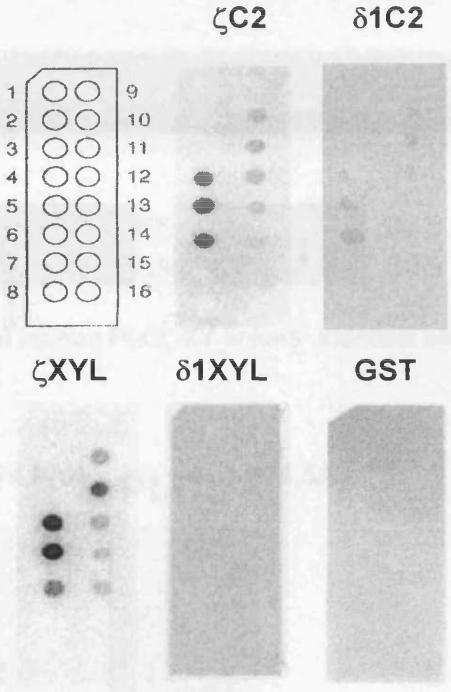

Figure 4.10 Binding of GST-tagged C2 domains and XY linkers to various phosphoinositides.

4.2.6 Expression and purification of GST-tagged PLCζ^{K374,5AA} mutant.

In order to further investigate the putative role of the XY linker region of mPLCζ on targeting the enzyme to PtdInsP$_2$, we made a mPLCζ mutant in which 2 positively charged amino acids [Lysines (K)] in the XY linker region (374 and 375 position) were mutated to 2 neutral amino acids [Alanines (A)], (Figure 4.11). This PLCζ^{K374,5AA} mutant had been made previously by Dr Chris Saunders in a pTarget vector and was subcloned into pGEX-5X-2 vector. The expression levels of this mutant were very low and 1 L of starting culture typically resulted to 0.05mg of purified GST- PLCζ^{K374,5AA} protein. Figure 4.10 shows purified GST-PLCζ^{K374,5AA} analysed by SDS-PAGE followed by

Coomassie Brilliant-Blue staining and immunoblot detection using the T103 antibody.

Figure 4.11 ClustalW alignment of mouse and human PLCζ XY linkers. Identical amino acids are shown in shaded black boxes.

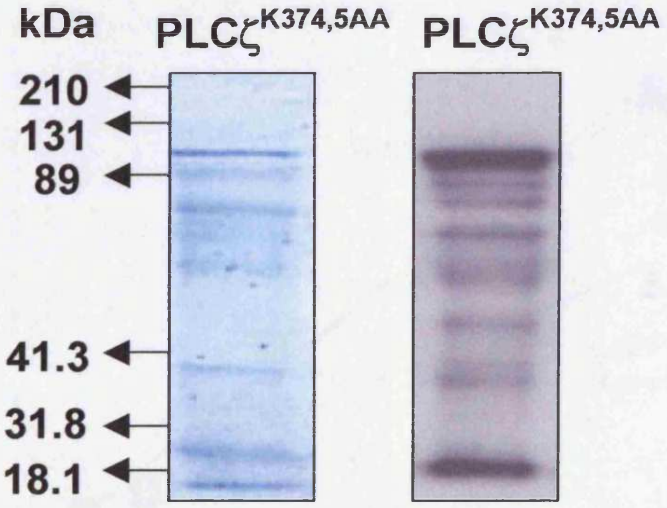

Figure 4.12 An 8% SDS-PAGE gel was used. 1μg of purified GST-PLCζ^{K374,5AA} was loaded into each lane and recombinant protein analysed by Coomassie Brilliant-Blue (left panel) and immunoblot analysis (right panel) using T103 antibody. The time of exposure was 2 seconds and the secondary antibody used was an anti-rabbit HRP conjugate.

4.2.7 Determination of *Km* values for ζΔC2, ζΔEF1,2 and PLCζ^{K374,5AA} mutants.

To determine the effect of deletion of EF hands or C2 domains on the affinity of mPLCζ for $PtdInsP_2$, we calculated the *Km*, for ζΔC2 and ζΔEF1,2 deletion constructs (Figure 4.13) using the $PtdInsP_2$ hydrolysis assay. We also calculated the *Km* value for the PLCζ^{K374,5AA} mutant to determine if the net positive charge in the XY linker region affected the affinity of mPLCζ for

PtdInsP$_2$. Figure 4.13 shows that deletion of EF hands resulted in a 2-fold increase of the *Km* (188μM) of mPLCζ (see Figure 3.11B). In contrast deletion of the C2 domain resulted in a dramatic 9-fold increase of the *Km* (802μM) of mPLCζ. Similarly the *Km* value for PLCζ^{K374,5AA} mutant was 8-fold higher (707μM) than that corresponding to the wild type mPLCζ (87μM). These results suggested that EF hands are not crucial for the high affinity of mPLCζ for its actual substrate, in contrast with the C2 domain and the positively charged XY linker region. Since mPLCζ lacks a PH domain, both C2 domain and XY linker region might play an important role and contributing to the high affinity of mPLCζ for PtdInsP$_2$.

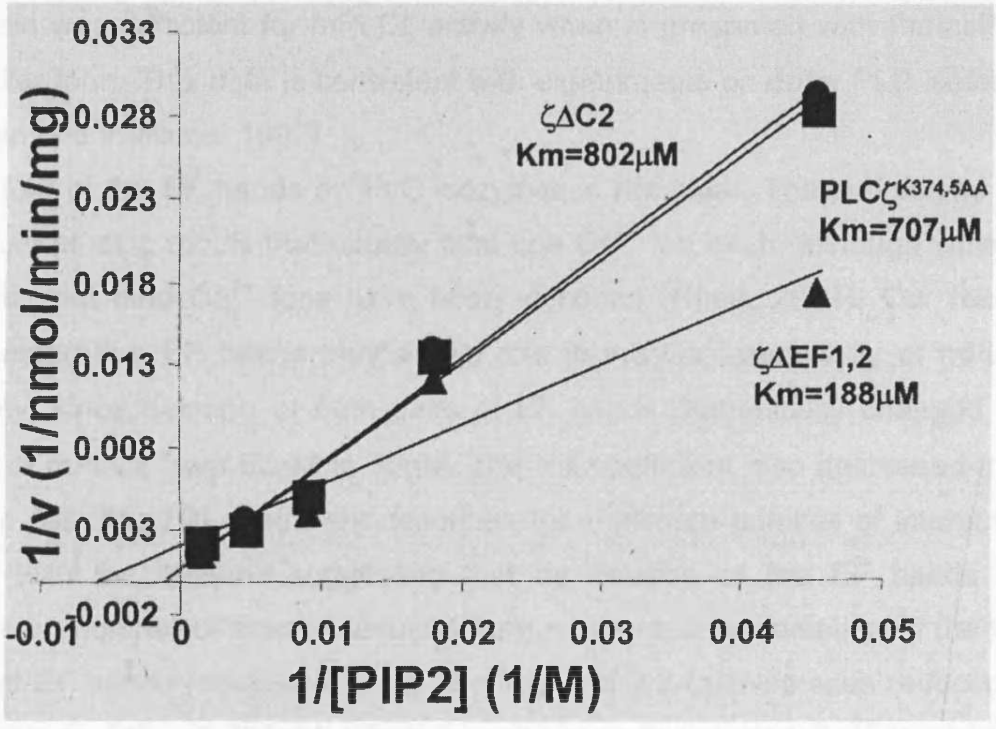

Figure 4.13 Lineweaver-Burk reciprocal plots for determination of the *Km* for PtdInsP$_2$, yielding values of 802μM, 707μM and 188μM for ζΔC2, PLCζ^{K374,5AA} and ζΔEF1,2 respectively. n=2 ± s.e.m, using 2 different batches of recombinant proteins. Each experiment was performed in duplicate.

4.3 Discussion.

In this chapter, in order to determine the role of selected domains of mPLCζ on its $PtdInsP_2$ hydrolysing activity *in vitro*, we generated a series of truncated constructs of mPLCζ with deletions of selected structural domains (Figure 4.1). These deletion constructs were expressed and purified as GST-tagged fusion proteins using the same bacterial system we used to express and purify GST-mPLCζ and GST-rPLCδ1 (Figure 4.2). Our data showed that the XY catalytic domain alone retained considerable activity (about 60%) compared of that of full-length mPLCζ. Furthermore, the proteins with deletions of either the EF hands or the C2 domains showed slightly reduced activity (~70%) compared that of full-length mPLCζ. Thus the XY catalytic domain was sufficient for mPLCζ activity when is presented with $PtdInsP_2$ in micellar form. This data is consistent with experiments on other PLC isoforms (Katan and Williams, 1997).

The role of the EF hands on PLC isozymes is not clear. These domains are calcium binding motifs that usually bind one Ca^{2+} ion each, although variants that do not bind Ca^{2+} ions have been identified (Rhee, 2001). Our results suggested that EF hands play a vital role in the Ca^{2+} sensitivity of mPLCζ activity, since deletion of both pairs of EF hands dramatically changed the EC_{50} of mPLCζ from 82nM to 30μM. The Hill coefficient also decreased from 4.3 to 0.6. The Hill coefficient describes the minimum number of interacting sites with the enzyme suggesting that by deletion of the EF hands the minimum number of sites is reduced from ~4 to ~1. Even deletion of the first pair of EF hands resulted to a Hill coefficient of 2.2 (actives sites reduced to ~2) and an EC_{50} of 734nM, which is well above the resting Ca^{2+} level in an egg. This suggests that Ca^{2+} binding to the EF hands is important for the interaction of the XY domain with the $PtdInsP_2$ and for mPLCζ hydrolysing activity. In contrast, deletion of the C2 domain did not have an effect on the EC_{50} of mPLCζ, even though the Hill coefficient was reduced from ~4 to ~1. Although mPLCζ loses Ca^{2+} binding sites after the deletion of the C2 domain, these appear not to be crucial for the enzymatic activity. C2 domains display

functional diversity and can be involved in binding to lipids, or proteins in a way that can be Ca^{2+}-dependent (Nalefski *et al*, 2001).

To investigate the putative role of C2 domain on targeting PLCζ to $PtdInsP_2$ we expressed and purified as GST-tagged fusion proteins the C2 domains of mPLCζ and rPLCδ1, and we tested their binding to phosphoinositides spotted on PIP strip membranes. GST-ζC2 strongly bound to all PtdInsPs and showed a reduced but remarkable affinity for $PtdIns(3,5)P_2$, $PtdIns(4,5)P_2$, in contrast with GST-δ1C2, which did not show any significant binding to any PtdInsP or $PtdInsP_2$, except some binding with low affinity to PtdIns(5)P and PtdIns(4)P. This result suggested that the C2 domain of mPLCζ could play an important role in targeting this enzyme to $PtdInsP_2$. This was confirmed by the Km values for ζΔC2 and ζΔEF1,2 deletion constructs (Figure 4.11). Deletion of C2 domain resulted in a dramatic 9-fold increase of the *Km* (802μM) of mPLCζ in contrast with deletion of EF hands, which resulted in a 2-fold increase of the *Km* (188μM) value for mPLCζ, suggesting that deletion of the EF hands does not dramatically affect the affinity of mPLCζ for $PtdInsP_2$.

Compared to rPLCδ1, mPLCζ has an extended and very positively charged XY linker region between the conserved X and Y catalytic domains in PLCζ, which might play a role in targeting PLCζ to $PtdInsP_2$ enriched biological membranes through interaction with the negatively charged $PtdInsP_2$. For this reason we expressed and purified, as GST-tagged fusion proteins, the XY linkers of mPLCζ and rPLCδ1, and we tested their binding to phosphoinositides using the PIP strip overlay assay. The XY linker of rPLCδ1 showed no binding to any phosphoinositides, in contrast with the XY linker of mPLCζ, which showed very high affinity for all PtdInsPs and $PtdIns(3,5)P_2$ and reduced affinity for $PtdIns(3,4)P_2$, $PtdIns(4,5)P_2$ and $PtdIns(3,4,5)P_3$. The GST-$PLC\zeta^{K374,5AA}$ mutant, in which 2 positively charged amino acids (K) in the XY linker region (374 and 375 position) mutated to 2 neutral amino acids (A), was tested to determine how this might affect the affinity of PLCζ for $PtdInsP_2$. The *Km* value for the $PLC\zeta^{K374,5AA}$ mutant was 8-fold higher (707μM) than that corresponding to the wild type mPLCζ (87μM).

In conclusion, the EF hand regions play an important role in the Ca^{2+} sensitivity of mPLCζ activity but are not important to the affinity of mPLCζ for $PtdInsP_2$. In contrast the C2 domain and the XY linker regions are not important to activity in the $PtdInsP_2$ hydrolysis assay but play an important role in binding to negatively charged phosphoinositides, which may be important in targeting mPLCζ to $PtdInsP_2$ enriched biological membranes.

Chapter 5

Expression of luminescent PLC constructs in mouse eggs.

5.1 Introduction.

In chapter 4 we used a series of domain-deletion constructs of mPLCζ expressed as GST-tagged fusion proteins, to investigate the role of EF hand, XY catalytic and C2 domains on the $PtdInsP_2$ hydrolysing activity and targeting of this protein. We demonstrated the importance of EF hands on the Ca^{2+} sensitivity of PLCζ and the importance of C2 domain on targeting of PLCζ to $PtdInsP_2$. It was therefore important to test how these deletions would affect the oscillatory activity of PLCζ *in vivo*. For this reason, 3 deletion constructs (Figure 5.1A) were made by a student in our laboratory. Constructs were cloned into pTarget vector, which allows the production of cRNA. Microinjection of cRNA, corresponding to these deletion constructs, into mouse eggs did not trigger any Ca^{2+} oscillations, in contrast with the wild type, full-length PLCζ (Figure 5.1B). This was a first indication that deletions of one or both EF hands and C2 domain prevent PLCζ from being able to cause Ca^{2+} oscillations in intact eggs.

Although the cRNA corresponding to each construct and used for the microinjection experiments was able to generate proteins of the correct size when expressed in an *in vitro* reticulocyte expression system (data not shown), we could not determine the expression levels of these constructs in mouse eggs. To verify that these deletion constructs of PLCζ were faithfully expressed in mouse eggs; and that loss of Ca^{2+} oscillations was not due to the lack of expression, we generated luciferase (LUC)-tagged versions of these constructs. These would enable us to quantify their relative protein expression in parallel with oscillatory activity.

As additional controls we made LUC-tagged versions of rPLCδ1 and ΔPH-rPLCδ1, so that their ability to trigger Ca^{2+} oscillations and the levels of protein expression could also be determined in mouse eggs.

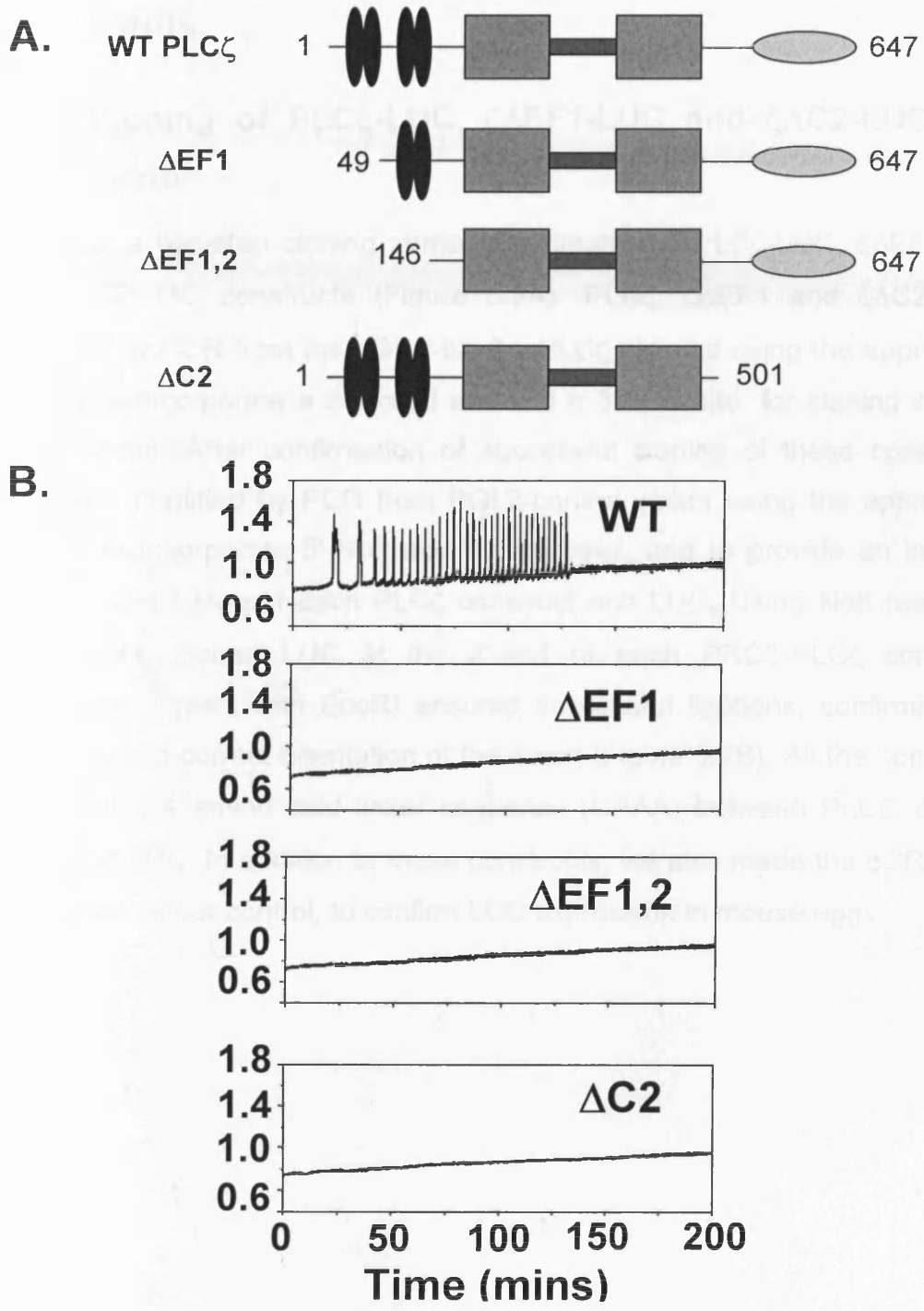

Figure 5.1 **A**. Schematic representation of the PLCζ domain-deletion constructs used for cRNA microinjections into mouse eggs. **B**. Changes in cytoplasmic [Ca^{2+}] in mouse eggs were measured by fluorescence excitation ratio measurements using intracellular fura-red. Recordings were obtained for over 3 hours after microinjection of cRNA into eggs for each PLCζ construct. Full-length PLCζ triggered Ca^{2+} oscillations approximately 18-22 minutes after cRNA microinjection into the eggs (n=10 ± s.e.m). 100% of the PLCζ control eggs produced Ca^{2+} oscillations; one representative trace is shown. Microinjection of cRNA for ΔEF1-PLCζ, ΔEF1,2-PLCζ or ΔC2-PLCζ failed to cause any Ca^{2+} oscillations in any of the eggs (n=10 for each cRNA). A representative trace is shown for each domain-deletion. (From Nomikos *et al*, 2005).

5.2 Results.

5.2.1 Cloning of PLCζ-LUC, ζΔEF1-LUC and ζΔC2-LUC into pCR3 vector.

We used a two-step cloning strategy to create the PLCζ-LUC, ζΔEF1-LUC and ζΔC2-LUC constructs (Figure 5.2A). PLCζ, ζΔEF1 and ζΔC2 were amplified by PCR from the pGEX-5X-2-mPLCζ plasmid using the appropriate primers to incorporate a 5'-EcoRI site and a 3'-NotI site, for cloning into the pCR3 vector. After confirmation of successful cloning of these constructs, LUC was amplified by PCR from PGL2-control vector using the appropriate primers to incorporate 5'-NotI and 3'-NotI sites; and to provide an in-frame ligation point between each PLCζ construct and LUC. Using NotI restriction enzyme we cloned LUC at the 3'-end of each PRC3-PLCζ construct. Restriction digests with EcoRI ensured successful ligations, confirming the presence and correct orientation of the insert (Figure 5.2B). All the constructs contained a 4 amino acid linker sequence (CAAA) between PLCζ, ζΔEF1, ζΔC2 and LUC. In addition to these constructs, we also made the pCR3-LUC to be used as our control, to confirm LUC expression in mouse eggs.

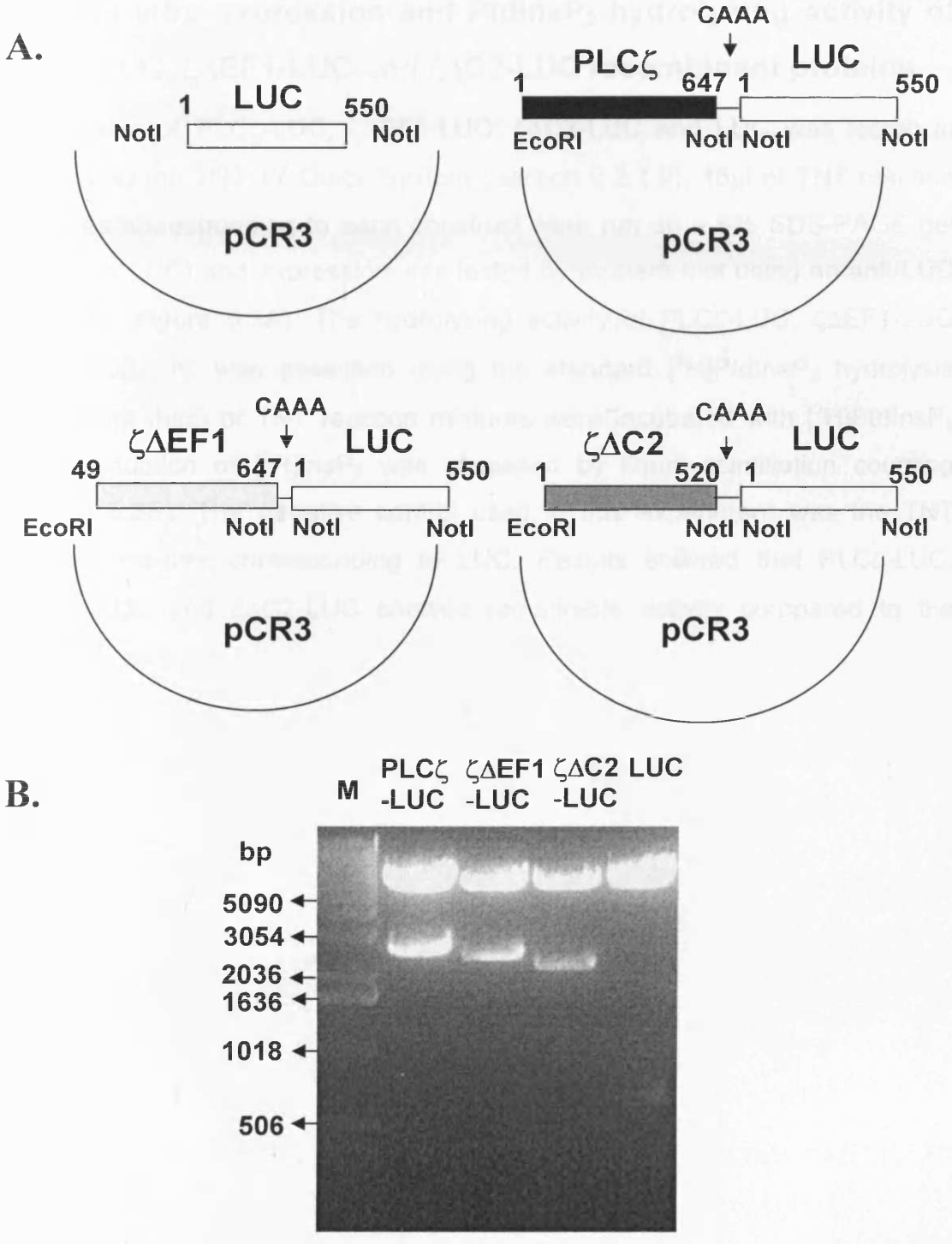

Figure 5.2 A. Cloning strategy for PLCζ-LUC, ζΔEF1-LUC and ζΔC2-LUC constructs. **B**. 1% agarose gel showing the products of enzymatic digestion of DNA maxi-preps corresponding to positive clones of PLCζ-LUC and LUC constructs, using EcoRI restriction enzyme. EcoRI cuts once in the multiple cloning site of pCR3 vector and once at the 587 position of LUC sequence, resulting into two bands for each construct. The exact size of the bands obtained after the digestion of each construct by EcoRI, confirming successful cloning are the following: For PLCζ-LUC 6156 and 2542, for ζΔEF1-LUC 6165 and 2396bp, for ζΔC2-LUC 6165 and 2161bp; and for LUC 6156 and 587bp.

5.2.2 *In vitro* expression and $PtdInsP_2$ hydrolysing activity of PLCζ-LUC, ζΔEF1-LUC and ζΔC2-LUC recombinant proteins.

Expression of PLCζ-LUC, ζΔEF1-LUC, ζΔC2-LUC and LUC was tested *in vitro* using the TNT T7 Quick System (Section 2.2.1.9). 16μl of TNT reaction mixtures corresponding to each construct were run on a 6% SDS-PAGE gel (7.5% for LUC) and expression was tested by western blot using an anti-LUC antibody (Figure 5.3A). The hydrolysing activity of PLCζ-LUC, ζΔEF1-LUC and ζΔC2-LUC was assessed using the standard [^{3}H]$PtdInsP_2$ hydrolysis assay. 8μl (half) of TNT reaction mixtures were incubated with [^{3}H]$PtdInsP_2$ and production of [^{3}H]$InsP_3$ was assessed by liquid scintillation counting (Figure 5.3B). The negative control used in this experiment was the TNT reaction mixture corresponding to LUC. Results showed that PLCζ-LUC, ζΔEF1-LUC and ζΔC2-LUC showed remarkable activity compared to the negative control.

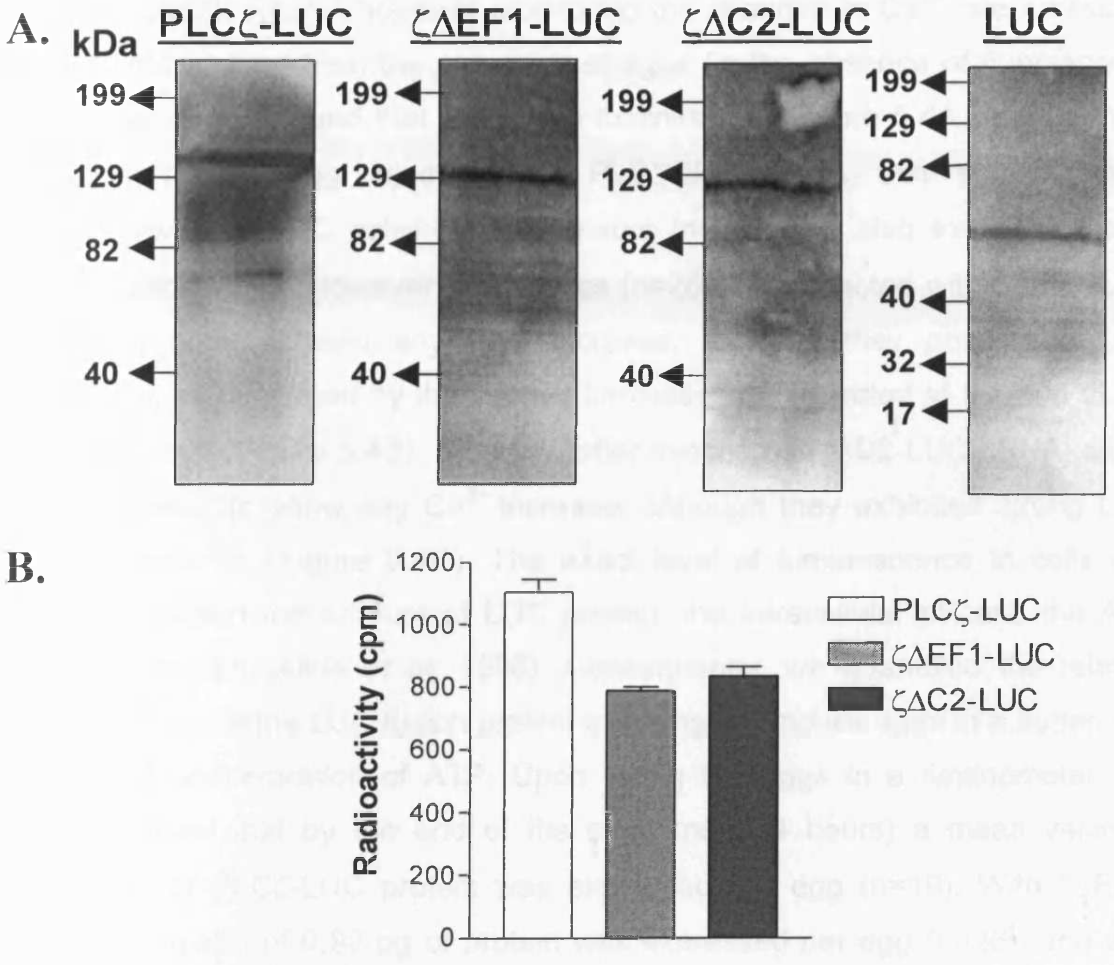

Figure 5.3 A. Western blots of 6% and 7.5% (for LUC) SDS-PAGE gels, showing recombinant protein products (16μl reaction/lane) of TNT-expressed PLCζ-LUC, ζΔEF1-LUC, ζΔC2-LUC and LUC constructs, using the anti-LUC antibody. The time of exposures vary from 30sec to 1min. **B.** $PtdInsP_2$ hydrolysis activity of PLCζ-LUC, ζΔEF1-LUC and ζΔC2-LUC (8μl) using the standard [^{3}H]$PtdInsP_2$ cleavage assay , n=2 ± s.e.m. The cpm value obtained for the negative control (LUC; 230cpm), has been subtracted from the final cpm values corresponding to PLCζ-LUC, ζΔEF1-LUC and ζΔC2-LUC recombinant proteins.

5.2.3 Expression of PLCζ-LUC, ζΔEF1-LUC and ζΔC2-LUC constructs in mouse eggs.

cRNAs corresponding to LUC constructs were prepared (as described in Section 2.2.1.10) and microinjected (by Karen Campbell) in mouse eggs. The left panel of Figure 5.4A shows that eggs injected with cRNA encoding PLCζ-LUC construct caused a series of Ca^{2+} oscillations in eggs. This indicates that a fusion tag at the C-terminus of PLCζ did not constrain the ability to generate Ca^{2+} oscillations, as has previously been shown for N-terminal tags (Saunders

et al, 2002). After 4 hours of monitoring the changes in Ca^{2+}, we measured the light emitted from the same set of eggs (in the absence of fluorescence excitation) and found that they were luminescent (Figure 5.4A right pannel). Every mouse egg injected with PLCζ-LUC cRNA that showed clear expression of LUC activity after 4 hours (n=19), had also exhibited robust Ca^{2+} oscillations. However, when eggs (n=26) were injected with ζΔEF1-LUC cRNA, none showed any Ca^{2+} increase, although they possessed LUC activity, as confirmed by the intense luminescence detected at the end of the experiment (Figure 5.4B). Similarly, after injection of ζΔC2-LUC cRNA, all 25 eggs failed to show any Ca^{2+} increase, although they exhibited strong LUC luminescence (Figure 5.4C). The exact level of luminescence in cells can depend upon the amount of LUC protein, the intracellular pH and the ATP concentration (Allue *et al*, 1996). Consequently, we quantified the relative expression of the LUC fusion protein by lysing the mouse eggs in a buffer with a fixed concentration of ATP. Upon lysing the eggs in a luminometer, we determined that by the end of the experiment (4 hours) a mean value of 0.19pg of PLCζ-LUC protein was expressed per egg (n=19). With ζΔEF1-LUC, a mean of 0.98 pg of protein was expressed per egg (n=26), and with ζΔC2-LUC a mean of 2.7pg of protein was expressed per egg (n=25). These data suggested that the PLCζ-LUC domain-deletion constructs that did not cause any Ca^{2+} oscillations were clearly expressed in the eggs that were injected with cRNA. The ζΔEF1-LUC and ζΔC2-LUC were expressed at levels that were 5- and 14-fold higher than that of PLCζ-LUC. This high level of expression of domain-deletion constructs more than compensates for the reduced specific activity of these proteins (~70%) relative to full-length PLCζ that we demonstrated in Chapter 2 (Figure 4.4). Because the threshold for PLCζ to cause a Ca^{2+} oscillation is around 50 fg (Saunders *et al*, 2002), the two domain-deletion constructs were expressed at levels that are 20-50 times the amount required to cause Ca^{2+} oscillations with the full-length PLCζ.

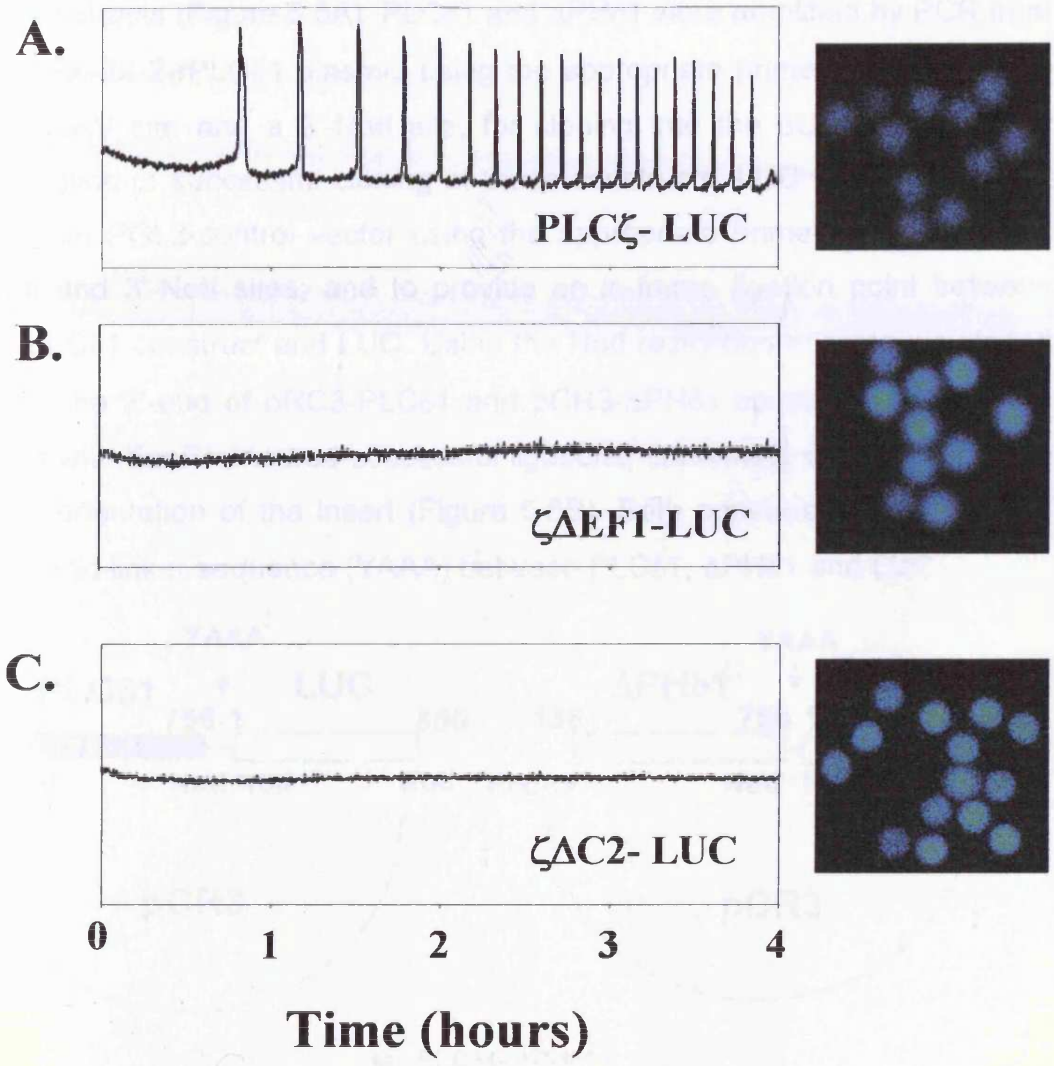

Figure 5.4 Eggs injected with LUC tagged versions of PLCζ. The fluorescence of eggs microinjected Oregon Green BAPTA-dextran was used to monitor Ca^{2+} as described in the Methods. Eggs were monitored in medium containing 100 μM luciferin. **A.** Left panel shows a representative fluorescence trace to measure Ca^{2+} from an egg injected with the wild type PLCζ-LUC cRNA; and right panel shows an integrated image of the LUC luminescence from the eggs injected with this construct. **B.** Left panel shows a sample Ca^{2+} recording from an egg injected with ζΔEF1-LUC cRNA and right pannel is a sample image of LUC luminescence. **C.** Left panel shows a sample fluorescence recording of Ca^{2+} and the right panel integrated luminescence of LUC from eggs injected with ζΔC2-LUC cRNA. The y-axes on the fluorescence traces are in arbitrary units, and each x-axis starts between 5-20 mins after the injection of eggs (From Nomikos *et al*, 2005).

5.2.4 Cloning of PLCδ1-LUC and ΔPHδ1-LUC into pCR3 vector.

In order to make PLCδ1-LUC and ΔPHδ1-LUC constructs we followed the same cloning strategy used to create the PLCζ-LUC, ζΔEF1-LUC and ζΔC2-

LUC constructs (Figure 5.5A). PLCδ1 and ΔPHδ1 were amplified by PCR from the pGEX-5X-2-rPLCδ1 plasmid using the appropriate primers to incorporate a 5'-EcoRV site and a 3'-NotI site, for cloning into the pCR3 vector. After confirmation of successful cloning of these constructs, LUC was amplified by PCR from PGL2-control vector using the appropriate primers to incorporate 5'-NotI and 3'-NotI sites; and to provide an in-frame ligation point between each PLCδ1 construct and LUC. Using the NotI restriction enzyme we cloned LUC at the 3'-end of pRC3-PLCδ1 and pCR3-ΔPHδ1 constructs. Restriction digests with EcoRI ensured successful ligations, confirming the presence and correct orientation of the insert (Figure 5.5B). Both constructs contained a 4 amino acid linker sequence (YAAA) between PLCδ1, ΔPHδ1 and LUC.

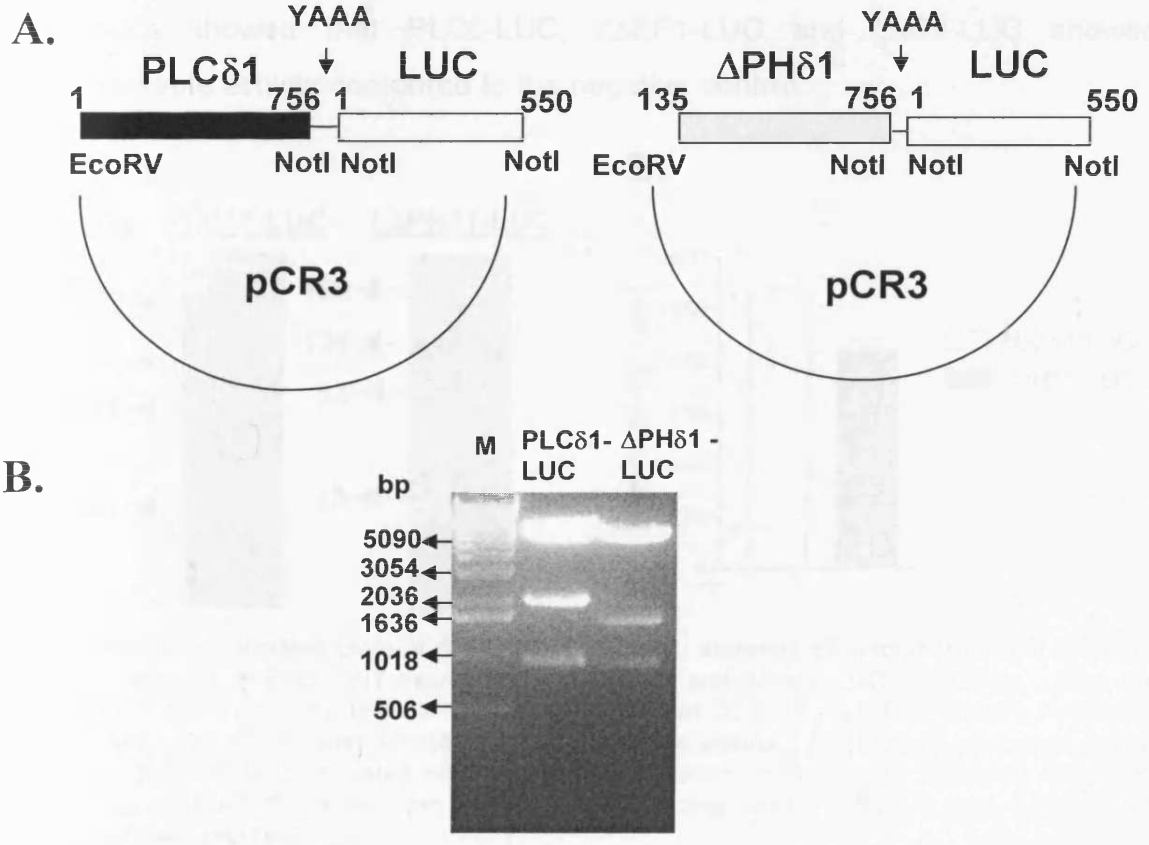

Figure 5.5 A. Cloning strategy for PLCδ1-LUC and ΔPHδ1-LUC constructs. **B**. 1% agarose gel showing the products of enzymatic digestion of DNA maxi-preps corresponding to positive clones of PLCδ1-LUC and ΔPHδ1-LUC constructs, using EcoRI restriction enzyme. EcoRI cuts once in the multiple cloning site of PCR3 vector, once at the 1942 position of PLCδ1 sequence and once at the 587 position of LUC sequence, resulting into three bands for each construct. The exact size of the bands obtained after the digestion of each construct by EcoRI confirming successful cloning are the following: For PLCδ1-LUC 6155, 1952 and 927bp; and for ΔPHδ1-LUC 6155, 1547 and 927bp.

5.2.5 *In vitro* expression and $PtdInsP_2$ hydrolysing activity of PLCδ1-LUC and ΔPHδ1-LUC recombinant proteins.

Expression of PLCδ1-LUC and ΔPHδ1-LUC was tested *in vitro* using the TNT T7 Quick System (Section 2.2.1.9). 16μl of TNT reaction mixtures corresponding to each construct were loaded into a 6% SDS-PAGE gel and expression was tested by western blot using the anti-LUC antibody (Figure 5.6A). The hydrolysing activity of PLCδ1-LUC and ΔPHδ1-LUC was assessed using the standard $[^3H]PtdInsP_2$ hydrolysis assay. 8μl (half) of TNT reaction mixtures were incubated with $[^3H]PtdInsP_2$ and production of $[^3H]InsP_3$ was assessed by liquid scintillation counting (Figure 5.6B). The negative control used in this experiment was the TNT reaction mixture corresponding to LUC. Results showed that PLCζ-LUC, ζΔEF1-LUC and ζΔC2-LUC showed remarkable activity compared to the negative control.

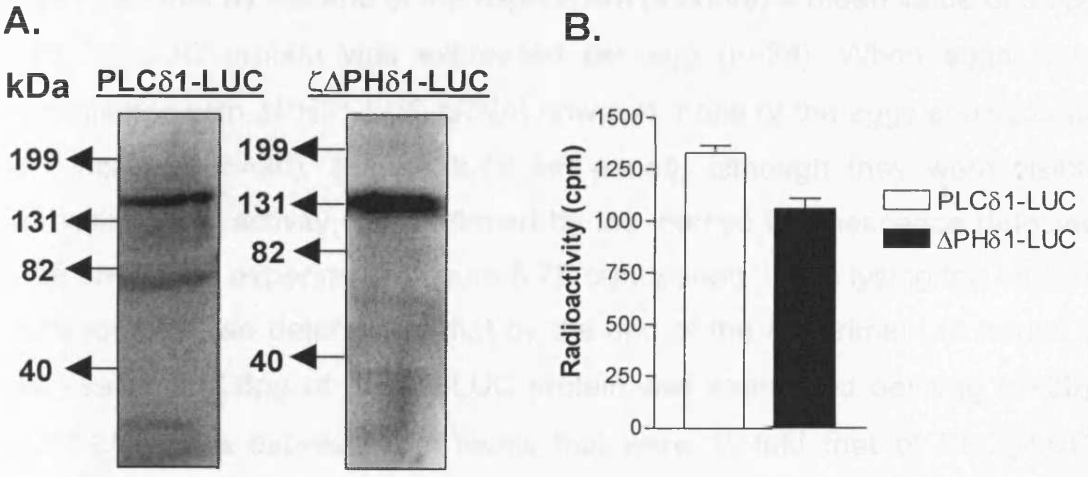

Figure 5.6 A. Western blots of 6% SDS-PAGE gels, showing recombinant protein products (16μl reaction/lane) of TNT-expressed PLCδ1-LUC and ΔPHδ1-LUC constructs, using the anti-LUC antibody. The time of exposures vary from 30 to 45sec. **B.** $PtdInsP_2$ hydrolysis activity of PLCδ1-LUC and ΔPHδ1-LUC (8μl) using the standard $[^3H]PtdInsP_2$ cleavage assay, n=2 ± s.e.m. The cpm value obtained for the negative control (LUC; 250cpm) has been subtracted from the final cpm values corresponding to PLCδ1-LUC and ΔPHδ1-LUC recombinant proteins.

5.2.6 Expression of PLCδ1-LUC and ΔPHδ1-LUC constructs in mouse eggs.

cRNAs corresponding to PLCδ1-LUC and ΔPHδ1-LUC constructs were prepared and microinjected (by Karen Campbell) in mouse eggs. The left panel of Figure 5.7A shows that eggs injected with cRNA encoding PLCδ1-LUC caused a series of Ca^{2+} oscillations in the eggs. The pattern and the frequency of Ca^{2+} oscillations that PLCδ1-LUC caused (2spikes/hr) were different compared to that triggered by PLCζ-LUC (6spikes/hr), (Figure 5.4A). At the end of 4 hours of monitoring the changes in Ca^{2+}, we measured the light emitted from the same set of eggs (in the absence of fluorescence excitation) and found that they were luminescent (Fig. 5.7A right pannel). Every mouse egg injected with PLCδ1-LUC cRNA showed clear expression of LUC activity after 4 hours (n=24). Upon lysing the eggs in a luminometer, we determined that by the end of the experiment (4 hours) a mean value of 3.3pg of PLCδ1-LUC protein was expressed per egg (n=24). When eggs were microinjected with ΔPHδ1-LUC cRNA, however, none of the eggs showed any Ca^{2+} increase (n=20), (Figure 5.7B left panel), although they were visibly expressing LUC activity, as confirmed by the intense luminescence detected at the end of the experiment (Figure 5.7B right panel). Upon lysing the eggs in a luminometer, we determined that by the end of the experiment (4 hours) a mean value of 7.6pg of ΔPHδ1-LUC protein was expressed per egg (n=20). PLCδ1-LUC was expressed at levels that were 17-fold that of PLCζ-LUC. Although PLCδ1-LUC was expressed at this high levels and it showed a 3-fold higher $PtdInsP_2$ hydrolysing activity *in vitro* (Figure 3.7) compared to PLCζ, its oscillatory activity was much lower than that of PLCζ. ΔPHδ1-LUC even though it was expressed at very high levels (7.6pg/egg) appeared to be unable to cause Ca^{2+} oscillations.

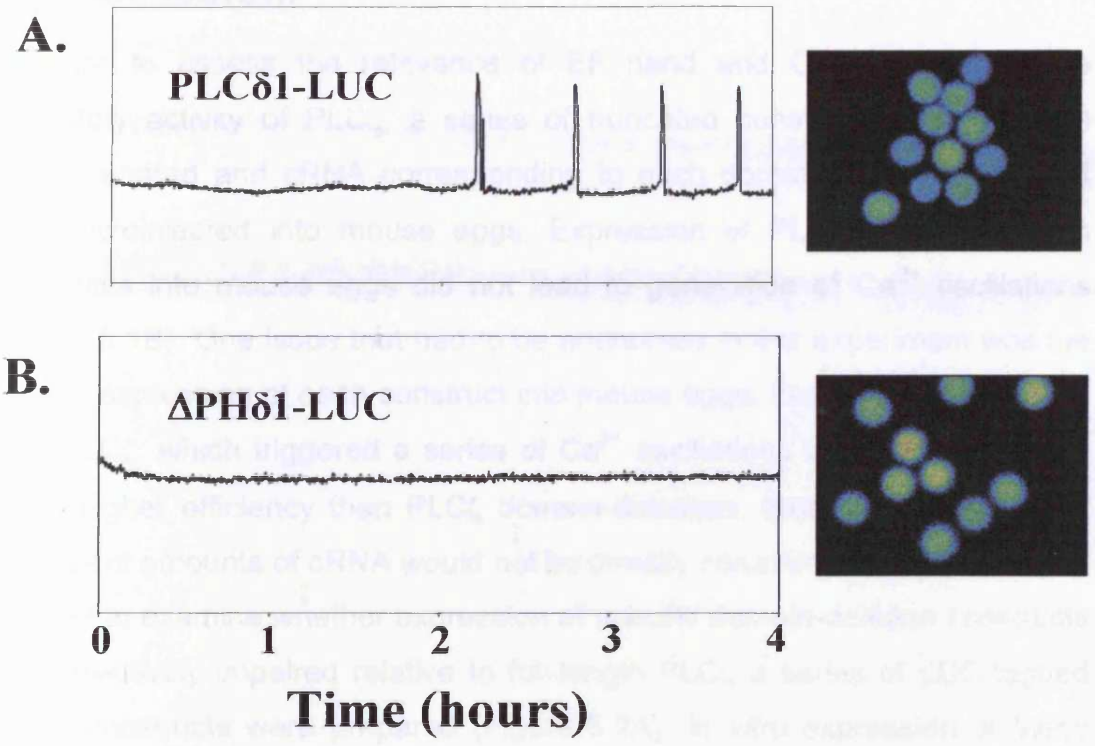

Figure 5.7 Eggs injected with LUC tagged versions of PLCδ1 and ΔPHδ1. The fluorescence of eggs microinjected Oregon Green BAPTA-dextran was used to monitor Ca^{2+} as described in the Methods. Eggs were monitored in medium containing 100 μM luciferin. **A.** Left panel shows a representative fluorescence trace to measure Ca^{2+} from an egg injected with PLCδ1-LUC cRNA; and right panel shows an integrated image of the LUC luminescence from the eggs injected with this construct. **B.** Left panel shows a sample Ca^{2+} recording from an egg injected with ΔPHδ1-LUC cRNA and right panel is a sample image of luciferase luminescence. The y-axes on the fluorescence traces are in arbitrary units, and each x-axis starts between 5-20 mins after the injection of eggs.

5.3 Discussion.

In order to assess the relevance of EF hand and C2 domains on the oscillatory activity of PLCζ, a series of truncated constructs (Figure 5.1A) were prepared and cRNA corresponding to each domain-deletion construct was microinjected into mouse eggs. Expression of PLCζ domain-deletion constructs into mouse eggs did not lead to generation of Ca^{2+} oscillations (Figure 5.1B). One issue that had to be addressed in this experiment was the level of expression of each construct into mouse eggs. For example if the wild type PLCζ, which triggered a series of Ca^{2+} oscillations was expressed with much higher efficiency than PLCζ domain-deletions, then microinjections of equivalent amounts of cRNA would not be directly comparable.

In order to examine whether expression of specific domain-deletion constructs was selectively impaired relative to full-length PLCζ a series of LUC-tagged fusion constructs were prepared (Figure 5.2A). *In vitro* expression of these constructs was tested using the TNT system and all LUC constructs were faithfully expressed (Figure 5.3A). The hydrolysing activity of these constructs was assessed using the standard [^{3}H]PtdInsP_2 hydrolysis assay. PLCζ-LUC and domain-deletions showed remarkable activity (Figure 5.3B). cRNA corresponding to PLCζ-LUC, ζΔEF1-LUC and ζΔC2-LUC constructs was microinjected into mouse eggs. It was notable that the Ca^{2+} oscillations observed upon injection of the full-length PLCζ-LUC cRNA occurred about 1 hr after injection and at the end of the experiment (4hr) the level of expressed PLCζ-LUC protein was determined to be 190fg/egg. If we assume a linear increase in PLCζ-LUC protein during the 4 hours of recording, then we can estimate that the amount of PLCζ-LUC required to initiate Ca^{2+} oscillations is around 50fg. This value is similar to previous estimations that 20-50fg of PLCζ is required to initiate Ca^{2+} oscillations in eggs (Saunders *et al*, 2002), as well as the estimate that 10-40fg of venusGFP-PLCζ is required to initiate Ca^{2+} release (Yoda *et al*, 2004). These data therefore suggest that the PLCζ-LUC has a similar efficiency in generating $InsP_3$ in eggs to other N-terminally tagged PLCζ fusion proteins.

The two domain-deletion PLCζ-LUC constructs showed significantly higher expression levels than that of the full-length PLCζ-LUC in mouse eggs (Figure 5.4); however, no Ca^{2+} oscillations were produced by any of these domain-deletions. PLCζ is not effective in stimulating Ca^{2+} oscillations when it lacks one or both of its EF hand domains. This result is consistent with previous observations with a short form of PLCζ that lacks the first 110 amino acids at the N-terminus (Kouchi *et al*, 2004). The basic ability to hydrolyse $PtdInsP_2$ *in vitro* would be preserved for these deletion constructs, so the lack of Ca^{2+} oscillation-inducing activity in eggs injected with EF hand domain-deletions of PLCζ may be explained by their differential response to Ca^{2+} regulation. EF hands appear to play a vital role in the Ca^{2+} sensitivity of PLCζ activity (Figure 4.4). The N-terminal truncation of EF hands would ablate the ability of this domain-deletion to generate $InsP_3$ in an intact cell with a Ca^{2+} level of around 100nM. In addition, the loss of the C2 domain from PLCζ also led to an inability to cause Ca^{2+} oscillations in intact eggs, although the EC_{50} for Ca^{2+} stimulation was unchanged. This result suggested two potential explanations. One possibility is linked to the significant change in the Hill coefficient, as C2 domain removal caused a marked reduction in the Hill coefficient for Ca^{2+} stimulation from ~4 to 1 (Table 4.1). This loss of cooperativity in Ca^{2+} stimulation could be important for generating Ca^{2+} oscillations. The other possibility is that the C2 domain plays an important role in targeting PLCζ to the correct subcellular source of $PtdInsP_2$ in eggs.

We also made LUC-tagged versions of PLCδ1 and ΔPHδ1 proteins. Both recombinant proteins were expressed *in vitro* (Figure 5.6A). The hydrolysing activity of these proteins was assessed using the standard $[^3H]PtdInsP_2$ hydrolysis assay and both PLCδ1-LUC and ΔPHδ1-LUC showed remarkable activity (Figure 5.6B). Although PLCδ1 possessed a much higher enzymatic activity *in vitro* compared to that of PLCζ (Figure 3.7), its oscillatory activity in mouse eggs was much lower (Figure 5.7). In addition PLCδ1 has not been detected in differentiated spermatids and spermatozoa (Lee *et al*, 1999) and is unlikely to be the sperm factor. But it was of great interest that microinjection and expression of cRNA, corresponding to ΔPHδ1, into mouse eggs was incapable of generating Ca^{2+} oscillations, even though ΔPHδ1

shares a considerable predicted domain homology and probably structure with PLCζ. It was clear that deletion of PH domain alone does not imbue a PLCδ-like isoform with oscillogenic activity. The fact that PLCδ1-LUC possessed some oscillatory activity in the eggs and given that the PH domain of PLCδ1 is primarily concerned with the targeting of the enzyme to a $PtdInsP_2$ substrate pool in the plasma membrane (Lemmon *et al*, 1995; Varnai and Balla, 1998, Dowler *et al*, 2000), suggested that PLCζ may target to a different (vesicular) pool of $PtdInsP_2$.

Chapter 6

Inhibition of $PtdInsP_2$ hydrolysing activity of human PLCζ (hPLCζ) by a mouse monoclonal antibody (mAb).

6.1 Introduction.

Antibodies can be used for immunological identification of proteins (western blot, Elisa), for detection of proteins in transfection studies, for separating proteins from other molecules in a cell lysate, as well as in a wide range of other experiments. The aim of these experiments was to produce and characterise anti-humanPLCζ (hPLCζ) mouse monoclonal antibodies (mAbs). mAbs have greater specificity than polyclonal antibodies and a single clone can produce unlimited quantities. The lack of a human anti-PLCζ (anti-hPLCζ) mAb from our laboratory necessitated its production.

A previous study showed that a mAb to the $InsP_3$ receptor completely blocked sperm-induced Ca^{2+} waves and Ca^{2+} oscillations in fertilised hamster eggs giving a first indication that Ca^{2+} release in fertilised hamster eggs is mediated by the $InsP_3$ receptor pathway (Miyazaki et al, 1992). Production of an anti-PLCζ mAb that could inhibit PLCζ hydrolysing activity *in vitro* and furthermore its oscillogenic activity in fertilised oocytes would be another indication that PLCζ is the sperm factor responsible for the Ca^{2+} oscillations during fertilisation.

The aim to produce a neutralising anti-hPLCζ mAb made the choice of the epitope very important. We designed two peptides corresponding to the XY linker sequence of hPLCζ (Figure 6.1) on the basis of our previous observations with mPLCζ that showed this region to play a significant role for targeting PLCζ to $PtdInsP_2$. Furthermore the basic amino acids in the sequence of these peptides could be highly immunogenic eliciting an enhanced immune response, an important factor for the successful production of mAbs.

Peptide A (299-312) KKIGTLKETHERKG

Peptide B (337-351) KKKTRKLKIALALSD

Figure 6.1 Sequence of peptides A and B, corresponding to portion of the XY linker region of hPLCζ, which were used as immunogens for the production of anti-hPLCζ mAbs.

6.2 Results.

6.2.1 Strategy for the production of anti-hPLCζ mAbs.

Peptides needed to be conjugated with a carrier protein to ensure immunogenicity of the antigen. We decided to conjugate each peptide with two different carrier proteins (BSA and KLH), obtaining two different versions of each peptide (A-BSA, A-KLH and B-BSA, B-KLH). This would help our screening strategy, avoiding any false positives to the carrier region, since one version of the peptide (for example A-BSA) would be used to immunise the mice and the other version (A-KLH) would be used for screening serum samples or media supernatants. 12 mice were injected with the peptides, in groups of three to each peptide. Two mice injected with B-BSA peptide and 1 mouse injected with B-KLH peptide died. This could be either a coincidence or the immunogenicity of peptide B may have been lethal for the mice. Tail bleeds from 8 mice were screened by ELISA (Figure 6.2) and the mouse number 2 (A2-BSA), which had been injected with A-BSA peptide and showed the strongest signal against A-KLH peptide was sacrificed. After the extraction of its spleen, fusion of the spleenocytes with myeloma cells was performed (section 2.2.4.4). The culture medium from the resulting hybridomas were screened against A-KLH peptide and 6 out 144 hybridomas which showed a reactivity with A-KLH peptide at least 10 times higher than background in the ELISA were regarded as positives (Table 6.1); and expanded 3-4 times in order to get a single clone producing the desired antibody. We successfully generated 3 mAbs, having lost the other 3 positives during the procedure of limiting dilution. All the mAbs (2A5, 5B6, 3C1) immunoreacted with both peptides A-BSA and A-KLH in an ELISA screen (Figure 6.3). The mAbs were isotyped using a commercial Isotyping kit (section 2.2.4.7) and found to be IgG1.

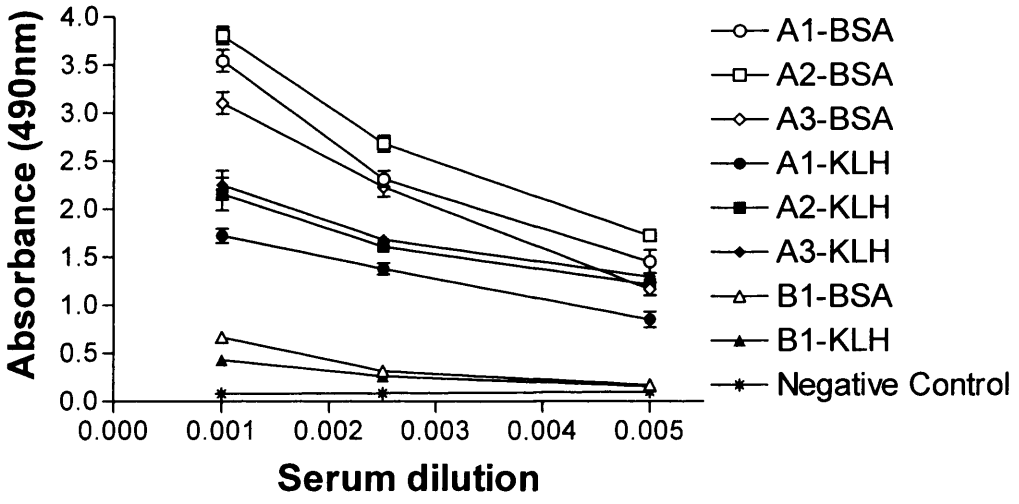

Figure 6.2 Pre-fusion ELISA screen of mice immunised with peptides A and B. Serum from eight test mice was tested by ELISA for immunoreactivity with A,B-KLH (open symbols) or A,B-BSA (solid symbols) depending on the antigen used for their immunisation. Serum from a non-immune mouse was used as negative control for this experiment. The spleen from mouse number 2, which had been injected with A-BSA peptide (A2-BSA) was used in the fusion since it showed the highest titre against A-KLH peptide.

Plate, well number	Absorbance (490nm)
2, A5	2.223 ± 0.233
3, C1	1.913 ± 0.178
4, B3	2.337 ± 0.210
4, C3	1.790 ± 0.121
5, A1	2.667 ± 0.301
5, B6	2.851 ± 0.165
Background	0.151 ± 0.035

Table 6.1 Wells of 96-well plates were coated with A-KLH peptide (1μg/well), blocked and incubated with 100μl supernatant from test fusion wells. Binding of the antibodies was detected using an HRPO-conjugated anti-mouse antibody and OPD development. Only a limited number of wells, which showed an absorbance value at least 10 times higher than background, and therefore can be regarded as positives are illustrated here. The majority of the remaining fusion wells showed an absorbance varied between 0.500 and 0.100.

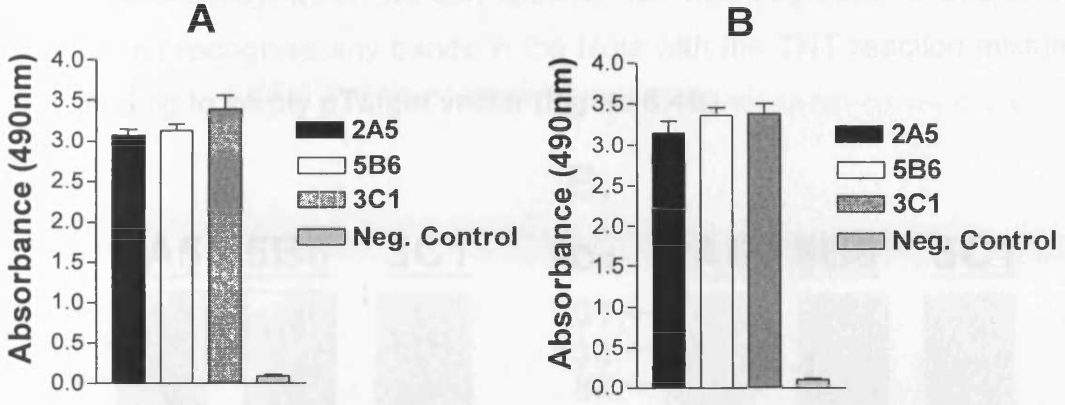

Figure 6.3 Elisa screening of the three mAbs. The wells of 96-well plates were coated with A-BSA (panel A) and A-KLH (panel B) peptide (1μg/well), blocked and incubated with 100μl supernatant from wells secreting the three monoclonal antibodies. Binding of the antibodies was detected using an HRPO-conjugated anti-mouse antibody and OPD development. Serum from non-immune mouse (1:1000 dilution) was used as negative control in this experiment.

6.2.2 Immunoreactivity of mAbs with recombinant hPLCζ expressed *in vitro*.

To test the ability of the mAbs to immunoreact with hPLCζ, attempts were made to express recombinant as a GST-tagged fusion protein. Although hPLCζ DNA was successfully cloned into pGEX-5X-2 and pBad vectors, for an unknown reason expression of recombinant protein was not possible in bacterial cells. We therefore used recombinant hPLCζ expressed *in vitro* using the TNT T7 Quick System. A pTarget-hPLCζ construct that had been previously made by Dr Llew Cox, was kindly provided. hPLCζ was expressed and the ability of mAbs to immunoreact with denatured recombinant hPLCζ was tested by western blot (Figure 6.4A). To test whether the antibodies bound unspecifically to any other products of the TNT reaction mixture, we used TNT reaction mixture corresponding to empty pTarget vector as negative control (Figure 6.4B). 15μl of TNT reaction mixtures corresponding to pTarget-hPLCζ construct and to the empty pTarget control were loaded into an 8% SDS-PAGE gel and blotted against the 3 mAbs. All mAbs recognised a 70kDa band corresponding to the correct size of hPLCζ plus some lower

bands (Figure 6.4B), which we can assume that was degraded hPLCζ since mAbs did not recognise any bands in the blots with the TNT reaction mixture corresponding to empty pTarget vector (Figure 6.4B).

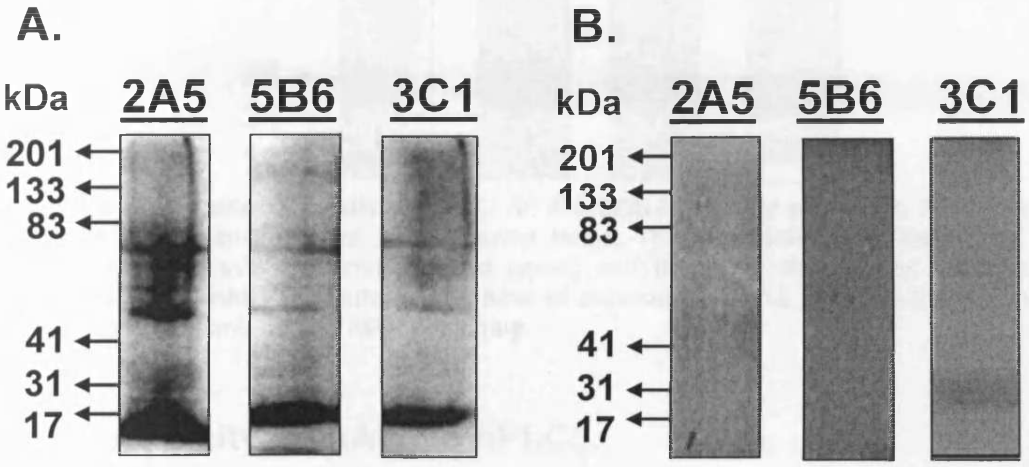

Figure 6.4 Recognition of recombinant hPLCζ. An 8% SDS-PAGE gel was used. **A.** 15μl of TNT reaction mixtures corresponding to pTarget-hPLCζ construct was loaded into each lane and immunoreactivity with the three mAbs (undiluted) was tested by western blot. The time of exposure was 10 min, **B.** 15μl of TNT reaction mixtures corresponding to empty pTarget vector was loaded into each lane and immunoreactivity with the three mAbs was tested by western blot. The time of exposure was 30 min. The secondary antibody used was anti-mouse.

6.2.3 Immunoreactivity of mAbs with native hPLCζ.

To test the ability of monoclonal antibodies to immunoreact with native hPLCζ, 100,000 sperm cells (of a control patient) were sonicated (in a water bath sonicator) for 5 minutes, diluted in 5x loading buffer (to 100μl final volume) and incubated for 30 min at 50 °C. The 100μl were split and 25,000 cell equivalents (25μl) were each loaded into 4 separate lanes of an 8% per cent SDS-PAGE gel. One resulting lane was stained by Coomassie Brilliant-Blue (Figure 6.5 last panel) and the other 3 lanes were blotted against the 3 mAbs (Figure 6.5 first 3 panels). All mAbs recognised a 70kDa band corresponding to the correct size of hPLCζ.

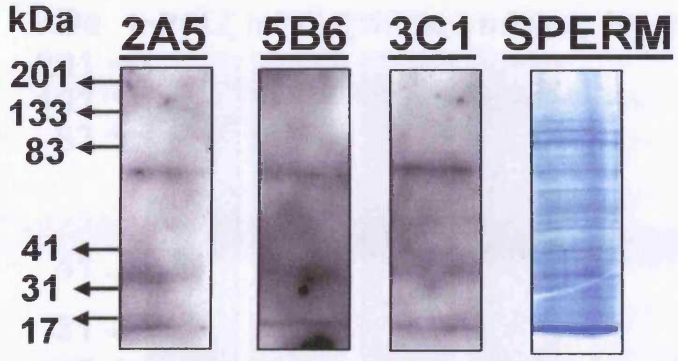

Figure 6.5 Recognition of native hPLCζ. An 8% SDS-PAGE gel was used; 25,000 sperm cells were loaded into each of four separate lanes. The four lanes were separated; one analysed by Coomasie Brilliant-Blue (last panel) and the other three lanes were blotted against the three mAbs (undiluted). The time of exposure was 15 min and the secondary antibody used was anti-mouse HRP conjugate.

6.2.4 Specificity of mAbs to hPLCζ.

Because there is a significant homology between peptide A (which corresponds to the XY linker sequence of hPLCζ and was used as the immunogen for the production of the mAbs) and 307-320 position of the XY linker sequence of mPLCζ (Figure 6.6), it was useful to test if the mAbs cross-reacted with mPLCζ. 1μg of recombinant GST-mPLCζ was loaded into 4 separate lanes of a 7.5% SDS-PAGE gel. After transfer to PVDF membrane, the 4 lanes were cut and blotted against the anti-GST (positive control antibody) and the 3 monoclonal antibodies (2A5, 5B6, 3C1), (Figure 6.7). The anti-GST antibody recognised a 100kDa band corresponding to the correct size of GST-mPLCζ plus some lower bands (degradation products), in contrast with the mAbs, which did not recognise any bands. This experiment was repeated twice. Even though there is a 10 out of 14 amino acids homology between peptide A and 307-320 position of the XY linker of mPLCζ, the mAbs did not cross-react with denatured recombinant mPLCζ. An important determinant for this could be the 3 positive charged Lysines (K) in the peptide A sequence, which are not present in the mPLCζ XY linker sequence. Epitope mapping of the mAbs would confirm this.

Mouse XY linker: 307 RKVGTLSETHERIG 320

PEPTIDE A: KKIGTLKETHERKG

Figure 6.6 Homology between 307-320 position of the XY linker of mPLCζ and peptide A.

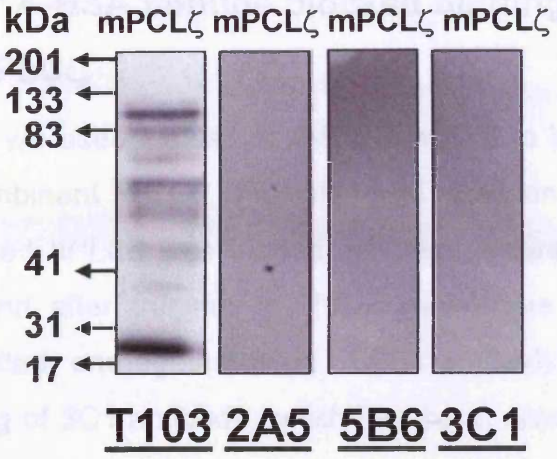

Figure 6.7 Cross-reactivity with mPLCζ. A 7.5% SDS-PAGE gel was used. 1μg of purified GST-mPLCζ was loaded into four separate lanes. The four lanes were separated and blotted against the T103 and the three mAbs (0 dilution). For the blot with T103 antibody, the time of exposure was 30 sec and the secondary antibody used was anti-rabbit. For the blots with 2A5, 5B6 and 3C1 mAbs, the time of exposure was 30 min and the secondary antibody used was anti-mouse HRP conjugate.

6.2.5 Purification of 3C1 mAb.

For further experiments, purification of mAbs from the crude supernatant was necessary. 1 L of crude 3C1 mAb was purified from crude supernatant using Montage® Antibody Purification kit (Section 2.2.4.9). We obtained a yield of 2.2 mg of purified antibody per Litre of crude supernatant. 10μg of purified 3C1 mAb was seperated on a lane of an 8% SDS-PAGE gel and analysed by Coomassie Brilliant-Blue (Figure 6.8).

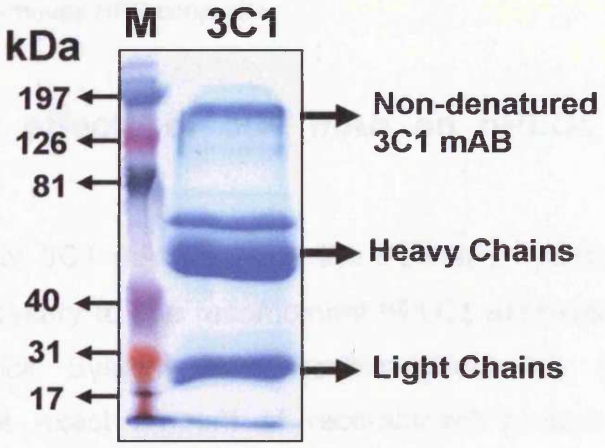

Figure 6.8 An 8% SDS-PAGE gel was used. 10μg of purified 3C1 mAb was analysed by Coomassie Brilliant-Blue.

6.2.6 Excess of A-BSA peptide blocked binding of 3C1 mAb to recombinant hPLCζ.

In this experiment we used excess of A-BSA peptide to block the binding of 3C1 mAb to recombinant hPLCζ. 15μl of a TNT reaction mixture containing unlabelled translated hPLCζ was loaded into two separate lanes of an 8% SDS-PAGE gel and after transfer to PVDF membrane the 2 lanes were separated and blotted; one against 36μg of 3C1 antibody (Figure 6.9A); and the other with 36μg of 3C1 antibody, which had been previously blocked with 60μg of A-BSA peptide at 4°C overnight (Figure 6.9B). Binding of A-BSA peptide to 3C1 antibody abolished its binding to hPLCζ.

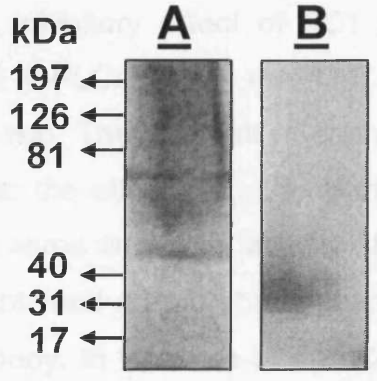

Figure 6.9 Specificity of 3C1 mAb. An 8% SDS-PAGE gel was used. 15μl of TNT reaction mixtures corresponding to pTarget-hPLCζ construct was loaded into two separate lanes. After transfer to PVDF membrane lanes were separated and one blotted against 36μg of 3C1 mAb (panel A) and the other with 36μg of 3C1 mAb, which had been previously blocked with 60μg of A-BSA peptide overnight at 4°C. The time of exposure was 20 min and the secondary antibody used was anti-mouse HRP conjugate.

6.2.7 Inhibitory effects of 3C1 mAb on hPLCζ hydrolysing activity.

To test the ability of 3C1 mAb to block the $PtdInsP_2$ hydrolysing activity of hPLCζ, it was necessary to use recombinant hPLCζ expressed *in vitro* using the TNT T7 Quick System as described previously (section 6.2.2). Quantitation of the exact amount of recombinant protein used in each experiment was not possible, but would give a preliminary idea for any inhibitory effects of 3C1 mAb. A pTarget-mPLCζ construct was kindly

provided. Recombinant mPLCζ was expressed as a negative control since we had previously shown that 3C1 mAb did not cross-react with mPLCζ. The hydrolysing activity of hPLCζ and mPLCζ was assessed using the standard [^{3}H]PtdInsP$_2$ hydrolysis assay. 7.5μl (half) of TNT reaction mixtures were incubated with [^{3}H]PtdInsP$_2$ and production of [^{3}H]InsP$_3$ was assessed by liquid scintillation counting. The negative control used in this experiment was a TNT reaction mixture corresponding to empty pTarget vector. Results showed that hPLCζ and mPLCζ possessed remarkable hydrolysing activity (Figure 6.10), with mPLCζ having a slightly higher activity. It was not possible to determine if this was related to this recombinant protein being expressed at higher levels or with a higher specific activity. Having established that both the hPLCζ and mPLCζ recombinant proteins were active, we set up a preliminary experiment to test the inhibitory effect of 3C1 mAb. We expressed new batches of hPLCζ and mPLCζ using the TNT system and the reaction mixtures were split into two. The first half of each reaction mixture was kept on ice for 4 hours and to the other half, 1.5 μg of 3C1 mAb was added and incubated on ice for the same time. The activity of all samples was tested. In the case of hPLCζ we obtained 48% of the total cpm counts after the addition of 3C1 monoclonal antibody. In the case of mPLCζ, addition of 3C1 antibody reduced its activity by only 6%. For a further confirmation we used increasing amounts of 3C1 antibody to block the activity of the recombinant proteins (Figure 6.11). The activity of hPLC was gradually reduced as we increased the amount of 3C1 antibody but in contrast the addition of different amounts of 3C1 antibody to mPLCζ did not significantly affect its hydrolysing activity.

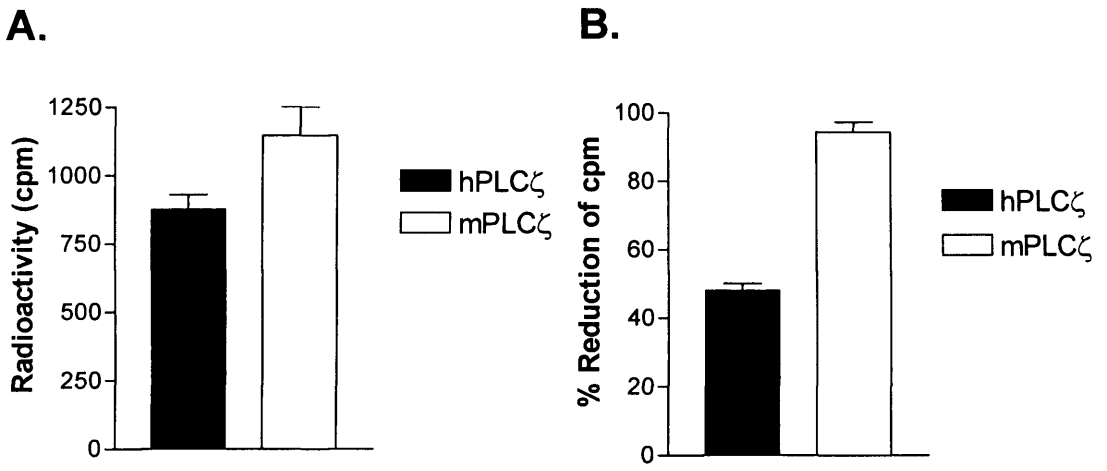

Figure 6.10 A. $PtdInsP_2$ hydrolysing activities of hPLCζ and mPLCζ (7.5µl) using the standard [^{3}H]$PtdInsP_2$ cleavage assay , n=2 ± s.e.m. The cpm value obtained for the negative control (empty pTarget vector; 190cpm), has been subtracted from the final cpm values corresponding to hPLCζ and mPLCζ recombinant proteins. **B.** % reduction of cpm values of hPLCζ and mPLCζ after addition of 1.5µg of 3C1 mAb to TNT reaction mixtures for 4 hours, prior standard [^{3}H]$PtdInsP_2$ cleavage assay , n=3 ± s.e.m using 3 different batches of TNT-expressed recombinant proteins.

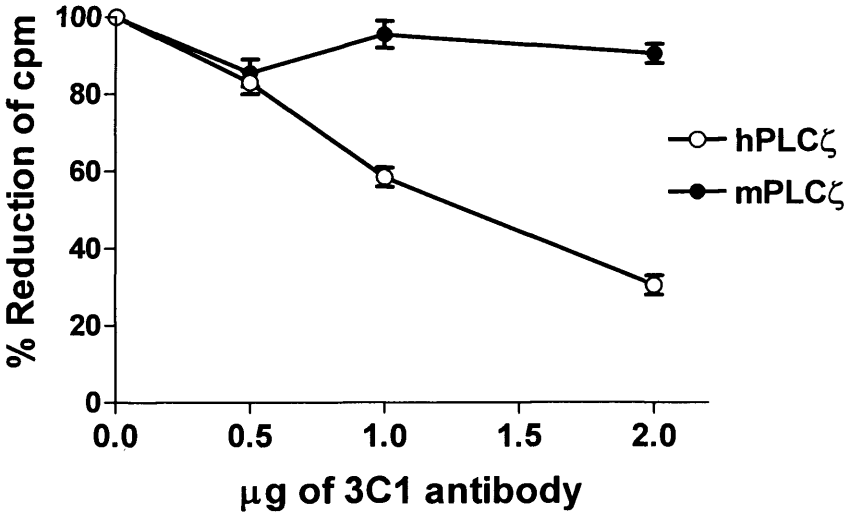

Figure 6.11 % reduction of cpm values of hPLCζ and mPLCζ after incubation with different amounts of 3C1 mAb added to TNT reaction mixtures for 4 hours, prior to the standard [^{3}H]$PtdInsP_2$ cleavage assay , n=2 ± s.e.m using 2 different batches of TNT-expressed recombinant proteins.

6.3 Discussion.

MAbs are essential laboratory tools enabling the characterisation of antigen distribution, structure and function. In addition they have two important advantages compared to polyclonal antibodies; their specificity and that they can be produced in unlimited quantities. Generation of mAbs to a specific protein traditionally requires purification of large amounts of native antigen for immunisation and screening. In our case, purification of large amounts of native hPLCζ from sperm was not possible. Another possible antigen could be recombinant hPLCζ. Recombinant protein would need a tag or other antibodies for purification purposes. In addition, it is very difficult to obtain 100% pure recombinant protein. To avoid all these problems we decided to use synthetic peptides as antigen. The disadvantage to the use of peptides could be that the mAbs raised against them will bind to the linearised antigen sequence rather than the folded conformation. We designed two peptides corresponding to the XY linker sequence of hPLCζ (Figure 6.1), with the aim of inhibiting hPLCζ hydrolytic activity based on our previous findings about the importance of this region to targeting of PLCζ to its substrate. Peptides were conjugated with 2 different carrier proteins (A-BSA and A-KLH) for screening purposes. 12 mice were injected with the peptides. ELISA screening of tail bleeds revealed that mice injected with A-BSA peptide gave the best signal against A-KLH peptide (Figure 6.2) and the mouse number 2 (A2-BSA), was chosen for the fusion. ELISA screening of supernatant from the resulting hybridomas revealed 6 positives against A-KLH peptide (Table 6.1), of which three reached the stage of mAb. The mAbs were isotyped and found to be IgG1. All the mAbs (2A5, 5B6, 3C1) immunoreacted with both peptides A-BSA and A-KLH in an ELISA screen (Figure 6.3), as well as with recombinant and native denatured hPLCζ on western blot (Figures 6.4; 6.5). Despite the significant homology between peptide A and 307-320 position of the mPLCζ XY linker sequence (Figure 6.6); mAbs appeared not to cross-react with mPLCζ. The reason is unknown since epitope mapping of the mAbs is required. 3C1 monoclonal antibody was purified from the crude supernatant and its inhibitory effects against hPLCζ hydrolysing activity were tested *in vitro*

with the TNT System, using mPLCζ expressed with the same TNT system, as a control. The $PtdInsP_2$ hydrolysing activity of hPLCζ was linearly reduced (in term of cpm values) with addition of increased amounts of 3C1 antibody in the TNT reaction mixture (without changing the final concentration of recombinant proteins in the cleavage assay). In contrast addition of different amounts of 3C1 antibody to mPLCζ did not significantly affect its hydrolysing activity (Figure 6.11).

The successful production of the 3C1 mAbs opens the way for a number of important experiments and has potential diagnostic value. MAbs could be used for immunocytochemistry and localisation experiments of hPLCζ in the sperm. It is likely that 3C1 mAb recognise the non-denatured hPLCζ protein as it neutralises activity of the folded recombinant protein. Also these antibodies can be used to screen sperm sample infertile men for absence of hPLCζ. Furthermore 3C1 mAbs may block the oscillogenic activity of hPLCζ into the oocytes and thus *in vivo* fertilisation providing further proof that PLCζ is indeed the sperm factor. Before this experiment can be performed a measure of the ratio of 3C1 mAb to of hPLCζ protein to block activity *in* vitro would be necessary. Thus, athough we managed to generate 3 anti-hPLCζ mAbs, further experiments are required for their characterisation and the characterisation of hPLCζ.

Chapter 7

General Discussion

7.1 PLCζ the trigger of Ca^{2+} oscillations during mammalian fertilisation.

The earliest signalling event in the activation of an egg by a sperm is a large, transient increase in intracellular free Ca^{2+} concentration (Stricker, 1999; Runft *et al*, 2002). In response to this Ca^{2+} signal, the fertilized egg completes meiosis and initiates the process of embryonic development (Lawrence *et al*, 1998). Several lines of evidence implicated the 1,4,5-trisphosphate ($InsP_3$) signaling pathway as the origin of the Ca^{2+} signals in mammalian eggs. Liberated $InsP_3$ causes Ca^{2+} release by binding to $InsP_3R$ located on the endoplasmic reticulum of eggs and oocytes (Wu *et al*, 2001). The essential role of $InsP_3$ and the $InsP_3R$ in fertilisation has been illustrated by studies in mouse and hamster eggs. Ca^{2+} oscillations at fertilization can be inhibited by microinjection of antibodies that inhibit $InsP_3R$ (Miyazaki *et al*, 1992), or by downregulation of $InsP_3Rs$ (Brind *et al*, 2000; Jellerette *et al*, 2000). In addition, it has been shown that sustained injection of $InsP_3$, or repeated photorelease of caged $InsP_3$, or microinjection of the $InsP_3$ analogue adenophostin, can all lead to a series of Ca^{2+} oscillations in eggs (Swann, 1994; Jones and Nixon 2000; Wu *et al*, 2001). Hence, in mammalian eggs, $InsP_3$ is both necessary and potentially sufficient to explain the Ca^{2+} oscillations observed at fertilization.

The sperm factor hypothesis was proposed as an alternative to receptor mediated activation of the $InsP_3$ pathway (Swann, 1990). Microinjection of sperm extracts, or whole sperm in eggs triggered Ca^{2+} oscillations similar to fertilization in a range of different species (Swann, 1990; Stricker, 1997; Wu *et al*, 1997; Kyozuka *et al*, 1998; Tang *et al*, 2000). The injection of such a sperm factor also triggered egg activation and embryo development at fertilisation (Fujimoto *et al*, 2004). The ability of soluble, mammalian sperm extracts to cause Ca^{2+} oscillations could be explained by the presence of a sperm-specific PLC activity (Jones *et al*, 2000; Parrington *et al*, 2002). A novel mammalian PI-PLC, phospholipase Cζ (PLCζ) was isolated from a spermatid cDNA library (Saunders *et al*, 2002). Microinjection of cRNA encoding the mouse (Saunders *et al*, 2002), human, and cynomolgus monkey PLCζ (Cox *et al*, 2002) into mouse eggs, triggered Ca^{2+} oscillations similar to those

observed at fertilisation. Furthermore, Ca^{2+} oscillations were abolished when PLCζ was immunodepleted from native sperm extracts (Saunders *et al*, 2002). The presence of PLCζ was also demonstrated in boar and hamster sperm (Saunders *et al*, 2002). Microinjection of recombinant PLCζ, synthesised using a baculovirus expression system, also triggered Ca^{2+} oscillations in mouse eggs (Kouchi *et al*, 2004). In addition, another recent study reported that sperm from transgenic mice expressing short hairpin RNAs had reduced amounts of PLCζ and triggered Ca^{2+} oscillations following *in vitro* fertilisation that terminated prematurely (Knott *et al*, 2005). One notable feature of PLCζ is that it is effective at causing Ca^{2+} oscillations in eggs at very low concentrations (e.g. 10fg/egg), (Saunders *et al*, 2002, Kouchi *et al*, 2004, Fujimoto *et al*, 2004). In contrast, other studies have shown that PLC isoforms of the β, γ or δ class are either ineffective (Jones *et al*, 2000), or at least much less effective than PLCζ at causing Ca^{2+} release, when microinjected in eggs (Runft *et al*, 2002, Kouchi *et al*, 2004).

In Figure 7.1 we propose a hypothetical mechanism of PLCζ-induced Ca^{2+} oscillations at fertilisation.

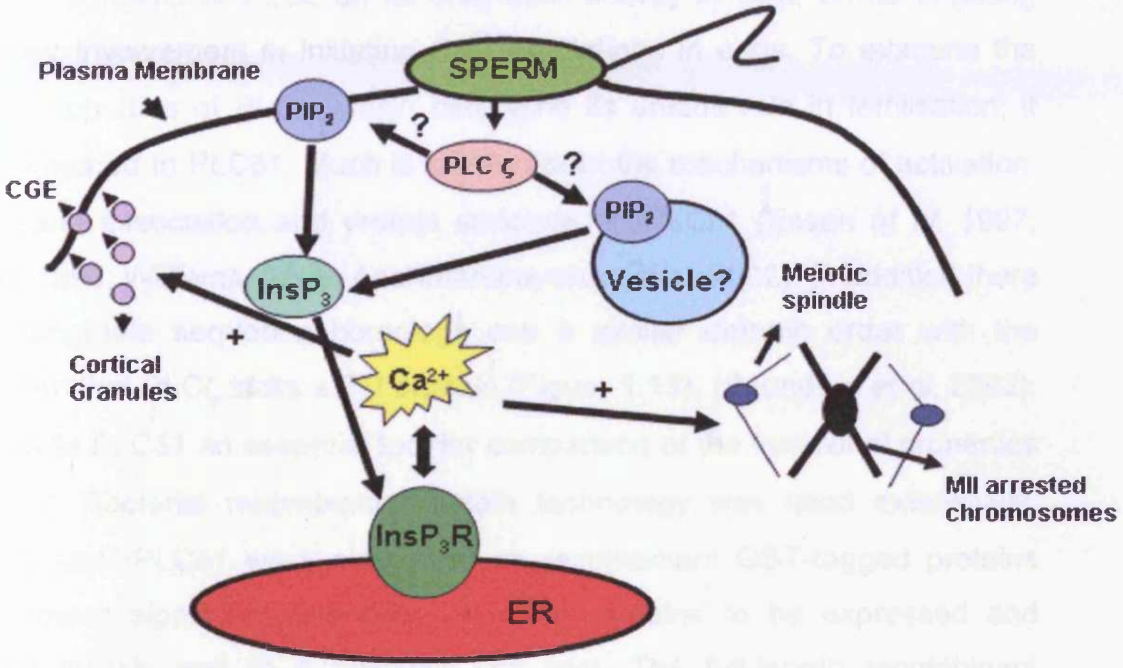

Figure 7.1 Summary of PLCζ-induced Ca^{2+} release at fertilisation.

PLCζ diffuses into oocyte cytosol from the sperm head. Reports from a recent study localised PLCζ to the post-acrosomal region of mouse sperm suggesting a mechanism by which PLCζ originates from an oocyte penetrating assembly, the sperm perinuclear matrix, to induce mammalian oocyte activation (Fujimoto *et al*, 2004). PLCζ then hydrolyses $PtdInsP_2$ in either plasma membrane or other intracellular vesicles and production of $InsP_3$ stimulates Ca^{2+} release from ER stores, which may feedback to attenuate both PLCζ activity and $InsP_3R$ sensitivity. Released Ca^{2+} may also cause activation of oocyte PLCs, adding to the pool of stimuli for repetitive Ca^{2+} release. Rise in $[Ca^{2+}]$ results in cortical granule exocytosis and resumption of meiosis.

7.2 Experimental Approach.

In this study we examined the biochemical properties and the importance of selected domains of PLCζ on its enzymatic activity *in vitro,* on its targeting and their involvement in initiating Ca^{2+} oscillations in eggs. To examine the critical properties of PLCζ, which determine its unique role in fertilisation, it was compared to PLCδ1. Much is known about the mechanisms of activation, membrane association and protein structure of rPLCδ1 (Essen *et al*, 1997; Katan, 1998; Williams, 1999; Ananthanarayanan *et al*, 2002). In addition there is considerable sequence homology and a similar domain order with the exception that PLCζ lacks a PH domain (Figure 1.13), (Saunders *et al*, 2002). This made PLCδ1 an essential tool for comparison of the functional properties of PLCζ. Bacterial recombinant protein technology was used extensively. mPLCζ and rPLCδ1 were expressed as recombinant GST-tagged proteins that allowed significant quantities of active proteins to be expressed and purified quickly and at a relatively low cost. The full-length recombinant proteins were used to study the kinetics of $PtdInsP_2$ hydrolysis and the effects of free Ca^{2+} concentration. These studies were extended to explore the role of the EF hand, C2 and XY linker domains by using a series of recombinant deletion constructs of these critical domains. These were examined for their effects on Ca^{2+} sensitivity of $PtdInsP_2$ hydrolysis and the targeting of PLCζ to $PtdInsP_2$ and other membrane phosphoinositides using both vesicle and PIP strip assays. Similar constructs tagged with luciferase (LUC) were made and cRNA corresponding to each of these constructs was injected into oocytes, in order to quantitate their expression levels and their potential to elicit Ca^{2+} oscillations. Finally we produced anti-hPLCζ monoclonal antibodies with the aim to primarily block the *in vitro* hydrolysing activity of hPLCζ and then to test any inhibitory effects of these antibodies in the initiation and/or the persistence of fertilisation-induced Ca^{2+} oscillations.

7.3 PtdInsP$_2$ hydrolysis, Ca^{2+} sensitivity and the role of EF hand domains.

The first critical property of mPLCζ is its high Ca^{2+} sensitivity compared to rPLCδ1. mPLCζ appeared to be 100 times more sensitive to Ca^{2+} than rPLCδ1 with an EC_{50} of 82nM, which is well within the range of reported resting Ca^{2+} concentrations in eggs. mPLCζ was maximally active at 1μM Ca^{2+} but rPLCδ1 was not fully activated until 30μM (Figure 3.12).

It was clear from our data that PLCζ was unable to stimulate Ca^{2+} release in oocytes when it lacked one or both of its EF hand domains (Figures 5.1, 5.4). This result is consistent with previous observations with a short form of PLCζ that lacks the first 110 amino acids at the N-terminus (Kouchi *et al.*, 2004). The basic ability to hydrolyse PtdInsP$_2$ *in vitro* (Figure 4.3) was preserved for these deletion constructs. However, deletion of both EF hands dramatically changed the EC_{50} for Ca^{2+} of PLCζ from 82 nM to 30 μM (Table 4.1, Figure 4.3). Even deletion of the first EF hand domain raised the EC_{50} for Ca^{2+} to >700nM, which is well above the resting Ca^{2+} level in an egg. Thus truncation of EF hands would ablate the ability of this domain-deletion to generate InsP$_3$ in an intact cell possessing a basal Ca^{2+} concentration of around 100nM. The Hill coefficients were also decreased by deletion of one or both of the EF hand domains. The Hill coefficient describes the minimum number of interacting active sites required for enzyme function, suggesting that upon removal of the EF hands the minimum number of sites for Ca^{2+} is reduced from ~4 to ~1. Ca^{2+} binding to the EF hands may therefore be important for the interaction of the XY domain with PtdInsP$_2$ substrate and thus for PLCζ enzyme activity. These results are in overall agreement with a similar and very recent PLCζ study where the authors indicated that the first half of the second pair of EF hands (EF2) is the important domain for the high Ca^{2+} sensitivity of PLCζ (Kouchi *et al*, 2005).

7.4 Targeting of PLCζ to $PtdInsP_2$.

A critical property of mPLCζ was its ability to bind with high affinity to $PtdIns(3,5)P_2$ and $PtdIns(4,5)P_2$ even though it lacked a PH domain from its sequence, which functions to target PLC isozymes such as PLCδ1 to $PtdIns(4,5)P_2$ sources (Lemmon *et al*, 1995; Varnai *et al*, 2002). We demonstrated the ability of mPLCζ to target $PtdIns(4,5)P_2$ using two different approaches, an overlay and a centrifugation/activity assay with a number of positive and negative controls (Figures 3.15, 3.16). The role of the C2 domain and the XY linker were examined as potential $PtdInsP_2$ membrane targeting domains.

7.4.1 Role of C2 domain of PLCζ.

The C2 domain has been well characterised as a membrane associating and intermolecular binding domain in a wide range of proteins (Medkova and Cho, 1999; Gerber *et al.*, 2001; Frazier *et al.*, 2002). Our data regarding the biological functions of the C2 domain imply that this domain has an essential role in the unique cellular function of PLCζ since deletion of the C2 domain from mPLCζ led to an inability to cause Ca^{2+} oscillations in intact eggs (Figures 5.1, 5.4). However the EC_{50} for Ca^{2+} stimulation was similar to that corresponding to full-length mPLCζ, in contrast to the effect of the deletion of EF hands (Table 4.1). There were two potential explanations for this result. One possibility was linked to the significant change in the Hill coefficient, as C2 domain removal caused a marked reduction in the Hill coefficient for Ca^{2+} stimulation from ~4 to 1 (Table 4.1). This loss of cooperativity in Ca^{2+} stimulation could be important for generating Ca^{2+} oscillations. The other possibility is that the C2 domain plays an important role in targeting PLCζ to the correct subcellular source of $PtdInsP_2$ in the eggs. To investigate the second hypothesis we expressed and purified the C2 domains of mPLCζ and rPLCδ1 as GST fusion proteins and we examined their binding to phosphoinositides spotted on PIP strip membranes. GST-ζC2 bound with high affinity to all PtdInsPs and showed a reduced but remarkable affinity for $PtdIns(3,5)P_2$, $PtdIns(4,5)P_2$, in contrast with GST-δ1C2, which did not show

any significant binding to any PtdInsP or $PtdInsP_2$, except some binding with low affinity to PtdIns(5)P, PtdIns(4)P and PtdIns(3,5)P_2 (Figure 4.10). This result suggested that the C2 domain of mPLCζ might not be sufficient for targeting the enzyme to $PtdInsP_2$, but could play an important role. Nevertheless, these results are not consistent with the other recent PLCζ study (Kouchi *et al,* 2005). The authors in that study used a similar PIP strip overlay assay and found that the C2 domain of mPLCζ bound to PtdIns(3)P and to lesser extend to PtdIns(5)P. Further confirmation for our result came when we calculated the *Km* values for ζΔC2 and ζΔEF1,2 deletion constructs (Figure 4.12). Deletion of C2 domain resulted in a dramatic 9-fold increase of the *Km* (802μM) of mPLCζ in contrast with deletion of EF hands, which resulted in a 2-fold increase of the *Km* (188μM) value for mPLCζ, suggesting that deletion of the C2 domain dramatically affects the affinity of mPLCζ for PtdIns(4,5)P_2 substrate. Further experiments with regard the importance of C2 domain on targeting of mPLCζ are required. It is also possible that association of PLCζ with its specific plasma membrane target may be mediated by interaction of C2 domain with another membrane-targeting protein, as has been previously demonstrated for the C2 domain of $PLA_2\alpha$ and its associations with vimentin. Vimentin is an intermediate filament component that acts as a perinuclear adapter for $PLA_2\alpha$ through its associations with the C2 domain of $PLA_2\alpha$ in a Ca^{2+}-sensitive manner (Nakatani *et al*, 2000).

7.4.2 Role of XY linker of PLCζ.

The XY linker is the sequence that links together the two domains forming the β/α catalytic barrel. It is the only sequence in the protein structure of PLCδ1 that has not been resolved by X-ray crystallography and its specific role in the molecular function of PLC is still unclear. The XY linker region of PLC ζ contains a cluster of basic residues not found in the unstructured homologous region of PLCδ1 (Figure 4.6). We hypothesised a putative role of this region on anchoring PLCζ to biological membranes by interactions with acidic lipids or even by direct binding to the $PtdInsP_2$ substrate. To test this hypothesis we expressed and purified the XY linkers of mPLCζ and rPLCδ1 as GST fusion

proteins and we tested their binding to phosphoinositides spotted on PIP strip membranes. The XY linker of rPLCδ1 showed no binding to any phosphoinositides, in contrast with the XY linker of mPLCζ, which showed very high affinity for all PtdInsPs and PtdIns(3,5)P_2 and some affinity for PtdIns(3,4)P_2, PtdIns(4,5)P_2 and PtdIns(3,4,5)P_3. This was a first indication that this region could be an important determinant in addition to the C2 domain on targeting mPLCζ to inositol phosphate enriched biological membranes. To further investigate the importance of this region on the high affinity of PLCζ for PtdIns(4,5)P_2, we constructed a mPLCζ mutant (expressed and purified as GST fusion protein), in which two amino acids with strong positive charge (K) in the XY linker region (374 and 375 position) had been replaced by two neutral amino acids (A); and we calculated the *Km* value for that mutant. The *Km* value for this PLCζ^{K374,5AA} mutant was 8 fold higher (707μM), (Figure 4.11) than that corresponding to the wild type mPLCζ (87μM) suggesting that this region could also play an important role in addition to the C2 on targeting PLCζ to its substrate. Although further investigation is required, it may be possible that the XY linker might plays a role in interaction of PLCζ with other membrane-associating cellular proteins. Nevertheless it has already been described that this region contains the nuclear localisation signal targeting PLCζ to the pronuclei. This pronuclear sequestration of PLCζ may explain the cell cycle-dependent regulation of Ca^{2+} oscillations following fertilisation (Larman *et al*, 2004).

In addition, recent experiments in which cRNA corresponding to hPLCζ-LUC construct (made by Dr Saunders) was microinjected in mouse eggs showed that the hPLCζ is more potent than its mouse counterpart (Laboratory communication). Given that the only significant sequence difference between hPLCζ and mPLCζ is that the mouse isozyme has 29 extra amino acids and a more negatively charged XY linker region compared to the Human (Figure 7.2). This small difference in the protein sequence appears to be critical for the difference in the oscillatory activity between the two species' PLCζ isoforms. This implies a significant role for the XY linker region in the activity of the PLCζ enzyme, as a small overall change in the peptide sequence of this region has a large effect on oscillatory activity.

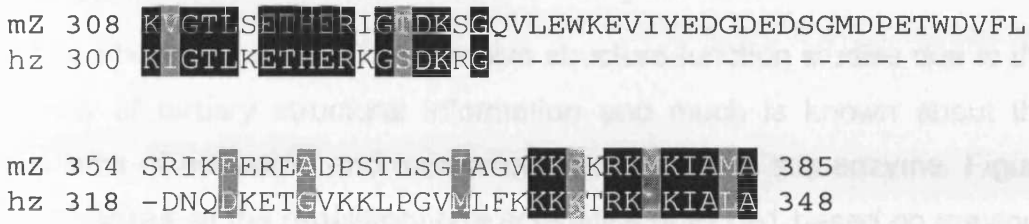

Figure 7.2 ClustalW alignment of mouse and human PLCζ XY linkers. Identical amino acids are shown in shaded black boxes; conservative substitutions are boxed in grey.

7.5 ΔPHPLCδ1 was ineffective in triggering Ca^{2+} oscillations in mouse eggs.

The two biochemical properties of PLCζ (its high Ca^{2+} sensitivity and its ability to bind $PtdInsP_2$ that we demonstrated in this thesis may be the source of explanation why PLCζ was so effective in triggering Ca^{2+} oscillations compared to PLCδ1, which appeared to be less effective when cRNAs corresponding to Luciferase tagged versions of these proteins microinjected in mouse eggs (Figure 5.7). PLCδ1 is unlikely to be the sperm factor because has not been detected in differentiated spermatids and spermatozoa (Lee *et al*, 1999). The Ca^{2+} oscillations triggered upon the microinjection of cRNA corresponding to PLCδ1-LUC could be the result of overexpression of this protein in mouse oocytes. This result is in overall agreement with the observations of another recent study, in which recombinant PLCδ1 triggered Ca^{2+} oscillations when microinjected in a 20-fold higher concentration than recombinant PLCζ (Kouchi *et al*, 2004).

We also investigated whether simplification in protein structure of PLCδ1 may be specifically responsible for the distinctive activity of PLCζ by creating a truncated clone of PLCδ1, missing the PH domain, creating a PLCδ1-derived clone with the same (predicted) domain structure as PLCζ (Figure 5.5A). This clone failed to trigger Ca^{2+} changes when microinjected in mouse eggs (Figure 5.7), despite the fact that it retained a higher enzymatic activity *in vitro* compared to mPLCζ (Figure 3.15).

7.6 A hypothetical mechanism of PLCζ action.

PLCδ1 has been the subject of extensive structure-function studies due to the availability of tertiary structural information and much is known about the mechanisms of activation and membrane association of this enzyme. Figure 7.3 summarises all the regulatory characteristics of PLCδ1 based on previous studies.

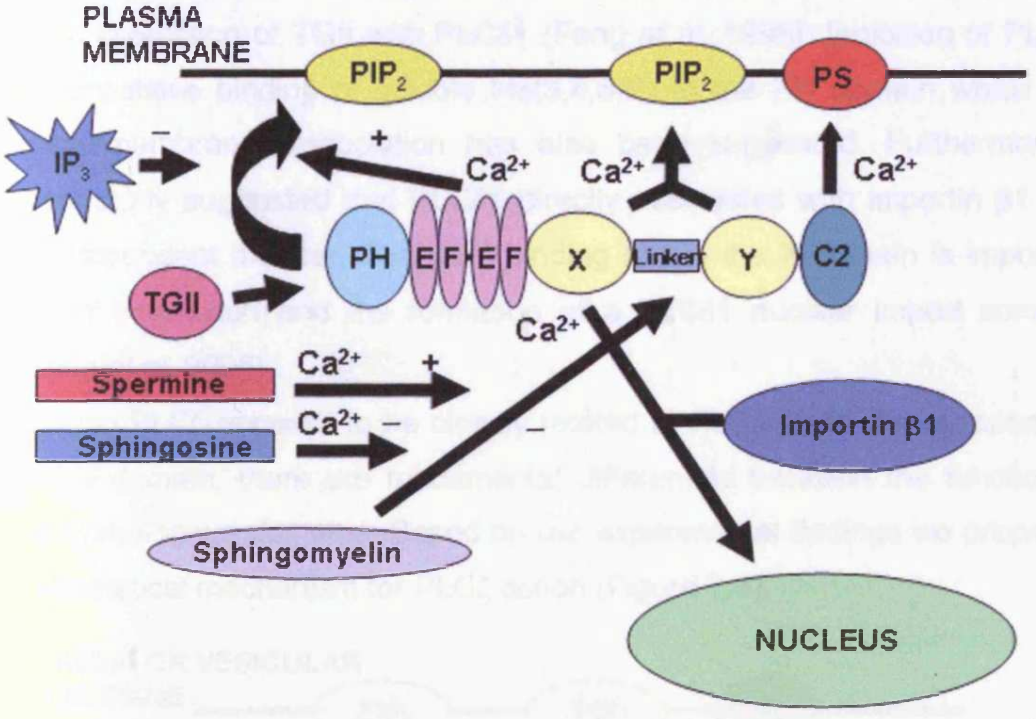

Figure 7.3 Summary of the control mechanisms of PLCδ1 characterised from a wide variety of studies (see text for explanation and references).

The PH and C2 domains are involved in the membrane attachment of PLCδ1. Crystallographic data suggested that the EF hand domain of PLCδ1 does not bind to Ca^{2+} but rather serves as a flexible link between the PH domain and the rest of the enzyme, allowing the C2 and catalytic domains to interact with the membrane after binding of the PH to PtdIns(4,5)P_2 (Rhee, 2001). However a more recent study suggested that the EF hand domain of PLCδ1 does bind Ca^{2+} and this is necessary for an efficient interaction of PH with PtdIns(4,5)P_2 (Yamamoto *et al*, 1999). In addition, Ca^{2+} binding to the C2 domain promotes the formation of an enzyme-phosphatidylserine-Ca^{2+} tertiary complex, increasing the affinity of the enzyme for substrate vesicles and leads

to enzyme activation (Lomasney *et al*, 1999). Once PLCδ1 is associated with the membrane PtdIns(4,5)P_2 the catalytic X/Y barrel binds and hydrolyses the inositol headgroup of PtdIns(4,5)P_2. Hydrolysis of PtdIns(4,5)P_2 is Ca^{2+} dependent and requires Ca^{2+} binding to one site in the catalytic domain (Grobler and Hurley, 1998). The activity of PLCδ1 is attenuated by interaction of the enzyme with sphingomyelin. This interaction is regulated by Ca^{2+}-dependent associations of spermine and sphingosine (Pawelczyk and Matecki, 1997). Additional regulatory mechanisms have been suggested such as the interaction of TGII with PLCδ1 (Feng *et al*, 1996). Inhibition of PLCδ1 by competitive binding of soluble Ins(3,4,5)P_3 to the PH domain which can induce membrane dissociation has also been suggested. Furthermore a recent study suggested that PLCδ1 directly associates with importin β1 in a Ca^{2+}-dependent manner. The Ca^{2+} binding site in the X domain is important for this interaction and the formation of a PLCδ1 nuclear import complex (Okada *et al*, 2005).

Although PLCζ appears to be closely related to PLCδ1 with the exception of the PH domain, there are fundamental differences between the function of their homologous domains. Based on our experimental findings we proposed a hypothetical mechanism for PLCζ action (Figure 7.4).

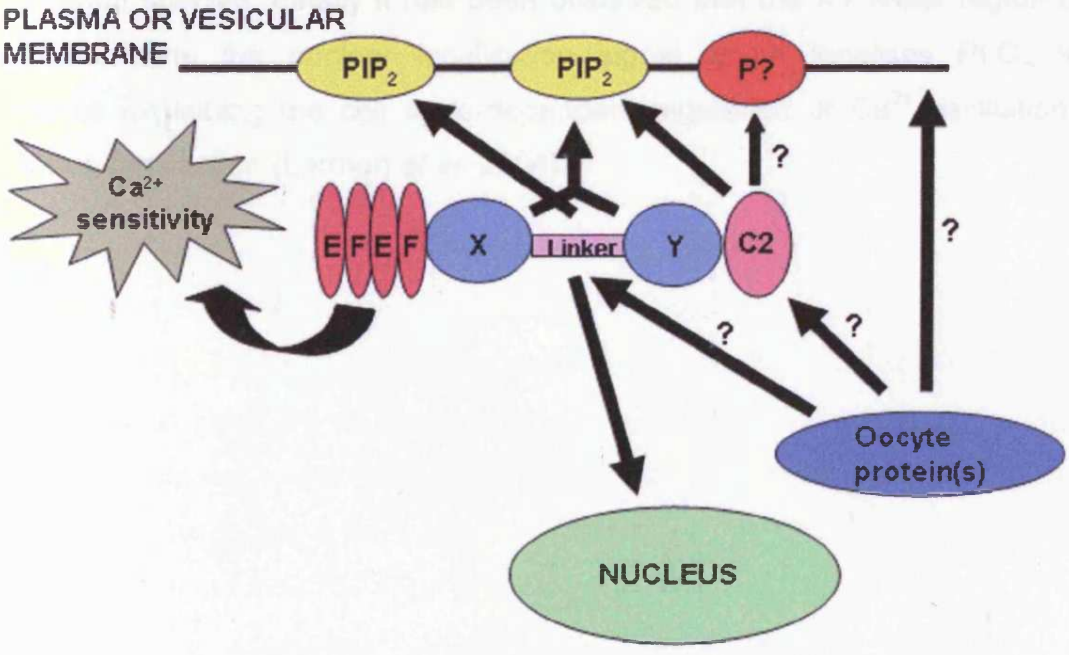

Figure 7.4 Summary of a hypothetical mechanism of PLCζ action based on our findings.

The type of membrane that PLCζ targets, is still not clear. PLCζ either targets a distinct vesicular $PtdInsP_2$-containing membrane, or a distinct $PtdInsP_2$-containing microdomain within the plasma membrane. EF hands confer the high Ca^{2+} sensitivity of PLCζ, which enables the enzyme to be active even at resting Ca^{2+} levels. If PLCζ is able to associate with a distinct $PtdInsP_2$ pool, then an important role in that association may be the positively charged XY linker region and/or the C2 domain, although they did not appear to be sufficient to target PLCζ to $PtdInsP_2$ on their own. The PIP strip and vesicle associated assays do not show that either domain is highly discriminatory for $PtdInsP_2$ compared to other phosphoinositides. Thus the mechanism of targeting to a specific $PtdInsP_2$ pool is not yet clear. However, both the XY linker region and the C2 domain may be necessary for an efficient interaction of PLCζ with $PtdInsP_2$. It is also possible that association of PLCζ with its specific plasma membrane target may be mediated by interaction of XY linker or C2 domain with another membrane-targeting protein but this requires further investigation.

Once PLCζ is associated with the membrane $PtdIns(4,5)P_2$ the catalytic X/Y barrel binds and hydrolyses its substrate. The non-conserved XY linker region may explain the different rates of $PtdInsP_2$ hydrolysis between PLCζ isoforms of different species. Finally it has been observed that the XY linker region of PLCζ contains the nuclear localisation signal which localises PLCζ to pronuclei explaining the cell cycle-dependent regulation of Ca^{2+} oscillations following fertilisation (Larman *et al*, 2004).

7.7 Future directions of this study.

We have demonstrated some critical biochemical properties of PLCζ. We propose on the basis of these findings a hypothetical mechanism of PLCζ action outlined above. In the course of this study, valuable and successful experimental approaches have been developed. Bacterial recombinant protein has proved a robust tool for measuring $PtdInsP_2$ hydrolysis and Ca^{2+} sensitivity for wild-type PLCζ and the series of deletion constructs. The design of LUC constructs has enabled confirmation and quantitation of expression of PLC constructs in oocytes, in parallel with the monitoring of their oscillogenic activity. In future these tools would be the basis for further studies to address the many questions remaining with regard to the mechanism of PLCζ action and its role in fertilisation.

A useful method for further investigation of the role of each domain on PLCζ function would be the construction of PLCζ/PLCδ1 chimeras. Swapping different domains between these proteins will enable us to investigate the specific role of each region on the enzymatic and oscillogenic activity of PLCζ. Recombination of PLCζ specific regions with the ΔPHδ1 protein would be interesting, testing the possibility to construct ΔPHδ1-PLCζdomain(s) chimera, with similar oscillogenic activity with PLCζ, demonstrating the combination of specific domains essential for the specific cellular activity of PLCζ. In addition construction of human/mouse/or other species PLCζ chimeras will be very useful, especially swapping XY linker regions, in order to understand better the importance of this region and its putative effects on enzymatic and thus oscillogenic activities of PLCζ from different species.

Another step forward in the analysis of the molecular properties of PLCζ will be the X-ray crystallography of high-fidelity purified PLCζ recombinant protein, preferably untagged. X-ray crystallography will reveal all the critical ion and lipid/protein-binding sites in the protein providing a useful tool for further investigation of putative interactions of PLCζ with ions, lipids or proteins, which may play an important role in its function.

To test whether subcellular localisation of PLCζ depends on interactions of the C2 domain or XY linker with oocyte cytosolic protein(s), which transport

the PLCζ enzyme to a $PtdInsP_2$ rich membrane, yeast-two-hybrid assay system will be useful. This can be followed by a more specific assay for the mechanisms of these interactions, such as immunoprecipitation.

To investigate PLCζ/lipid interactions the technique of surface plasmon resonance (SPR) can be used. This technique measures the kinetics of intermolecular associations with high degree of accuracy, in real time. SPR has been successfully used previously to investigate the lipid binding kinetics of other C2 domains, including those of PLA_2, PKC (Stahelin and Cho, 2001) and PLCδ1 (Ananthanarayanan *et al*, 2002).

The production of the anti-hPLCζ monoclonal antibodies could be invaluable although further work is required for their characterisation. If these monoclonal antibodies inhibit the initiation and/or persistence of fertilisation-induced Ca^{2+} oscillations it will be another confirmation that hPLCζ is the sole molecule responsible for the generation of Ca^{2+} oscillations at fertilisation. In addition these antibodies can be used for analysis of human sperm providing a better understanding for male infertility since 40% of failed fertilisation ICSI are reported to be due to failure of egg activation (Rawe *et al*, 2000).

Further experimental work on PLCζ activation and regulatory mechanisms is required. This would contribute to a greater understanding of the fundamental mechanisms of the earliest events in oocyte activation and embryogenesis.

APPENDIX I. ABBREVIATIONS

A	alanine
AA	amino acid
Ab	antibody
ADP	adenosine diphosphate
ADPR	ADP-ribose
ATP	adenosine triphosphate
BAPTA	1,2-bis(2-aminophonoxy)ethane-N,N,N',N'-tetraacetic acid
BCA	bicinchoninic acid
bp	base pair(s)
BSA	bovine serum albumin
C	cysteine
C2 domain	PKC homology domain type 2
Ca^{2+}	calcium ion
cADP	cyclic ADP
cADPR	cyclic ADP-ribose
CaM	calmodulin
cAMP	cyclic adenosine monophosphate
cDNA	complementary DNA
CGE	cortical granule exocytosis
cRNA	complementary RNA
CSF	cytostatic factor
C-terminus	carboxyl terminus
DAG	diacylglycerol
DEPC	diethylpyrocarbonate
DMSO	dimethyl sulphoxide
DNA	deoxyribonucleic acid
dNTP	2'-deoxyribonucleotide 5'-triphosphate
DTT	dithiothreitol
E. Coli	*Escherichia Coli*
EDTA	ethylene-diamine-tetraacetic acid
EF hand domain	elongation factor hand domain

EGF	epidermal growth factor
EGFR	epidermal growth factor receptor
EGTA	ethyleneglycolbib-(β-aminoethylether)-N,N,N',N'-tetraacetic acid
ELISA	enzyme-linked immunosorbent assay
EPG	epidermal growth factor
ER	endoplasmic reticulum
EST	expressed sequence tag
FCS	foetal calf serum
FKBP12	FK506-binding protein 12
FSH	follicle stimulating hormone
GFP	green fluorescent protein
G-protein	guanine nucleotide-binding protein
GPCRs	G-protein coupled receptors
GSH	glutathione reduced
GST	glutathione S-transferase
GVBD	germinal vesicle breakdown
HAT	selection medium containing hypoxanthine, methotrexate thymidine
hCG	human chorionic gonadotrophin
HEPES	N-2-hydroxyethyliperazine-N'2-ethanesulphonic acid
hPLCζ	human PLCζ
ICSI	intracytoplasmic sperm injection
$InsP_3$	Inositol 1,4,5-trisphosphate
$InsP_3R$	Inositol 1,4,5-trisphosphate receptor
IPA	isopropyl alcohol
IPTG	isopropyl β-D-1-thiogalactopyranoside
K	lysine
K_m	Michaelis-Menten constant
kb	kilobase(s)
kDa	kiloDalton(s)
KLH	keyhole limpet hemocyanin protein
LB	Luria's broth

LUC	luciferase
LUVs	Large Unilamellar Vesicles
MAb	monoclonal antibody
MAPK	mitogen-activated protein kinase
MCS	multiple cloning site
MDa	megaDalton(s)
MPF	maturation promoting factor
mPLCζ	mouse PLCζ
MW	molecular weight
NAD	β-nicotinamide adenine dinucleotide
NADP	β-nicotinamide adenine dinucleotide 2'-phosphate
NAADP	nicotinic acid adenine dinucleotide phosphate
NE	nuclear envelope
NFG	nerve growth factor
NO	nitric oxide
NRTK(s)	nonreceptor tyrosine kinase(s)
N-terminus	amino terminus
PA	phosphatidic acid
PAGE	polyacrylamide gel electrophoresis
PBS	phosphate buffered saline
PC	phosphatidylcholine
PCR	polymerase chain reaction
PDGF	platelet-derived growth factor
pfu	plaque-forming units
PH domain	pleckstrin homology domain
PKA	protein kinase A
PKC	protein kinase C
PLA	phospholipase A
PLC	phospholipase C
PS	phosphatidylserine
$PtdInsP_2$	phosphatidylinositol 4,5-bisphosphate
PTK(s)	protein tyrosine kinase(s)
PTPases	protein tyrosine phosphatases

PVDF	polyvinylidene fluoride
RACE	rapid amplification of cDNA ends
RA domain	Ras-association domain
RGS	regulators of G-protein signalling
RNA	ribonucleic acid
ROCC	receptor-operated calcium channel
ROS	reactive oxygen species
RPMI	Roswell Park Memorial Institute medium
RTK(s)	receptor tyrosine kinase(s)
RyR	ryanodine receptor
S1P	sphingosine 1-phosphate
SDS	sodium dodecyl sulphate
SERCA	sarco/endoplasmic reticulum Ca^{2+}-ATPase
SF	sperm factor
SFK(s)	Src-family of protein tyrosine kinase(s)
SH2	Src homology 2 domain
SH3	Src homology 3 domain
SOCC	store-operated calcium channel
SR	sarcoplasmic reticulum
TAE	Tris-acetate-EDTA buffer
TBS	Tris buffered saline
TBS-T	TBS-Tween20
TEMED	N,N,N',N'-tetramethylethylenediamine
T_m	melting temperature
TNT	coupled *in vitro* transcription and translation
Tris	tris(hydroxymethyl)aminomethane
VOCC	voltage-operated calcium channel
Y	tyrosine
ZP	zona pellucida

APPENDIX II. BIBLIOGRAPHY

Abou-Haila, A. and Tulsiani, D.R. (2000) Mammalian sperm acrosome: formation, contents, and function. *Archives of Biochemistry and Biophysics* **379**; 173-182

Aitken, R.J. (1997) Molecular mechanisms regulating human sperm function. *Molecular Human Reproduction* **3**; 169-173

Allue, I., Gandelman, O., Dementieva, E., Ugarova, N. and Cobbold, P. (1996) Evidence for rapid consumption of millimolar concentrations of cytoplasmic ATP during rigor-contracture of metabolically compromised single cardiomyocytes. *Biochemical Journal* **319**; 463-469

Ananthanarayanan, B., Das, S., Rhee, S.G., Murray, D. and Cho, W. (2002) Membrane targeting of C2 domains of phospholipase C-delta isoforms. *Journal of Biological Chemistry* **277**; 3568-3575

Arbuzova, A., Wang, L., Wang, J., Hangyas-Mihalyne, G., Murray, D., Honig, B. and McLaughlin, S. (2000) Membrane binding of peptides containing both basic and aromatic residues. Experimental studies with peptides corresponding to the scaffolding region of caveolin and the effector region of MARCKS. *Biochemistry* **39(33)**; 10330-10339

Berridge, M. (1993) Inositol trisphosphate and calcium signalling. *Nature* **361**; 315-325

Berridge, M. (1997) Elementary and global aspects of calcium signalling. *Journal of Physiology* **56**; 297-319

Berridge, M.G., Bootman, M.D. and Lipp, P. (1998) Calcium – a life and death signal. *Nature* **395**; 645-648

Berridge M. J., Lipp P. and Bootman M. D (2000) The Versatility and Universality of Calcium Signalling. *Nature Reviews Molecular Cell Biology* **1**; 11 - 21

Beutner, G., Sharma, V., Giovannucci, D., Yule, D. and Sheu, S. (2001) Identification of a ryanodine receptor in rat heart mitochondria. *Journal of Biological Chemistry* **276**; 21482-21488

Bezprozvanny, I., Watras, J. and Ehrlich, B.E. (1991) Bell-shaped calcium response curves of Ins(1,4,5)P3- and calcium gated channels from endoplasmic reticulum of cerebellum. *Nature* **351**; 751-754

Bleil, J.D., Greve, J.M. and Wassarman, P.M. (1998) Identification of a secondary sperm receptor in the mouse egg zona pellucida: role in maintenance of binding of acrosome-reacted sperm to eggs. **128**; 376-385

Blondel, O., Takeda, J., Janssen, H., Seino, S. and Bell, G.I. (1993) Sequence and functional characterisation of a third inositol triphosphate receptor subtype, IP3R-3, expressed in pancreatic islets, gastrointestinal tract, and other tissues. *Journal of Biological Chemistry* **268**; 11356-11363

Boehning, D. and Joseph, S. (2000) Functional properties of recombinant type I and type III inositol 1, 4, 5,-triphosphate receptor isoforms expressed in COS-7 cells. *Journal of Biological Chemistry* **275**; 21492-21499

Boguslavsky, V., Rebecchi, M., Morris, A.J., Jhon, D.Y., Rhee, S.G. and McLaughlin, S. (1994) Effect of monolayer surface pressure on the activities of phosphoinositide-specific phospholipase C-beta 1, -gamma 1, and -delta 1. *Biochemistry* **33**; 3032-3037

Bonaccorsi, L., Luconi, M., Forti, G. and Baldi, E. (1995) Tyrosine kinase inhibition reduces the plateau phase of the calcium increase in response to progesterone in human sperm. *FEBS Letters* **364; 83-86**

Bootman, M.D. and Lipp, P. (1999) Calcium signalling: ringing changes to the 'bell-shaped curve'. *Current Biology* **9**; R876-R878

Bootman, M.D., Collins, T.J., Peppiatt, C.M., Prothero, L.S., Mackenzie, L., Desmet, D., Travers, M., Torey, S.C., Seo, J.T., Berridge, M.J., Ciccalin, F. and Lipp, P. (2001) Calcium signalling – An overview. *Cell and Developmental Biology* **12**; 3-10

Breitbart, H. (2002) Intracellular calcium regulation in sperm capacitation and acrosomal reaction. *Molecular and Cellular Endocrinology* **187**; 139-541

Breitbart, H., Rubinstein, S. and Nass-Arden, L. (1985) The role of calcium and Ca^{2+}-ATPase in maintaining motility in ram spermatozoa. *Journal of Biological Chemistry* **260**; 11548-11553

Brind, S., Swann, K. and Carroll, J. (2000) Inositol 1,4,5-trisphosphate receptors are downregulated in mouse oocytes in response to sperm or adenophostin A but not to increases in intracellular Ca^{2+} or egg activation. *Developmental Biology* **223(2)**; 251-265

Buser, C.A. and McLaughlin, S. (1998) Ultracentrifugation technique for measuring the binding of peptides and proteins to sucrose-loaded phospholipid vesicles. *Methods in Molecular Biology* **84**; 267-281

Carroll, J. (2001) The initiation and regulation of Ca^{2+} signalling at fertilisation in mammals. *Seminars in Cell and Developmental Biology* **12**; 37-43

Carroll, J., Ramarao, C.S., Mehlmann, L.M., Roche, S., Terasaki, M. and Jaffe, L.F. (1997) Calcium release at fertilisation in starfish eggs is mediated by phospholipase Cγ. *Journal of Cell Biology* **138**; 1303-1311

Chen, M.S., Tung, K.S., Coonrod, S.A., Takahashi, Y., Bigler, D., Chang, A., Yamashita, Y., Kincade, P.W., Herr, J.C. and White, J.M. (1999) Role of the integrin-associated protein CD9 in binding between sperm ADAM 2 and the egg integrin alpha6beta1: implications for murine fertilization. *Proceedings for the National Academy of Sciences* **96**; 11830-11835

Chini, E.W. and Dausa, T.P. (1995) Nicotinate-adenine dinucleotide phosphate-induced Ca^{2+} release does not behave as a Ca^{2+}-induced Ca^{2+}-release system. *Biochemical Journal* **316**; 709-711

Clapham, D. (1995) Calcium signalling. *Cell* **80**; 259-268

Coronado, R., Morrissettee, J., Sukhareva, M. and Vaughan, D. (1994) Structure and function of ryanodine receptors. *American Journal of Phisiology* **266**; C1485-C1504

Cortvrindt R., Smitz J. and Van Steirteghem A.C. (1997) Assessment of the need for follicle stimulating hormone in early preantral mouse follicle culture in vitro. *Human Reproduction* **12**; 759-768

Cox, L.J., Larman, M.G., Saunders, C.M., Swann, K. and Lai, F.A. (2002) Sperm phospholipase Cζ from humans and cynomolgus monkeys triggers Ca^{2+} oscillations, activation and development of mouse oocytes. *Reproduction* **124**; 611-623

Cran, D.J., Moor, R.M. and Irvine, R.F. (1988) Initiation of cortical reaction in hamster and sheep oocytes in response to inositol trisphopshate. *Journal of Cell Science* **91**; 139-144

Cross, N.L. and Razy-Faulkner, P. (1997) Control of human sperm intracellular pH by cholesterol and its relationship to the response of the acrosome to progesterone. *Biology of Reproduction* **56**; 1169-1174

Cuthbertson, K.S.R. and Cobbold, P.H. (1985) Phorbol ester and sperm activate mouse oocytes by inducing sustained oscillations in cell Ca^{2+}. *Nature* **316**; 541-542

Da Silva, C. and Guse, A. (2001) Intracellular Ca^{2+} release mechanisms: multiple pathways having multiple functions within the same cell type? *Biochimica et Biophysica Acta* **1498**; 122-133

Degucchi, R., Shirakawa, H., Oda, S., Mohri, T. and Miyazaki, S. (2000) Spatiotemporal analysis of Ca^{2+} waves in relation to the sperm entry site and animal-vegetal axis during Ca^{2+} oscillations in fertilised mouse eggs. *Developmental Biology* **218**; 299-313

Dekel, N. (1988) Regulation of oocyte maturation: the role of cAMP. *In "In Vitro Fertilization and other Assisted Reproduction"* Academic Science, NY; 211-216

Dostalova, Z., Calvete, J.J., Sanz, L. and Topfer-Petersen, E. (1995) Boar spermadhesin AWN-1. Oligosaccharide and zona pellucida binding characteristics. *European Journal of Biochemistry* **230**; 329-336

Dowler, S., Currie, R.A., Campbell, D.G., Deak, M., Kular, G., Downes, C.P and Alessi, D.R. (2000) Identification of pleckstrin homology domain-containing proteins with novel phosphoinositide-binding specificities. *Biochemical Journal* **351**; 19-31

Duchen, M. (1999) Contributions of mitochondria to animal physiology: from homeostatic sensor to calcium signalling and cell death. *Journal of Physiology* **516**; 1-17

Duchen, M. (2000) Mitochondria and calcium: from cell signalling to cell death. *Journal of Physiology* **529**; 57-68

Ducibella, T., Huneau, D., Angelichio, E. Xu, Z., Schultz, R.M., Kopf, G.S., Fissore, R., Madoux, S. and Ozil, J.P. (2002) Egg to embryo transition is driven by differential responses to Ca(2+) oscillation number. *Developmental Biology* **250**; 280-291

Edwards, R.G. (1965) Maturation in vitro of mouse, sheep, cow, pig, rhesus monkey and human ovarian oocytes. *Nature* **208**; 349-351

Ehrlich, B., Kaltan, E., Bezprozvannaya, S. and Bezprozvanny, I. (1994) The pharmacology of intracellular Ca^{2+} release channels. *Trends in Pharmacological Sciences* **15**; 145-149

Ellis, M.V., James, S.R., Perisic, O., Downess, C.P., Williams, R.L. and Katan, M. (1998) Catalytic domain of phosphoinositide-specific phospholipase C (PLC): Mutational analysis of residues within the active site and hydrophobic ridge of PLC delta 1. *Journal of Biological Chemistry* **273**; 11650 -11659

Emori, Y., Homma, Y., Sorimachi, H., Kawasaki, H., Nakanishi, O., Suzuki, K. and Takenawa, T. (1989) A second type of rat phosphoinositide-specific phospholipase C containing an src-related sequence not essential for phosphoinositide-hydrolysing activity. *Journal of Biological Chemistry* **254**; 21885-21890

Eppig J.J. (1991) Intercommunication between mammalian oocytes and companion somatic cells. *Bioessays* **13**; 569-574

Eppig, J.J. (1993) Regulation of mammalian oocyte maturation. *In "The Ovary"* (A.Y. Adashi, P.C.K. Leung, Eds.) Raven Press, NY; 185-208

Eppig, J.J., Ward-Bailey, P.F. and Coleman, D.L. (1985) Hypoxanthine and adenosine in murine ovarian follicular fluid: concentrations and activity in maintaining oocyte meiotic arrest. *Biology of Reproduction* **33**; 1041-1049

Essen, L.O., Perisic, O., Cheung, R., Katan, M. and Williams, R.L. (1996) Crystal structure of a mammalian phosphoinositide-specific phospholipase-C delta. *Nature* **380**; 595-602

Essen, L.O., Perisic, O., Katan, M., Wu, Y., Roberts, M.F. and Williams, R.L. (1997) Structural Mapping of the Catalytic Mechanism for a Mammalian Phosphoinositide-Specific Phospholipase C. *Biochemistry* **36**; 1704 – 1718

Fabiato, A. (1981) Myoplasmic free calcium concentration reached during the twitch of an intact isolated cardiac cell and during calcium-induced release of calcium from the sarcoplasmic reticulum of a skinned cardiac cell from the adult rat or rabbit ventricle. *Journal of General Physiology* **78(5)**; 457-497

Feng, J.F., Rhee, S.G. and Im, M.J. (1996) Evidence that phospholipase C delta1 is the effector in the Gh (transglutaminase II)-mediated signalling. *Journal of Biological Chemistry* **271**; 16451-16454

Ferguson, K.M., Lemmon, M.A., Schlessinger, J. and Sigler, P.B. (1995) Structure of the high affinity complex of inositol trisphosphate with a phospholipase C pleckstrin homology domain. *Cell* **83**; 1037-1046

Fill, M. and Copello, S.A. (2002) Ryanodine Receptor Calcium Release Channels. *Physiological Reviews* **82**; 893-922

Fissore, R. A. and Robl, J.M. (1994) Mechanisms of calcium oscillations in fertilized rabbit eggs. *Developmental Biology* **166**; 634-642

Flesch, F.M. and Gadella B.M. (2000) Dynamics of the mammalian sperm plasma membrane in the process of fertilization. *Biochimica et Biophysica Acta* **1469**; 197-235

Frazier, A.A., Wisner, M.A., Malmberg, N.J., Victor, K.G., Fanucci, G.E., Nalefski, E.A., Falke, J.J. and Cafiso, D.S. (2002) Membrane orientation and position of the C2 domain from cPLA2 by site-directed spin labelling. *Biochemistry* **41**; 6282-6292

Fujimoto, S., Yoshida, N., Fukui, T., Amanai, M., Isobe, T., Itagaki, C., Izumi, T. and Perry, A.C. (2004) Mammalian phospholipase Czeta induces oocyte activation from the sperm perinuclear matrix. *Developmental Biology* **96**; 317-323

Fukami, K. (2001) Structure, regulation and function of phospholipase C isozymes. *Journal of Biochemistry* **131**; 293-299

Fukami, K., Nakao, K., Inoue, T., Kataoka, Y., Kurokawa, M., Fissore, R.A., Nakamura, K., Katsuki, M., Mikoshiba, K., Yoshida, N. and Takenawa, T. (2001) Requirement of phospholipase Cδ4 for the zona pellucida-induced acrosome reaction. *Science* **292**; 920-923

Fulton, B.P. and Whittingham, D.G. (1978) Activation of mammalian oocytes by intracellular injection of calcium. *Nature* **273**; 149-151

Furuichi, T., Simon-Chazottes, D., Fujino, I., Yamada, N., Hasegawa, M., Miyawaki, A., Yoshikawa, S., Guenet, J.L. and Mikoshiba, K. (1993) Widespread expression of inositol 1,4,5-trisphosphate receptor type 1 gene ($InsP_3R1$) in the mouse central nervous system. *Receptors Channels* **1**; 11-24

Galione, A. and Ruas, M. (2005) NAADP receptors. *Cell Calcium* **38**; 273-280

Galione, A., Patel, S. and Churchill, G. (2000) NAADP-induced calcium release in sea urchin eggs. *Biology of the Cell* **92**; 197-204

Gerber, S.H., Rizo, J. and Südhof, T.C. (2001) The top loops of the C2 domains from synaptotagmin and phospholipase A_2 control functional specificity. *Journal of Biological Chemistry* **276**; 32288-32292

Ghosh, T., Bain, J. and Gill, D. (1994) Sphingosine 1-phosphate generated in the endoplasmic reticulum membrane activates release of stored calcium. *Journal of Biological Chemistry* **269**; 22628-22635

Giannini, G., Conti, A., Mammarella, S., Scrobogna, M. and Sorrentino, V. (1995) The ryanodine receptor/calcium channel genes are widely and differentially expressed in murine brain and peripheral tissues. *Journal of Cell Biology* **128**; 893-904

Graham, L.J., Stoica, B.A., Shapiro, M., DeBell, K.E., Rellahan, B., Laborda, J. and Bonvini, E. (1998) Sequences surrounding the Src-homology 3 domain of phospholipase C-γ1 increase the domain's association with Cbl. *Biochemical and Biophysical Research Communications* **249;** 537-541

Grobler, J.A. and Hurley, J.H. (1998) Catalysis by phospholipase-C delta1 requires that calcium bind to the catalytic domain, but not the C2 domain. *Biochemistry* **37**; 5020-5028

Grunwald, R. and Meissner, G. (1995) Lumenal sites and C-terminus accessibility of the skeletal muscle calcium release channel (ryanodine receptor). *Journal of Biological Chemistry* **270**; 11338-11347

Guse, A. (1999). Cyclic ADP-ribose: a novel Ca^{2+}-mobilising sound messenger. *Cell signal* **11**; 309-316

Hagorr, R., Burgstahler, A., Nathanson, M.H. and Mignery, G.A. (1998) Type III $InsP_3$ receptors stay open in the presence of increased calcium. *Nature* **396**; 81-84

Hajnoczky, G., Csordas, G., Madesh, M. and Pacher, P. (2000) The machinery of local Ca^{2+} signalling between sarco-endoplasmic reticulum and mitochondria. *Journal of Physiology* **529**; 69-81

Hemler, M.E. (1998) Integrin associated proteins. *Current Opinion of Cell Biology* **10**; 578-585

Hohenegger, M., Suko, J., Gscheidlinger R., Drobny, H. and Zidar, A. (2002) Nicotinic acid adenine dinucleotide phosphate, NAADP, activates the skeletal muscle ryanodine receptor. *Biochemical Journal* **367**; 423-431

Homa S.T. and Swann, K. (1994) A cytosolic sperm factor triggers calcium oscillations and membrane hyperpolarizations in human oocytes. *Human Reproduction* **9**; 2356-2361

Houvila, A.J., Almeida, E.A.C. and White, J.M. (1996) ADAMs and cell fusion. *Current Opinion of Cell Biology* **8**; 692-699

Hurley, J. and Misra, S, (2000) Signalling and subcellular targeting by membrane-binding domains. *Annual Review of Biophysics and Biomolecular Structure* **29;** 49-79

Hwang, J.I., Heo, K., Shin, K.J., Kim, E., Yun, C., Ryu, S.H., Shin, H.S. and Suh, P.G. (2000) Regulation of phospholipase C-β3 activity by Na^+/K^+ exchanger regulatory factor 2. *Journal of Biological Chemistry* **275**; 16632-16637

Hwang, J.I., Oh, Y.S., Shin, K.J., Kim, H., Ryu, S.H. and Suh, P.G. (2005) Molecular cloning and characterization of a novel phospholipase C, PLC-eta. *Biochemical Journal* **389**; 181-186

Hwang, S.C., Jhon, D.Y., Bae, Y.S., Kim, J.H. and Rhee, S.G. (1996) Activation of phospholipase C-gamma by the concerted action of tau proteins and arachidonic acid. *Journal of Biological Chemistry* **271**; 18342-18349

Hyslop, L.A., Nixon, V.L., Levasseur, M., Chapman, F., Chiba, K., Mc Dougal, A., Venables, J.P., Elliot, D.J. and Jones, K.T. (2004) Ca^{2+} promoted cyclin B1 degradation in mouse oocytes requires the establishment of a metaphase arrest. *Developmental Biology* **269**; 206-219

Jaffe, L.F. (1983) Sources of calcium in egg activation: a review and hypothesis. *Developmental Biology* **99**; 256-276

Jaffe, L.F. (1991) The path of calcium in cytosolic calcium oscillations: A unifying hypothesis. *Proceedings of the National Academy of Science USA* **88**; 9883-9887

James, S.R., Paterson, A., Harden, T.K., Demel, R.A. and Downes, C.P. (1997) Dependence of the activity of phospholipase C beta on surface pressure and surface composition in phospholipid monolayers and its implications for their regulation. *Biochemistry* **36**; 848-855

Jellerette, T., He, C.L., Wu, H., Parys, J.B. and Fissore, R.A. (2000) Down-regulation of the inositol 1,4,5-trisphosphate receptor in mouse eggs following fertilization or parthenogenic activation. *Developmental Biology* **223**; 238-250

Jeyakumar, L.H., Ballister, L., Cheng, D.S., McInistyre, J.O., Chang, P., Olivey, H.E., Rollins-Smith, L., Barnett, J.V., Murray, K., Xin, H.B. and Fleischer S. (2001) FKBP binding characteristics of cardiac microsomes from diverse verterbrates. *Biochemical Biophysical Research Communications* **281**; 979-986

Jones, G.A. and Carpenter, G. (1993) The regulation of phospholipase C-gamma 1 by phosphatidic acid. Assessment of kinetic parameters. *Journal of Biological Chemistry* **268**; 20845-20850

Jones, K.T., Soeller, C. and Cannell, M.B. (1998a) The passage of Ca^{2+} and fluorescent markers between the sperm and egg after fusion in the mouse. *Development* **125**; 4627-4635

Jones, K.T., Cruttwell, C., Parrington, J. and Swann, K. (1998b) A mammalian sperm cytosolic phospholipase C activity generates inositol trisphosphate and causes Ca^{2+} release in sea urchin homogenates. *FEBS Letters* **437**; 297-300

Jones, K.T., Matsuda, M., Parrington, J., Katan, M. and Swann, K. (2000) Different Ca^{2+} releasing abilities of sperm extracts compared with tissue extracts and phospholipase C isoforms in sea urchin homogenate and mouse eggs. *Biochemical Journal* **346**; 743-749

Jones, K.T. and Nixon V.L. (2000) Sperm-induced Ca^{2+} oscillations in mouse oocytes and eggs can be mimicked by photolysis of caged inositol 1,4,5-trisphosphate: evidence to support a continuous low level production of inositol 1,4,5-trisphosphate during mammalian fertilization. *Developmental Biology* **225**; 1-12

Jones, R. and Jansen, S. (1993) Mechanism of gamete recognition and adhesion during fertilization in mammals. *Journal of Reproduction and Development* **39** (Suppl.); 47

Katan, M. and Parker, P.J. (1987) Purification of a phosphoinositide-specific phospholipase C from a particulate fraction of bovine brain. *European Journal of Biochemistry* **168**; 413-418

Katan, M. and Williams, R.L. (1997) Phosphoinositide-specific phospholipase-C: structural basis for catalysis and regulatory interactions. *Seminars in Cell and Developmental Biology* **8**; 287-296

Katan, M. (1998) Families of phosphoinositide-specific phospholipase-C: structure and function. *Biochimica et Biophysica Acta* **1436**; 5-17

Kelley, G.G., Reks, S.E., Ondrako, J.M. and Smrcka, A.V. (2001) Phospholipase Cε: a novel Ras effector. *EMBO Journal* **20**; 743-754

Kim, M.J., Chang, J.S., Park, S.K., Hwang, J.I., Ryu, S.H. and Suh, P.G. (2000) Direct interaction of SOS1 Ras exchange protein with the SH3 domain of phospholipase C-γ1 *in vivo*. *Biochemistry* **39;** 8674-8682

Kim, N.H., Day, B.N., Lee, H.T. and Chung, K.S. (1996) Microfilament assembly and cortical granule distribution during maturation, parthenogenetic activation and fertilization in the porcine oocyte. *Zygote* **4**; 145-149

Kim, S., Lakhani, V., Costa, D., Sharara, A., Fitz, J., Huang, L.-W., Peters, K. and Kindman, L. (1995) Sphingolipid-gated Ca^{2+} release from intracellular stores of endothelial cells is mediated by a novel Ca^{2+}-permeable channel. *Journal of Biological Chemistry* **270**; 5266-5269

Kim, U.H., Fink, D., Kim, H.S., Park, D.J., Contreras, M.L., Guroff, G. and Rhee, S.G. (1991) Nerve growth factor stimulates phosphorylation of phospholipase C-gamma in PC12 cells. *Journal of Biological Chemistry* **266**; 1359-1362

Kindman, L., Kim, S., McDonald, T. and Gardner, P. (1994) Characterisation of a novel intracellular sphingolipid-gated Ca^{2+}-permeable channel from rat basophilic leukaemia cells. *Journal of Biological Chemistry* **269**; 13088-13091

Knott, J.G., Kurokawa, M., Fissore, R.A., Schultz, R.M. and Williams, C.J. (2005) Transgenic RNA interference reveals role for mouse sperm phospholipase Czeta in triggering Ca2+ oscillations during fertilization. *Biology of Reproduction* **72**; 992-996

Kouchi, Z., Fukami, K., Shikano, T., Oda, S., Nakamura, Y., Takenawa, T. and Miyazaki, S. (2004) Recombinant phospholipase Czeta has high Ca2+ sensitivity and induces Ca2+ oscillations in mouse eggs. *Journal of Biological Chemistry* **279**; 10408-10412

Kouchi, Z., Shikano, T., Nakamura, Y., Shirakawa, H., Fukami, K. and Miyazaki, S. (2005) The role of EF-hand domains and C2 domain in regulation of enzymatic activity of phospholipase Czeta. *Journal of Biological Chemistry* **280**; 21015-21021

Kuo, R.C., Baxter, G.T., Thompson, S.H., Stricker, S.A., Patton, C., Bonaventura, J. and Epel, D. (2000) NO is necessary and sufficient for egg activation at fertilisation. *Nature* **406**; 633-636

Kupker, W., Diedrich, K. and Edwards, R.G. (1998) Principles of mammalian fertilization. *Human Reproduction* **1**; 20-32

Kyozuka, K., Deguchi, R., Mohri, T. and Miyazaki, S. (1998) Injection of sperm extract mimics spatiotemporal dynamics of Ca^{2+} responses and progression of meiosis at fertilization of ascidian oocytes. *Development* **125**; 4099-4105

Larman, M.G., Saunders, C.M., Carroll, J., Lai, F.A. and Swann, K. (2004) Cell cycle-dependent Ca2+ oscillations in mouse embryos are regulated by nuclear targeting of PLCzeta. *Journal of Cell Science* **117**; 2513-2521

Lawrence, Y., Whitaker, M. and Swann, K. (1997) Sperm-egg fusion is the prelude to the initial Ca^{2+} increase at fertilisation in the mouse. *Development* **124**; 233-294

Lawrence, Y., Ozil, J.P. and Swann, K. (1998) The effects of a Ca^{2+} chelator and heavy-metal-ion chelators upon Ca^{2+} oscillations and activation at fertilisation in mouse oocytes suggest a role for repetitive Ca^{2+} increases. *Biochemical Journal* **335**; 335-342

Lax, Y., Rubinstein, S. and Breitbart, H. (1994) Epidermal growth factor induces acrosomal exocytosis in bovine sperm. *FEBS Letters* **339**; 234-238

Lee, C.W., Lee, K.H., Lee, S.B., Park, D. and Rhee, S.G. (1994) Regulation of phospholipase C-beta 4 by ribonucleotides and the alpha subunit of Gq. *Journal of Biological Chemistry* **269**; 25335-25338

Lee, H. (1997) Mechanisms of calcium signalling by cyclic ADP-ribose and NAADP. *Physiological Reviews* **77**; 1133-1164

Lee, H. (2001) Physiological functions of cyclic ADP-ribose and NAADP as calcium messengers. *Annual Reviews in Pharmacology and Toxicology* **41**; 317-334

Lee, S.B, Shin, S.H., Hepler, J.R., Gilman, A.G. and Rhee, S.G. (1993) Activation of phospholipase C-beta 2 mutants by G protein alpha q and beta gamma subunits.*Journal of Biological Chemistry* **268**; 25952-25952.

Lee, W.K., Kim, J.K., Seo, M.S., Cha, J.H., Lee, K.J., Rha, H.K., Min, D.S., Jo, Y.H. and Lee, K.H. (1999) Molecular cloning and expression analysis of a mouse phospholipase C-delta1. *Biochemical and Biophysical Research Communications* **261**; 393-399

Lemmon, M.A., Ferguson, K.M., O'Brien, R., Sigler, P.B. and Schlessinger, J. (1995) Specific and high-affinity binding of inositol phosphates to an isolated pleckstrin homology domain. *Proceedings of the National Academy of Science USA* **92**; 10472-10476

Lemmon, M.A. and Ferguson, K.M. (2000) Signal-dependent membrane targeting by pleckstrin homology (PH) domains. *Biochemical Journal* **335**; 335-342

Lemmon M.A. (2003) Phosphoinositide recognition domains. *Traffic* **4(4)**; 201-213

Lim, D., Kyozuka, K., Gragnaniello, G., Carafoli, E. and Santella, L. (2001) $NAADP^+$ initiates the Ca^{2+} response during fertilization of starfish oocytes. *FASEB Journal* **15**; 2257-2267

Lipp, D. and Niggli, E. (1994) Sodium current-induced calcium signals in isolated guinea-pig ventricular myocytes. *Journal of Physiology* **474**; 439-446

Lomasney, J.W., Ceng, H.F., Wang, L.P., Kuan, Y.S., Liu, S.M., Fesik, S.W. and King, K. (1996) Phosphatidylinositol 4,5-bisphosphate binding to the pleckstrin homology domain of phospholipase C-δ1 enhances enzyme activity. *Journal of Biological Chemistry* **271**; 25316-25326

Lomasney, J.W., Cheng, H.F., Roffler, S.R. and King, K. (1999) Activation of phospholipase C delta1 through C2 domain by a Ca^{2+}-enzyme-phosphatidylserine ternary complex. *Journal of Biological Chemistry* **274**; 21995-22001

Lopez, I., Mak, E.C., Ding, J., Hamm, H.E. and Lomasney, J.W. (2001) A novel bifunctional phospholipase C that is regulated by Gα12 and stimulates the Ras/MAP kinase pathway. *Journal of Biological Chemistry* **276**; 2758-2765

Lu, C.C., Brennan, J. and Robertson, E.J. (2001) From fertilization to gastrulation: axis formation in the mouse embryo. *Current Opinion in Genetics and Development* **11**; 384-392

Mackrill, J. (1999) Protein-protein interactions in intracellular Ca^{2+}-release channel function. *Biochemical Journal* **337**; 345-361

Mao, C., Kim, S., Almenoff, J., Rudner, X., Kearney, D. and Kindman, L. (1996) Molecular cloning and characterisation of SCaMPER, a sphingolipid Ca^{2+} release-mediating protein from endoplasmic reticulum. *Proceedings of the National Academy of Sciences USA* **93**; 1993-1996

Marangos, P., FitzHarris, G. and Carroll, J. (2003) Ca^{2+} oscillations at fertilization in mammalas are regulated by the formation of pronuclei. *Development* **130 (7)**; 1461-1472

Marx, S.O., Reiken, S., Hisamatsu, Y., Jayaraman, T., Burkoff, D., Rosemblit, N. and Marks, A.R. (2000). PKA phosphorylation dissociates FKBP12.6 from the calcium release channel (ryanodine receptor): defective regulation in coupling hearts. *Cell* **101**; 365-376

Masui, Y. and Market, C.L. (1971) Cytoplasmic control of nuclear behaviour during meiotic maturation of frog oocytes. *Journal of Experimental Zoology* **177**; 129-146

Matecki, A. and Pawelczyk, T. (1997) Regulation of phospholipase C delta1 by sphingosine. *Biochimica et Biophysica Acta* **1325;** 287-296

McAvey, B.A., Wortzman, G.B., Williams, C.J. and Evans, J.P. (2002) Involvement of calcium signalling and the actin cytoskeleton in the membrane block to polyspermy. *Biology of Reproduction* **67**; 1342-1352

Medkova, M. and Cho, W. (1999) Interplay of C1 and C2 domains of protein kinase C-alpha in its membrane binding and activation. *Journal of Biological Chemistry* **274**; 19852-19861

Mehlmann, L.M., Carpenter, G., Rhee, S.G. and Jaffe, L.A. (1998) SH2 domain-mediated activation of phospholipase C is not required to initiate Ca^{2+} release at fertilisation of mouse eggs. *Developmental Biology* **203**; 221-232

Mehlmann, L.M., Chattopadhyay A., Carpenter, G. and Jaffe, L.A. (2001) Evidence that Phospholipase C from the sperm is not responsible for initiating Ca^{2+} release at fertilisation of mouse eggs. *Developmental Biology* **236**; 492-501

Meissner, G. (1994) Ryanodine receptor/Ca^{2+} release channels and their regulation by endogenous effectors. *Annual Reviews of Physiology* **56**; 485-508

Meldolesi, J. and Pozzan, T. (1998) The endoplasmic reticulum Ca^{2+} store: a view from the lumen. *Trends in Biochemical Sciences* **23**; 10-14

Meldolesi, J. (2001) Rapidly exchanging Ca^{2+} stores in neurons: molecular, structural and functional properties. *Progress in Neurobiology* **65**; 309-338

Meldolesi, J. and Grohovaz, F. (2001) Total calcium ultrastructure: advances in excitable cells. *Cell Calcium* **30**; 1-8

Mikoshiba, K. Furuichi, T. and Miyawaki, A. (1994) Structure and function of $InsP_3$ receptors. *Seminars in Cell Biology* **5**; 273-281

Mikoshiba, K. (1997) The $InsP_3$ receptor and intracellular Ca^{2+} signalling. *Current Opinion in Neurobiology* **7**; 339-345

Miller, D.J., Gong, X. and Shur, B.D. (1993) Sperm require beta-N-acetylglucosaminidase to penetrate through the egg zona pellucida. *Development* **118**; 1279-1289

Miyado, K., Yamada, G., Yamada, S., Hasuwa, H., Nakamura, Y., Ryu, F., Suzuki, K., Kosai, K., Inoue, K., Ogura, A., Okabe, M and Mekada, E. (2000) Requirement of CD9 on the egg plasma membrane for fertilisation. *Science* **287**; 321-324

Miyazaki, S. (1988) Inositol 1,4,5-trisphosphate-induced calcium release and guanine nucleotide-binding protein-mediated periodic calcium rises in golden hamster eggs. *Journal of Cell Biology* **106**; 345-353

Miyazaki, S., Yuzaki, M., Nakada, K., Shirakawa, H., Nakanishi, S., Nakade, S. and Mikoshiba, K. (1992) Block of Ca^{2+} wave and Ca^{2+} oscillations by antibody to the inositol 1,4,5-trisphosphate receptor in fertilized hamster eggs. *Science* **257**; 251-255

Miyazaki, S., Shirakawa, H., Nakada, K. and Honda, Y. (1993) Essential role of the inositol 1,4,5-trisphosphate/Ca^{2+} release channel in Ca^{2+} waves and Ca^{2+} oscillations at fertilization of mammalian eggs. *Developmental Biology* **58**; 62-78

Mojzisova, A., Krizanova, O., Zacikova, L., Kominkova, V. and Ondrias, K. (2001) Effect of nicotinic acid adenine dinucleotide phosphate on ryanodine calcium release channel in heart. *Pflugg Arch* **441**; 674-677

Morales, P., Vigil, P., Franken, D.R., Kaskar, K., Coetzee, K. and Kruger, T.F. (1994) Sperm-oocyte interaction: studies on the kinetics of zona pellucida binding and acrosome reaction of human spermatozoa. *Andrologia* **26**; 131-137

Murase, T. and Roldan, E.R. (1996) Progesterone and the zona pellucida activate different transducing pathways in the sequence of events leading to diacylglycerol generation during mouse sperm acrosomal exocytosis. **320**; 1017-1023

Murthy, S.N., Lomasney, J.W., Mak, E.C. and Lorand, L. (1999) Interactions of G(h)/transglutaminase with phospholipase Cdelta1 and with GTP. *Proceedings of National Academy of Science U S A* **96**; 11815-11819

Nakahara, M., Shimozawa, M., Nakamura, Y., Irino, Y., Morita, M., Kudo, Y. and Fukami, K. (2005) A novel phospholipase C, PLC(eta)2, is a neuron-specific isozyme. *Journal of Biological Chemistry* **280**; 29128-29134

Nakai, J., Imagawa, T., Hakamat, Y., Shigekawa, M., Takeshima,H., Numa, S. (1990) Primary structure and functional expression from cDNA of the cardiac ranodine receptor/ calcium release channel. *FEBS letters* **271**; 169-177

Nakano, Y., Shirakawa, H., Mitsuhashi, N., Kuwubara, Y. and Miyazaki, S. (1997) Spatiotemporal dynamics of intracellular calcium in the mouse egg injected with a spermatozoon. *Molecular Human Reproduction* **3**; 1087-1093

Nakaoka, H., Perez, D.M., Baek, K.J., Das, T., Husain, A., Misono, K., Im, M.J. and Graham, R.M. (1994) Gh: a GTP-binding protein with transglutaminase activity and receptor signalling function. *Science* **264**; 1593-1596.

Nakashima, S., Banno, Y., WatanabeT., Nakamura, Y., Mizutani T., Sakai, H., Zhao, Y., Sugimoto, Y. and Nozawa Y. (1995) Deletion and site-directed mutagenesis of EF-hand domain of phospholipase C-delta1: effects on its activity. *Biochemical and Biophysical Research Communications* **211**; 365-369

Nakatani, Y., Tanioka, T., Sunaga, S., Murakami, M. and Kudo, I. (2000) Identification of a cellular protein that functionally interacts with the C2 domain of cytosolic phospholipase $A_2\alpha$. *Journal of Biological Chemistry* **275**; 1161-1168

Nalefski, E.A. and Falke, J.J. (1996) The C2 domain calcium-binding motif: structural and functional diversity. *Protein Science* **5**; 2375-2390

Nalefski, E.A., Wisner, M.A., Chen, J.Z., Sprang, S.R., Fukuda, M., Mikoshiba, K. and Falke, J.J. (2001) C2 domains from different Ca2+ signaling pathways display functional and mechanistic diversity. *Biochemistry* **40(10)**; 3089-3100

Nishimura, H., Cho, C., Branciforte, D.R., Myles, D.G. and Primakoff, P. (2001) Analysis of the loss of adhesive function in sperm lacking cyritestin or fertilin β. *Developmental Biology* **233**; 204-213

Nomikos, M., Blayney, L.M., Larman, M.G., Campbell, K., Rossbach, A., Saunders, C.M., Swann, K. and Lai, F.A. (2005) Role of phospholipase C-zeta domains in Ca2+-dependent phosphatidylinositol 4,5-bisphosphate hydrolysis and cytoplasmic Ca2+ oscillations. *Journal of Biological Chemistry* **280 (35)**; 31011-31018

Nottola, S.A., Macchiarelli, G., Familiari, G., Stallone, T., Sathananthan A.H. and Motta P.M. (1998) Egg-sperm interactions in humans: ultrastructural aspects. *Italian Journal of Anatomy and Embryology* **103**; 85-101

O'Neil, A.F., Hagar, R.E., Zippel, W.R., Nathanson, M.H. and Ehlrich, B.E. (2002) Regulation of the type III $InsP_3$ receptor by $InsP_3$ and calcium. *Biochemical and Biophysical Research Communications* **294**; 719-725

Okada, M., Ishimoto, T., Naito, Y., Hirata, H. and Yagisawa, H. (2005) Phospholipase Cdelta1 associates with importin beta1 and translocates into the nucleus in a Ca2+-dependent manner. *FEBS Letters* **579**; 4949-4954

Ottini, L., Marziali, G., Conti, A., Charlesworth, A. and Sorentino, V. (1996) Alpha and beta isoforms of ryanodine receptor from chicken skeletal muscle are the homologous of mammalian RyR1 and RyR3. *Biochemical Journal* **315**; 207-216

Palermo, G., Joris, H., Devroey, P. and Van Steirteghem, A.C. (1992) Pregnancies after intracytoplasmic injection of single spermatozoon in an oocyte. *Lancet* **340**; 17-18

Park, D., Jhon, D.Y., Lee, C.W., Ryu, S.H. and Rhee, S.G. (1993) Removal of the carboxyl-terminal region of phospholipase C-beta1 by calpain abolishes activation by G alpha q. *Journal of Biological Chemistry* **268**; 3710-3714

Park, E.S., Won, J.H., Han, K.J., Suh, P.G., Ryu, S.H., Lee, H.S., Yun, H.Y., Kwon, N.S. and Baek, K.J. (1998) Phospholipase C-δ1 and oxytocin receptor signalling: evidence of its role as an effector. *Biochemical Journal* **331**; 283-289

Parrington, J., Swann, K., Shevchenko, V.I., Sesay, A.K. and Lai, F.A. (1996) Calcium oscillations in mammalian eggs triggered by a soluble sperm protein. *Nature* **379**; 364-368

Parrington, J., Brind, S., De Smedt, H., Gangeswaran, R., Lai, F. A., Wojcikiewicz, R. and Carroll, J. (1998) Expression of inositol 1,4,5-trisphosphate receptor in mouse oocytes and early embryos: the type I isoform is upregulated in oocytes and downregulated after fertilization *Developmental Biology* **203**; 451-461

Parrington, J., Jones, M.L., Tunwell, R., Devader, C., Katan, M. and Swann, K. (2002) Phospholipase C isoforms in mammalian spermatozoa: potential components of the sperm factor that causes Ca^{2+} release in eggs. *Reproduction* **123**; 31-39

Patel, S., Joseph, S. and Thomas, A. (1999) Molecular properties of inositol 1, 4, 5-trisphosphate receptors. *Cell Calcium* **25**; 247-264

Patel, S., Churchill, G. and Gallione, A. (2001) Coordination of Ca^{2+} signalling by NAADP. *Trends in Biochemical Sciences* **26**; 482-489

Pawelczyk, T. and Lowenstein, J.M. (1997) The effect of different molecular species of sphingomyelin on phospholipase C delta 1 activity. *Biochimie* **79**;741-748.

Pawelczyk, T. and Matecki, A. (1997a) Expression, purification and kinetic properties of human recombinant phospholipase C delta 3. *Acta Biochimica Polonica* **44**; 221-230

Pawelczyk, T. and Matecki, A. (1997b) Structural requirements of phospholipase C δ1 for regulation by spermine, sphingosine and sphingomyelin. *European Journal of Biochemistry* **248**; 459-465

Pawson, T. and Nash, P. (2000) Protein-protein interactions define specificity in signal transduction. *Genes Development* **14;** 1027-1047

Perez, P.J., Ramos-Franco, J., Fill, M. and Magnery, G.A. (1997) Identification and functional reconstitution of the type2 inositol 1,4,5 triphosphate receptor from ventricular cardiac myocytes. *Journal of Biological Chemistry* **272**; 23961-23969

Petersen, O.H., Petersen, C.C.H. and Kusai, H. (1994) Calcium and hormone action. *Annual Reviews of Physiology* **56**; 297-319

Piatrowska, K. and Zernicka-Goetz, M. (2001) Role for sperm in spatial patterning of the early mouse embryo. *Nature* **409**; 517-521

Ponting, C.P. and Benjamin, D.R. (1996) A novel family of Ras-binding domains. *Trends in Biochemical Science* **21**; 422-425

Pozzan, T., Rizzuto, R., Volpe, P. and Meldolesi, J. (1994) Molecular and cellular physiology of intracellular calcium stores. *Physiological Reviews* **74**; 595-636

Pyne, S. and Pyne, N. (2000) Sphingosine 1-phosphate signalling in mammalian cells. *Biochemical Journal* **349**; 385-402

Ramos-Franco, J., Fill, M. and Mignery, G.A. (1998) Isoform-specific function of single inositol 1,4,5-triphosphate receptor channels. *Biophysical Journal* **75**; 834-839

Rawe, V.Y., Brugo-Olmedo, S., Nodar, F.M., Doncel, G.D., Acosta, A.A. and Vitullo, A.D. (2000) Cytoskeletal defects and abortive activation in human oocytes and IVF and ICSI. *Human Reproduction* **6**; 510–516

Rawlings, N.C., Evans, A.C., Honaramooz, A. and Bartlewski, P.M. (2003) Antral follicle growth and endocrine changes in prepubertal cattle, sheep and goats. *Animal Reproduction Science* **78(3-4)**; 259-270

Rebecchi, M.J. and Pentyala, S.N. (2000) Structure, function and control of phosphoinositide-specific phospholipase C. *Physiological Review* **80**; 1291-1335

Rhee, S.G. and Bae, Y.S. (1997) Regulation of phosphoinositide-specific phospholipase C isozymes. *Journal of Biological Chemistry* **272**; 15045-15048

Rhee, S.G. (2001) Regulation of phosphoinositide-specific phospholipase C. *Annual Review of Biochemistry* **70**; 281-312

Rice, A., Parrington, J., Jones, K.T. and Swann, K. (2000) Mammalian sperm contain a Ca^{2+} sensitive phospholipase C activity that can generate $InsP_3$ from PIP_2 associated with intracellular organelles. *Developmental Biology* **228**; 125-135

Richardson, R.T., Yamasaki, N. and O'Rand, M.G. (1994) Sequence of a rabbit sperm zona pellucida binding protein and localization during the acrosome reaction. *Developmental Biology* **165**; 688-701

Runft, L.L., Watras, J. and Jaffe, L.A. (1999) Calcium release at fertilization of *Xenopus* eggs requires type I IP_3 receptor, but not SH2 domain-mediated activation of PLCγ or G_q-mediated activation of PLCβ. *Developmental Biology* **214**; 399-411

Runft, L.L., Jaffe, L.A. and Mehlmann, L.M. (2002) Egg activation at fertilization: where it all begins. *Developmental Biology* **245**; 237-254

Rutter, G. and Rizzuto, R. (2000) Regulation of mitochondrial metabolism by ER Ca^{2+} release: an intimate connection. *Trends in Biochemical Sciences* **25**; 215-221

Sagata, N., Watanabe, N., Vande Woude, G.F. and Ikawa, Y. (1989) The c-mos proto-oncogene product is a cytostatic factor responsible for meiotic arrest in vertebrate eggs. *Nature* **342**; 512-518

Sato, K., Tokmakov, A.A., Iwasaki, T. and Fukami, Y. (2000) Tyrosine kinase-dependent activation of phospholipase C gamma is required for calcium transient in *Xenopus* egg.fertilization. *Developmental Biology* **224**; 453-469

Saunders, C.M., Larman, M.G., Parrington, J., Cox, L.J., Royse, J., Blayney, L.M., Swann, K. and Lai, F.A. (2002) PLCζ: a sperm-specific trigger of Ca^{2+} oscillations in eggs and embryo development. *Development* **129**; 3533-3544

Schultz, R. M. and Kopf, G. S. (1995) Molecular basis of mammalian egg activation. *Current Topics in Developmental Biology*. **30;** 21-62

Seedorf, K., Kostka, G., Lammers, R., Bashkin, P., Daly, R., Burgess, W.H., Van der Bliek, A.M., Schlessinger, J. and Ullrich, A. (1994) Dynamin binds to SH3 domains of phospholipase C-γ and GRB-2. *Journal of Biological Chemistry* **269**; 16009-16014

Sette, C., Bevilacqua, A., Bianchini, A., Mangia, F., Geremia, R. and Rossi, P. (1997) Parthenogenetic activation of mouse eggs by microinjection of a truncated c-kit tyrosine kinase present in spermatozoa. *Development* **124**; 2267-2274

Shearer, J., De Nadai, C., Emily-Fenouil, F., Gache, C., Whitaker, M. and Ciapa, B. (1999) Role of phospholipase Cγ at fertilisation and during mitosis in sea urchin eggs and embryos. *Development* **126**; 2273-2284

Shull, G. (2000) Gene knockout studies of Ca^{2+}-transporting ATPases. *European Journal of Biochemistry* **267**; 5284-5290

Smrcka, A.V., Hepler, J.R., Brown, K.O. and Sternweis, P.C. (1991) Regulation of polyphosphoinositide-specific phospholipase C activity by purified Gq. *Science* **251**; 804-807

Smrcka, A.V. and Sternweis, P.C. (1993) Regulation of purified subtypes of phosphatidylinositol-specific phospholipase C beta by G protein alpha and beta gamma subunits. *Journal of Biological Chemistry* **268**; 9667-9674

Soler, C., Beguinot, L. and Carpenter, G. (1994) Individual epidermal growth factor receptor autophosphorylation sites do not stringently define association motifs for several SH2-containing proteins *Journal of Biological Chemistry* **269**; 12320-12324

Song, C., Hu, C.D., Masago, M., Kariyai, K., Yamawaki-Kataoka, Y., Shibatohge, M., Wu, D., Satoh, T. and Kataoka, T. (2001) Regulation of a novel phospholipase C, PLC-epsilon, through membrane targeting by Ras. *Journal of Biological Chemistry* **276**; 2752-2757

Sorrentino, A. and Rizzuto, R. (2001) Molecular genetics of Ca^{2+} stores and intracellular Ca^{2+} signalling. *Trends in Pharmacological Sciences* **22**; 459-464

Sorrentino, V. and Volpe, D. (1993) Ryanodine receptors: how many, where, and why? *Trends in Pharmacological Science* **14(3)**; 98-103

Spungin, B., Margalit, I. and Breitbart, H. (1995) Sperm exocytosis reconstructed in a cell-free system. Evidence for the involvement of phospholipase C and actin filaments in membrane fusion. *Journal of Cell Science* **108**; 2525-2535

Steinhardt, R.A., Epel, D., Caroll, E.S. and Yanagimachi, R. (1974) Is calcium ionophore a universal activator for eggs? *Nature* **252**; 41-43

Stricker, S.A. (1997) Intracellular injections of soluble sperm factor trigger calcium oscillations and meiotic maturation in unfertilized oocytes of a marine worm. *Developmental Biology* **186**; 185-201

Stricker, S.A. (1999) Comparative biology of calcium signalling during fertilization and egg activation in animals. *Developmental Biology* **211**; 157-176

Swann, K. (1990) A cytosolic sperm factor stimulates repetitive calcium increases and mimics fertilisation in hamster eggs. *Development* **110**; 1295-1302

Swann, K. (1994) Ca^{2+} oscillations and sensitization of Ca^{2+} release in unfertilized mouse eggs injected with a sperm factor. *Cell Calcium* **15;** 331-339

Swann, K. (1996) Soluble sperm factors and Ca^{2+} release in eggs at fertilisation. *Reviews of Reproduction* **1**; 33-39

Takeshima, H., Nishimura, S., Matsumoto, T., Ishida, H., Kangawa, K. Minamino, N., Matsuo, H., Ueda, M., Hanaoka, M., Hirose, T (1989) Primary structure and expression from complementary DNA of skeletal muscle ryanodine receptor. *Nature* **339**; 439-445

Tang, T.S., Dong, J.B., Huang, X.Y. and Sun, F.Z. (2000) Ca^{2+} oscillations induced by a cytosolic sperm factor are mediated by a maternal machinery that functions only once in mammalian eggs. *Development* **127**; 1141-1150

Taylor, C. (1998) Inositol trisphosphate receptors: Ca^{2+}-modulated intracellular Ca^{2+} channels. *Biochimica et Biophysica Acta* **1436**; 19-33

Taylor, C., Genazzini, A. and Morris, S. (1999) Expression of inositol trisphosphate receptors. *Cell Calcium* **26**; 237-251

Taylor, S.J., Chae, H.Z., Rhee, S.G. and Exton, J.H. (1991) Activation of the beta 1 isozyme of phospholipase C by alpha subunits of the Gq class of G proteins. *Nature* **350**; 516-518

Tesarik, J., Pilka, L., Drahorad, J., Cechova, D. and Veselsky, L. (1988) The role of cumulus cell-secreted proteins in the development of human sperm fertilizing ability: implication in IVF. *Human Reproduction* **3**; 129-132

Tesarik, J., Sousa, M. and Testart, J. (1994) Human oocyte activation after intracytoplasmic sperm injection. *Human Reproduction* **9**; 511-518

Thrower, E., Hagar, R. and Ehrlich, B. (2001) Regulation of $Ins(1,4,5)P_3$ receptor isoforms by endogenous modulators. *Trends in Pharmacological Sciences* **22**; 580-586

Timeramn, A.P., Ogumbumni, E., Freund, E., Wiederrecht, G., Marks, A.R., and Fleicher, S. (1993) The calcium release channel of sarcoplasmic reticulum is modulated by FK-506 binding protein. Dissociation and reconstitution of FKBP-12 to the calcium release of skeletal muscle sarcoplasmic reticulum. *Journal of Biological Chemistry* **268**; 22992-22999

Timerman, A.P., Onoke, H., Xin, H.B., Bag, S., Copello, J., Wiederrecht, G. and Fleischer, S. (1996) Selective binding of FKBP12.6 by the cardiac ryanodine receptor. *Journal of Biological Chemistry* **271**; 20385-20391

Toepfer-Petersen, E., Calvete J.J., Sanz, L. and Sinowatz, F. (1993) Spermadhesins: a novel group of carbohydrate-binding proteins that function in fertilization. *Journal of Reproduction and Development* **39** (Suppl.); 45

Toepfer-Petersen, E., Petrounkina, A.M. and Ekhlasi-Hundrieser M. (2000) Oocyte-sperm interactions. *Animal Reproduction Science* **60-61**; 653-662

Tosti, E., Palumbo, A. and Dale, B. (1993) Inositol trisphosphate in human and ascidian spermatozoa. *Molecular Reproduction and Development* **3**; 373-383

Trump, B.F. and Berezesky, I.K. (1995) Calcium-mediated cell injury and cell death. *FASEB Journal* **9**; 219-228

Tsafriri, A. and Dekel, N. (1994) Molecular mechanisms in ovulation: *In "Molecular Biology of the Female Reproductive System"* (J.K. Findlay, Ed.) Academic Press, San Diego; 207-258

Varnai, P. and Balla, T. (1998) Visualisation of phosphoinositides that bind pleckstrin homology domains: calcium- and agonist-induced dynamic changes and relationship to the *myo*-[^{3}H]inositol-labelled phosphoinositide pools. *Journal of Cell Biology* **143**; 501-510

Varnai, P., Lin, X., Lee, S.B., Tuymetova, G., Bondeva, T., Spat, A., Rhee, S.G., Hajnoczky, G. and Balla, T. (2002) Inositol lipid binding and membrane localization of isolated pleckstrin homology (PH) domains. Studies on the PH domains of phospholipase C delta 1 and p130. *Journal of Biological Chemistry* **277**; 27412-27422

Verkhratsky, M. and Shmigol, A. (1996) Calcium-induced calcium release in neurons. *Cell Calcium* **22**; 11-14

Verkhratsky, M. and Petersen, O. (1998) Neuronal calcium stores. *Cell calcium* **24**; 333-343

Visconti, P.E., Moore, G.D., Bailey, J.L., Laclerc, P., Connors, S.A., Pan, D., Olds-Clarke, P. and Kopf, G.S. (1995) Capacitation in mouse spermatozoa. II. Protein tyrosine phosphorylation and capacitation are regulated by a cAMP-dependant pathway. *Development* **121**; 1139-1150

Visconti, P.E. and Kopf, G.S. (1998) Regulation of protein phosphorylation during sperm capacitation. *Biology of Reproduction* **59**; 1-6

Wahl, M.I., Nishibe, S., Suh, P.G., Rhee, S.G. and Carpenter, G. (1989) Epidermal growth factor stimulates tyrosine phosphorylation of phospholipase C-II independently of receptor internalization and extracellular calcium. *Proceeding of the National Academy of Science* **86**; 1568-1572

Wang, T., Pentyala, S., Rebecchi, M.J. and Scarlata, S. (1999) Differential association of the pleckstrin homology domains of phospholipases C-beta 1, C-beta 2, and C-delta 1 with lipid bilayers and the beta gamma subunits of heterotrimeric G proteins. *Biochemistry* **38**; 1517-1524

Wang, T., Dowal, L., El-Maghrabi, M.R., Rebecchi, M.J. and Scarlata, S. (2000) Pleckstrin homology domain of PLC-beta2 confers G-βγ activation of the catalytic core. *Journal of Biological Chemistry* **275**; 7466-7-34

Wehrens, X.H.T., Lehnart, S.E. and Marks, A.R. (2005) Intracellular calcium release and cardiac disease. *Annual Reviews of Physiology* **67**; 69-98

Wing, M.R., Houston, D., Kelley, G.G., Der, C.J., Siderovski, D.P. and Harden, T.K. (2001) Activation of PLC-ε by heterotrimeric G protein βγ-subunits. *Journal of Biological Chemistry* **276**; 48257-48261

Whitaker, M. Swann, K. and Crossley, I. (1989) What happens during the latent period at fertilisation? *In "Mechanisms of Egg Activation"* (R.Nucchitelli, G.N.Cherr and W.H.Clark, Eds.) Plenum Press, NY; 157-171

Williams, C.J., Mehlmann, L.M., Jaffe, L.F., Kopf, G.S. and Schultz, R.M. (1998) Evidence that the Gq family G proteins do not function in mouse egg activation at fertilisation. *Developmental Biology* **198**; 116-127

Williams, R.L. (1999) Mammalian phosphoinositide-specific phospholipase-C. *Biochimica et Biophysica Acta* **1441**; 255-267

Wolny, Y.M., Fissore, R.A., Reiss, M.M., Colomero, L.T., Ergun, B. Rosenwaks, Z. and Palermo, G.D. (1999) Human glucosamine-6-phosphate isomerase, a homologue of hamster oscillin, does not appear to be involved in Ca^{2+} release in mammalian oocytes. *Molecular Reproduction and Development* **52**; 277-287

Wolosker, H., Kline, D., Bian, Y., Blackshaw, S., Cameron, A.M., Fralich, T.J., Schnaar, R.L. and Snyder, S.H. (1998) Molecularly cloned mammalian glucosamine-6-phosphate deaminase localises to transporting epithelium and lacks oscillin activity. *FASEB Journal* **12**; 91-99

Wu, D.Q., Jiang, H.P., Katz, A. and Simon, M.I. (1993) Identification of critical regions on phospholipase C-beta1 required for activation by G-proteins. *Journal of Biological Chemistry* **268**; 3704-3709

Wu, H., He, C.L. and Fissore, R.A. (1997) Injection of a porcine sperm factor triggers calcium oscillations in mouse oocytes and bovine eggs. *Molecular Reproduction and Development* **46**; 176-189

Wu H., He, C.L., Jehn, B., Black, S.J. and Fissore, R.A. *(1998) Partial characterisation of the calcium-releasing activity of porcine sperm cytosolic extracts.* Developmental Biology ***203; 369-381***

Wu, H., Smythe, J., Luzzi, V., Fukami, K., Takenawa, T., Black, S.L., Allbritton, N.L. and Fissore, R.A. (2001) Sperm factor induces intracellular free calcium oscillations by stimulating the phosphoinositide pathway. *Biology of Reproduction* **64**; 1338-1349

Yagisawa, H., Sakuma, K., Paterson, H.F., Cheung, R., Allen, V., Hirata, H., Watanabe, Y., Hirata, M. and Katan, M. (1998) Replacement of single basic amino acids in the pleckstrin homology domain of phospholipase C-δ1 alter the ligand binding, phospholipase activity, and interaction with the plasma membrane. *Journal of Biological Chemistry* **273**; 417-424

Yamagata, K., Murayama, K., Okabe, M., Toshimori, K., Nakanishi, T., Kashiwabara, S. and Baba, T. (1998) Acrosin accelerates the dispersal of sperm acrosomal proteins during acrosome reaction. *Journal of Biological Chemistry* **273**; 10470-10474

Yamamoto, T., Takeuchi, H., Kanematsu, T., Allen, V., Yagisawa, H., Kikkawa, U., Watanabe, Y., Nakasima, A., Katan, M. and Hirata, M. (1999) Involvement of EF hand motifs in the Ca^{2+}-dependant binding of the pleckstrin homology domain to phosphoinositides. *European Journal of Biochemistry* **265**; 481-490

Yoda, A., Oda, S., Shikano, T., Kouchi, Z., Awaji, T., Shirakawa, H., Kinoshita, K. and Miyazaki, S. (2004) Ca2+ oscillation-inducing phospholipase C zeta expressed in mouse eggs is accumulated to the pronucleus during egg activation. *Developmental Biology* **268(2)**; 245-257

Yuan, R., Primakoff, P. and Myles, D.G. (1998) A role for the disintegrin domain of cyritestin, a sperm surface protein belonging to the ADAM family, in mouse sperm-egg plasma membrane adhesion and fusion. *Journal of Cell Biology* **137**; 105-112

Zheng, L., Krishnamoorthi, R., Zolkiewski, M. and Wang, X. (2000) Distinct Ca^{2+} binding properties of novel C2 domains of plant phospholipase Dα and β. *Journal of Biological Chemistry* **275**; 19700-19706

Zhou, C., Horstman, D., Carpenter, G. and Roberts, M.F. (1999) Action of phosphatidylinositol-specific phospholipase Cgamma1 on soluble and micellar substrates. Separating effects on catalysis from modulation of the surface. *Journal of Biological Chemistry* **274**; 2786-2793

Zucchi, R. and Ronca-Testoni, S. (1997) The sarcoplasmic reticulum Ca^{2+} channel/ryanodine receptor: modulation by endogenous effectors, drugs and disease states. *Pharmacological Reviews* **49**; 1-51

APPENDIX III. OLIGONUCLEOTIDE PRIMERS

Primers raised against mPLCζ

Primer	*Sequence*	*Length(Bp)*	*Comments*
mPLCzF (193-215)	ATTC**GAATTC**TCATGGA AAGCCAACTTCATGAG	33	Sense primer to amplify full length PLCζ, ζΔC2, PLCζ-LUC, ζΔC2-LUC; Contains EcoRI restriction site
mPLCzF (342-362)	ACCG**GAATTC**ATATTTT TAAGGAAAATGAC	30	Sense primer to amplify ζΔEF1, ζΔEF1-LUC; Contains EcoRI restriction site
mPLCzF (625-647)	ACCG**GAATTC**GATACA TGTTTTCATCAGAATGT	33	Sense primer to amplify ζΔEF1,2, ζXY; Contains EcoRI restriction site
mPLCzR (2124-2144)	AATG**GTCGAC**ATGCGT CACTCTCTGAAGTA	30	Antisense primer to amplify full length PLCζ, ζΔEF1, ζΔEF1,2; Contains SalI restriction site
mPLCzR (1720-1749)	GATG**GTCGAC**ATATTCT GGTTAATTGGGGT	30	Antisense primer to amplify ζΔC2, ζXY; Contains SalI restriction site
ZXYlinkF	TA**GAATTC**GGAAAGTG GGAACCTTATCTGAAAC	33	Sense primer to amplify ζXY linker; Contains EcoRI restriction site
ZXYlinkR	AATG**GTCGAC**AAGGCC ATGGCTATTTTCATCT	32	Antisense primer to amplify ζXY linker; Contains SalI restriction site
LPLCzR	ATGT**GCGGCCGC**GCAC TCTCTGAAGTACCAAAC A	34	Antisense primer to amplify full length PLCζ-LUC, ζΔEF1-LUC; Contains NotI restriction site
ZC2dR	TAAT**GCGGCCGC**AACT GGATGGTCGTCATATT C	33	Antisense primer to amplify ζΔC2-LUC; Contains NotI restriction site
PLCζ con-9 (53-80)	ATTTTTCCACCTCTGAA AAGTCATCCTGAA	30	Sequencing of antisense strand

PLCζ con-10 (138-170)	CTGTCATTTGTCCTTAA AAATACCTGTTTCACAT GA	36	Sequencing of antisense strand
PLCζ con-11 (178-207)	TCTAAACTTCTTCATAT GGTGATTCTTCCTTG	32	Sequencing of antisense strand
PLCζ con-12 (1757-1782)	TGGCATTGATACGTTTT GTTGTTGAA	26	Sequencing of sense strand
PLCζ con-13 (1843-1875)	TGCATGAACAAAGGTTA TCGTCGTGTTCCTCTG	33	Sequencing of sense strand

Primers raised against rPLCδ1

Primer	***Sequence***	***Length(Bp)***	***Comments***
PLCdelta1F	CTTC**GTCGAC**CATGGA CTCGGGTAGGGAC	29	Sense primer to amplify full length PLCδ1; Contains SalI restriction site
PLCdelta1R	CACC**GCGGCCGC**TTAG TCCTGGATGGAGATCT TC	34	Antisense primer to amplify full length PLCδ1, ΔPHδ1; Contains NotI restriction site
ΔPHd1F	TTC**GTCGAC**TGGGCTC CATGGACCAGCGGCAG AAGC	36	Sense primer to amplify ΔPHδ1; Contains SalI restriction site
DXYlinkF	TA**GAATTC**GGAAGAAG CTGGGAGGGCTGCTGCC T	34	Sense primer to amplify δ1XY linker; Contains EcoRI restriction site
DXYlinkR	ATG**GTCGAC**TCCGGCA CCAGCTTTAGTTTATCC	33	Antisense primer to amplify δ1XY linker; Contains SalI restriction site
PHF	TA**GAATTC**TCATGTGC GGCCGCGCCGGAGTG GTG	34	Sense primer to amplify PHδ1; Contains EcoRI restriction site
PHR	GA**GTCGAC**CCAGCCTT TCGCAAGC	24	Antisense primer to amplify PHδ1; Contains SalI restriction site
LPLCd1F	TATC**GATATC**ATGGACT CGGGTAGGGACTTCCT G	34	Sense primer to amplify PLCδ1-LUC; Contains EcoRV restriction site
LDPHd1F	TATC**GATATC**ATGGAC CAGCGGCAGAAGCTGC AG	34	Sense primer to amplify ΔPHδ1-LUC; Contains EcoRV restriction site

LPLCd1R	ATGT**GCGGCCGC**GTAG TCCTGGATGGAGATCT TCA	35	Antisense primer to amplify PLCδ1-LUC, ΔPHδ1-LUC; Contains NotI restriction site
Delta1F (1-28)	ATGGACTCGGGTAGGG ACTTCCTGACCC	28	Sequencing of sense strand
EFD1F (402-431)	ATGGACCAGCGGCAGA AGCTGCAGAACTG	29	Sequencing of antisense strand

Primers raised against LUCIFERASE

Primer	*Sequence*	*Length(Bp)*	*Comments*
LuciF	TACT**GCGGCCGC**GATG GAAGACGCCAAAAACA TA	34	Sense primer to amplify LUC and all LUC chimeras; Contains NotI restriction site
LuciR	TT**GCGGCCGC**TTACAA TTTGGACTTTCC	28	Antisense primer to amplify LUC and all LUC chimeras; Contains NotI restriction site
LIs	CAATCAAATCATTCCGG ATACTGCGATT	28	Sequencing of sense strand
Luc-int2	AGTATGAACATTTCGCA G	18	Sequencing of antisense strand